UNIVERSITY OF CANTERBURY
DEPARTMENT OF CIVIL ENGINEERING

Equivalent Fire Resistance Ratings of Construction Elements Exposed to Realistic Fires

By Jonathan F Nyman

May 2002

Equivalent Fire Resistance Ratings of Construction Elements Exposed to Realistic Fires

by

Jonathan F Nyman

Supervised by

Dr Andrew H Buchanan

and

J T (Hans) Gerlich

A research report presented as partial fulfilment of the requirements for the Degree of Master of Engineering in Fire Engineering.

Department of Civil Engineering
University of Canterbury
Christchurch, New Zealand

May 2002

Abstract

The New Zealand Building Code Approved Documents have recently incorporated reductions in the life safety F-ratings, which determine the fire resistance rating (FRR) requirements of fire barriers in buildings. This reduction has led to concern that in the event of a real fire exposure, where modern synthetic materials increase both the speed of fire growth, peak heat release rates and temperatures within a compartment, fires more severe than the AS1530.4 standard furnace test exposure may result. In such cases construction elements may not provide suitable fire protection for the life safety requirements of the Building Code. These requirements include provision for safe evacuation of occupants and fire service rescue activities.

Three full-scale compartment tests were carried out, establishing the actual times to failure of numerous light timber framed (LTF) and light steel framed (LSF) non-loadbearing wall and LTF ceiling/floor assemblies. Each test assembly selected had detailed temperature data available from its respective standard furnace test, which had previously been undertaken to determine the assemblies FRRs. The compartment assemblies, of ISO 9705 room geometry, were exposed to fires of varying severity based on the fuel load energy density within the compartment and the ventilation opening dimensions. Synthetic materials were selected to replicate the initial fast fire growth associated with upholstered furniture. Wooden cribs were used to provide bulk fuel for the remainder of the FLED requirement.

A method of predicting assembly failure times when exposed to real fire exposures has been established. The method is based on a correlation of the cumulative radiant heat energy that would impact on an assembly up to the point of its failure during a standard test, and the equivalent time at which a real fire exposure would have produced the same level of cumulative energy. The method provides good agreement and reasonably conservative prediction of a non-loadbearing assembly's insulation failure. Further validation is required to establish factors of safety to the method for determining assembly integrity failure. The method was found to be non-conservative for use on loadbearing assemblies.

Acknowledgements

Substantial financial support was provided by the Building Industry Authority (BIA), Winstone Wallboards Ltd, and the Foundation for Research, Science and Technology, in the form of a Technology for Industry Fellowship (TIF). Additional thanks go to BRANZ for staffing time and testing costs. Many thanks to these sponsors.

Special thanks go to my supervisors, Dr Andrew Buchanan (University of Canterbury) and Hans Gerlich (Winstone Wallboards Ltd.), for their enthusiasm and guidance throughout all aspects of the research.

Winstone Wallboards Ltd, James Hardie Building Products Ltd and BRANZ provided all materials and instrumentation for the testing.

All compartment fire tests were carried out at the fire research facilities of the Building Research Association of New Zealand (BRANZ), Wellington, New Zealand. Many thanks to the staff at BRANZ, for provision of an office and access to all their resources and technical expertise, and particularly for showing such interest in this project.

Additional thanks go to Dr Geoff Thomas (Victoria University of Wellington) for assistance on this area of research, and Cliff Barnett (Macdonald Barnett Partners Ltd, Auckland) for checking preliminary calculations and ongoing feedback of test results.

Thanks also to the New Zealand Fire Services Commission for their continued support of the ME Fire program.

Proof reading was carried out by Colleen Wade (BRANZ) and Hans Gerlich (Winstone Wallboards Ltd). Thanks again.

A very special thanks go to my good friends Chris and Sharon Wilkinson for allowing me stay with them and putting up with me during my 6 month stay in Wellington. You kept me relatively sane through the whole experience and I am truly indebted to you.

Table of Contents

List of Figures

List of Tables

Nomenclature

Symbol	Description	Units
A_f	Floor area of compartment	m^2
A_t	Total area of internal bounding surfaces (including openings)	m^2
A_v	Area of vent opening	m^2
A_{wood}	Surface area of wood	m^2
b	√Thermal Inertia = $\sqrt{(k \rho C_p)}$	
b_v	Vertical opening factor	
C_p	Specific heat capacity	J/kgK
D	Crib stick thickness	m
E	Heat release per mass of O_2 consumed (≈13.1MJ/kg)	MJ/kg
E_{total}	Total energy content of fuel	MJ
e_f	Fuel load per m^2 floor area	MJ/m^2
F_v	Opening factor	$m^{0.5}$
H_r	Height of compartment	m
H_v	Height of vent opening	m
h	Heat transfer coefficient	W/m^2K
h_a	Nett calorific value	MJ/kg
h_c	Crib height	m
h_n	Oven dry calorific value	MJ/kg
$\Delta h_{c.eff}$	Effective heat of combustion	MJ/kg
k	Thermal conductivity	W/mK
k_b	CIB formula compartment linings parameter	min $m^{2.25}/MJ$
k_c	Eurocode formula compartment linings parameter	min m^2/MJ
M_{O_2}	Molecular weight of oxygen (32g/mol)	g/mol
M_a	Molecular weight of combustion air (29g/mol for dry air)	g/mol
m_c	Moisture content by weight	%
m_i	Initial mass of specimen	g
m_f	Final mass of specimen	g
$\dot{m}$	Ventilation controlled burning rate for wood cribs	kg/s

$\dot{m}''_{wood}$	Surface burning rate for wood	kg/s/m²
$\dot{m}_e$	Mass flow rate of exhaust combustion products	kg/s
n	Number of crib sticks per row	
$\dot{q}$	Heat release rate	kW
$\dot{q}''_{peak}$	Peak heat release rate per unit exposed area	kW/m²
q''_{total}	Total heat release per unit exposed area	MJ/m²
$\dot{Q}''$	Emissive heat release	kJ/m²
Q_{total}	Total heat release	MJ
$\dot{Q}_{peak}$	Peak heat release	kW
Q_{fo}	Heat release rate to cause flashover	MW
Q_v	Ventilation controlled heat release rate	MW
RH	Relative humidity	%
S	Crib clear spacing between sticks	m
t_b	Burning time	Secs
t_e	Time equivalent	Mins
t_{hr}	Time	Hrs
t_{min}	Time	Mins
t_{secs}	Time	Secs
t*	Ficticious time	Hrs
Δt	Sampling time interval	secs
T	Temperature	°C
T_{ref}	Ambient temperature	K
T_0	Ambient Temperature	°C
w_f	Ventilation factor	$m^{-0.25}$
V	Volume	m³
$X^a_{H_2O}$	Actual mole fraction of water vapour in the combustion air	
$X^a_{CO_2}$	Actual mole fraction of carbon dioxide in the combustion air	
$X^{A^a}_{O_2}$	Measured mole fraction of oxygen in the combustion air	
$X^{A^e}_{O_2}$	Measured mole fraction of oxygen in the exhaust flow	

α	Volumetric expansion factor =1.105 (Janssens 1995)	
α_h	Horizontal openings ratio	
α_v	Vertical openings ratio	
ε	Emissivity	
Γ_{ECmod}	Eurocode parametric curve ficticious time constant	
ρ	Density	kg/m^3
σ	Stefan Boltzmann Constant (5.67×10^{-11})	kW/m^2K^4
ϕ	Oxygen depletion factor	

1 Introduction

1.1 Background

In New Zealand, the minimum requirements for building fire safety design as set out by the New Zealand Building Code (NZBC 1992) are largely performance based. The Approved Documents (BIA 2001), which are non-mandatory, are used substantially in New Zealand by building designers and engineers to provide prescriptive methods to arrive at NZBC compliant fire safety design solutions. These designate building elements to have specific fire resistance ratings for life safety and fire fighting access. The fire resistance of load bearing and non-load bearing light frame building elements and components, such as walls, doors, services penetration fittings and the like, has traditionally been determined using standard fire tests to provide a fire resistance rating (FRR). Testing methods to establish fire resistance are similar around the world. The level of FRR required by the prescriptive methods of the Approved Documents has little relation to the likely severity of a real compartment fire and the performance of fire rated building elements.

The recently updated Approved Documents (BIA 2001) have seen a reduction in the FRR's required from building elements, for what is deemed to provide appropriate protection time in the event of a fire, for safe evacuation, fire service intervention and search and rescue activities. Previous research (Jones 2001) has shown qualitatively that the actual fire resistance of building elements exposed to real building fires can be significantly less than the intended evacuation times implied by the NZBC. As a consequence, there is some concern that in a real building fire, where modern synthetic materials are used, which increase both the speed of fire growth and the peak heat release rates and temperatures, construction elements may not ensure safe evacuation, or offer the required life safety of the building occupants and the fire services as is intended by the building codes.

1.2 Project Objective

The aim of the project was to conduct fully instrumented full scale fire compartment tests and to quantify the variation in fire resistance of non-load bearing building elements exposed to realistic fast growth fires, compared with standard furnace test results for those same construction elements. The project's objective is to establish a correlation, between standard fire test severity and the expected real fire severity. Such a correlation would be applied by designers and

engineers to fire resistance ratings (FRR's) to establish the time to failure of elements when exposed to real fire conditions.

The project examines the fire resistance of building elements, including non-load bearing walls and floor/ceiling systems comprising gypsum plasterboard and cementicious board systems, which are described in Section 3. In addition, a fire door was examined, to establish whether any correlation may be applicable to these too. Additional information on charring rates of timber in realistic fires will also be documented in Section 4 of the report.

This report initially overviews the topic of fire resistance by means of a literature review in Section 2, which will cover:

- basic definitions of the subjects of fire resistance, fire severity and fire resistance ratings (FRR's)
- standard fire FRR testing methods and history
- realistic fire testing and previous works undertaken to assess FRR's for realistic fires

Three full-scale fire compartment tests have been undertaken to establish the times to failure of a variety of assemblies in a realistic fire. Descriptions of the full-scale fire compartment testing are provided in Section 3 of the report, which will incorporate:

- realistic fire requirements, including fuel materials, geometry and prediction of expected fire severity for each test scenario
- technical details of building elements under test, including construction methods and standard fire FRR ratings
- details of dummy column set up to record charring rates
- testing apparatus set up and equipment.

All results and test observations, including comparisons of the time to failures of the building elements under the standard fire test and from the full-scale fire compartment tests are incorporated in Section 4.

In the analyses (Section 5), the report finally establishes a correlation for use in realistic fire situations, where the time to failure of a barrier can be established for a real fire, based upon the fuel load, compartment geometry, ventilation openings and building element construction in use.

Calorimeter tests undertaken, to establish heat release rates and heat of combustion of the synthetic materials used in the compartment tests, are described in Section 6 of the report.

Finally, the project is summarised and conclusions are provided in Section 7. All recommendations arising from the research are described in Section 8.

2 Fire Safety, Resistance and Severity

2.1 General

An explanation of the building fire safety requirements of the NZBC is provided within this chapter, which will show why fire resistance is important for provision of life safety to building occupants in the event of a fire. This section will provide definitions explaining fire resistance, and additionally explains how fire resistance ratings (FRR's) of construction elements are determined within New Zealand. Descriptions of the historical background of determining a fire resistance rating (FRR) is given, which in conjunction with an understanding of fire severity, will examine the appropriateness of current FRR's and their relevance to fire severity and 'realistic' fires.

2.2 Fire Safety Objectives

2.2.1 Building Code Requirements

Performance-based building codes, such as those applied in the New Zealand Building Code (NZBC 2001), require that buildings be constructed and operated such that fire safety in buildings is provided to an appropriate level. The NZBC sets out fire safety requirements to an extent that the following objectives must be met;

(a) Clause C1 OUTBREAK OF FIRE – Requires that outbreak of fire be minimised, safeguarding people from injury or illness caused by fire.
(b) Clause C2 MEANS OF ESCAPE – Requires that people be safeguarded from injury or illness from a fire when escaping to a safe place and that fire rescue operations be facilitated.
(c) Clause C3 SPREAD OF FIRE – Requires that people be safeguarded from injury or illness when evacuating a building during a fire, and that fire service personnel are protected during fire fighting operations. Additionally, fire protection of adjacent properties and safeguarding of the environment from adverse effects of fire are also required by this clause.
(d) Clause C4 STRUCTRURAL STABILITY DURING A FIRE – Requires that people be safeguarded from injury, and that household units and other property be protected from damage due to loss of structural stability.

From the above general objectives, adequate fire protection must be provided to protect occupants and fire service personnel within the building during a fire. Additionally, outside of the building during a fire, neighbouring properties and the environment must be protected. These objectives can be met by incorporating either passive or active fire protection/control methods into the building design.

Active and passive control is defined by Buchanan (Buchanan 2001a), where active control refers to the control of the fire by some action taken by a person or an automatic device, and passive control refers to the control of the fire by systems that are built into the structure or fabric of the building, not requiring operation by people or automatic controls. Fire resistance of a building element to prevent both fire spread and collapse of the structure is the most important element of passive fire protection.

This report will be examining only the passive protection, and in particular fire resistance necessary to provide the fire safety objectives for safety of people and fire services operations within the building only. Fire safety protection requirements of adjacent properties and the environment are beyond the scope of this report.

2.2.2 Life Safety Requirements and F-ratings

The most common objective in providing life safety from fire in a building is to ensure safe escape (Buchanan 2001a). In addition to alerting the building occupants of the occurrence of a fire, it is essential that occupants are not affected adversely by fire or smoke whilst evacuating using the escape paths provided. In some circumstances, such as hospitals or institutions, building occupants may not be able to escape to safety. Where such instances occur, building construction elements need to have appropriate levels of fire resistance to withstand the effects of a fire, until rescue operations can be carried out, or the fire has been extinguished.

Internally within a building, fire resistance can be provided by employing barriers, which prevent the spread of fire and smoke for a specific period of time whilst evacuation, rescue and fire fighting operations are being undertaken. Such barriers include wall partitions, doors, ceiling/floors and other similar building construction components. Paper-faced gypsum plasterboard linings are most commonly used for internal barriers, particularly when fire resistance is required. Fire resistance requirements of a compartment in the Building Code

(NZBC 1992) is intended to be the appropriate level of resistance to meet the life safety, as described in Section 2.2.1. It must be noted that the NZBC does not aim to protect property, other than adjacent property under separate ownership.

The Approved Documents (BIA 2001) provide prescriptive methods of compliance with the NZBC. These methods are not mandatory. The Approved Documents are commonly used as a basis for fire engineering design by building designers, for building fire safety. Since the Approved Documents cater for all building types (excluding buildings of fire loads greater than 1500MJ/m^2 and firecells with inadequate ventilation), significant use of specific fire engineering design is not necessarily employed for a significant number of building fire safety designs (Buchanan 1994). In certain circumstances this may be detrimental to building fire safety. Examination of such circumstances is beyond the scope of this project.

Levels of fire protection and resistance levels required for buildings and fire compartments of various use, size and levels are designated by the Approved Documents (BIA 2001). Life safety 'F ratings' are assigned to a fire compartment and corresponding FRR's are then ascertained for the compartment's barriers. These fire-cell 'F-ratings' are selected t provide the minimum time that is required for safe evacuation and rescue activities from that compartment. They identify the level of resistance to internal spread of fire that must be provided and are applicable to all fire separations, such as walls and floors, and their associated supporting elements. Building fire safety designs in New Zealand rely heavily on active systems. Automatic sprinklers are required in all buildings 25 metres and higher, and in buildings of lesser height depending on use and occupant numbers.

F-ratings are not calculated and would appear to be arbitrary 'real time' values (Duncan 2001). Approved Document F-ratings, required for life safety, have recently been reduced to 30 minutes for most building types (Buchanan et al 2001). This reduction is shown in Table 2.1. The figures denoted in brackets are the F-ratings prior to being reduced. This reduction is of particular cause for concern in the early evacuation and rescue stages of a fire, and it has been suggested that in light of recent research undertaken by Jones (2001), specifically in cases where the building fire is more severe than the standard fire resistance test, the actual available evacuation time required could, in some cases, be much less than the F-ratings imply.

Purpose Group	Escape Heights							
	Single storey	2 Floors	3 Floors	<25m	<34m	<46m	<58m	>58m
CS - Crowd small	**F0** (F0)	**F30** (F30/60)	**F30** (F60)	**F45** (F60)	**F30** (F60)	**F30** (F60)	**F30** (F60)	**F60** (F60)
CM – Merchandise	**F0** (F0)	**F30** (F30/60)	**F30** (F30/60)	**F45** (F60)	**F30** (F60)	**F30** (F60)	**F30** (F60)	**F60** (F60)
CL – Crowd large	**F0** (F0)	**F30** (F30/60)	**F30** (F60)	**F45** (F60)	**F30** (F60)	**F30** (F60)	**F30** (F60)	**F60** (F60)
WL/ WM/ WH – Work light/ medium/ heavy	**F0** (F0)	**F30** (F30/60)	**F30** (F30/60)	**F45** (F60)	**F30** (F60)	**F30** (F60)	**F30** (F60)	**F60** (F60)
WF – Work fast fire	**F0** (F0)	**F30** (F30/60)	**F30** (F60)	**F30** (F60)	**F30** (F60)	**F30** (F60)	**F30** (F60)	**F60** (F60)
SC/ SD – Sleep care/ detention	**F0** (F0)	**F30** (F30)	**F30** (F30)	**F30** (F30)	**F30** (F30)	**F30** (F60)	**F30** (F60)	**F60** (F60)
SA – Sleep accommodation	**F0** (F0)	**F30** (F30)	**F30** (F60)	**F45** (F60)	**F30** (F30)	**F30** (F60)	**F30** (F60)	**F60** (F60)
SR – Sleep residential	**F0** (F0)	**F30** (F30)	**F30** (F30)	**F45** (F60)	**F30** (F30)	**F30** (F60)	**F30** (F60)	**F60** (F60)

Table 2.1 – Approved Document 'F-ratings'

For purpose groups where high levels of modern synthetic materials and plastics (i.e. polyurethane (PU) foam) are used in the form of large quantities of upholstered furniture or plastics, it is suggested that the F-ratings are too low. Where such synthetic materials are evident in a particular occupancy, the available safe egress times (ASET) will be reduced, as fire severity will potentially be worse than standard fire test FRR's provide for. This will result in less time for occupants to evacuate safely, as construction elements will fail in a shorter duration of time. In the Approved Documents, purpose groups such as hotels, motels, apartments, restaurant and dining facilities, hospitals, plastic and synthetic material or chemical manufacture and storage, retail and merchandising, executive commercial offices and other similar applications may offer a particularly high risk to occupants due to rapid fire growth and severity, particularly where high rise buildings are involved. Additionally, where occupants are unable to evacuate immediately or require assistance to evacuate, such as in sleeping or medical occupancies, actual evacuation times required will be noticeably longer, due to pre-movement times involved with waking up

from sleep, evaluating the fire danger, alerting other occupants, getting dressed and evacuation decision making.

2.3 Fire Resistance

2.3.1 Introduction

The fire resistance of a building element, or barrier, is that property which gives a barrier the ability to withstand, or give a level of protection to, a fire of a certain severity. The level to which a barrier continues to exhibit such fire resistance is defined as the fire endurance, and is usually represented by the time elapsed, to assembly failure, when exposed to a fire.

2.3.2 Fire Resistance of Lightweight Construction Assemblies

The fire resistance of a light framed construction is assigned to the complete assembly, not to individual components of that assembly. A number of parameters affect the fire resistance performance of light timber framed (LTF) and light steel framed (LSF) assemblies. The parameters of significance, as outlined by Sultan et al (2000), are:

- Lining type (gypsum, cementitious fibre, etc.)
- Lining thickness
- Number of layers
- Insulation type
- Insulation width
- Glass fibre in gypsum board
- Gypsum density
- Stud type

In a series of standard fire tests on steel framed and timber framed wall assemblies, Sultan et al (2000) established the effect on an assembly's fire resistance, when altering any of the above parameters. For all tests, the quality and type of fixings was to recommended manufacturers' standards. It was found that the effect of insulation type on the fire resistance performance varied. Ordinarily, insulation in assemblies result in higher temperatures on the exposed lining, causing earlier falloff and failure. However, Sultan et al found in their tests, that for unloaded

steel stud walls, use of glass fibre insulation did not affect the fire resistance, whereas mineral fibre insulation increased the fire resistance by 54% and cellulose fibre insulation increased fire resistance by 4 %. The difference was largely due mineral fibre insulation maintaining its integrity and protecting the studs and the unexposed lining after the fire-exposed lining has fallen off, whereas the glass fibre insulation melts when exposed to higher, post flashover temperatures. For the loaded timber framed walls, the use of mineral or glass fibre insulation made no difference to the fire resistance, as failure in all cases was structural. Cellulose insulation was found not to alter the fire resistance, since the failure of the assembly was determined by the failure of the fire-exposed lining. The insulation width was found to play a significant role in the fire resistance of the assembly. In a steel stud framed wall, tighter fitting insulation, as opposed to loose fitting insulation, within the frame was found to increase fire resistance by 66%. The other significant observation was that the addition of a second lining on the exposed face increased fire resistance by 55%.

Increased density generally improves the fire performance of gypsum lining, as there are fewer air voids within the board and a greater quantity of moisture of crystallisation to be driven off.

Gypsum linings containing glass fibre reinforcing provide greater fire resistance, as shrinkage of the board is controlled. When linings shrink, they can pull away from fixings to the frame. Glass fibres incorporated into the lining reduce such premature failure of the lining, which is common with standard type gypsum linings.

2.3.3 Fire Resistance Ratings

Fire barriers are designed to control the fire for an extended period of time within the compartment of origin. This period of time needs to be sufficiently long for building occupants to evacuate and the fire service to carry out search and rescue activities. If additionally required by the building owner, the barriers may provide sufficient time for the fire service to control and extinguish the fire before spread occurs to other compartments.

The extent to which the barriers provide protection from a fire for a period of time is determined by assigning that barrier, or construction element, with a fire resistance rating (FRR). For fire compartment barriers it is most often quantified as a measure of time, usually in hours or parts of hours, in which the building element can meet a certain criteria when exposed to the

standard fire test. The criteria in tests, which determine an elements fire resistance when exposed to a fire, are stability, integrity and insulation. These are described in more detail in Section 2.3.5. Most countries have building codes that specify FRR's for building elements. Buchanan et al (2001a) explain that European countries commonly require ratings 2-3 times higher than that required in New Zealand. In Australia, the required ratings are 2-4 times higher. It should be noted, however, that these countries do not specify life safety F ratings separately from structural S ratings. Therefore, these countries fire ratings may be over conservative for simply providing fire resistance for evacuation and fire rescue operations alone. Also, building regulations in other countries often require a degree of property protection, whereas the NZBC has a life safety focus and leaves the protection of property, with the exception of adjacent property under separate title, to market forces (the insurance industry).

2.3.4 Fire Resistance Testing Methods

In New Zealand, the fire resistance rating of a barrier, or assembly, is determined by physical testing or by seeking an opinion from a fire expert or laboratory. Extensive testing is required by the present regulations. The tests provide a means of initial acceptance and additionally act as a data source, which can be used to support variations by assessment (Collier 2000).

Full-scale testing is the most common method of obtaining FRR's. In New Zealand, such tests are carried out at the Building and Research Association of New Zealand (BRANZ). At BRANZ, the fire resistance testing of building elements is carried out to AS 1530 Part 4 (SAA 1990), ISO 834 (ISO 1975), or BS 476 (BSI 1987) Parts 20-23, as required. There is similarity in the approved methods of testing and general requirements of these codes. The full-scale furnace used for such fire resistance testing can cater for building assemblies up to dimensions of 4m high by 3m wide. Floor, wall and door constructions can be tested using such a furnace. A typical full-scale test furnace can be seen in operation in Figure 2.1.

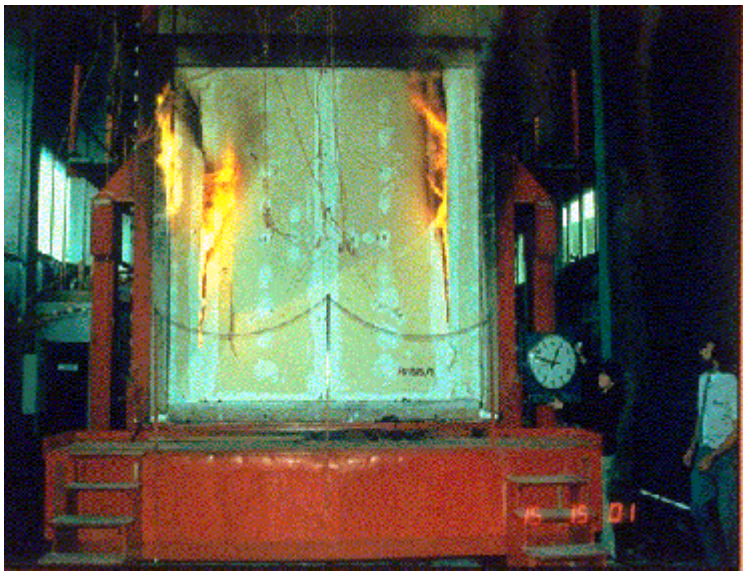

Figure 2.1 – Full scale test furnace at BRANZ.

Additionally, small scale furnace fire resistance testing can be undertaken using a pilot furnace, shown in Figure 2.2, with an opening size of 2.1m high by 1m wide. However, Buchanan (2001a) explains that although such small scale testing is cheaper than full-scale testing, full assessment of the potential problems caused by construction connections, shrinkage, deflections and gaps between panels of lining materials, is not possible with small-scale testing. Pilot scale testing is most commonly used to supplement data already gathered from a full-scale test.

Figure 2.2 – Pilot scale test furnace at BRANZ.

2.3.5 Test Failure Criteria

The fire resistance rating of a construction element is defined as being the time to failure, under the standard fire test, when one or more of the following general failure criteria apply (SAA 1990):

- Stability (or Structural) failure – An element of construction under test is deemed to have structurally failed when collapse, excessive deflection or significantly reduced load bearing capacity has occurred.
- Integrity failure – An element of construction under test is deemed to have an integrity failure when collapse, or the development of cracks, fissures, or other openings allow the passage of hot gases or flames through the construction element.
- Insulation failure – An element of construction under test is deemed to have an insulation failure when either the average surface temperature on the unexposed side of the test element exceeds 140°C, or when any point on the unexposed side exceeds a temperature of 180°C.

The first failure criterion does not apply to non-load bearing construction elements. Additionally, England et al (2000) note that there may be different particular requirements defining failure for specific types of constructions and in these cases, the relevant standard should be examined for such cases.

FRR's are designated to construction elements in the form --/--/--, where the time, in minutes, of fire resistance to the standard fire are ordered 'stability/integrity/insulation' respectively.

2.3.6 Quality of Construction Workmanship and Fire Resistance Performance

For LTF and LSF construction, the linings and framing construction are an essential part of the fire resistive construction. The quality of the lining and its fixings to the frame, whether it be gypsum based or other type, are extremely important.

Poor workmanship and construction quality will inevitably lead to a reduction in fire resistance of the element. Although quality of construction is hard to quantify in terms of determining fire resistance of an element, some efforts have been made to do this. Blackmore et al (1999) found

in a series of full-scale room tests and standard furnace tests that bad workmanship can significantly reduce the fire resistant performance of plasterboard and masonry wall systems. Based on insulation failure criteria, 'badly' constructed plasterboard systems were found to fail 5 minutes earlier, on average, than 'standard' construction walls. Masonry walls were found to collapse (integrity failure) prior to reaching insulation failure when 'bad' construction was evident. This was in contrast to 'standard' constructed masonry walls, which was found to fail on insulation criteria primarily.

2.3.7 Barrier Construction Quality in Fire Tests

Since the manufacturer of the system to be fire tested requires the longest FRR possible to be achieved, for marketing reasons, the quality of construction of fire test specimens is usually superior to that found on any building site. During preparation for fire resistance tests at BRANZ, it was observed by the author that construction of a test system is supervised by the system manufacturer, and more time and effort is spent ensuring the system is installed to the highest workmanship standards and quality, as this will maximise the system integrity and result in optimum FRR test results. Such time allocated to the construction of a single building element in a 'real' building construction is rare, if existent, and the quality of construction in the building industry reflects this shortfall in time expenditure. Therefore it is unlikely that a system installed in the construction industry will achieve the same level of fire resistance if exposed to the standard fire test exposure.

2.3.8 Standard Fire Time-Temperature Curve

New Zealand fire resistance tests are based on the requirements of standard AS 1530 Part 4 (SAA 1990), or BS 476 (BSI 1987). The standard time-temperature relationship for the fire used in such tests has been standardised internationally by ISO 834 (ISO 1975).

ISO 834 defines the time-temperature relationship of that fire, where:

$$T = 345 \log_{10} (8t_{\min} + 1) + T_0 \qquad \textbf{Equation 2-1}$$

The resulting time-temperature relationship can be seen in Figure 2.3.

2.3.9 History of the Standard Fire

There is much debate on the appropriateness of the standard fire as to whether it is representative of fire conditions in the modern building environment. Many fire resistance tests have been undertaken, at great expense, and a vast database of FRR's has been collated over the years, which allow good comparison between construction elements. To discuss whether the standard fire time-temperature relationship is appropriate, it is necessary to understand how this time-temperature relationship evolved.

Duncan's (2001) report overviews the full history of the standard time-temperature fire curve. As outlined by Babrauskas et al (1978b), the origins of the standard time-temperature fire curve date back as far as 1903, with the first standard for this curve being introduced in 1917 by the American Society for Testing and Materials (ASTM). This curve was originally based on wood fuel burning furnaces. It was modified slightly to give a faster temperature rise in the first ten minutes. This was done to apparently represent gas fired furnace temperatures. However, the approach was not based on knowledge of the intensities of building fires. The modified standard became ASTM E119 in 1918 (now ASTM E119, 1995). This fire testing time-temperature regime has not been significantly modified since 1918. Other countries adopted their standard fire test exposure in a similar fashion. Figure 2.3 compares the ASTM E119 heating regime with the standard curves as designated by ISO 834 (ISO1975) and BS 476 (BSI 1987). These time-temperature relationships can generally be considered the same when comparing fire resistance test methods.

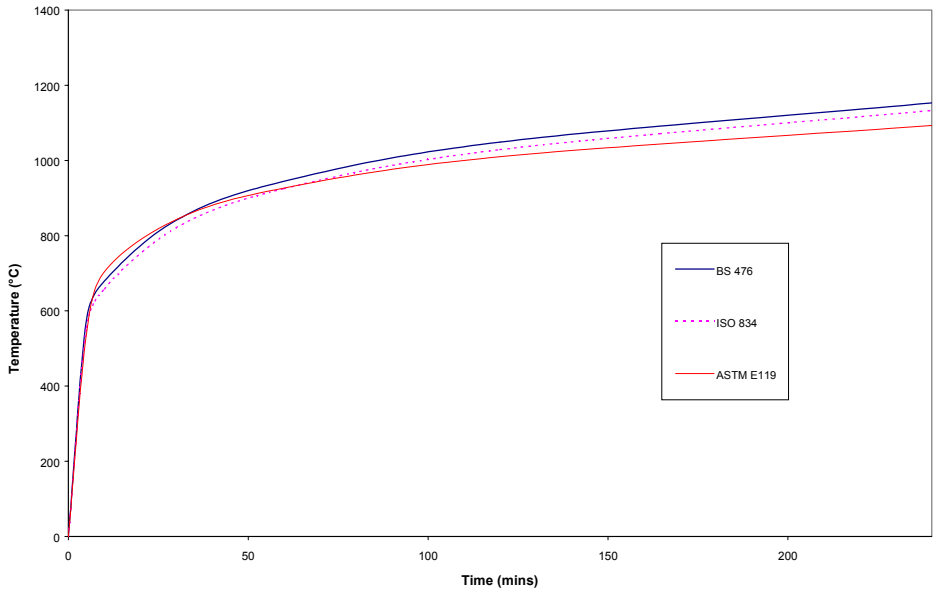

Figure 2.3 – Comparison of standard time-temperature curves

All further reference to the standard time-temperature fire curve shall be to the ISO 834 standard fire.

2.4 Fire Severity

2.4.1 Stages of Fire Development

In order to better appreciate the concept of fire severity, it is necessary to understand the stages of development of a fire. The distinct stages of a fire are:

- Incipient phase and ignition
- Growth phase and flashover
- Fully developed burning phase
- Decay phase.

Figure 2.4 shows these stages of development of a fire, graphically, as a temperature-time relationship.

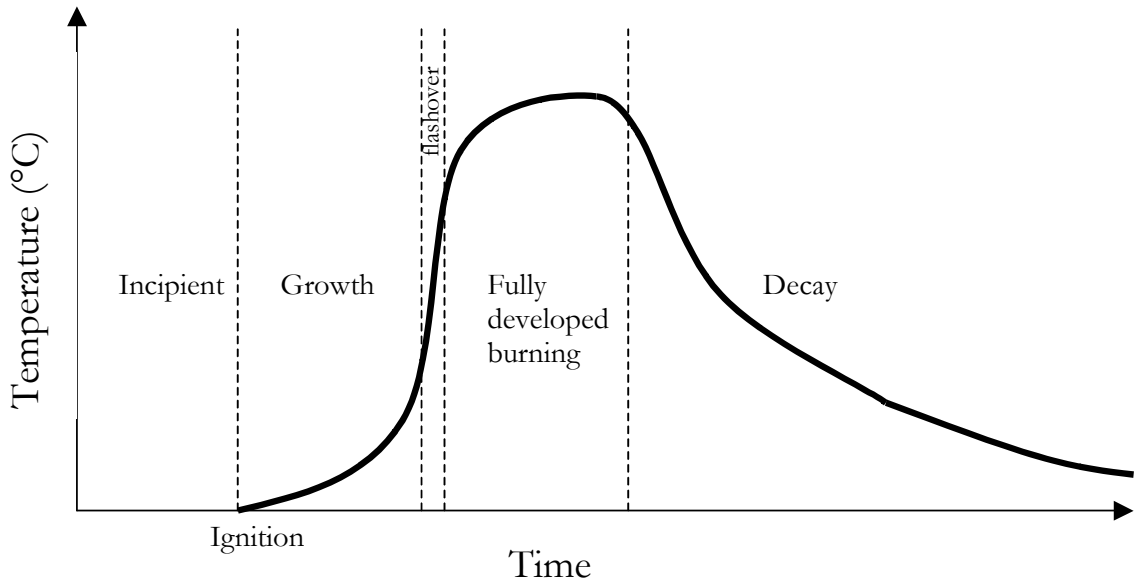

Figure 2.4 – Stages of development of a fire

Fire ignition is always preceded by an incipient phase, which is when heating and gasification of a combustible is occurring. The incipient phase can be from milliseconds to days depending on the fuel, ambient conditions and many other variable factors required for ignition of a fuel. An

incipient phase fire can often be detected prior to ignition, due to occupants smelling smoke, or by the activation of a smoke detector. Buchanan (2001b) suggests that a fire is in its incipient phase when the dominant form of heat transfer is not radiation, which as a rule of thumb is a fire of about 20kW or less.

Ignition of a combustible is the process which produces a chemical reaction characterised by an increase in temperature much above ambient. Ignition can be piloted ignition by a spark, match, or other source. Additionally, ignition may be a spontaneous event resulting from the accumulation of heat in a fuel.

Fire growth after ignition may be at a slow or fast rate, depending on several factors:

- Fuel type
- Combustion type
- Fire interaction with surroundings
- Availability of oxygen

Smouldering type combustion may occur after ignition. This is a particularly slow fire development, in which energy release rates and temperatures are relatively low. This type of combustion is synonymous with the production of high quantities of toxic gases and products of incomplete combustion, which present an extreme hazard to life.

Flaming combustion is a much more rapid form of fire growth which can occur in the presence of sufficient levels of oxygen (fuel controlled), where flame spread is possible over the surface of a combustible fuel, and additionally where the radiant heat flux from the flame is sufficiently large enough to ignite adjacent fuel sources.

A compartment flaming fire may be sustained, such that it has sufficiently large growth for the phenomena of flashover to occur. Flashover is the transitional stage between growth and fully developed stages, when all combustibles in the compartment ignite. Flashover lasts an extremely short duration, often seconds. Flashover is generally caused by the increasing temperatures within the compartment due primarily to increasingly hot upper layer smoke temperatures and radiation, along with levels of re-radiation from objects and the compartment construction itself.

It occurs when the upper layer temperature reaches approximately 600°C and the heat flux to the floor is about 20kW/m².

Following flashover, the fire is described as fully developed. During this stage of the fire, when the room is fully involved, the energy released from the fire into the room is at it's highest, and it's burning ability is often limited by the availability of oxygen. This type of burning is called ventilation controlled burning, and is governed by the size and number of any openings a compartment may have. During ventilation controlled burning, it is normal to witness flames burning out through the openings, as any unburnt gases, which leave through the opening will be able to burn due to the new supply of outside oxygen. Temperatures within a compartment during this stage can reach upto 1200°C, and may possibly exceed these temperatures under considerably long fire exposures. Fully developed burning will continue as long as there are sufficient quantities of fuel and ventilation.

The decay phase is considered to commence when ventilation controlled burning within a compartment becomes fuel controlled, where the burning rate is governed by the quantity of available fuel remaining within an environment having a sufficiently large air supply. Decay will continue until the fuel is consumed and/or the fire goes out. With burning thermoplastics and liquid hydrocarbon fuels, the decay phase can be extremely short. However, with cellulosic materials, such as wood, which chars, the decay stage is much longer and is of primary interest when examining the fire resistance of structural elements of a building. England et al (2000) suggest that for smaller enclosures, decay is the period of the fire from when the temperature within the enclosure has decreased to below 80% of its peak. Buchanan (2001b) also uses a value of 80% for the transition to decay stage, however, the value is for when 80% of the fuel has been consumed.

2.4.2 Fire Severity - Definition

The fundamental requirement when designing for fire safety is to ensure that the fire resistance of an element is greater than the severity of the fire to which that building element is exposed.

Buchanan (2001a) defines fire severity as "the measure of the destructive impact of a fire, or the measure of the forces or temperatures as a result of a fire, which would cause failure or collapse". It is a measure of thermal actions, products of combustion and differential pressures

to which an element is exposed, as a result of a fire. England et al (2000) explain that it is most commonly represented in terms of:

- time-temperature relationship in an enclosure
- heat release rate (HRR)-time relationship for a fire
- heat flux-time relationship within the enclosure of fire origin
- equivalent time of exposure to the standard heating regime

The severity of a fire is dependant on fuel type and geometry, fire compartment construction and geometry, and the size and location of ventilation openings.

In the 1920's, Ingberg developed the concept that fire severity was related to the fuel load (Babrauskas 1976). This relationship was for wooden fuels only. Such a concept, although groundbreaking at the time in terms of fire engineering, does not hold true for all combustibles, particularly those, such as synthetic fuel types, which have a high heat release rate (Cooper et al 1996).

With regards to geometry, the physical size of the compartment will influence the severity of a fire to construction elements of that compartment. Girgis (2000) found in his research that the larger the space in which furniture burnt, the less hazardous the effects compared to if the same furniture burnt in a smaller space. Additionally, the geometry of a compartment may result in certain elements having different fire exposures from a fire.

The most intense burning occurs when stoichiometric combustion conditions exist, and when there is just enough oxygen to react with the fuel. The larger the ventilation opening(s), the hotter and faster becomes the burning of fire. Such fires tend to have shorter durations compared with fires in compartments with fewer or smaller openings, which experience cooler, slower fires of long burning duration. Such time effects are significant with regards to fire resistance. A hot, short fire may not burn for sufficient time for heat to penetrate a structure, despite high gas temperatures. However a long, cool fire may have time for heat to penetrate, despite lower temperatures, and may therefore be more severe. As mentioned earlier in this section of the report, fire severity can be plotted as time-temperature relationship or HRR-time relationship. Figure 2.5 shows fires of differing severities. One curve is representation of the

ISO 834 standard fire test heating regime, whilst the other two represent a short hot fire and long cool fire respectively.

The size and geometry of ventilation openings of a compartment become important when examining fire severity when the fire is ventilation controlled and these parameters have an influence on the burning rate. Buchanan (2001a) overviews the various burning rate empirical relationships of openings and air flow and shows that the rate of burning, in many empirical equations, tends to be a function of the ventilation parameter $A_v \sqrt{H_v}$ (Units - $m^{3/2}$).

The amount of ventilation available in a fire compartment is described by fire engineers in terms of the opening factor, F_v, where:

$$F_v = \frac{A_v \sqrt{H_v}}{A_t} \qquad \textbf{Equation 2-2}$$

Additionally, the ventilation factor, w_f, defines the ventilation parameters of a compartment, and is often used by engineers when examining the concept of equivalent fire severity and time equivalence. These ventilation factors are detailed in section 2.5.7 and 2.5.8 of this report.

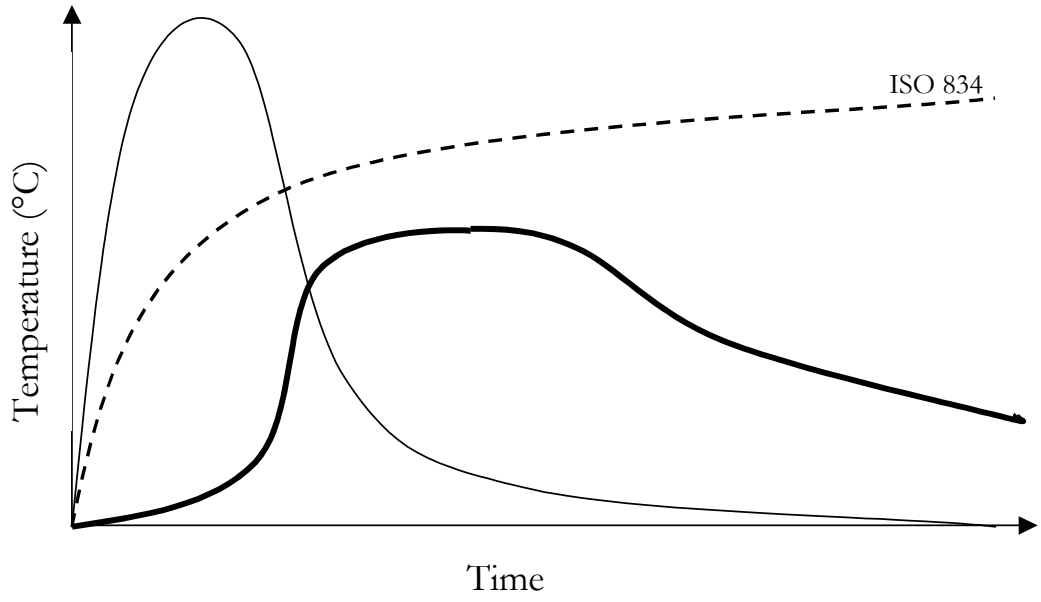

Figure 2.5 – Time-temperature representation of different fire severities

2.4.3 Realistic Fires

2.4.3.1 Introduction

The stages of development of a real fire and the factors determining a fires' severity have been discussed in previous sections. This section will highlight the factors that are responsible for making the severity of a real fire significantly worse, than the equivalent early stages of the standard ISO 834 time-temperature relationship. A brief overview will be provided of previous research, which undertook a number of full-scale compartment burns, and provided information on time-temperature histories of real fires. The overview will highlight the significant observations of relevance to this research project.

2.4.3.2 Thermoplastic Materials and Modern Furnishings

As was described in previous sections, the standard heating regime originates from the application of wood burning furnaces. The reality of modern typical commercial and residential properties is that they incorporate both wooden items such as tables, chairs, desks and bookshelves and additionally items such as upholstered furniture, mattresses, and many other items, which make use of thermoplastic materials, including synthetic foams and fabrics. In fact, increasing levels of use of thermoplastic materials is evident in many occupancies. Caro et al (1995) conducted a survey of office occupancies and fuel loads. Although limited in the number of buildings surveyed, the findings showed that since the previous similar survey undertaken in 1975 (Culver 1976), fuel loads (in energy terms) in such buildings have increased. This was particularly due to the widespread application of desktop computers and use of fabric coated partitioning used in modern office applications.

In New Zealand there is currently no regulatory control for the flammability of upholstered furniture, unlike the United Kingdom and parts of the United States of America. Previous research projects undertaken at Canterbury University, specifically looking at the flammability of NZ upholstered furniture and combinations of foams and fabrics (Firestone 1999, Denize 2000, Coles 2001), have attempted to apply the CBUF Model I (Sundström 1995), developed for European furniture, to assess NZ upholstered furniture contributions to a fire's severity. It was found that New Zealand upholstered furniture has been shown to present a more significant fire hazard than its European equivalent, by reaching higher peak heat release rates in shorter time duration (Enright 2000), resulting in a faster growth of room temperatures. Therefore, a real fire

situation in New Zealand, in which upholstered furniture is present as a fuel source, will be more severe during these early growth phases of a fire than an equivalent upholstered furniture fire overseas.

The burning behaviour of thermoplastics is detailed in an analytical description provided by Babrauskas et al (1979a). They explain how during a fire, thermoplastic materials melt and flow to the floor, where they burn as pool fires. Such pool fires burn significantly faster, with higher heat release rates, compared to burning where such pooling is not evident. The burning rate of thermoplastic materials depend highly on surrounding gas and wall temperatures, and the mass loss rate of the fuel, which is in turn a function of the net heat flux onto the material and material heat of gasification (Yii 2000).

Since use of thermoplastics in furniture can result in fires being significantly more severe in early stages than the ISO 834 standard fire, it is evident that the ISO 834 standard fire curve used in fire resistance tests would not appear to accurately represent the early fire time-temperature history of a real fire involving thermoplastics.

2.4.3.3 Realistic Time-Temperature Fire Histories

Jones (2001) reported a number of full-scale compartment burns in his research. Three burns were carried out in compartments constructed of LTF and gypsum plasterboard internal walls and ceiling, following standard New Zealand building practices. Each compartment was 2.4 m wide by 2.4 m deep by 2.4 m high, with a 2.0 m high by 0.8 m wide ventilation opening and 0.4 m by 0.26 m glazed viewing window. The three burns represented rooms with different occupant uses, consisting of a lounge, bedroom and office respectively. Each compartment was furnished with items relevant to that occupancy, including upholstered furniture. Thermocouple trees and spot thermocouples were located throughout the compartments. Each test was ignited in a manner that was representative of how a fire may start in that occupancy, and each fire was extinguished shortly after flashover. As a result of the extinguishment, the full duration of the fire and potential peak temperatures cannot be reported on. The lounge test results showed an incipient phase of 120 seconds, followed by a growth stage with flashover at 300 seconds. The bedroom test results showed an incipient phase of 50 seconds, followed by a growth stage with flashover at 240 seconds. The office test results showed an incipient phase of 10 seconds, followed by a growth stage with flashover at only 90 seconds. In all cases, temperatures reached

up to 1000°C prior to the fire being extinguished. It is extremely likely that had the fire been allowed to burn for significantly longer after flashover, the compartment temperatures would have been noticeably higher than those recorded.

Blackmore et al (1999) undertook five full-scale compartment fire tests, each furnished with combustible items and floor linings, averaging a total theoretical fuel load energy density (FLED) of 808MJ/m². The test compartments were of dimensions 3.6m (L), 3m (W) and 3m (H). An opening of 2m (H) by 0.8m (W) was located centrally in one of the short walls, and a window of 2m (L) by 1.8m (H) was located in one of the long walls such that the top of the window was level with the false ceiling. The false ceiling was located at a height of 2.4m above floor level. The test walls of the compartment had a nominal 1 hour rating. The walls were of masonry construction or of light framed plasterboard construction, and were located at the opposite wall to the door opening. Room test results of temperatures within the compartment and temperatures through the tested wall constructions were compared with equivalent standard furnace test results. Quality of construction was also considered when comparing results. It was found that in the early stages of the real fire the severity was greater than that of the standard furnace test, with temperatures in lightweight construction compartments reaching 1100°C, and in masonry constructed compartments reaching almost 1000°C. These temperatures were reached well within 5 minutes of ignition. As the real fire progressed and went into decay, the standard furnace test becomes more severe. With regards to construction, the findings are previously discussed in Section 2.3.6. For the light framed plasterboard construction, failures by insulation for the 'standard' constructed assemblies were generally around 78 minutes. Poorly constructed assemblies failed on the insulation criteria several minutes earlier.

2.4.4 Equivalent Fire Severity

Fire engineers and researchers have always endeavoured to quantify the exposure, or severity of a real enclosure fire. One approach to this has been to quantify the severity of one fire in terms of another fire. This is defined as the determining the equivalent fire severity of a fire. Several approaches have been used to determine the equivalent severity of a fire. Of particular significance are the 'equal area' and 'time equivalent' concepts of equivalent fire severity.

2.4.5 Equal Area Concept of Fire Severity

The equal area concept of fire severity was developed by Ingberg in the 1920's. He defined the integral (area) under the time-temperature curve as the fire severity. The area of consideration was above a baseline temperature of 150°C. The baseline was considered to be 300°C when dealing with heavy non-combustible structural members. This theory and it's suitability for modern fire engineering application is detailed by Babrauskas (1976 & 1978b). Further to comparison of the standard test fire severity and realistic fires, where areas under the time-temperature curves were examined, major shortfalls of using the equal area concept were found, particularly in applications where lightweight constructions and modern furnishings involving significant quantities of synthetic fuels are used. The equal area concept cannot be proved theoretically. This is because the heat energy directly input into a compartment's walls, floor and ceiling, is not directly proportional to the temperature. At high temperatures, radiation is the predominant mode heat energy transfer into the construction. Radiation is proportional to the temperature difference raised to the fourth power. Therefore, such a method of comparing severity would underestimate the severity of short hot fires and overestimate long cooler fires severity. It was suggested that the method be dropped from useage.

Cooper et al (1996) go on to explain that although the equal area concept of fire severity is technically obsolete, it may be useful in the following occasions:

- when high heat release rates are not involved, due to thermal shock effects on integrity
- when the time-temperature relationship is not significantly higher or lower than the standard fire test heating regime.

2.4.6 Time Equivalence

The most common approach to quantifying fire severity is to equate the performance of an element exposed to a real fire in terms of an equivalent exposure to the standard heating regime applied in the standard fire test. This approach to quantifying fire severity is known as determining the 'time equivalence' of a fire. Thomas, G (1997) defines time equivalence as "the time at which the equivalent worse value of a specific failure criteria at a characteristic location in the element is reached when exposed to the ISO 834 standard fire". For temperature, this is the equivalent time of exposure to the standard fire an element would need to be exposed to, to reach a maximum temperature achieved during exposure to a real fire. For structural fire

resistance, this is the equivalent time of exposure to the standard fire to reach a maximum loading achieved during exposure to a real fire.

Numerous structural time equivalent formulae have been developed for application in fire engineering design of buildings. The accepted approaches use formulae, which are based on the maximum temperature of protected steel members exposed to real fires. The two main time equivalent formulae for structural fire resistance, commonly used for fire engineering design shall be detailed in this report. They are the CIB formula and Eurocode formula, respectively. For details of alternative time equivalent formulae, refer to reviews carried out by Harmathy (1987) and Law (1997)

2.4.7 CIB Formula

The CIB formula (CIB 1986) is the more commonly used time equivalent formula. The time equivalent, t_e, to an ISO 834 test is given by the equation:

$$t_e = k_c \, w_f \, e_f \qquad \text{(mins)} \qquad \textbf{Equation 2-3}$$

where the ventilation factor, w_f is defined by:

$$w_f = \frac{A_f}{\left(A_v \, A_t \, H_v^{\,0.5}\right)^{0.5}} \qquad \textbf{Equation 2-4}$$

The ventilation factor defines the ventilation parameters of a compartment, when examining the concept of time equivalent. The CIB formula is only valid for compartments with vertical openings in walls. It is not valid for compartments with roof openings.

2.4.8 Eurocode Formula

The Eurocode formula (EC1 1996) is similar to the CIB formula, however, the compartment lining parameter, k_b is replaced with k_c. Additionally, the ventilation factor is altered to allow for horizontal openings in the roof of the compartment.

The Eurocode time equivalent formula is derived from:

$$t_e = k_b \, w_f \, e_f \qquad \text{(mins)} \qquad \textbf{Equation 2-5}$$

where, ventilation factor, w_f is defined by:

$$w_f = \left(\frac{6.0}{H_r}\right)^{0.3} \left[0.62 + \frac{90(0.4-\alpha_v)^4}{1+b_v \alpha_h}\right] > 0.5 \qquad \textbf{Equation 2-6}$$

and, $\alpha_v = A_v / A_f \qquad 0.05 \le \alpha_v \le 0.25$ **Equation 2-7**

$$\alpha_h = A_h / A_f \qquad \alpha_h \le 0.20 \qquad \textbf{Equation 2-8}$$

$$b_v = 12.5\left(1 + 10\alpha_v - \alpha_v^{\,2}\right) \qquad \textbf{Equation 2-9}$$

Buchanan (2001a) explains in detail the applications of the formulae and the differences between them. Additionally appropriate values for the compartment lining factors, k_c and k_b, are given. These are shown in Table 2.2, where the high, medium and low 'b' values represent steel construction, normal and lightweight concrete, and constructions using gypsum plaster and better insulating materials respectively. Where:

$$b = \sqrt{Thermal\ inertia} = \sqrt{k \rho C_p} \qquad \textbf{Equation 2-10}$$

Formula	Term	b			General
		High (> 2500)	Medium (720-2500)	Low (< 720)	
CIB	k_c	0.05	0.07	0.09	0.10
Eurocode	k_b	0.04	0.055	0.07	0.07

Table 2.2 – Time equivalent formulae k_c & k_b values

Kirby et al (1994) recommend some modifications to the Eurocode values shown in Table 2.2, for large spaces. For such large spaces, the values for k_b are 0.05, 0.07, and 0.09 for high, medium, and low values of 'b' respectively. The general value of b to be used is 0.09 (Buchanan 2001a).

The Approved Documents (BIA 2001) apply the Eurocode time equivalence, to cater for real fire severity, when evaluating structural 'S-ratings', which determine level of structural protection for complete burn out of a fire. These ratings are used to provide protection of neighbouring property.

The above time equivalent formulae are generally accepted as being for use for protected steel members and reinforced concrete members only. They are not intended for use on unprotected steel members, or timber construction. Thomas, G (1997), in his research described in section 2.5.4 of this report, suggests that for many cases, the time equivalent formulae used to predict the response of structures to fire in terms of exposure to the standard fire test are inadequate, usually on the unsafe side.

2.4.9 Safe Egress Time

There are currently no existing time equivalent formulae for use with non-loadbearing barriers, such as walls and fire doors etc. As a consequence, there is no time equivalence applied to the life safety 'F-ratings' in the Approved Documents, and real fire severity is not accounted for in evaluating the required FRR of elements. For fire resistance, establishing a time equivalence, or similar approach, for such barriers would be a major aid to fire engineers in achieving a required level of 'real' fire resistance.

Thomas, G et al (2002) have recently developed what is termed a 'factor of safety' , which can be applied to establish a time equivalent approach to fire resistance ratings of lightweight constructions to real fires. The design approach is, by the Thomas' own admission, not a highly accurate method, and in certain instances may be non-conservative, although not significantly. However, Thomas sees it as an alternative approach to current, simplistic design approaches made by building owners, architects and even engineers who apply the Approved Documents (BIA 2001) fire resistance ratings (FRR) literally, on the assumption that this will meet the safe egress time requirements for life safety in a real fire. In most cases applying the FRR will be

highly non-conservative and in a real fire the assembly will have failed well before the occupant required safe egress time (RSET) has been met. The RSET includes detector response time, occupant response time, evacuation travel time, and time for fire service rescue operations. Thomas et als' method, based on use of existing FRRs, calculates what is termed the ASET, which is essentially an estimation of the 'time to failure' (t_{fail}) of an assembly in a real fire.

Since ASET is the terminology for a widely used and accepted model for predicting the smoke filling process in a room and evaluating the available egress time before occupancy tenability limits are reached (Cooper 1995), and to avoid further confusion, this report will refer to Thomas et als' ASET term as the t_{fail} of an element.

The basic design approach to calculating the t_{fail} of an assembly, as given by Thomas et al, is as follows:

1. Total fuel load, E (MJ) is determined by:

$$E = A_f e_f \qquad \textbf{Equation 2-11}$$

2. Assumes all windows are broken post flashover. Establish window/vent opening area, A_v, and window/vent height, H_v.
3. The ventilation controlled heat release rate, Q_v (MW), is calculated using:

$$Q_v = 1.5 A_v \sqrt{H_v} \qquad (Buchanan\,2001b) \qquad \textbf{Equation 2-12}$$

4. Calculate burn time, t_b (secs), from:

$$t_b = \frac{E}{Q_v} \qquad \textbf{Equation 2-13}$$

   This assumes no unburnt fuel remaining in the compartment.
5. Calculate ventilation factor, w_f, from Equation 2-6.
6. Calculate time equivalent, t_e (mins), from Equation 2-5.
7. Ascertain FRR of element. If FRR significantly more than t_e, element will not fail.
8. Calculate the t_{fail} (mins) of the element using:

$$t_{fail} = FRR \times {t_b}/{t_e} \qquad \textbf{Equation 2-14}$$

The compartment tests undertaken for this research project will be used for verification of the Thomas, G et al (2002) method (Section 5).

2.4.10 Standard Fire Vs Realistic Fire

It can be seen from the information detailed earlier in this section of the report, regarding the ISO 834 standard fire test heating regime, and the severity of real fires, that the standard test is not representative of realistic fires.

The standard test is conservative for long duration fires, as the ISO 834 time-temperature relationship has no decay phase, whereas in a real fire compartment temperature will reduce with the duration of the decay phase.

For shorter duration fires, particularly where upholstered furniture and thermoplastics may be involved in a real fire, the standard curve may be non-conservative. Such a realistic fire can be more severe than the standard fire in the early stages of fire development, when evacuation and rescue activities are required to be undertaken. It is important to note that the compartment temperatures of real fires, involving upholstered furniture, can reach up to 1300°C relatively soon after of ignition, although temperatures of 1000-1100°C are more common (Thomas 2002). The standard ISO 834 fire is still only at 834°C after 30 minutes of the heating regime. This is of particular significance as many of the life safety 'F-ratings' are F30 (Table 2.1).

The reliance in New Zealand on active fire protection and the focus on life safety (not property protection) means that the required levels for passive fire protection are low compared with overseas requirements, particularly Europe and Australia, as described earlier in section 2.3.3. Considering the limitations of the standard furnace testing, it is suggested that New Zealand F rating requirements may not conservative enough.

2.5 Establishing 'Realistic' Fire Resistance Ratings for Lightweight Construction Assemblies

2.5.1 Introduction

This section of the report will briefly discuss previous attempts made to establish fire resistance ratings for building elements when exposed to more severe fires than the standard ISO 834 fire, particularly detailing use of fire testing with modified heating regimes and computational modelling.

2.5.2 Severe Fire Pilot Furnace Testing

Jones (2001) undertook a pilot scale furnace test of a nominally 60 minute rated steel stud gypsum lined wall assembly. Applying a time-temperature curve more severe than the standard curve resulted in the wall failing on the integrity criteria at 28 minutes. Figure 2.6 shows the severity of the fire used in the test, compared with the standard ISO 834 fire curve.

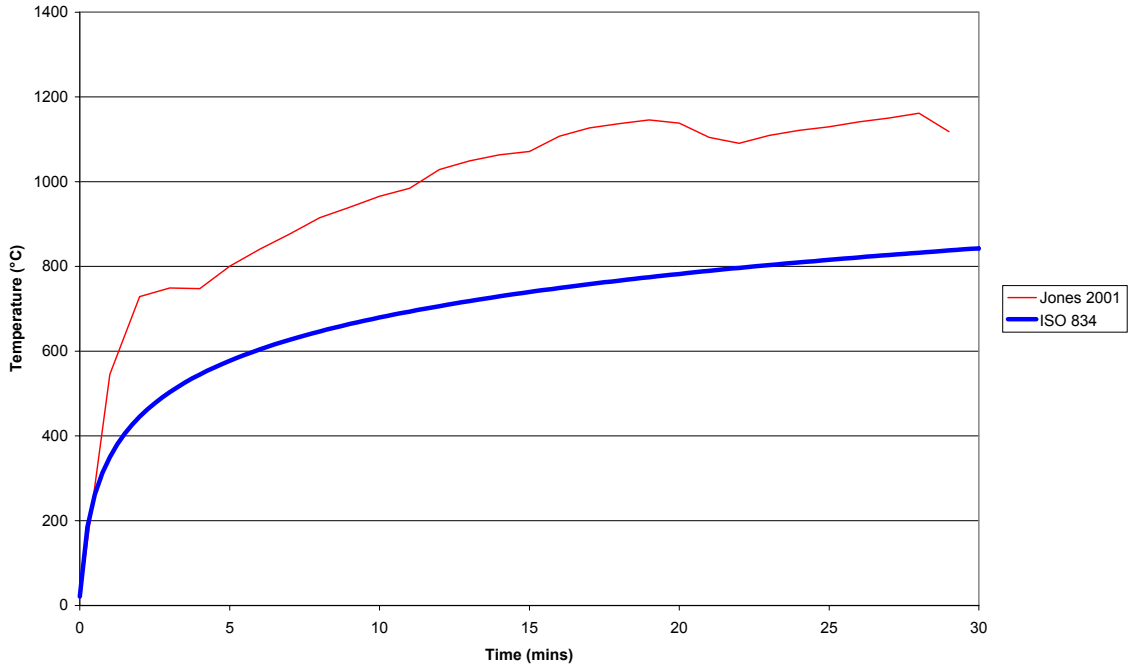

Figure 2.6 – 'Real fire' pilot furnace fire resistance test temperatures

The test showed the limitations of using the existing furnaces to reproduce realistically severe fires. The temperatures obtained in the early stages of the curve were the maximum the furnace could achieve.

2.5.3 Hydrocarbon Fire Test Heating Regime

The hydrocarbon heating regime, as defined by the Eurocode (EC1 1996), was developed for furnace testing on construction elements for the petrochemical industry to more accurately reflect the early stages of some fire scenarios, and the flashover phenomenon. It is the only alternative curve widely used for fire testing of construction elements. The historical development of this alternative time-temperature curve is fully detailed by Cooper et al (1996).

The time-temperature relationship is defined by the equation:

$$T = 1080\left(1 - 0.325e^{-0.167t_{\min}} - 0.675e^{-2.5t_{\min}}\right) + 20 \qquad \textbf{Equation 2-15}$$

Figure 2.7 shows this time-temperature relationship compared with the less severe standard fire curve. England et al (2000) suggest that the hydrocarbon curve may be incorporated into future versions of the Australian Standard AS 1530.4 (SAA 1990) to simulate fires involving significant quantities of thermoplastics and where enclosure boundaries may have a low thermal inertia.

Use of such a curve, to simulate rapid fire growth, could also be made for fire resistance testing in New Zealand. However, due to the limitations of the existing furnaces heat output, major upgrading of test furnaces would be required to reproduce the rapid temperature rises in the early stages of the hydrocarbon heating regime.

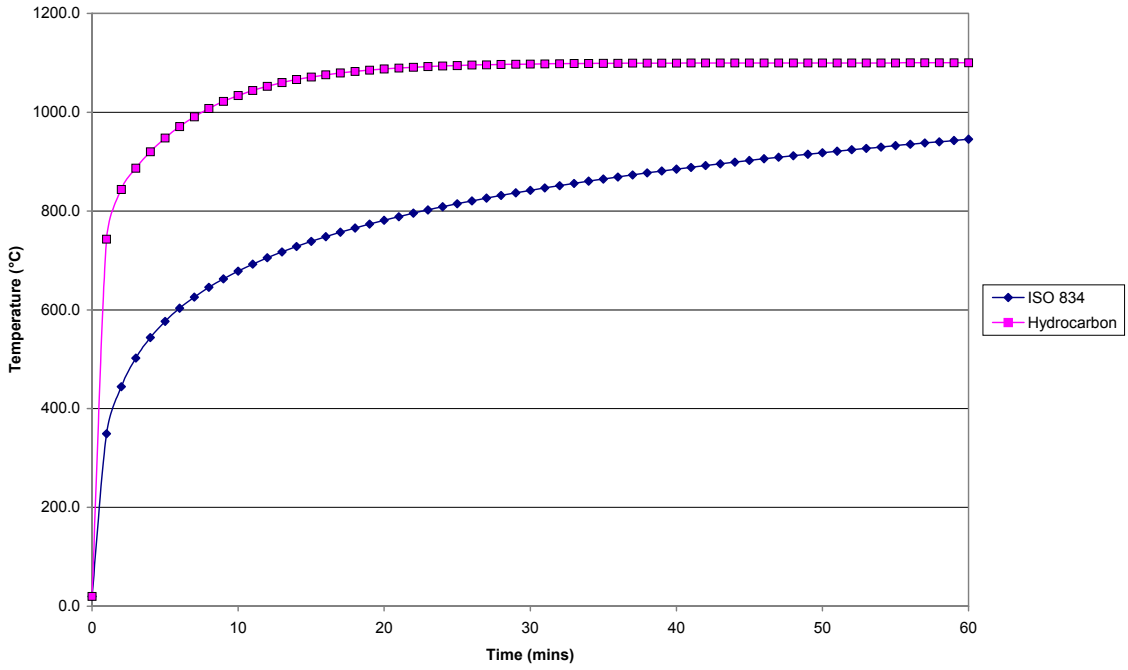

Figure 2.7 – Hydrocarbon heating regime

2.5.4 Computational Modelling

A number of software packages have been used in attempts to assess and predict the performance of building elements when exposed to realistic fires. The following brief review is in the form of a literature survey of such previous research.

Temperature Analysis of Structures Exposed to Fire (TASEF) is a heat transfer modelling software package. Gerlich (1995) applied a thermal model using TASEF to predict a steel framed plasterboard wall construction's time-temperature history. The results of this model showed that TASEF could be used with a certain level of accuracy when the system was modelled to the standard fire. However, when a realistic fire profile was applied to the model, he found that the temperatures provided by the model were too low and non-conservative. This was predominantly due to the fact that TASEF was unable to account for mass loss during fire conditions, and in particular was not able to model the ablation of gypsum plasterboard (erosion due to heating). Ablation occurs at high temperatures, usually 500°C-700°C for standard gypsum board and 700-900°C for fire-rated glass fibre reinforced plasterboard (Collier 2000).

Thomas, G (1997) used existing computer models to examine the applicability of using time equivalent concepts, as outlined in the Eurocode (EC1 1996), for realistic fires acting on various types of wall and floor constructions. He examined thermal and structural time equivalence using TASEF, COMPF-2 (Babrauskas 1979) and ABAQUS. He found that as a thermal analysis program, ABAQUS, a finite element model, compared similarly with TASEF. Similarly to Gerlich, he also confirmed that failures, due to loss of integrity, could not be predicted by TASEF thermal models. Thermal models, in general, cannot predict integrity failures. ABAQUS, a finite element structural modelling package, was also used to examine structural time equivalent prediction of failure for light timber framed and steel concrete structures with some success.

Cooper (1997) developed a simulation model called GYPST, a subroutine of FORTRAN, which simulates the thermal response of steel stud framed gypsum wall systems. The simulation achieved favourable comparison to the experimental validation test results. The GYPST models use is limited to steel stud plasterboard wall constructions exposed to standard fire conditions only.

Cooper et al (2000) further developed the use of GYPST by incorporating the subroutine into the existing zone model simulation program CFAST (Jones et al 1990). The resulting prototype fire model, called CFAST.GYPST, evaluates thermal performance of light steel framed plasterboard wall systems. With the additional subroutine added, CFAST.GYPST can simulate fire in a room with such barriers and evaluate the performance of these barriers. Simulation and experimental validation of the new fire model included standard furnace testing results to establish whether CFAST.GYPST results corresponded appropriately with the standalone GYPST model. A second set of simulations and compartment experiments used for validation were for more severe fires, with initial rapid rising upper layer temperatures (above that of the standard fire) within the first few minutes of ignition, followed by a drop below the standard fire temperatures as decay of the fire occurs. CFAST.GYPST simulated thermal wall responses were found to compare favourably with furnace tested thermal wall responses. The simulations modelling realistic fire exposures determined that thermal failure to the assembly would not have occurred. The simulation was shown to provide estimates of the fire resistance of light steel framed plasterboard systems, but only with respect to the potential for thermal failure. Further development work on the CFAST.GYPST model is ongoing, with a view to developing a special purpose fire/thermal/structural computer model (CFAST.GYPST/SAFIR) which would be capable of predicting thermal and structural fire resistance performance of LSF plasterboard systems.

A user-friendly software package has been developed by Collier (2000), which on completion, is expected to be able to model and evaluate the thermal performance of a wall system subjected to a 'real' time-temperature fire exposure. The model is based upon a finite difference heat transfer model of linings and cavities. Plasterboard ablation characteristics are incorporated. Charring of timber and reduction of steel strength for LTF and LSF constructions, respectively, are incorporated to determine structural failure of studs. The model currently gives generally reliable prediction of thermal performance and insulation failure of cavity walls for standard and non-standard fires. However, necessary refinements are ongoing and the model and software is being updated at the time of writing this report. It is assumed that data gathered from this report's compartment tests will assist in further validation procedures of the software.

SAFIR computer modelling was undertaken by Jones (2001) to evaluate whether the program was suitable for prediction of thermal behaviour and fire resistance performance of steel stud framed plasterboard wall systems. The modelling was tested against the results of a number of

pilot scale furnace tests, in which the test walls were subjected to standard and non-standard time-temperature heating regimes. It was found from the model that SAFIR did not predict insulation failures of the non-standard fire tests well. The limitations of modelling with the SAFIR program were described as being the size of the time steps used, the run time of the model, the level of input and output obtained, all of which are pre-determined by the user. SAFIR was also unable to model moisture movement, ablation and shrinkage of plasterboard linings.

Computer modelling of assemblies exposed to realistic fire exposures have not yet been able to establish good predictions of assembly failures in realistic fires. Hence, a more quantitative approach of undertaking the compartment tests has been used for this research.

3 Compartment Fire Resistance Testing

3.1 Introduction

Three full-scale fire tests have been carried out to obtain substantial temperature data and establish times to failure of assemblies exposed to fires more severe than the standard fire test exposure. The compartments were constructed to enable simultaneous testing of various lightweight timber and steel framed walls and ceiling/floor systems, including a fire door. All systems have prescribed fire resistance ratings, previously determined by standard fire resistance tests undertaken at BRANZ, according to AS1530.4 (SAA 1990). Each construction had detailed standard furnace test temperature data available for comparison and analysis.

This section details the compartment constructions and the fuels selected for the test fires, as well as instrumentation used.

3.2 General Construction Description

All compartments were constructed such that all walls and ceiling assemblies formed an interacting structure, as would be found in a real building situation. The compartments geometry was based upon the ISO 9705 (ISO 1993) standard test room dimensions as shown in Figure 3.1. All test compartments had identical internal dimensions of 3600mm (L) x 2400mm (W) x 2400mm (H). Dimensions of the vent opening size for the compartment tests were kept uniform for two of the tests and increased in size for the final test. Vent opening dimensions for each test are shown in Table 3.1. The geometries and setting out of the test compartments constructions can be seen in Figures 3.1, 3.2 and 3.10. Assembly location references are as given in Table 3.2.

Test Reference	Vent Opening Dimensions (m)	
	Height	Width
#1	2.0	0.8
#2	2.0	0.8
#3	2.0	1.2

Table 3.1 – Compartment tests vent opening dimensions

3.3 Test #1 and Test #3 Constructions

All assemblies in Test #1 and #3 were of a nominal 30 minute FRR. Compartment geometry and construction set out for Test #1 and #3 is shown in Figures 3.1 and 3.2, respectively. As can be seen in the diagrams, the compartments are geometrically identical, with the exception of the vent opening widths in each test.

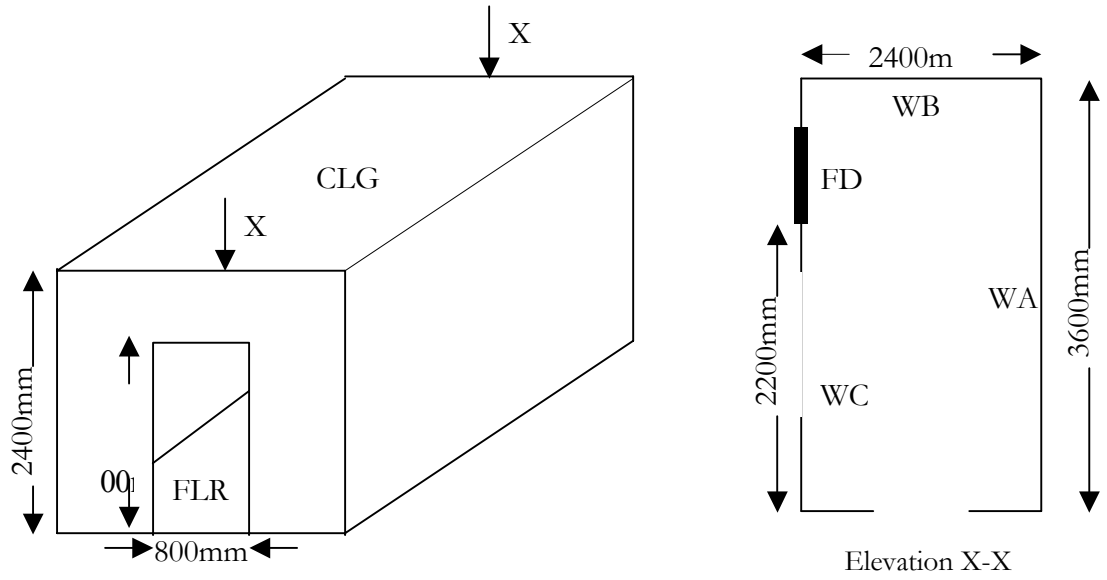

Figure 3.1 – Test #1 Compartment geometry and construction set out

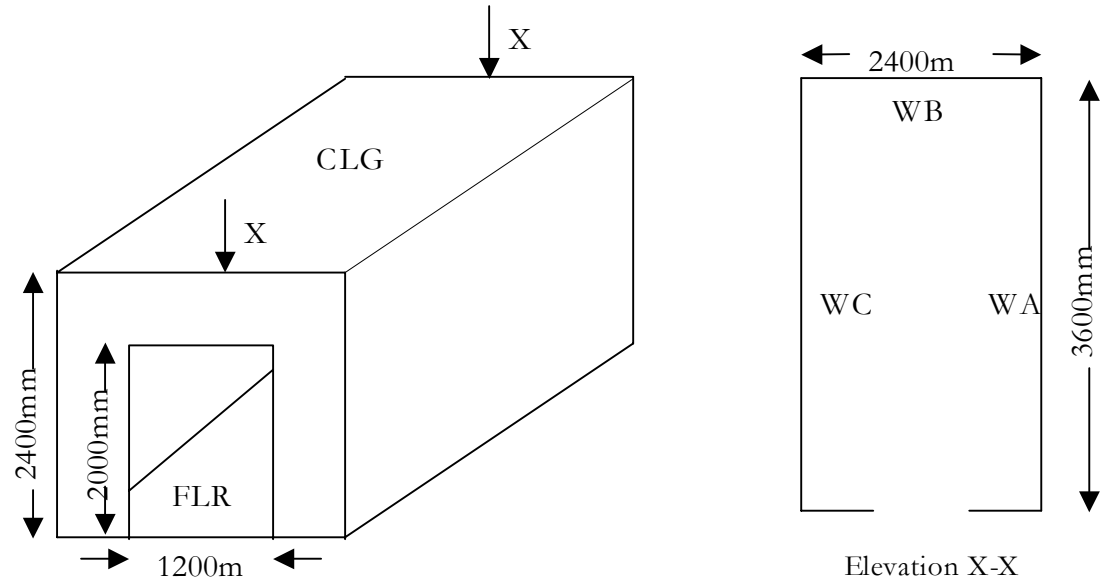

Figure 3.2 – Test #3 Compartment geometry and construction set out

Building Element Reference	Abbreviation
Wall A	WA
Wall B	WB
Wall C	WC
Ceiling	CLG
Floor	FLR

Table 3.2 –Assembly location references and abbreviations

3.3.1 Assembly 1 - 30 Minute Rated LTF Gypsum Plasterboard Lined Assembly

This assembly construction was located at Wall A (WA) in both compartment tests. The assembly was constructed identically to the construction specification used when tested to the standard furnace test, as detailed by the fire resistance test report FR1712 (BRANZ FR1712).

Figure 3.3 shows a representation of the cross section through the wall. Consisting of a load bearing timber framed wall, lined with a single layer of 10mm 'Fyreline' gypsum plasterboard to each side. Timber framing was constructed using nominal 90mm x 45mm kiln dried No. 1 framing grade Radiata pine for the studs, dwangs, and top and bottom plate. Studs were placed at 600mm centres. Dwangs were fixed between the studs at 1200mm centres vertically, starting at the bottom. Sheets were fixed to the timber frame with vertical joints at the sheet edges staggered 600mm between the exposed and unexposed linings. The sheets were fastened with 41mm (Size 6) gold passivated screws at 300mm centres around the perimeter of each sheet and along each stud. The internal faces were taped and stopped using a bedding compound and paper reinforcing tape.

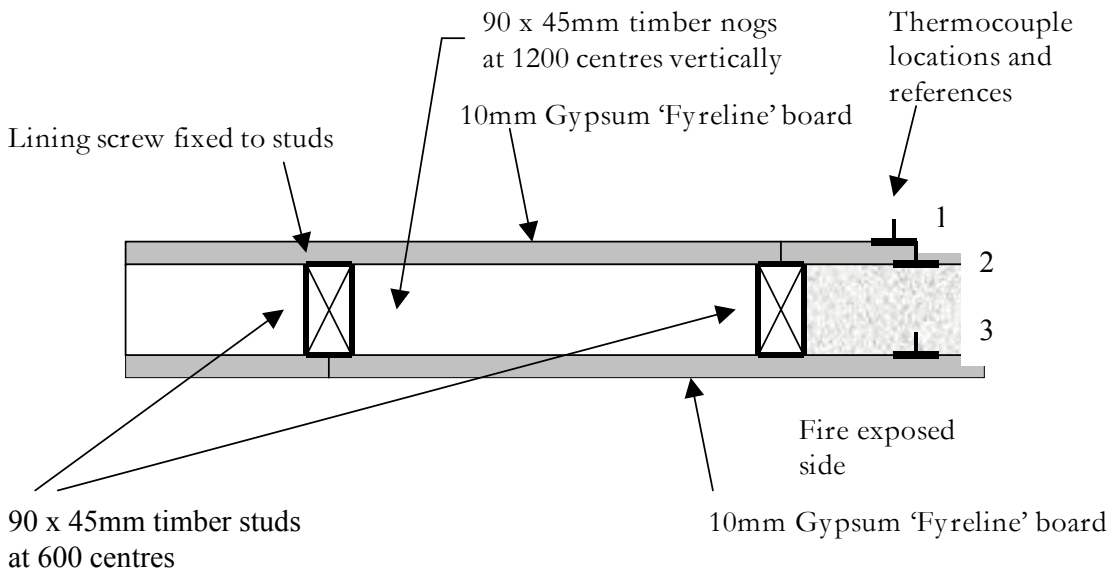

Figure 3.3 –Assembly 1 cross section

3.3.2 Assembly 2 - 30 Minute Rated LTF Fibre-Cementitious & Gypsum Plasterboard Lined Assembly

This assembly construction was located at Wall B (WB) in compartment test #1, and Wall C (WC) in test #3. This wall assembly was constructed identically to the construction specification used when tested to the standard furnace test, as detailed by the fire resistance test report FR2454 (BRANZ FR2454).

Figure 3.4 shows a representation of the cross section through the wall. Consisting of a load bearing timber framed wall, lined with a single layer of 13mm 'Fyreline' gypsum plasterboard on the unexposed face and a layer of 9mm compressed fibre-cement sheet on the exposed face. 'Flamestop' building paper was used behind the fibre cement sheet on the cavity side of the wall. The wall was insulated with R1.8 fibreglass batts of nominal 75mm thickness. The timber framing was constructed using nominal 90mm x 45mm kiln dried No. 1 framing grade Radiata pine for the studs, dwangs, and top and bottom plates. Studs were placed at 600mm centres. Dwangs were fixed between the studs at 800mm centres vertically, starting at the bottom. 'Fyreline' linings on the unexposed side were fixed to the timber frame with vertical joints at the sheet ends staggered 600mm between the unexposed and exposed linings. The 'Fyreline' sheets were fastened with 41mm (Size 6) gold passivated screws at 300mm centres around the perimeter of each sheet and along each stud at 300mm centres. The fibre-cement sheets on the exposed face were fixed to the timber with vertical joints at sheet ends staggered 600mm to the

unexposed lining. The sheets were fixed with 2.7 mm diameter x 40mm long clouts at 150mm centres around the perimeter of each sheet and along each stud. The internal sheet joints were filled and initially plastered with layers of cementitious plaster and embedded fibreglass reinforcing tape, with a final finishing plaster product then applied.

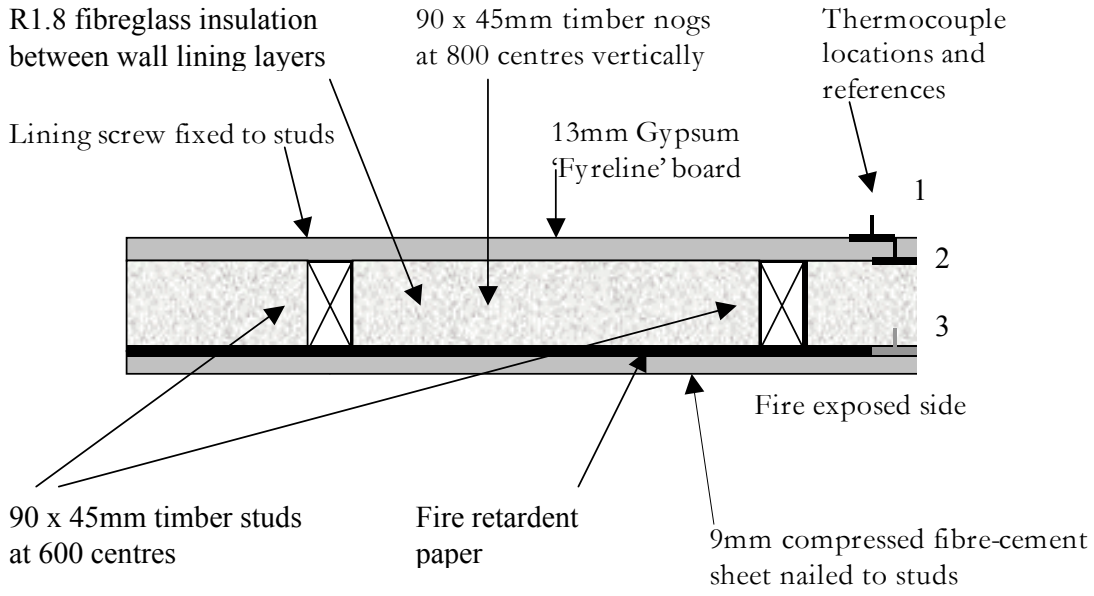

Figure 3.4 – Assembly 2 cross section

3.3.3 Assembly 3 - 30 Minute Rated LSF Gypsum Plasterboard Lined Assembly

This assembly construction was located at Wall C (WC) in compartment test #1, and Wall B (WB) in test #3. The wall was constructed identically to the construction specification used when tested to the standard furnace test, as detailed by the fire resistance test report FR1391 (BRANZ FR1391).

Figure 3.5 shows a cross section through the wall. Consisting of a non-loadbearing steel framed wall, lined with a single layer of 13mm 'Standard' gypsum plasterboard to each side. Steel framing was constructed using 64mm x 34mm x 0.55mm thick galvanised steel studs with 30mm diameter holes in the web at 300mm centres. Studs were placed at 600mm centres. There was an expansion gap of 15mm at the top of each stud, and studs were fixed to the channel runners with soft aluminium rivets at the top and bottom. Sheets were fixed to the steel frame with vertical joints at the sheet ends staggered 600mm between the exposed and unexposed linings. The sheets were fixed to the steel studs with 25mm bugle head type 'S' screws at 300mm centres around the perimeter of the sheets and along centre studs. The internal faces were taped and

stopped using a bedding compound and paper reinforcing tape. All screw heads were additionally stopped.

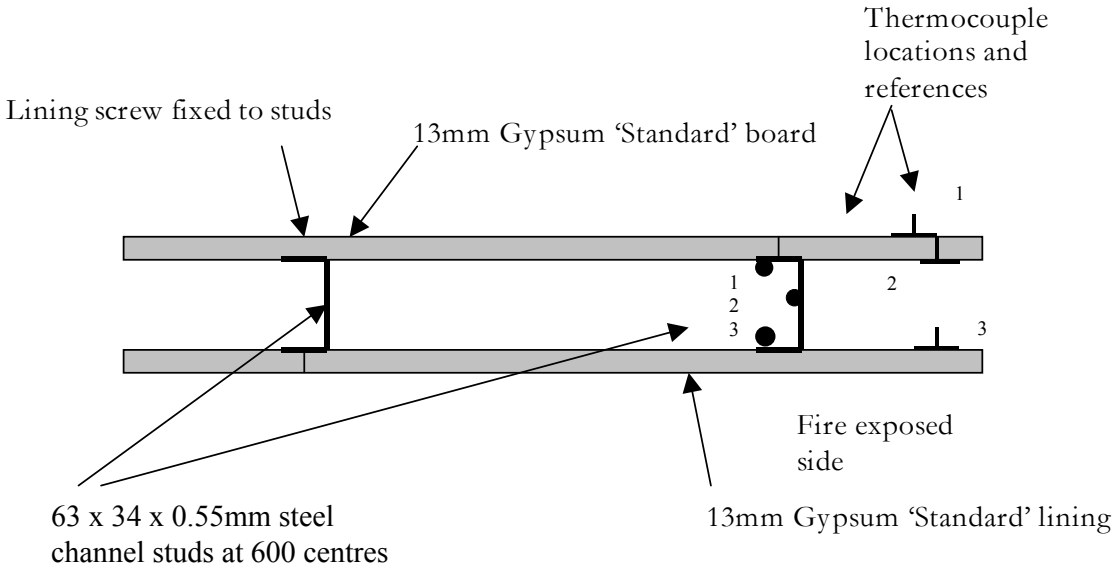

Figure 3.5 – Assembly 3 cross section

3.3.4 Assembly 4 - 30 Minute Rated Ceiling Assembly

This ceiling assembly was used for both compartment tests #1 and #3. The ceiling was constructed identically to the construction specification used when tested to the standard furnace test, as detailed by the fire resistance test report FR1572 (BRANZ FR1572).

Figure 3.6 shows a representation of the cross section through the ceiling. Consisting of a floor/ceiling system using 240mm composite timber joists, with one layer of 13mm 'Fyreline' gypsum plasterboard on the ceiling and a layer of 20mm particle board on the floor. The timber framing comprised the composite joists spanning the 3.6m nominal length of the compartment. The joists were supported by 90mm x 45mm bearers, which were a part of the timber framed wall constructions. The joists were spaced at 600mm centres, with floor dwangs at 600mm intervals and solid blocking half way across the span. The underside layer of 13mm 'Fyreline' gypsum plasterboard was fixed to the joists and solid blocking, with joints being formed over the dwangs. Fixing entailed the use of 51mm (Size 7) gold passivated screws at 150mm centres on the perimeter of each sheet and 200mm centres along joists and dwangs. All wall/ceiling joints were stopped using a bedding compound and paper reinforcing tape. All screw heads were additionally stopped. The flooring sheets were laid across the joists and fixed to joists and

dwangs using 50mm (Size 8) yellow zinc screws at 150mm centres around the perimeter of each sheet and at 200mm centres on all other joists and dwangs.

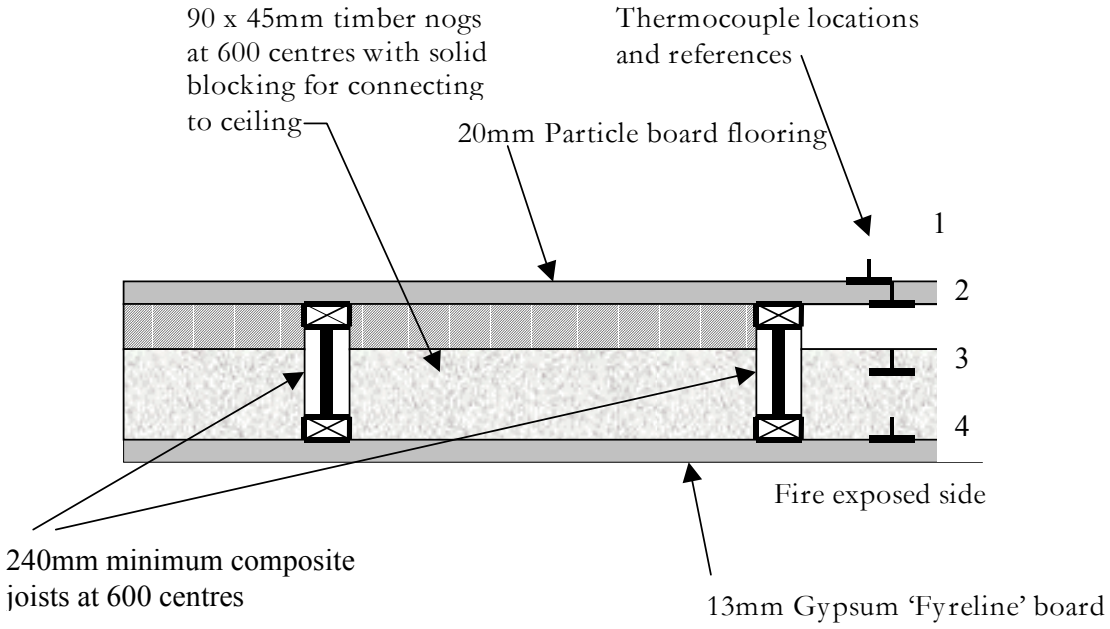

Figure 3.6 – Assembly 4 cross section

3.3.5 Assembly 9 - 30 Minute Rated Fire Door Assembly

This assembly was tested in compartment test #1 only, and located as indicated in Figure 3.1. The fire door was of identical construction specification as the door tested to the standard furnace test and detailed by the fire resistance test report FR1405 (BRANZ FR1405).

Figure 3.7 shows a picture of the fire door assembly used in Test #1. The door consisted of a side hung single leaf doorset mounted in a nominal 90mm x 45mm timber framed wall (as detailed for Wall A). The door leaf was of nominal 2020mm high x 1020mm wide x 45mm thick dimensions. Incorporated in the door construction were intumescent seals in the rebate in the doorjambs, head, and opposite the centre of the door leaf, and additionally under the escutcheons of the lockset. The door was installed as originally tested, with the door opening in towards the compartment.

Figure 3.7 – Assembly 9 - Fire door

3.3.6 Floor Construction

The following description of the floor construction is identical for all compartment tests and was designed with a view to ensuring that the floor system survived the fire exposure of all tests, to enable re-use. Further description of the floor will not be repeated in this report.

Figure 3.8 shows a cross section of the floor assembly used in all tests. Consisting of a loadbearing floor system using 240mm composite timber joists. Directly on the joists was one layer of 20mm particle board flooring, with two layers of 10mm gypsum fibre board on top of the fire-exposed side of the particle board. The timber framing comprised composite joists spanning the 3.6m nominal length of the compartment. The joists were supported by two steel I beams clamped onto two steel construction trolleys. The trolleys enabled the compartments to be wheeled outside upon completion of construction, when tests were ready to be undertaken (Figure 3.9). The joists were spaced at 600mm centres, with floor dwangs at 600mm intervals and solid blocking half way across the span. All flooring sheets were laid across the joists and fixed to joists and dwangs using 50mm (Size 8) yellow zinc screws at 150mm centres around the perimeter of each sheet and at 200mm centres on all other joists and dwangs.

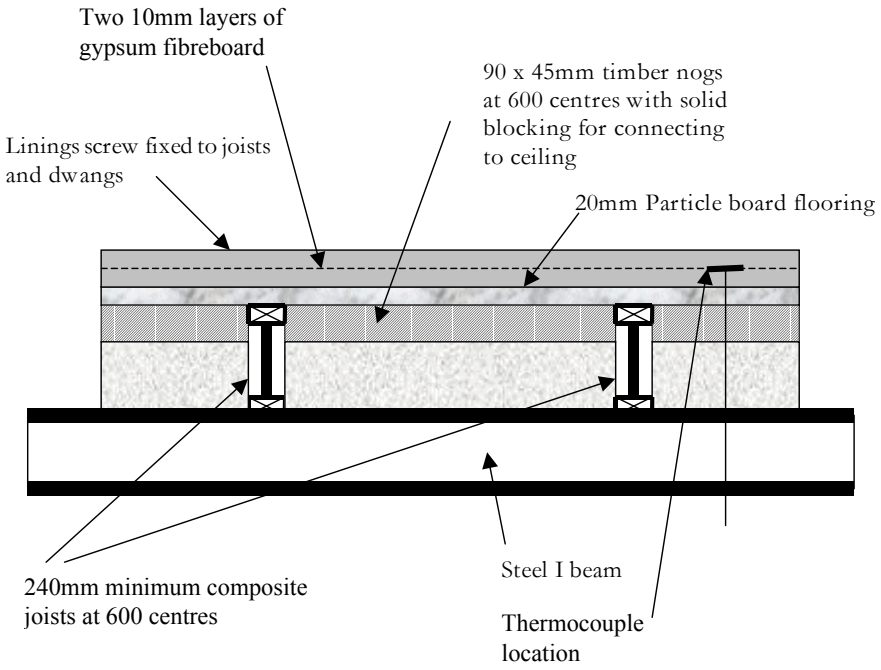

Figure 3.8 – Compartment floor cross section

3.3.7 Tests #1 and #3 Wall with Vent Opening

Construction of the wall with the vent opening was of nominal dimensions as shown in Figures 3.1 and 3.2, and to the same construction details as previously described for Assembly 1. An additional shield was constructed above this wall to prevent re-radiation from flames burning outside the compartment from affecting the thermocouples on the ceiling/floor system (Figure 3.9).

Figure 3.9 – Typical compartment on trolleys, with protective shield

3.4 Test #2 Constructions

All elements tested were of a nominal 60 minute FRR. Compartment geometry and construction set out are shown in Figure 3.10. No fire door was incorporated in the construction of test #2.

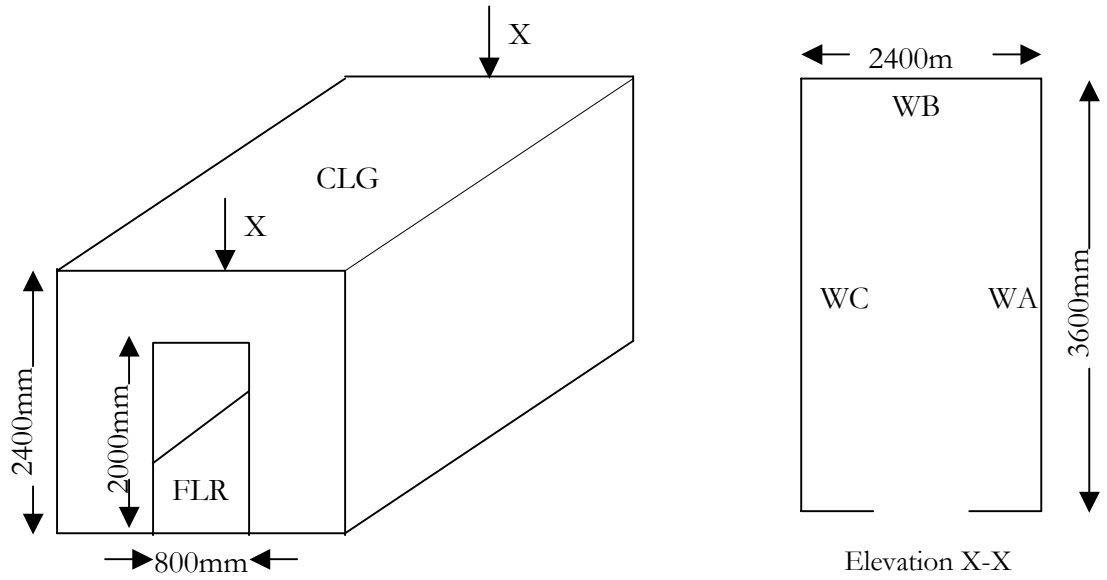

Figure 3.10 – Test #2 Compartment geometry and construction set out

Compartment building element references are as given previously (Table 3.2).

3.4.1 Assembly 5 - 60 Minute Rated LTF Gypsum Plasterboard Lined Assembly

This assembly was located at WA in compartment test #2. The wall was constructed identically to the construction specification used when tested to the standard furnace test, as detailed by the fire resistance test report FR1571 (BRANZ FR 1571).

Consisting of a load bearing timber framed wall, lined with a single layer of 13mm 'Fyreline' gypsum plasterboard to each side. Details of framing construction, fixings and surface finishing were identical to that previously described for Assembly 1. Refer to Figure 3.3 for typical cross section details.

3.4.2 Assembly 6 - 60 Minute Rated LTF Fibre-Cementitious & Gypsum Plasterboard Lined Assembly

This wall assembly was located at WB in compartment test #2. The wall was constructed identically to the construction specification used when tested to the standard furnace test, as detailed by the fire resistance test report FR2493 (BRANZ FR 2493).

Figure 3.11 shows a typical cross section detail of the construction.

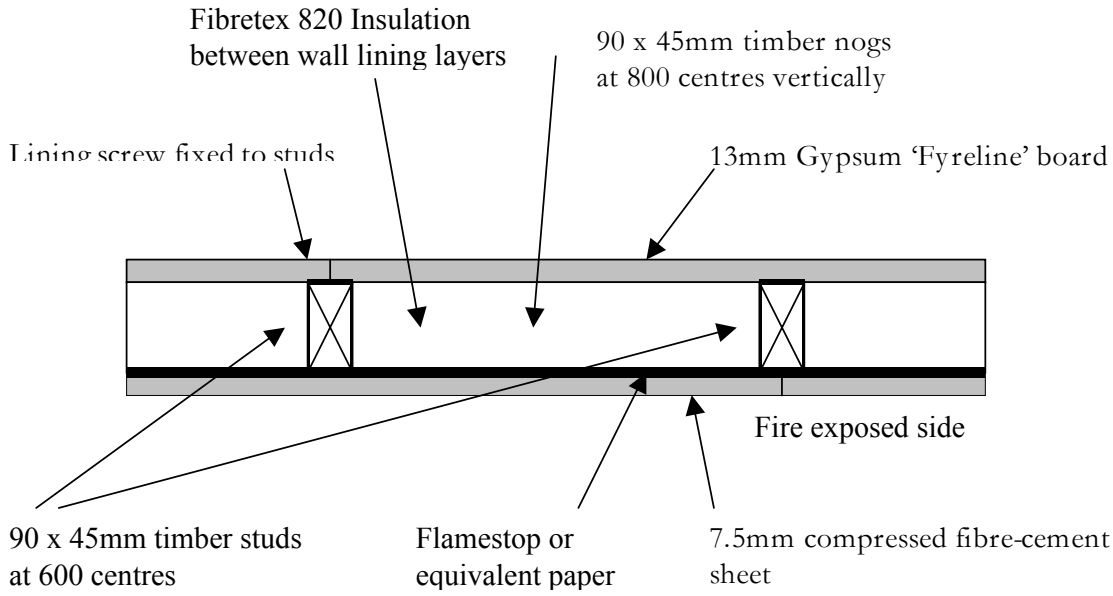

Figure 3.11 – Assembly 6 cross section

Consisting of a load bearing timber framed wall, lined with a single layer of 13mm 'Fyreline' gypsum plasterboard on the unexposed face and a layer of 7.5mm compressed fibre-cement sheet on the exposed face. 'Flamestop' building paper was used to line the fibre cement sheet on the cavity side of the wall. The wall was insulated with one layer mineral insulation blanket, having a density of 120kg/m³ and a nominal 38mm thickness. Details of framing construction, fixings and surface finishing were identical to that previously described for Assembly 2.

3.4.3 Assembly 7 - 60 Minute Rated LSF Gypsum Plasterboard Lined Assembly

This wall assembly was located at WC in compartment test #2. The wall was constructed identically to the construction specification used when tested to the standard furnace test, as detailed by the fire resistance test report FR1579 (BRANZ FR 1579).

Consisting of a non-load bearing steel framed wall, lined with a single layer of 13mm 'Fyreline' gypsum plasterboard to each side. Details of framing construction, fixings and surface finishing were identical to that previously described for test Assembly 3. Refer to Figure 3.5 for typical cross section details.

3.4.4 Assembly 8 - 60 Minute Rated Ceiling Assembly

The ceiling/floor was constructed identically to the construction specification used when tested to the standard furnace test, as detailed by the fire resistance test report FR1370 (BRANZ FR1370).

Consisting of a floor/ceiling system using 240mm composite timber joists, with one layer of 16mm 'Fyreline' gypsum plasterboard on the ceiling and a layer of 20mm particle board on the floor. Details of framing construction, fixings and surface finishing were identical to that previously described for Assembly 4. Refer to Figure 3.6 for typical cross section details.

3.4.5 Test #2 Wall with Vent Opening

Construction of the wall with the vent opening was of nominal dimensions as shown in Figure 3.10, and to the same construction details as previously described for Assembly 5. As done with success in test #1 an additional shield was constructed above this wall to prevent re-radiation from flames burning outside the compartment from affecting the thermocouples on the ceiling/floor system (Figure 3.9).

3.4.6 Summary of Test Assemblies

Table 3.3 summarises the test assemblies and their compartment test locations references shown in Figures 3.1, 3.2 and 3.10.

Construction Element	Description and Nominal FRR	Tests Reference #	Location Ref.
Assembly 1	30 mins. rated LTF gypsum plasterboard lined wall assembly	#1 #3	WA WA
Assembly 2	30 mins. rated LTF fibre-cementitious and gypsum plasterboard lined wall assembly	#1 #3	WB WC
Assembly 3	30 mins. rated LSF gypsum plasterboard lined wall assembly	#1 #3	WC WB
Assembly 4	30 mins. rated LTF gypsum plasterboard lined ceiling assembly	#1	CLG
Assembly 5	60 mins. rated LTF gypsum plasterboard lined wall assembly	#1 #3	WA WA
Assembly 6	60 mins. rated LTF fibre-cementitious and gypsum plasterboard lined wall assembly	#2	WB
Assembly 7	60 mins. rated LSF gypsum plasterboard lined wall assembly	#2	WC
Assembly 8	60 mins. rated LTF gypsum plasterboard lined ceiling assembly	#2	CLG
Assembly 9	30 mins. Rated fire door	#1	FD

Table 3.3 – Compartment test assembly descriptions

3.5 Standard Test Fire Resistant Ratings of Compartment Assemblies

The FRR's for all test assemblies and their original standard fire test failure times and mechanisms of failure are shown in Table 3.4.

Element Reference	BRANZ Fire Test Report	Standard test failure time (mins)	Criteria of Failure	Cause of Standard test failure
Assembly 1	FR1712	42	Insulation	Individual thermocouple (tc) exceeded 180°C rise.
Assembly 2	FR2454	39	Insulation	Individual thermocouple (tc) exceeded 180°C rise.
Assembly 3	FR1391	34 (assessment)	Insulation	Furnace test terminated after 32 minutes
Assembly 4	FR1572	55	Structural	Significant deflection due to failure of one or more joists
Assembly 5	FR1571	68 (49)	Insulation (Structural)	Average of thermocouple (tc) exceeded 140°C rise. (Failed when tested under structural loading criteria)
Assembly 6	FR2493	58	Insulation	Individual thermocouple (tc) exceeded 180°C rise.
Assembly 7	FR1579	63	Insulation	Average of thermocouple (tc) exceeded 140°C rise.
Assembly 8	FR1370	74	Structural	Significant movement and cracking due to failure of one or more joists
Assembly 9	FR1405	32	Integrity	Sustained flaming exceeding 10 seconds at head of door.

Table 3.4 – Fire resistance ratings of test compartments building elements

With reference to the comments given regarding the original standard test structural failure of assembly 5 indicated in Table 3.4, it should be noted that this is the failure of the wall as a load bearing structure. Since the scope of this report is examining only non-load bearing systems (with the exception of the floor/ceiling system), the insulation criteria failure time is the non-load bearing fire resistance rating of this element and will be used for future comparison and analysis.

3.5.1 FRR Rating 'By Assessment' of Assembly 3

The standard fire test for assembly 3 (BRANZ FR1391) was terminated at 32 minutes, which was prior to failure of that assembly being reached. The reasons for this are unknown to the author and other parties involved in the test at the time. As a result, the nominal 30 minute FRR steel stud system has been given a failure time of 34 minutes for insulation, by the authors assessment. This failure time was determined by detailed examination of the standard test data

and a conduction model calculation. Figure 3.12 shows the wall profile temperatures of the nominally 30 minute FRR rated steel stud framed wall assembly when tested to the standard fire during furnace testing (BRANZ FR1391).

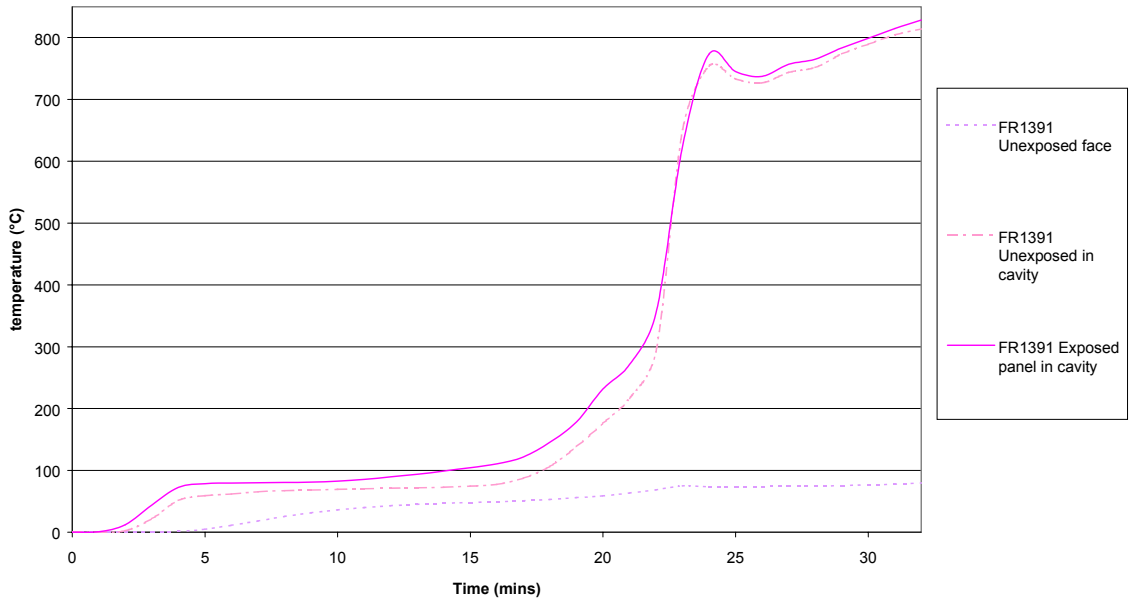

Figure 3.12 – Assembly 3 wall temperatures in the standard fire test, FR1391

The rapid rise in cavity temperatures on the exposed and unexposed linings, at 22 minutes, indicate the internal lining has fallen away, and the external lining of the assembly is exposed to the furnace fire exposure temperatures. At the time of the test termination (32 minutes), the unexposed face has risen to a temperature of 94.5°C. Where the previous two recorded temperature rises, prior to termination of the test, were 92.4°C and 92.9°C for 30 and 31 minutes respectively, the temperature rise for the following minute time step can be estimated using the similar ratio of temperature rise. Therefore the temperature rise of 5°C on the unexposed face, gives a temperature of 99.5°C by 33minutes. This is sufficiently close enough to 100°C, to assume that beyond 33 minutes of the standard furnace exposure, the moisture removal plateau experienced by gypsum plasterboard on the steel stud system has been exceeded, and from then on, the temperature on the unexposed face will continue to rise due to conduction through the plasterboard lining. At 33 minutes into the standard furnace test, the unexposed lining within the cavity is approaching furnace temperature, at 825°C. Applying a two-dimensional steady state finite difference conduction calculation to the plasterboard lining, whereby the heat transfer model can be represented by the diagram shown in Figure 3.13, provides an estimate of the time to failure of the wall assembly can be made. Incropera and

DeWitt (1996) explain how to derive the energy balance equations at each node, and therefore determine the temperature profile at a given time. The calculation assumes that the exposed side (Node 5) of the lining is at furnace temperature, as shown by the thermocouple readings, and the unexposed face is 100°C at the beginning of the calculation (ie at 33 minutes into the standard furnace test).

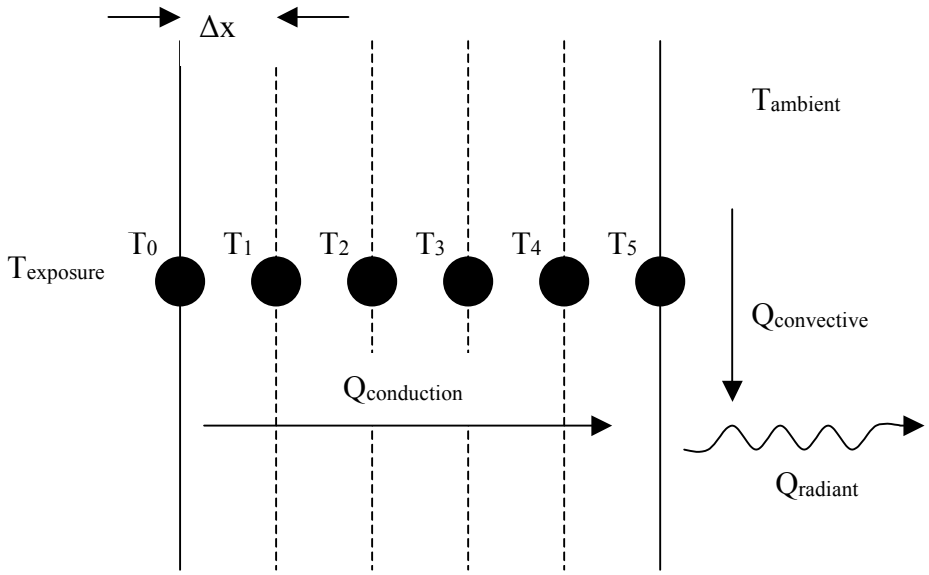

Figure 3.13 – Conduction heat transfer model through standard gypsum plasterboard lining

Assuming thermal properties for the gypsum plasterboard are:

k	=	0.12 W/mK	(Buchanan 2001b)
Cp	=	2000 J/kgK	(Buchanan 2001b)
ρ	=	670 kg/m³	(Winstones Wallboards 2001)

and

h	=	6 W/m²K	(Incropera and DeWitt 1996)
σ	=	5.67 E-8 W/m²K⁴	(Incropera and DeWitt 1996)
ε	=	0.88 assumed	(Incropera and DeWitt 1996)

The conduction equations used, are:

Node0 $T_{0'}$ = Unexposed lining in cavity temperature **Equation 3-1**

Internal nodes 1 –4 $$T_{i'} = \frac{\Delta t\, k}{\rho\, Cp\, \Delta x^2}\left(\left(T_{i+1} - T_i\right) + \left(T_{i-1} - T_i\right)\right) + T_i$$ **Equation 3-2**

Where $T_{i'}$ is the temperature of the node in the current time step, and T_i is the temperature at that node in the previous time step. T_{i-1} and T_{i+1} are the adjacent nodes before and after the internal node, respectively.

Node 5 $$T_{5'} = \frac{2\,\Delta t}{\rho\, Cp\, \Delta x}\left(\frac{k\left(T_4 - T_5\right)}{\Delta x} - k\left(T_5 - T_\infty\right) - \sigma\varepsilon\left(T_5^{\,4} - T_\infty^{\,4}\right)\right) + T_5$$ **Equation 3-3**

(Note: temperatures should be in K for radiant components of the equations)

Where T_∞ is the ambient temperature ($T_{ambient}$ in Figure 3.13).

Therefore, applying these calculations in a spreadsheet format provides a temperature rise, on the unexposed face, between 100°C and failure at 140°C as shown in Figure 3.14. It should be noted that average thermocouple temperatures of the test data are being applied and therefore failure was determined as the time to reach 140°C.

The temperature of the unexposed face of the steel stud framed, 13mm 'standard' plasterboard lined wall assembly, exceeds 140°C after 34 minutes. Therefore, 'by assessment', the derived FRR for the steel framed wall assembly lined either side with 13mm 'standard' plasterboard is 34 minutes.

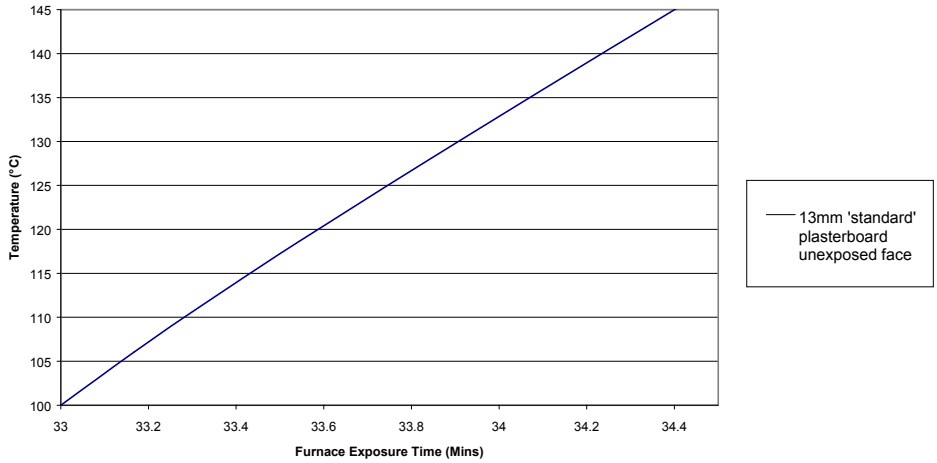

Figure 3.14 – Temperature rise of unexposed face of standard plasterboard from 100°C to failure.

3.6 Design Fire Fuels

3.6.1 Basis of Realistic Fire Fuel Load Selection

The basis of the design fire was to simulate the rapid growth in fire severity associated with upholstered furniture, followed by a continued duration of burning to maintain the required fire severity, for a sufficiently long period of time in accordance with the associated fuel load energy density (FLED) for the fire hazard categorisation as given in the Approved Documents (BIA 2001). Two FLEDs were used for the tests as shown in Table 3.5. These FLEDs were selected to ensure that failure of assemblies would occur and enable comparison of assembly failure times with differing fire exposures. Without assembly failure, correlation between assembly realistic fire time to failures and standard fire test time to failures was not envisaged to be feasible.

Test Reference Number	Fire Load Energy Density (MJ/m^2)	Fire Hazard Category
Test #1	800	2
Test #2	1200	3
Test #3	800	2

Table 3.5 – Compartment tests FLED's

All three tests were intended to have similar severity of fire growth, with the variation being the duration burning time increasing as the FLED increases. Polyurethane (PU) foam cushions with an appropriate synthetic fibre covering were used to provide a rapid initial fire growth as would

be expected by upholstered furniture in a real fire situation. The foam cushions were selected to take the test fire to flashover conditions, after which point, wooden cribs were designed to provide sufficient burning rates to maintain a ventilation controlled fire through to the start of the decay stage.

3.6.2 Selection and Geometry of Foam and Fabric

Selection of the upholstery cushion's foam and fabric materials was made on the basis of previous research undertaken at the University of Canterbury, with an aim that the experiment could be repeated should any future similar tests be undertaken.

The previous research used in determining the foam fabric selection were studies where application of the European combustion behaviour of upholstered furniture (CBUF) model (Sundström 1995) had been made to NZ upholstered furniture, comprising various foam and fabric upholstery combinations. The main factors arising from these research projects and considered of primary importance to the fuel and fabric selections for this project are listed as follows:

- Denize (1999) shows that non-fire retardant PU foam produces higher peak heat release rates in a quicker duration of time compared to fire retardant foam selection.

- Firestone (1999) showed that foam and fabric interaction is a crucial factor in determining the combustion severity. It was therefore necessary to select an appropriate foam and fabric combination, which would provide the most severe likely fire growth representative of foams and fabrics in common use in NZ.

- In a large variety of foam and fabric combinations tested, Coles (2001) showed that two specific combinations provided the most severe fire growth rate and peak heat release. Although the foam and fabric combination (coded according to the CBUF modelling convention (Sundström 1995)), type L (approx 38kg/m^3) foam with an olefin (100% olefin) fabric gave fastest growth and higher peak heat release rates, this combination was not selected as that foam's use is predominantly for public auditoriums and maritime berths and seating, which has a less common usage over the majority of building upholstered furniture applications. Instead, further to informed discussions with PU

foam manufacturers, the type K foam (approx 29kg/m³) used for domestic and commercial seatbacks and cushions, with 100% olefin fabric cover was selected. This combination provides a slightly less severe fire growth and peak result than the aforementioned combination, but still significantly more severe than the alternative foam and fabrics tested by Coles (2001). The actual PU foam selected from the manufacturers considerable available range was non-fire retardant PU foam with a density of 30kg/m³ (±1 kg/m³).

- Girgis (2000) showed that the presence of arm rests in upholstered furniture accelerate the development of a fire, leading to a shorter duration to reach the peak heat release rate of the furniture. For this reason, the geometry of the foam cushions to be burnt was selected such that the foam and fabric combination resemble the shape of a couch with armrests.

The geometry of a two-seater couch (Figure 3.15) was selected for Test #1, as this was deemed to have the fuel load required to take the compartment to flashover, whilst giving the severest fire growth and peak heat release of upholstered furniture. To confirm that sufficient quantity of foam fuel was available to take the compartment fire to flashover, the two-seater couch geometry was tested in the ISO room calorimeter (refer to Section 6 of this report).

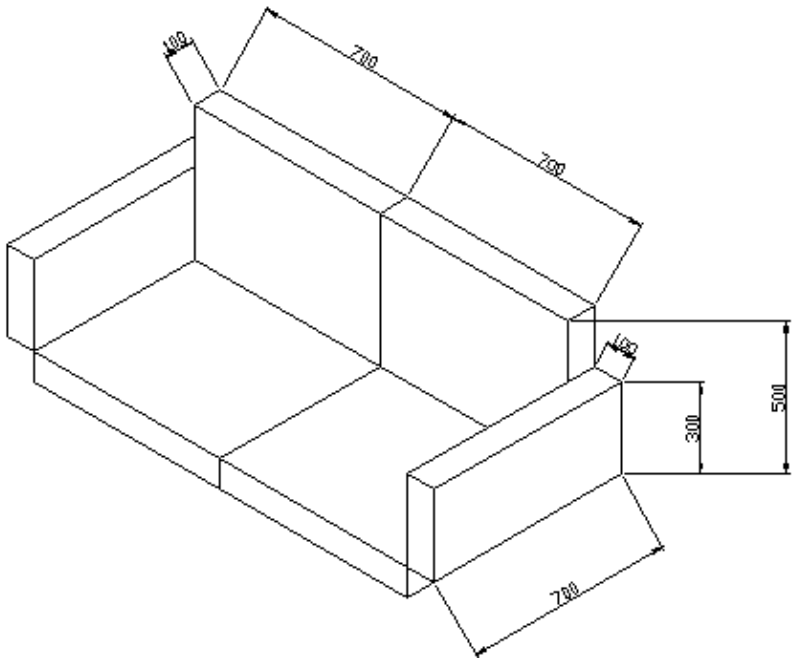

Figure 3.15 – Two-seater foam and fabric fuel geometry

Tests #2 and #3 used a three-seater couch geometry. The couch geometry, and therefore, PU foam fuel source was increased for tests #2 and #3, since the fuel load was to be increased by 50% to 1200MJ/m² (Test #2) and the vent opening size was increased (Test #3). Therefore a third seat of 700mm width was incorporated into the design (Figure 3.16).

In order that the foam cushions retained their geometry and position above the ground during the fire test, and so as to achieve the thermoplastic pooling that occurs from burning upholstered furniture at floor level, three steel seat frames were constructed. Two were used for Test #1 and three for Tests #2 and #3. Construction details of a single seat frame are detailed in Figure 3.17.

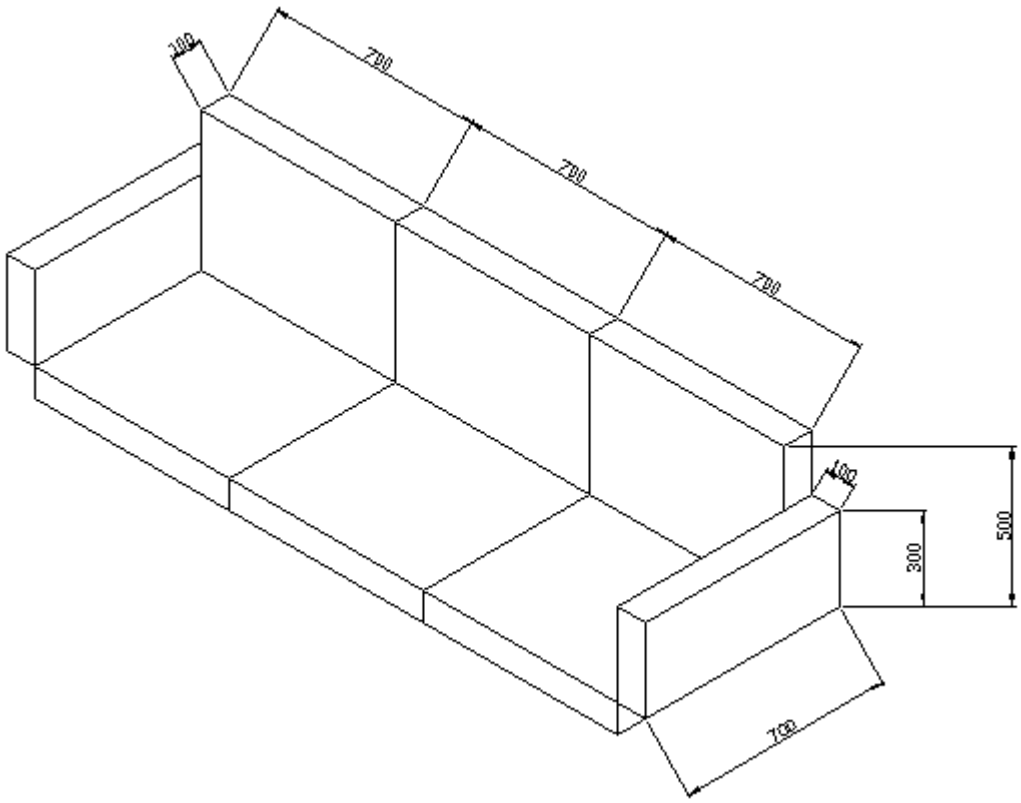

Figure 3.16 – Three-seater foam and fabric fuel arrangement

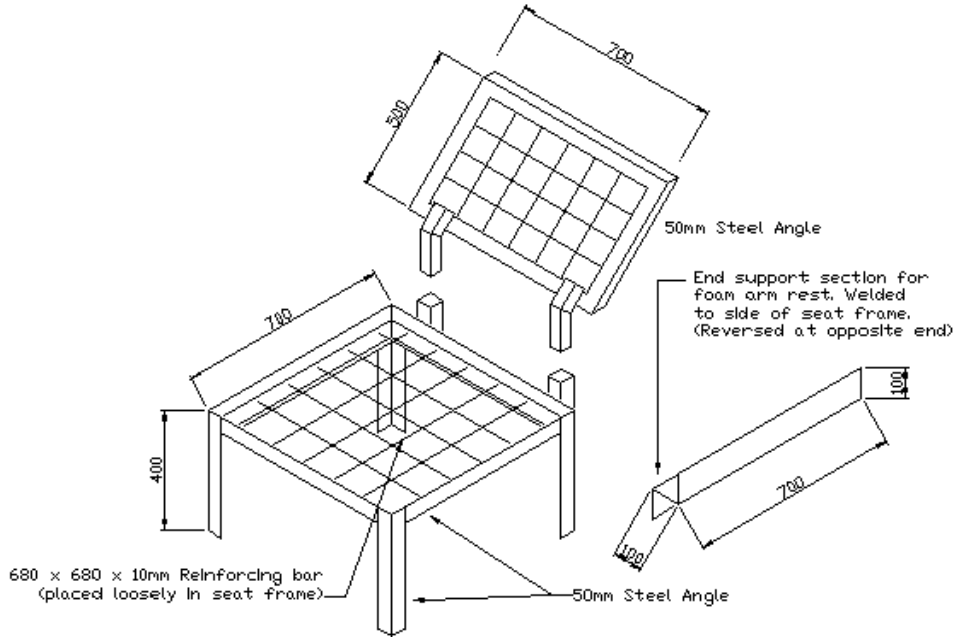

Figure 3.17 – Steel seat frame construction

3.6.3 Ignition Source

The ignition source for all fire tests was a cotton wool swab moistened lightly with methylated spirits. The swab was located at the join between the seat cushions and the seat back cushions in the centre of the two, or three seater chairs (Figure 3.18), and ignited using a match.

Figure 3.18 – Ignition source location

3.6.4 Wood Cribs Geometry

Untreated 'rough sawn' Radiata pine wood cribs were designed to the geometry as given by Babrauskas (1995). The typical crib geometry can be seen in Figure 3.19. The numbers of cribs and crib dimensions to be used in each test, were selected such that the required FLED was achieved by the combination of foam and wood fuels, and additionally so the fuel surface area of the wood fuel ensured achieving the ventilation controlled heat release rate. The calculations for this are as detailed in section 3.7.4.

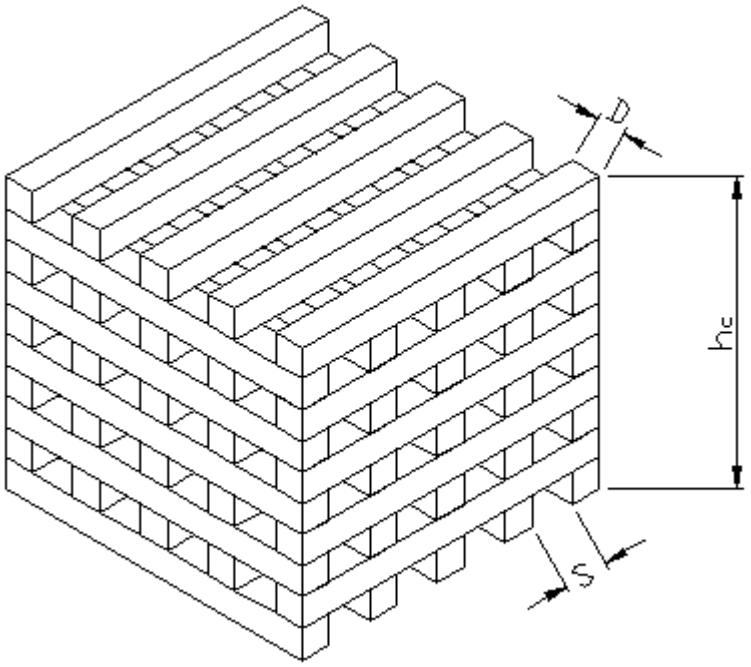

Figure 3.19 – Wood crib fuel geometry

Due to cost constraints and availability of timber, crib sticks were made from untreated timber of nominal 50mm x 50mm cross section. The dimensions selected for all cribs used in the tests are as shown in Table 3.7. The term A_{wood} in the Table is the actual surface area of the wood cribs at the start of each test.

Test Ref.	D (m)	S (m)	h_c (m)	n	No. of cribs	V (m^3)	Mass (kg)	Total Wood fuel load (MJ)	Wood FLED (MJ/m^2)	Actual A_{wood} (m^2)
#1	0.05	0.1	1	5	6.9	1.12	563	6,752	781	70.4
#2	0.05	0.1	1	5	10.4	1.69	848	10,177	1,178	106.1
#3	0.05	0.1	1	5	6.9	1.12	563	6,752	781	70.4

Table 3.7 – Preliminary Calculations - Wood crib dimensions and FLEDs

3.6.5 Wood Crib Moisture Content

Prior to each test, the moisture contents of two samples of crib sticks were recorded. Initially, measurements were taken from the samples using a pre-calibrated moisture meter. Additionally, the sample crib sticks had their weight measured using pre-calibrated electronic scales and recorded. The sticks were then placed in a drying oven and their weight was monitored daily, until no further weight/moisture loss from the sticks was observed. The moisture content of the crib sticks was then calculated and average moisture content recorded (Table 3.8).

Compartment Test	Density at time of test (kg/m^3)	Average Moisture Content (%)
		Oven drying method
#1	496.5	14.6
#2	451.6	13.9
#3	487.8	16.2

Table 3.8 – Moisture content of wood samples at time of tests

3.6.6 Preliminary Fuel Quantities Calculations

For the preliminary estimation of the required quantities of fuels, the densities of the fuel types were taken from measured samples at BRANZ, where a timber density of $502.7kg/m^3$ and the PU foam density of $30.1kg/m^3$, were measured. The calorific value of PU foam was initially taken as being 25.5MJ/kg (Buchanan 2001b). The actual heat of combustion for the PU foam and olefin fabric fuels was established using ISO 9705 room and cone calorimetry, which is described in detail in Section 6 of this report. It should be noted that calorimetry was not able to be undertaken until after the compartment tests. Therefore all estimates of fuel quantities were obtained using the above assumed values.

Using the required FLED's for each test as a basis for the fuel quantities, and with a knowledge of the quantities of PU foam required for the couch geometries, quantities and dimensions of both foam fuels and wood crib fuels were established, and are shown in Tables 3.9 and Table 3.7 respectively.

Compartment Test	Volume of PU foam (m^3)	Mass (kg)	Total PU foam fuel load (MJ)	PU foam FLED (MJ/m^2)
#1	0.21	6.3	161.3	18.7
#2	0.294	8.9	225.8	26.1
#3	0.294	8.9	225.8	26.1

Table 3.9 – PU foam FLEDs

The remaining wood crib component of the FLED requirement for the compartment tests was determined using the effective heat of combustion, Δh_{ceff}, of 12MJ/kg (Babrauskas 1995), as shown in Table 3.7.

3.6.7 Tested Fuel Load Energy Densities

Further to information gained from the cone calorimeter tests, which were undertaken after the compartment tests (refer to Section 6), this sub-section of the report provides details of the actual fuel loads used in the compartment tests.

The foam and fabric samples tested using the cone calorimeter established a heat of combustion, Δh_c, of 27.7MJ/kg for the PU foam and olefin fabric composite. Applying this in conjunction with the weights of the cushions, the fuel load contributed to the compartment tests by the cushions have been calculated and are shown in Table 3.10.

Test #	Mass of PU foam (kg)	Mass of PU foam and olefin fabric composite (kg)	Total PU foam and olefin fuel load (MJ)	PU foam cushions FLED (MJ/m^2)
#1	5.99	7.87	218.0	25.23
#2	8.37	10.94	303.0	35.07
#3	8.37	10.83	300.0	34.72

Table 3.10 – PU foam cushions fuel load

The mass for each wood crib stick was taken as being the average of that taken from two sample sticks prior to each test. Applying an effective heat of combustion, Δh_{ceff}, of 12MJ/kg (Babrauskas 1995), the fuel load potential of the wood cribs in each test was as shown in Table 3.11.

Test #	Mass of wood sticks (kg)	Total mass of wood cribs (kg)	Total wood cribs fuel load (MJ)	Wood cribs FLED (MJ/m²)
#1	0.795	548.55	6582.6	761.88
#2	0.720	748.80	8985.6	1040.0
#3	0.755	520.95	6251.52	723.56

Table 3.11 – Wood cribs fuel load at time of tests

3.6.8 Fuel Layout

The crib and chair upholstery fuels for each test were laid out as symmetrically as possible to attempt to achieve similar fire severities at each wall assembly. Cribs were stacked at heights of 1-1.5m in tests #1 and #3, and at 1.5-2m for test #2. A typical layout is shown in Figure 3.20. Cribs were positioned 300 mm from the wall assemblies, with the exception of the front two cribs, which were 150mm from the walls in order to avoid blockage of the vent opening.

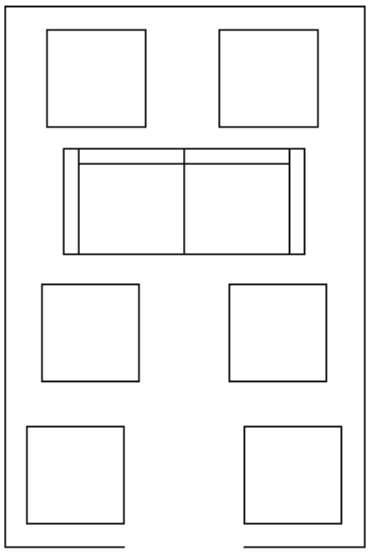

Figure 3.20 – Compartment tests fuel layout

It should be noted that varying the location of the foam seat around the compartment would result in differing fire severities to each test assemblies. The experiment has attempted to provide an even distribution of fire severity to each building element. However, in reality, upholstered furniture is likely to be located hard against a wall assembly and a fire from the seat in such a location would be more severe to that system. In order to optimise the number of systems tested, the fuel layout selected was deemed to be the preferred option for testing so many systems in a single fire test.

3.7 Compartment Design Fire Calculations

3.7.1 Introduction

This sub-section of the report describes briefly the design fire calculations undertaken to evaluate and predict the likely fire severity of each compartment test fire. The calculations are based upon the geometry and fuel loads envisaged (Section 3.6.6). As previously mentioned in Section 2.4.2, Girgis (2000) found that the larger the space in which furniture burnt, the less hazardous the effects were, compared to if the same furniture burnt in a smaller space. Therefore, it was expected that the relatively small ISO room compartment geometry, which is comparable in volume to the standard test furnace, produces more hazardous conditions, than a larger compartment under the same test fuel loads, providing conservative fire resistances for fire engineering design applications. In theory, however, the most severe conditions occurs when the oxygen supply just matches the fuel vapours so that all the fuel is just burned inside the room (stiochiometry). Therefore, the room size shouldn't make any difference to the results, if the fuel and combustion conditions are right. However, it was envisaged that greater uniformity in combustion is more likely in the small ISO room, than in larger spaces. Such uniformity is generally acheived in the full-scale furnace, of similar small volume.

3.7.2 Compartment Ventilation and Opening Factors

Using the vent opening dimensions previously given in Table 3.1, the compartment opening factors and Eurocode ventilation factor (EC1 1996), as calculated by Equations 2-2 and 2-6, respectively, are shown in Table 3.12.

Test Reference	Opening Factor, F_v	Eurocode formula ventilation factor, w_f
#1	0.049	1.07
#2	0.049	1.07
#3	0.074	0.84

Table 3.12 – Compartment tests vent opening dimensions

3.7.3 Heat Release Rate for Flashover

The heat release rate for flashover to occur within a compartment can be estimated using Thomas's flashover correlation (Walton et al 1995), where the heat release rate, Q_{fo}, can be determined by:

$$Q_{fo} = 0.0078 A_t + 0.378 A_v \sqrt{H_v}$$ **Equation 3-4**

The predicted heat release rates for each test are tabulated in Table 3.13.

Test Reference	Q_{fo} (MW)
#1	1.21
#2	1.21
#3	1.64

Table 3.13 – Compartment tests predicted HRR for flashover

The ISO room calorimeter test, as described later in Section 6 of this report, shows that the two-seater arrangement achieved a heat release rate in excess of 2.5MW in an otherwise empty compartmernt. Allowing for some of this heat release to be absorbed by the wooden cribs, which will act as a heat sink to some extent, flashover was expected to occur in the compartment tests.

3.7.4 Ventilation Controlled Heat Release Rate and Crib Burning Rate

The ventilation controlled burning of the fuels within the test compartment is anticipated to occur after flashover, when the PU foam couch has ceased to burn and the wooden cribs become the single burning fuel items within the compartment. Therefore, the ventilation controlled burning rate for wood cribs, $\dot{m}$, is calculated using Babrauskas' (1995) derivation, where:

$$\dot{m} = 0.12\, A_v \sqrt{H_v} \qquad \textbf{Equation 3-5}$$

and the ventilation controlled heat release rate, Q_v, is derived from:

$$Q_v = \dot{m}\, \Delta h_{c.eff} \qquad \textbf{Equation 3-6}$$

Where $\Delta h_{c.eff}$ is 12 MJ/kg for wood (Babrauskas 1995). Now, using a surface burning rate, $\dot{m}''_{wood}$, of 0.0056 kg/s/m² (Buchanan 2001b), the total surface area of wood, A_{wood}, required to maintain ventilation controlled burning, can be established using:

$$A_{wood} = \frac{\dot{m}}{\dot{m}''_{wood}} \qquad \textbf{Equation 3-7}$$

The ventilation controlled burning rates, heat release rates and required surface area of wood, for each test, are tabulated in Table 3.14.

Compartment Test	*FLED* (MJ/m²)	$\dot{m}$ (kg/s)	Q_v (MW)	Required A_{wood} (m²)
#1	800	0.27	3.26	48
#2	1200	0.27	3.26	48
#3	800	0.41	4.89	73

Table 3.14 –Predicted ventilation controlled burning rates and wood surface area requirements

From the above estimations of the required crib surface area required to maintain ventilation controlled burning, initial estimates of fuel quantities and actual surface areas, as shown in Table 3.7, suggest that the surface area of wood used in test #3 may have been slightly insufficient to achieve, based on the design FLED requirements.

3.7.5 Eurocode Method Temperature Prediction

The modified Eurocode parametric equation (EC1 1996), as described in detail by Buchanan (2001a) was applied to provide a prediction of the burning time and fire severity time-temperature relationship. The equation for temperature is derived from:

$$T = 1325\left(1 - 0.324\,e^{-0.2t^*} - 0.204\,e^{-1.7t^*} - 0.472\,e^{-19t^*}\right) \qquad \textbf{Equation 3-8}$$

where the 'modified' fictitious time (hours), t*, is given by the equation:

$$t^* = \Gamma_{EC\,\mathrm{mod}}\, t_{hr} \qquad \textbf{Equation 3-9}$$

and

$$\Gamma_{EC\,\mathrm{mod}} = \frac{\left(F_v / \ 0.04\right)^2}{\left(b / \ 1900\right)^2} \qquad \textbf{Equation 3-10}$$

The design fire duration of burning, t_d, and the decay rate, $\frac{dT}{dt}$, are determined respectively by:

$$t_d = 0.00013\,E_{total} \Big/ \left(A_v \sqrt{H_v}\right) \qquad \textbf{Equation 3-11}$$

and

$$\frac{dT}{dt} = \left(\frac{dT}{dt}\right)_{ref} \frac{\sqrt{F_v / 0.04}}{\sqrt{b/1900}} \qquad \textbf{Equation 3-12}$$

The reference decay, $\left(\frac{dT}{dt}\right)_{ref}$, is 625°C/hr for fires of burning duration of less than half an hour, decreasing to 250°C/hr for fires with a burning duration of greater than two hours.

Equations 3-5 to 3-9 provide a time-temperature relationship for each test as shown in Figure 3.21.

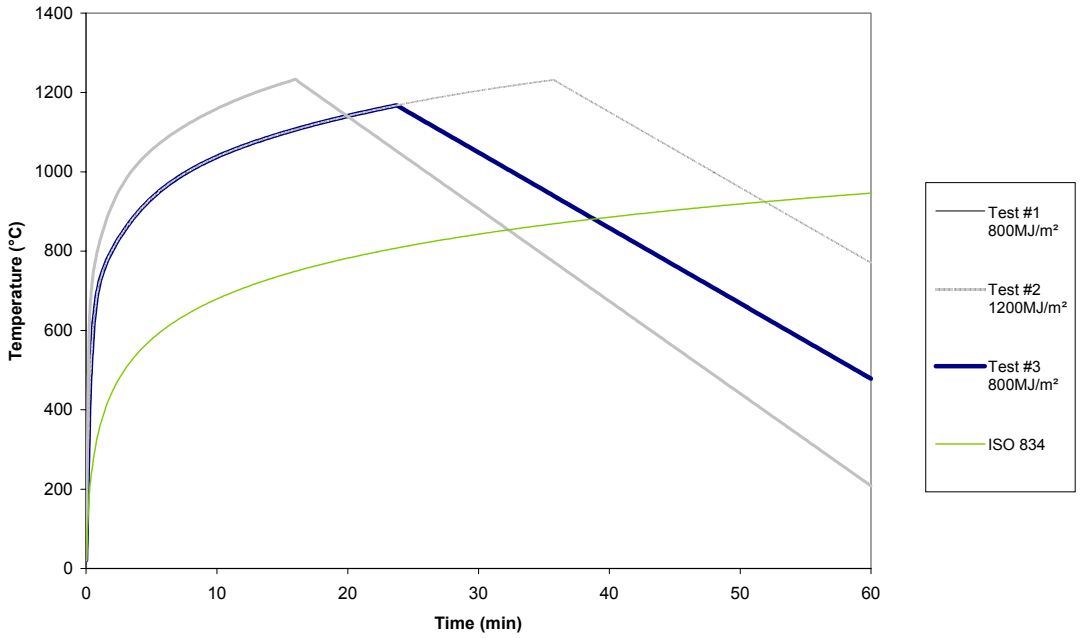

Figure 3.21 – Eurocode modified parametric method - predicted compartment temperatures

3.7.6 BRANZFIRE Modelling Temperatures and Heat Release Rate Prediction

To assist BRANZ in their development of the computer software simulation modelling package, BRANZfire 2002.2 (BRANZ 2000 & Appendix E addendum notes) was used to simulate the compartment fires and provide estimations of the time-temperature fire severity curves. BRANZfire 2002.2 is a user friendly fire simulation modelling package, with windows type screen interface (Figure 3.22). The data obtained from the compartment tests will be used by BRANZ to assist them in their validation process for the software development.

Inputting of appropriate design data, including compartment geometry, ventilation openings, construction properties, design fire FLED, and fuel quantities and properties can be carried out as a new data input. Alternatively, as was the case for the tests, inputs were selected from the

BRANZfire existing data base, and modified where appropriate. Simulations were carried out assuming no change in the size of the vents during the test.

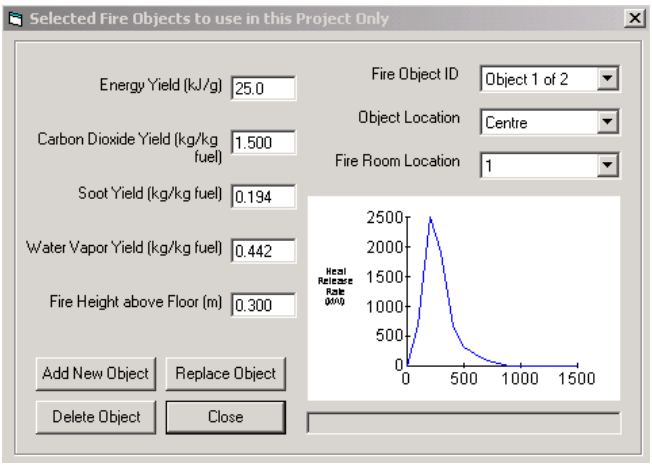

Figure 3.22 – BRANZfire 2002.2 typical input screen

The fire simulation run time for each test was the calculated duration of burning for a test (Equation 3.9), with an additional 20 minutes of decay. The resulting temperature-time, HRR-time and mass loss-time charts obtained from the simulations are shown in Figures 3.23, 3.24, and 3.25 respectively.

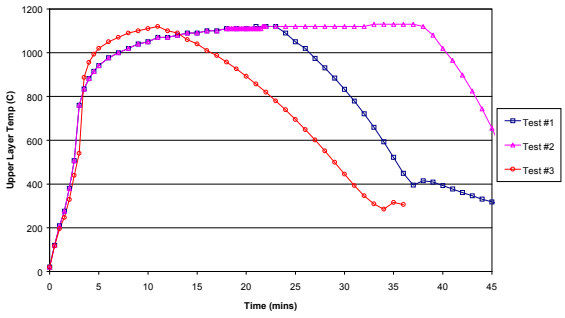

Figure 3.23 – BRANZ fire 2002.2 temperature prediction

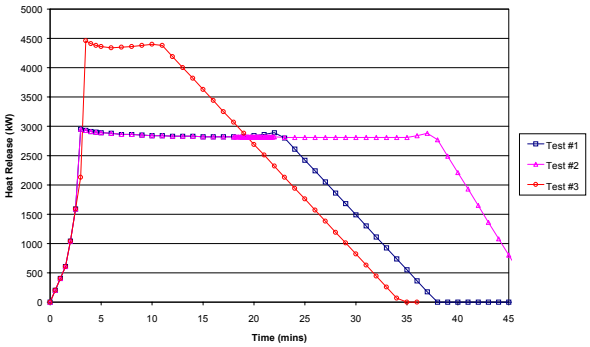

Figure 3.24 – BRANZ fire 2002.2 heat release rate prediction

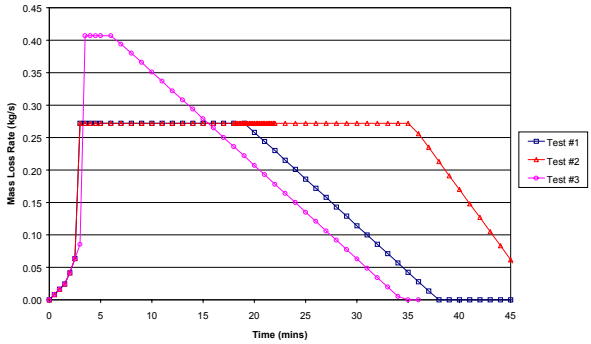

Figure 3.25 – BRANZ fire 2002.2 mass loss rate prediction

3.8 Timber 'Dummy' Column

3.8.1 Introduction

Charring rates for timber structural fire design are as specified in the New Zealand Code of Practice for Timber Design (NZS 1993), where a charring rate of 0.65mm/min is generally used for design. Minor modifications of charring rates can additionally be applied, based on wood types and density as provided by the Eurocode (EC5 1994).

To assess the variations in charring rates with differing fire severities, a nominal 1000 x 90 x 90 mm 'dummy' column was installed within each fire test compartment.

3.8.2 Dummy Column Experimental Setup

Location and general installation of the columns are shown in Figures 3.26-3.28.

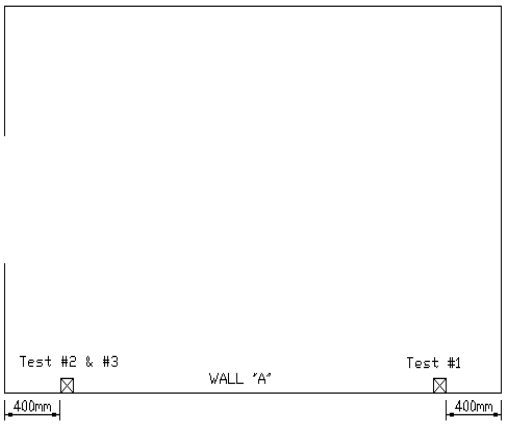

Figure 3.26 – Dummy column layout

The dummy column, as shown in Figure 3.27, was located at a height, such that the sheath thermocouples were at a height of 1800mm above the floor level (i.e. the same as the tree thermocouple height).

Figure 3.27 – Dummy column installation (typical)

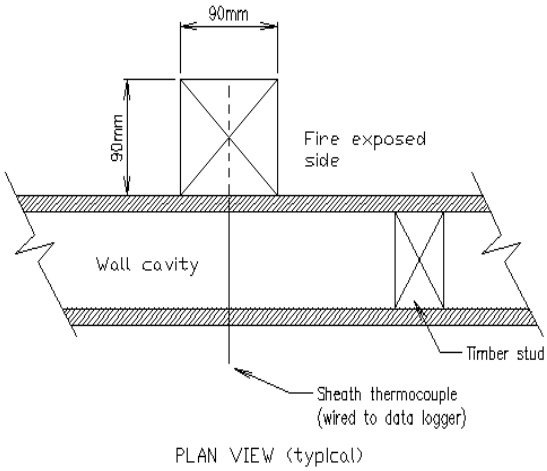

Figure 3.28 – Dummy column installation plan section (typical)

For each test, the untreated Radiata pine timber column was instrumented internally with sheathed thermocouples, to enable readings of the temperature distrbution through the timber column to be recorded for points at distances of 5, 10, 20, 30, 40 and 50mm from the fire exposure. The thermocouples general arrangement and wiring can be seen in Figures 3.29 and 3.30.

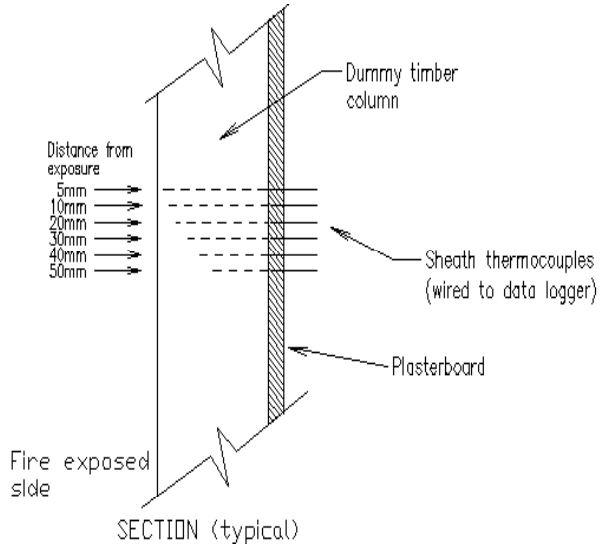

Figure 3.29 – Dummy column thermocouple positioning

Figure 3.30 – Dummy column thermocouple installation and wiring

The exposure of the fire, for each test column location, was taken as the nearest tree thermocouple to the column in that test. Table 3.15 summarises the reference number of the thermocouple tree and height of the thermocouple from which the fire severity at the dummy columns were taken. For locations of thermocouple trees, refer to Section 3.9.1.

Test Reference	Tree Location Reference	Height of thermocouples (mm)
#1	1 and 2 (average)	1800
#2	6	1800
#3	6	1800

Table 3.15 – Dummy column fire exposure thermocouple tree and height reference

3.9 Instrumentation

3.9.1 Thermocouples

3.9.1.1 Fire Exposed Thermocouples

The principal instrumentation for measurement of fire exposure within each of the test compartments consisted of thermocouple trees located 100mm from each test wall assembly and a single thermocouple tree at the centre of the compartment. Figure 3.31 shows the layout of the thermocouple trees for each test.

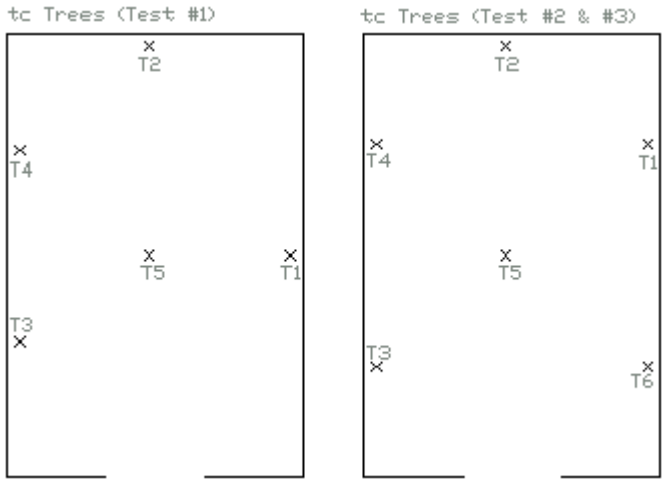

Figure 3.31 – Compartment thermocouple tree layout

Tree thermocouples consisted of Type K Alumel/Chromel, 24 gauge, 0.5mm diameter, glass braid insulated and sheathed thermocouple wire with crimped tip thermocouples. Thermocouples were installed at heights as shown in Table 3.16. A thermocouple located at the ignition source (Figure 3.18) was to the same specification as for the tree thermocouples.

Additionally, sheathed thermocouples were installed at height of 2300mm from floor level through each wall assembly (with the exception of Assembly 2 in Test #1. The sheathed thermocouple tip was located 100mm from, and central to, the wall assembly (Figures 3.32-3.34). These were employed as a back up of data in case any of the tree thermocouples were to get damaged, or malfunction, during the test. The wall penetrations for the sheathed thermocouples were stopped to maintain wall integrity.

Test Reference	Thermocouple Heights above floor (mm)					
	Tree 1	Tree 2	Tree 3	Tree 4	Tree 5	Tree 6
#1	1800 1100 600	1800 1200 600	1440 960 480	1800 1200 600	2400 2300 2100 1800 1200 300 100	-
#2 and #3	1800 1100 600	1800 1200 600	1800 1200 600	1800 1200 600	2400 2300 2100 1800 1200 300 100	1800 1100 600

Table 3.16 – Tree thermocouple locations and height positioning

3.9.1.2 Compartment Assemblies Thermocouples (Non fire exposed)

Measurement of temperatures within the various test assemblies was carried out to be comparable with similar measuring locations used for each assembly's respective standard fire

test. Disc thermocouples of type K, 0.5mm wire silver soldered to 12mm diameter x 0.2 nun thick copper disc, with 30mm square insulating pads were used for temperature measurement through the assemblies. Insulating pads were removed for temperature measurement of the unexposed lining within the cavity. The positions at which the disc thermocouples were located on the assemblies are indicated in Figures 3.32-3.35.

Disc thermocouples within the assemblies were located on the unexposed face, unexposed lining in the cavity, mid cavity, and exposed lining within the cavity, for both the hour rated and half hour rated assemnlies, where Figure 3.3 shows locations for assembly 1 and 5, Figure 3.4 shows locations for assembly 2 and 6, Figure 3.5 shows locations for assembly 3 and 7, and Figure 3.6 shows locations for assembly 4 and 8. Assembly 9 (fire door) thermocouples were all located on the unexposed face only.

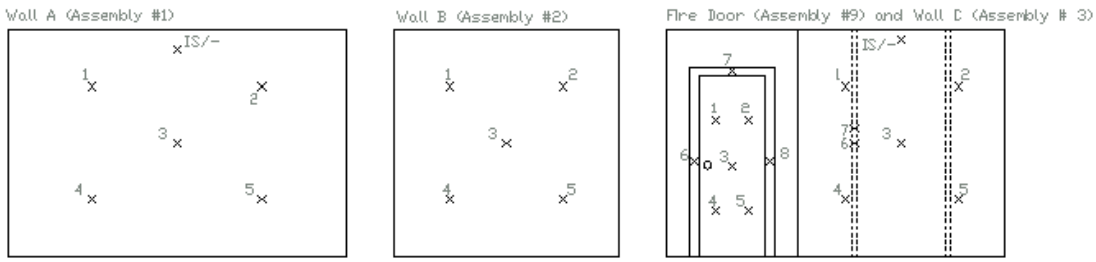

Figure 3.32 – Thermocouple positions (elevation view) on wall and door assemblies – Test#1

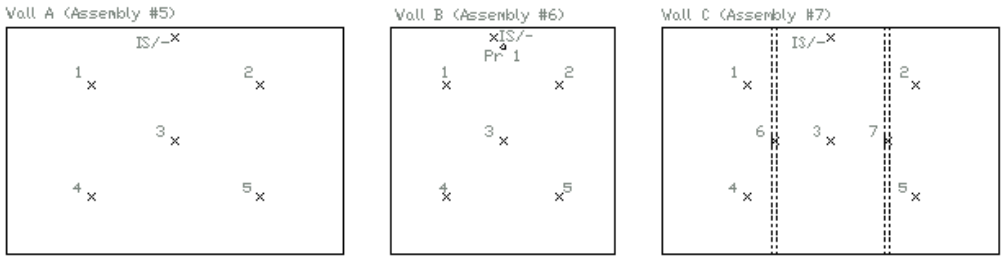

Figure 3.33 – Thermocouple positions (elevation view) on wall assemblies –Test#2

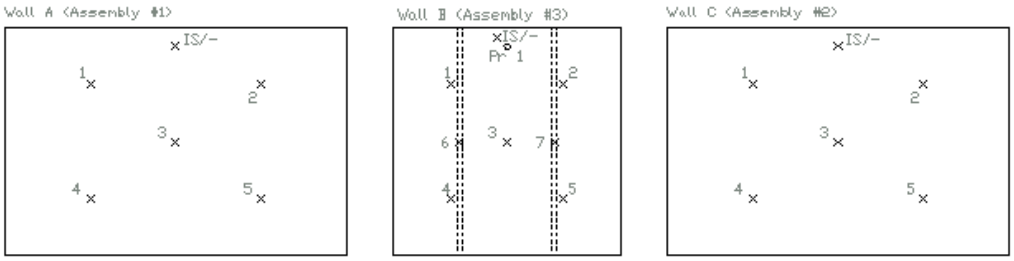

Figure 3.34 – Thermocouple positions (elevation view) on wall assemblies –Test#3

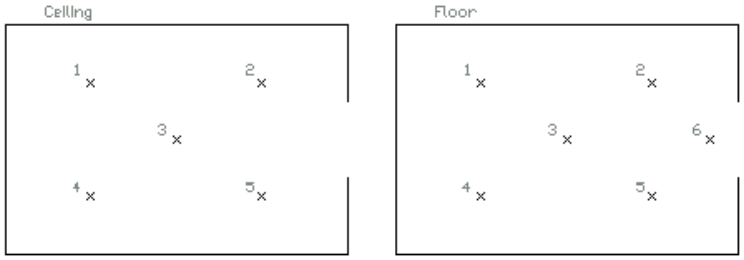

Figure 3.35 – Thermocouple positions (plan view) on ceiling and floor assemblies –Tests #1 - #3

For temperature measurement at the steel studs, twisted end Type K thermocouple wire was riveted to the studs at locations within the studs, as shown in Figure 3.5.

All thermocouple wiring external to the compartment was carried out using PVC insulated type K thermocouple wire.

To assist Winstone Wallboards Ltd in their assessment of thermal characteristics of a new flooring product, thermocouples were included to measure the temperature profiles between the compartment floor linings. The location of the disc between the compartment floor lining is indicated in Figure 3.8. Evaluation and assessment of the results is beyond the scope of this project, and is not discussed further in this report.

In excess of one hundred thermocouples were used in each compartment test and connected to the data logger (Figure 3.36). Thermocouple data logger channel reference tables are included in the Appendices of this report.

Figure 3.36 – Data logger acquisition equipment

3.9.2 Load Cells

To assist research by others in developing an empirical model for fire compartment temperatures (Barnett 2002), four electronic load cells were used to measure the mass loss rate of the compartment during each test. The load cells were located at the end of each beam supporting the compartment, to evenly distribute the mass of the compartment to each cell, as shown in Figure 3.37.

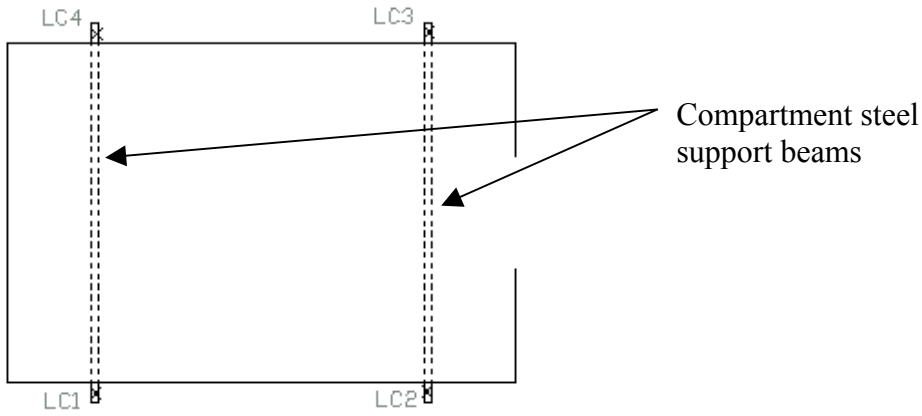

Figure 3.37 – Load cell locations

3.9.3 Pressure Probes and Measurement

Following Test #1, it was decided that obtaining compartment pressures would be beneficial to validating many of the results obtained. Therefore, a stainless steel seamless pressure probe and manometer, connected to the load cell data acquisition equipment was applied. The location of the probe was central in Wall B at a height of 2300mm above the floor (Figures3.33 and 3.34), with the probe tip 200mm away from the wall assembly.

3.9.4 Video and Photographic Equipment

A stationary video camera was located in front of the compartment at a distance of approximately 15m from the compartment. Additionally, a roving video camera was utilised during each test to record events at all external locations of the test compartments. Numerous cameras were used during each test by various people, enabling photos of all external compartment locations to be taken for incorporation into the report.

4 Compartment Test Results

4.1 General

This section of the report describes the compartment temperatures during each test, highlighting significant events that were observed, which may have impacted the severity of the test fire at any given time. The general compartment fire behaviour and exposures for each test are described in relation to the centrally located thermocouple tree 5.

Additionally, the results obtained, from both the load cells and pressure monitoring equipment, during the tests are provided in this section. A detailed analysis of these results is beyond the scope of this report.

4.2 Compartment Test #1 Fire Exposure

The compartment temperatures at each thermocouple on tree 5, from the time of ignition, are shown in Figure 4.1. Additionally plotted on the graph, is the ISO 834 standard fire exposure curve, and the predicted fire severities derived using the Eurocode modified parametric curve and BRANZ fire (Sections 3.7.5 and 3.7.6 respectively).

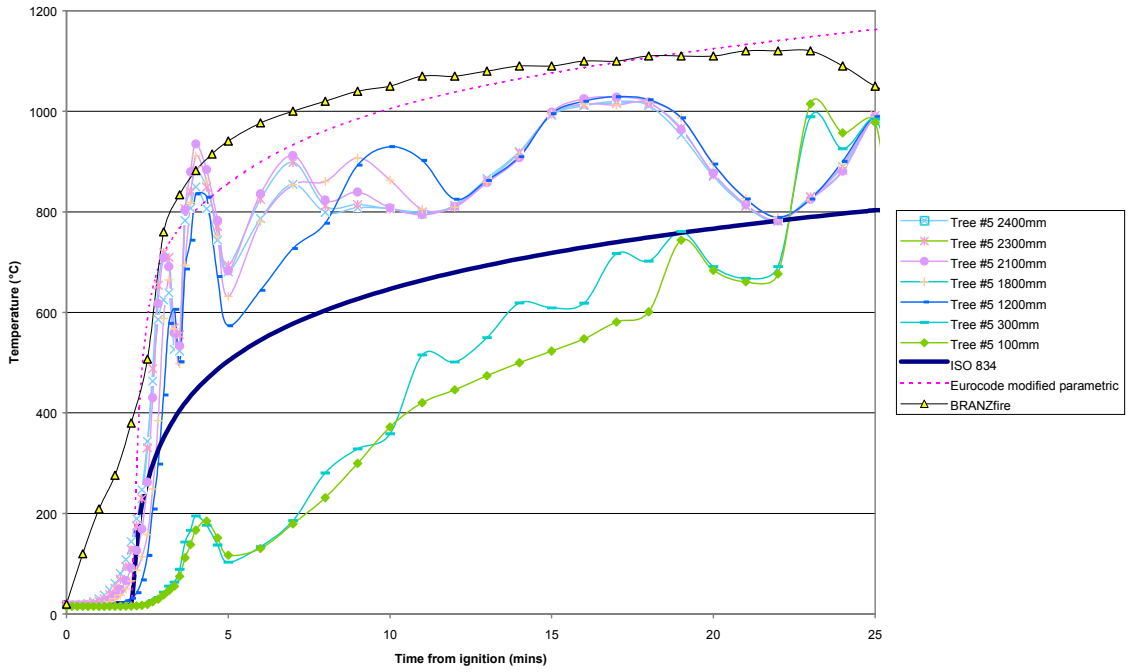

Figure 4.1 – Compartment test #1 exposure at tree 5

Test #1 flashover occurred at 3 minutes 30 seconds after ignition, with the temperature peaking at 950°C shortly after this. This burning was observed to be almost entirely that of the PU foam and fabric cushions. Beyond the peak, from 4 minutes and 15 seconds, the severity of the fire can be seen to diminish to approximately 700°C, due to the cushion burning being in decay. From 5 minutes onwards, crib burning then takes over as the dominant burning regime, raising the temperature to 900°C at 7 minutes, and becoming the sole fuel source when the cushions have totally burnt out. The exposure temperature then generally rises steadily during a period of ventilation controlled crib burning, until a point after 18 minutes, when the cribs begin to collapse within the compartment. This collapsing of cribs reduced the amount of surface area of wood fuel within the compartment and additionally blocked the ventilation opening (air supply) to some extent. This phenomenon would have resulted in a significant reduction of heat release, and the resulting drop in temperature is evident as temperatures fall from over 1000°C to below 800°C, between 18 and 22 minutes respectively. At 22 minutes, Wall C had a large integrity failure, which involved a section of the assembly falling outwards from the compartment. The new opening provided an increased air supply for the fuels to burn more readily, which can be seen by the increased temperatures from 22 minutes until the test was terminated at 25 minutes after ignition. The test was terminated earlier than originally had been envisaged, to protect neighbouring constructions from the exposure created when Wall C collapsed outwards.

4.3 Compartment Test #2 Fire Exposure

The compartment temperatures, from the time of ignition, are shown in Figure 4.2. Additionally plotted on the graph is the ISO 834 standard fire exposure curve, and the predicted fire severities derived using the Eurocode modified parametric curve and BRANZ fire (Sections 3.7.5 and 3.7.6 respectively).

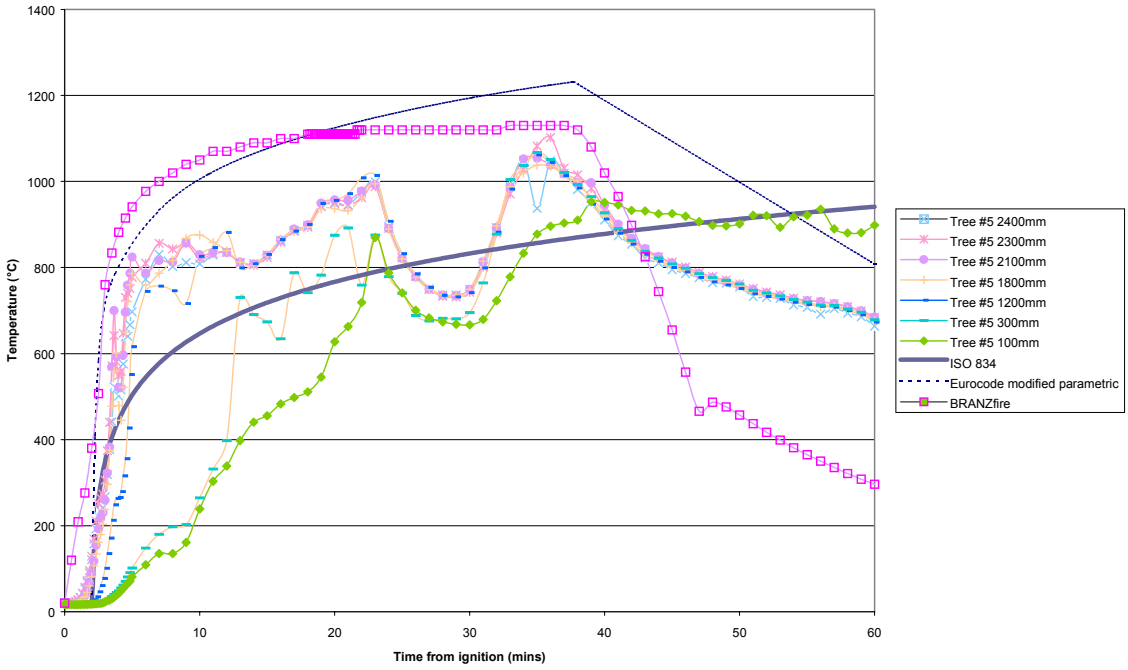

Figure 4.2 – Compartment test #2 exposure at tree 5

Test #2 flashover occurred at 4 minutes 30 seconds after ignition, with the temperature rising steadily beyond the initial peak of 900°C at 5 minutes. Beyond this time, cribs were observed to ignite at various locations, prior to the PU foam cushions having burnt out fully. This accounts for the smoother transition from foam to crib burning regimes, which is evident in test #2, with no considerable drop in temperatures, compared with the transition in test #1. At 6 minutes 30 seconds, the PU foam burning was observed, by a change in smoke colour, to have burnt out and crib burning then took over as the sole burning regime. Crib ventilation controlled burning continues, resulting in steadily rising temperatures until a point at 22 minutes, where an extremely significant fall in compartment temperature is observed (Figure 4.2). As described for test #1, this is the point when the cribs begin to collapse inwards within the compartment. This drop in temperature is more pronounced than was in test #1 due to the greater crib heights and volume of wood, which blocked the ventilation opening significantly. The resulting fall in compartment temperatures, from 1000°C to 700°C are largely due to a reduced air supply and additionally the reduction in the surface area of fuel exposed to the fire. At 30 minutes, the temperature begins to rise back to a temperature approaching 1100°C. This rise is the result of further breakdown of the cribs into smaller ember pieces at floor level, which unblocks the ventilation opening to allow more air into the compartment for combustion. Decay of the exposure commences from 36 minutes until the termination of the test at 60 minutes.

4.4 Compartment Test #3 Fire Exposure

The compartment temperatures, from the time of ignition, are shown in Figure 4.3. Additionally plotted on the graph is the ISO 834 standard fire exposure curve, and the predicted fire severities derived using the Eurocode modified parametric curve and BRANZfire (Sections 3.7.5 and 3.7.6 respectively).

Test #3 flashover occurred at 3 minutes 15 seconds after ignition, with the temperature peaking at 900°C shortly after this. This burning was observed to be purely that of the PU foam and fabric cushions. Beyond the peak, from 4 minutes and 30 seconds, the severity of the fire can be seen to diminish to approximately 750°C, due to the cushion burning being in decay. From 5 minutes onwards, crib burning then takes over as the dominant burning regime, raising the temperature to in excess of 900°C at 7 minutes, and becoming the sole fuel source when the cushions have totally burnt out. The exposure temperature then generally rises steadily during a period of ventilation controlled crib burning, until a point after 19 minutes, when the cribs begin to collapse within the compartment.

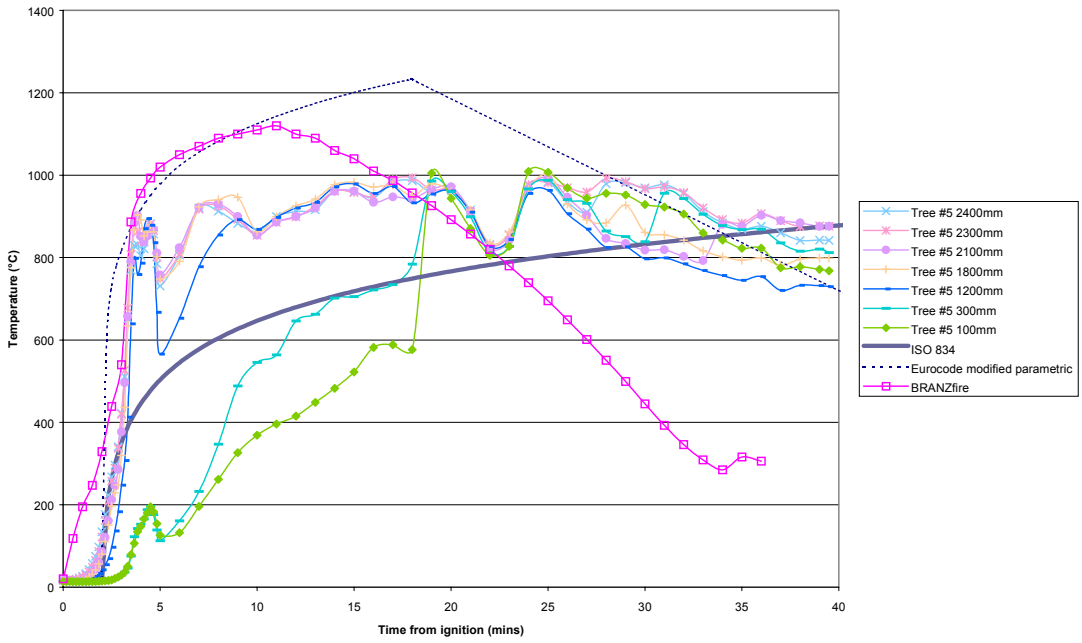

Figure 4.3 – Compartment test #3 exposure at tree 5

As described for test #1 and #2, this collapsing of cribs reduces the amount of surface area of wood fuel within the compartment and additionally blocked the ventilation opening (air supply) to some extent. The resulting drop in temperature is evident as temperatures fall from about 1000°C to below 800°C, between 19 and 23 minutes respectively. At 23 minutes 15 seconds,

Wall B had a large integrity failure, which involved approximately half of the assembly falling outwards from the compartment. The increased air supply enables more combustion to take place, resulting in the higher recorded temperatures, peaking at above 1000°C at approximately 25 minutes. After this point, the fire was clearly fuel controlled and decay was evident from observations. After 25 minutes 20 seconds, the ceiling lining fell within the compartment. It is believed that beyond this point the thermocouples within tree #5 collapsed from the supporting tree into the burning embers at floor level, due to the falling ceiling lining. Evidence of this pattern of exposure from within the burning embers is clearly evident for the 100mm high thermocouple in test #2 (Figure 4.2), which has clearly been immersed in fallen crib embers, whilst the other, higher thermocouples are not immersed and are recording the compartment fire decay. For this reason, no decay is evident from Figure 4.3. The actual decay can be seen from the data obtained, and is shown in the later sub-section, which discusses individual assembly exposures (Section 5.2.2).

4.5 Additional Comments of Test Fire Exposure Results

Crib stick sizes were limited by budget and availability of materials in the quantities required within the project program time for the experiments. As a result only 50mm x 50mm crib sticks could be obtained. Ideally larger sticks with smaller surface area would have been preferred, to ensure all combustion products from the fuels burnt within the compartment and prevent cribs from collapsing too early. Cribs falling over and suppressing the fire, with subsequent drop in severity, meant that the potential FLED did not burn as severely as possible for the maximum duration, or entirely within the compartment.

4.6 Test #1 Mass Loss History

The mass loss history for the compartment can be seen in Figure 4.4.

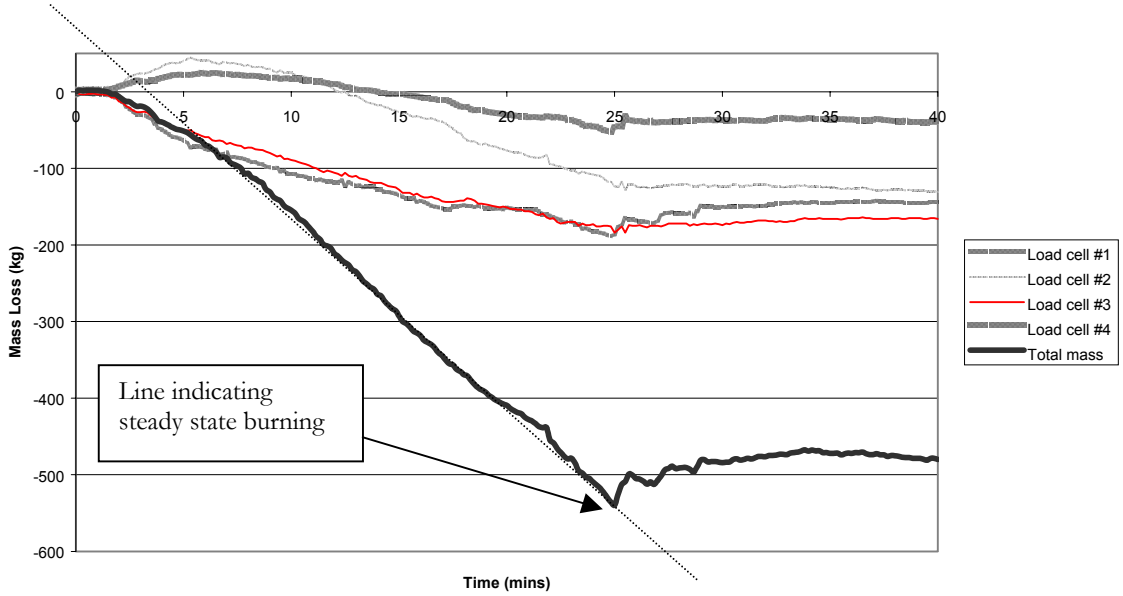

Figure 4.4 – Test #1 Compartment mass loss history

It can be seen in the graph that the mass at load cells 2 and 4 appears to increase in the initial stages for approximately 6 minutes, whilst load cells 1 and 3 appear to lose mass at an equivalent rate for a similar duration of time. These load cells are at opposite corners, and it seems reasonable to deduce that some minor twisting or deformation of the compartment in these early stages of burning has occurred. This assumption would appear to be reasonable in view of the total mass loss curve providing results, which concur with all observations and the time line of the compartment test, indicating that the total mass was redistributed to load cells 1 and 3.

The history of the total mass loss rate shows the initial increasing mass loss rate of the PU foam and olefin fabric cushions. There is a sharp increase in mass loss at 3 minutes 30 seconds after ignition, when flashover of the room occurred, possibly due rapid change in the average density of the room gases, resulting in a corresponding change in the mass of the gases in the room. This rise in mass loss rate occurs for approximately 45 seconds, at which point it was observed that the cushion combustion had completed and the wood crib slower burning rate continued. From approximately 4 minutes 15 seconds after ignition, the wood crib mass loss rate increases steadily until a point when steady state mass loss is evident between the times of 9-17 minutes after ignition. The end of the steady mass loss rate at 17 minutes after ignition corresponds with the time at which the cribs began falling and the fire began being suppressed due to a reduction in oxygen levels created by fallen cribs blocking the air path into the compartment and

additionally due to reduced exposed surface area of burning materials. This slow decline in the mass loss rate is evident until 21minutes 55 seconds, when Wall C failed. At failure of Wall C, there is a rapid mass loss of 16.4kg over a 10 second monitoring period, which can be attributed mainly to the weight of the wall structure falling away from the compartment. The resulting opening created by the linings of Wall C falling outwards allowed more air into the compartment and an increased level of burning mass loss rate is evident, until 23 minutes 30 seconds, when the Wall A integrity failure created an additional opening. At this time, another mass loss of 10 kg over a 10 second period can be attributed to the mass of the Wall A structure falling outwards from the compartment. From this time, until the test was terminated at 25 minutes, the mass loss continues at a generally steady rate.

The total mass loss over the 25 minute duration of the test was 540kg. This is the combined mass loss from combustion, moisture draw off from plasterboard and wood construction elements, and additionally the mass loss due to construction elements collapsing away from the compartment due to integrity failure. The moisture loss due to re-hydration of the gypsum plasterboard is estimated to rise to approximately 60kg at 15 minutes based on a 20% weight loss of the internal fire exposed linings.

4.7 Test #2 Mass Loss History

The mass loss history for the compartment can be seen in Figure 4.5. It can be seen that the apparent twisting/deformation of the compartment, as observed in Test #1, has not occurred in Test #2.

The history of the total mass loss rate shows an increasing mass loss rate until approximately 12 minutes, when steady mass loss from the compartment is evident. The end of the steady mass loss rate at 22 minutes after ignition corresponds with the time at which the cribs began falling and the suppressed the fire due to a reduction in oxygen levels created by fallen cribs blocking the air path into the compartment and additionally due to reduced exposed surface area of burning materials. This slow decline in the mass loss rate is evident until 37 minutes, when Wall C failed. When failure of Wall C occurred, there is a rapid mass loss of 13kg over a 10 second monitoring period, which can be attributed mainly to the weight of the wall structure falling away from the compartment. The resulting opening created by the linings of Wall C falling outwards allowed more air into the compartment. However, the fire was well into decay by this

time, and even with the additional air supply created by the collapse of Wall C, no increased burning rate occurred. Decay continues at the rate similar to that prior to the wall collapse, until the time of the test termination at 60 minutes.

The total mass loss over the 60 minute duration of the test was 931kg. This is the combined mass loss from combustion, moisture draw off from plasterboard and wood construction elements, and additionally the mass loss due to construction elements collapsing away from the compartment due to integrity failure. The moisture loss due to re-hydration of the gypsum plasterboard is estimated to rise to approximately 80kg at 15 minutes based on a 20% weight loss of the internal fire exposed linings.

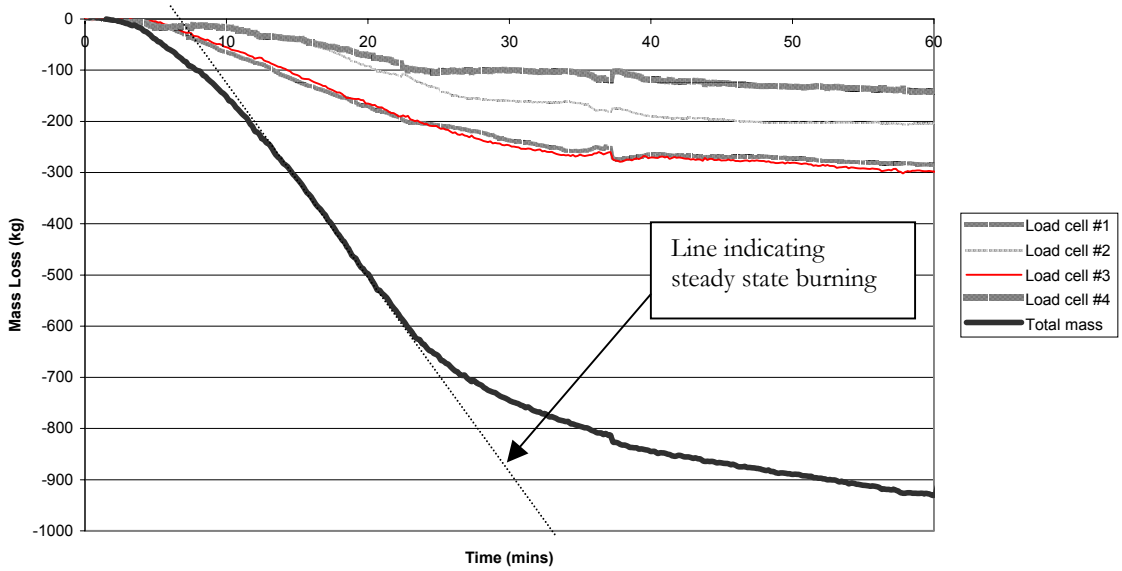

Figure 4.5 – Test #2 Compartment mass loss history

4.8 Test #3 Mass Loss History

The mass loss history for the compartment can be seen in Figure 4.6. Load cell #3 malfunctioned during the course of the test and no results for that cell were obtained, so no specific details of the fire can be seen graphically in the mass loss history. However, an estimate of load cell #3 mass loss has been made to give an indication only.

Based on the mass loss profiles shown in Tests #1 and #2 (Figures 4.4 and 4.5 respectively), the cells appear to experience similar mass loss measurement of the corresponding opposite corner load cell. Therefore the estimate of load cell 1 has been derived from the value of load cell 3, plus or minus the difference between cells 2 and 4. This provides a general total

mass loss history as shown in Figure 4.6. When plotted against the total mass loss of test #1, test #3 has a larger/quicker mass loss, which would be expected from the more severe fire.

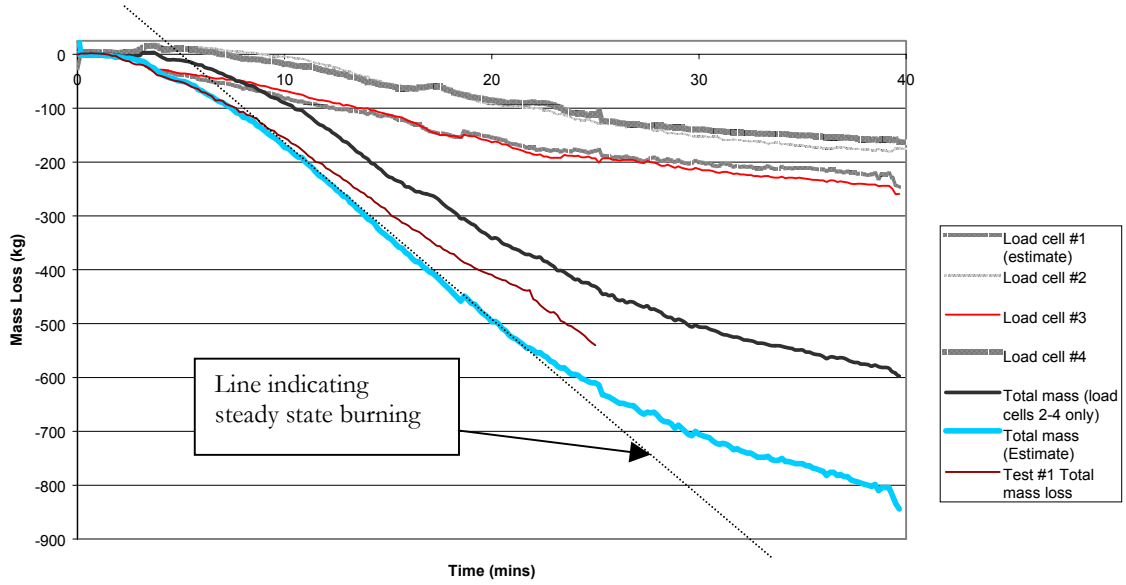

Figure 4.6 – Test #3 Compartment mass loss history

4.9 Assembly Failure Times and Fire Exposures

4.9.1 General

The various failure times in the tests, of each assembly, is given in this section of the report.

For ease of reading of this report, only those assembly temperature profiles which have been used for analysis, and are referred to, are incorporated in the main body of the report. All further temperature profiles of assemblies are included in the Appendices of this report for further information only.

4.9.2 Test Errors and Omitted Thermocouple Readings

It should be noted that in Test #1, the disc thermocouples located on the inside of the unexposed linings, within the cavity, were installed with the pads still attached to them for all construction assemblies. This resulted in the pads insulating the disc thermocouple from the heat on the fire-exposed side, suppressing the temperature readings obtained during the early stages of heat development (generally assumed to be up to temperatures of 100°C). Such readings were not considered to be unrepresentative for temperatures above 100°C. Above this

temperature, it is assumed that any insulating moisture, or the like, within the pads has been drawn off, and the pads will be approximately the same temperature as the unexposed lining in the cavity. The results for the Wall A, B and C beyond 100°C are therefore included for analysis. Assembly #4 ceiling temperatures within the cavity on the unexposed panel are not included for analysis, as temperatures recorded did not exceed 100°C.

Two disc thermocouples that malfunctioned during test #1 have been excluded from any analyses and calculations conducted. These thermocouples were on differing assemblies and are considered to not affect the significance of the results obtained.

4.9.3 Assembly Times to Failure

From test observations, collected data, and by assessment where appropriate, the assembly times to failure, t_{fail}, from the start of exposure, as shown in Table 4.1 have been obtained.

Assembly Reference	Test Ref.	Standard test failure time (mins)	Test Time to Failure (mins)		Compartment Test Mode of Failure
			From Ignition	From Exposure,t_{fail}	
1	#1	42	23	21	Insulation
1	#3	42	20	18	Insulation
2	#1	39	38	36	Insulation
2	#3	39	26	24	Insulation
3	#1	34	21	19	Integrity
3	#3	34	19	17	Integrity
4	#1	55	32	30	Structural
4	#3	55	30	28	Structural
5	#2	68	53	51	Insulation
6	#2	58	57	55	Insulation
7	#2	63	37	35	Integrity
7 (Jones 2001)	BRANZ FP2881	63	-	28	Integrity
8	#2	74	-	$58 < t_{fail} < 75$	Structural
9	#1	32	22	20	Integrity

Table 4.1 – Test assemblies fire resistance failure times

4.9.4 Assembly Failure Mode Descriptions

Assembly 1 was deemed to have failed under the insulation criteria in tests #1 and #3 when darkening and scorching became apparent on the unexposed face. Since the scorching observed was not in the general location of the wall thermocouples, recorded temperatures did not achieve an average temperature rise of 140°C, or a peak rise at a thermocouple of 180°C. However, these specific failure temperatures were being approached, as can be seen in Figure 4.7.

Assembly 2 did not fail within the duration of tests #1 and #3 respectively. As a result, failure of this assembly, under the insulation criteria, was derived, by the author, 'by assessment'. This assessment of the failure time is described in detail in the following sub-section (4.9.5).

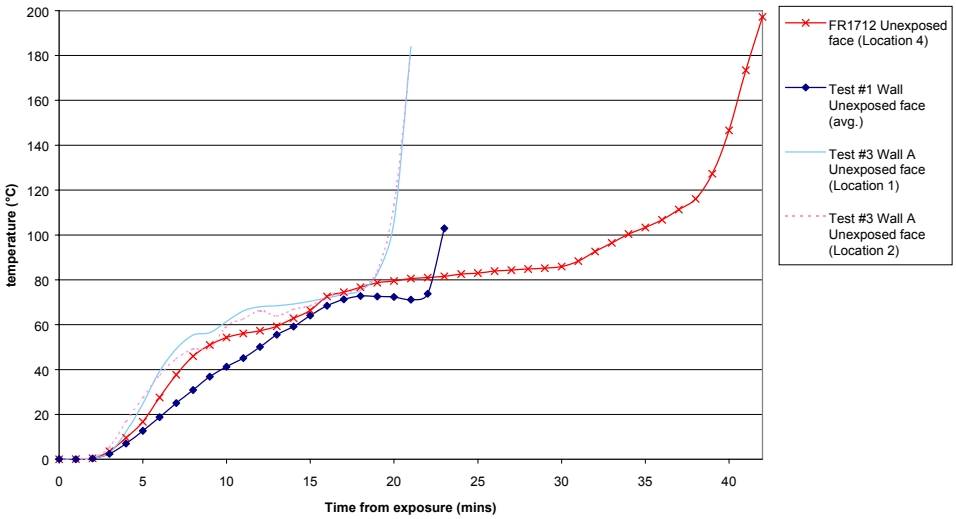

Figure 4.7 - Assembly 1 unexposed face temperature rise profiles at failure locations

With reference to the LSF assemblies 3 and 7, it is clear from the Table 4.1, that when exposed to a fire of higher severity than the standard fire in the early stages, these assemblies fail on the integrity criteria significantly sooner than the unexposed face temperature profiles would indicate (Figures 4.8 and 4.9).

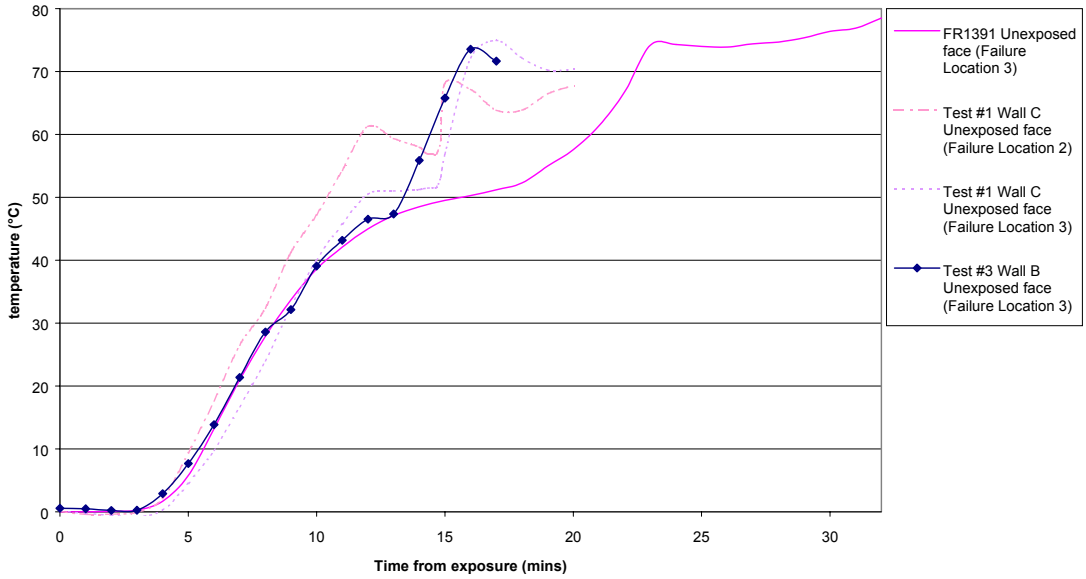

Figure 4.8 - Assembly 3 unexposed face temperature rise profiles at failure locations

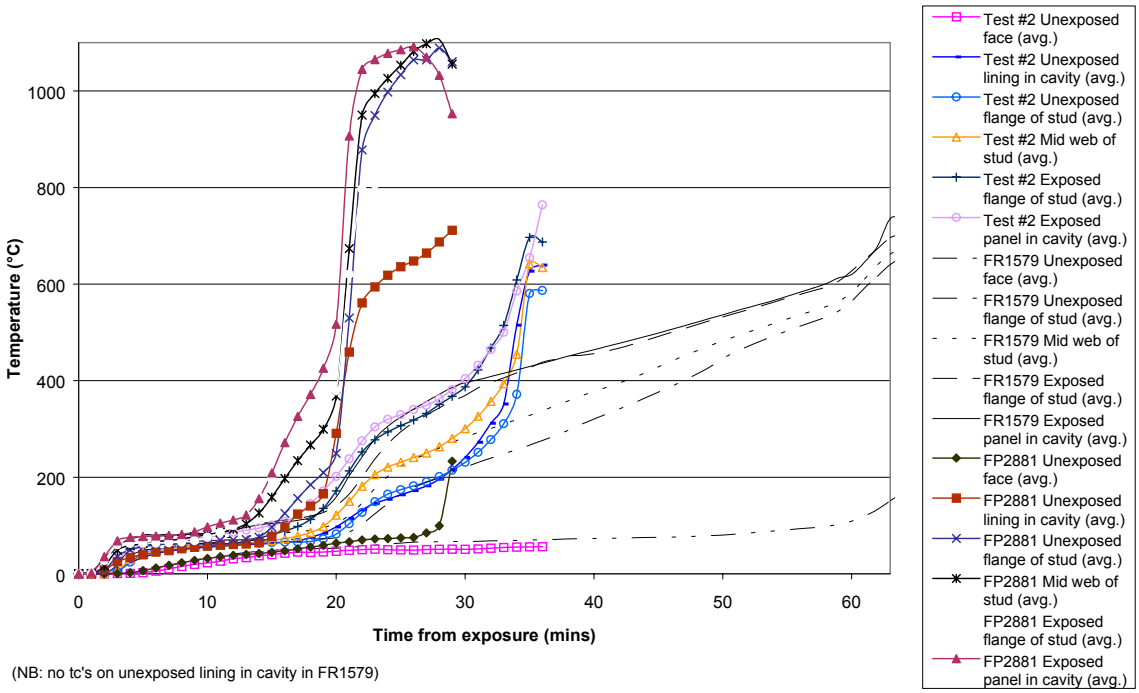

Figure 4.9 - Assembly 7 temperature rise profiles at failure locations

The failures of Assemblies 3 and 7 in all tests, as observed, were caused by rapid and sizeable deflections in the steel studs, which effectively made the unexposed linings 'pop out' from the framing. It is worth noting that Assembly 7 also failed on the integrity criteria in the pilot furnace test research undertaken by Jones (2001 and BRANZ FP2881), as described previously in Section 2.5.2.

With reference to the ceiling floor assemblies 4 and 8, the failure times, which have been assessed by the author (refer to Sub-section4.9.6 and 4.9.7), have been assumed to be to failure under the structural criterion. This assumption is deemed reasonable, as the standard test failures for these assemblies also occurred under the same failure mode.

Assembly 5 was deemed to have failed under the insulation criteria in test #2 at 57 minutes due to a peak rise at a thermocouple (Location 3) of 180°C. This rise can be seen in Figure 4.10.

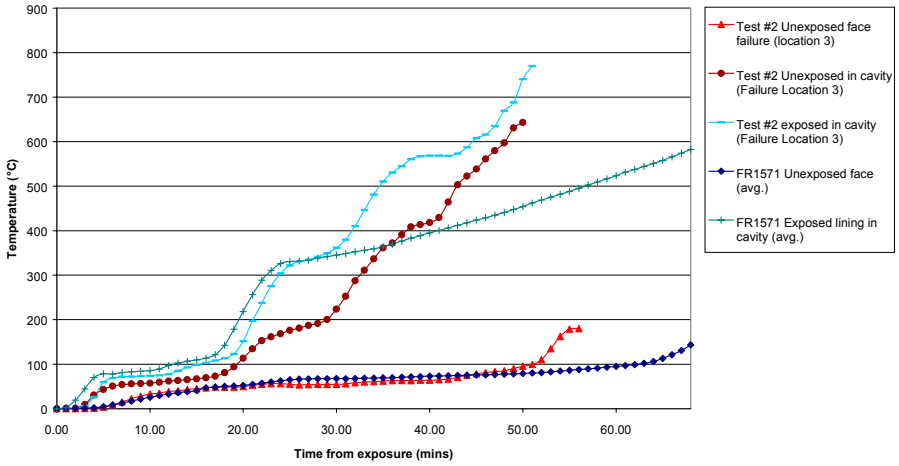

(NB: no thermocouples on unexposed cavity lining in FR1571)

Figure 4.10 - Assembly 5 temperature rise profiles at failure locations

Assembly 6 was deemed to have failed under the insulation criteria in test #2 due to darkening and scorching apparent on the unexposed face. Since the scorching observed was not in the general location of the wall thermocouples, recorded temperatures did not achieve an average temperature rise of 140°C, or a peak rise at a thermocouple of 180°C. However, these specific failure temperatures were being approached, as can be seen in Figure 4.11.

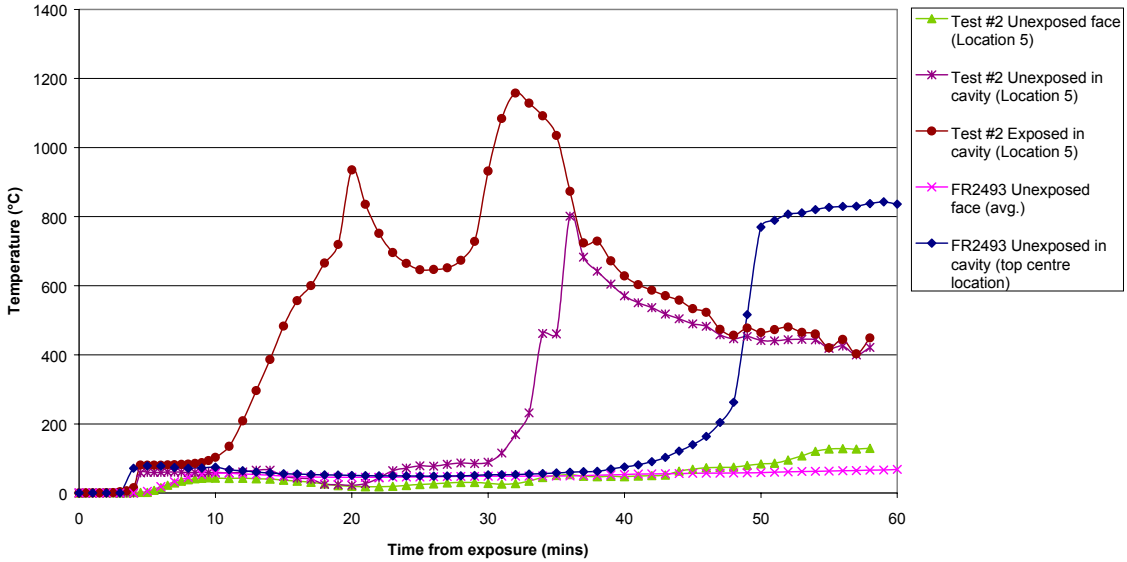

(NB: no thermocouples on exposed lining in cavity in FR2493)

Figure 4.11 - Assembly 6 temperature rise profiles at failure locations

Assembly 9 was deemed to have failed on the integrity criteria, when flames were protruding from the top corner of the door. This is a typical mode of failure for this type of fire door in standard fire tests.

4.9.5 Time to Failure of Assembly 2 in Tests #1 and #3 'by Assessment'

Assembly 2 did not fail during the duration of tests #1 and #3. Therefore, failure times to the actual and predicted exposure have been obtained by the author's assessment, using the compartment test data and the standard test data (BRANZ FR2454). The following assessment of compartment test failure times is carried out with reference to Figures 4.12-14.

In test #1, assembly 2 did not fail within the 25 minute duration of the test. Figure 4.12 shows the exposure to the wall assembly in tests #1 and #3, and shows that the test #1 exposure is slightly more severe in the first 5 minutes of exposure than the standard ISO 834 fire exposure, after which time, the exposure becomes very similar to that of the standard curve.

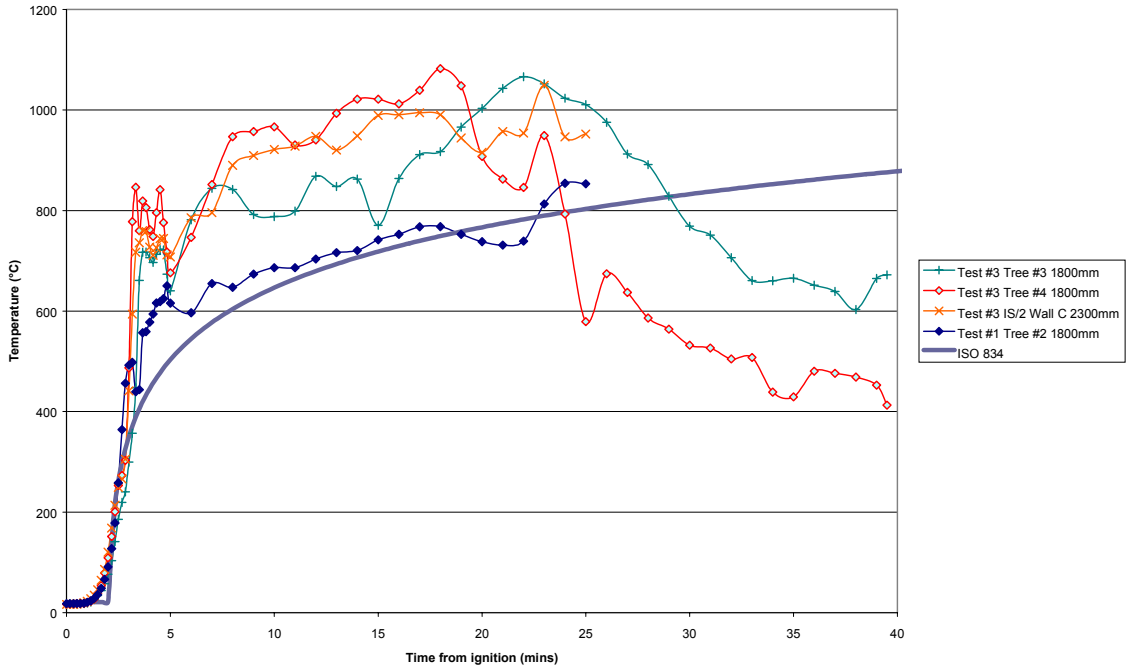

Figure 4.12 – Assembly 2 fire exposures

Therefore, using the temperature on the unexposed face as a reference (Figure 4.13), it can be seen when comparing the test #1 and standard furnace test (BRANZ FR2454) results that there is a lag of 3 minutes to reaching the first temperature plateau (at 9 minutes from the start of exposure) in the standard test results. Since beyond this point, test #1 can be assumed to have the equivalent standard ISO834 fire exposure, the failure time is reasonably estimated at 36 minutes from exposure 'by assessment'.

The failure time for Assembly 2 in test #3 was necessary, since 13mm gypsum 'Fyreline' plasterboard was used as an external lining instead of the specified 10mm required to give the nominal half hour assembly (refer to Assembly 2 system description in Section 3). As a result, the assembly did not fail in the duration of test #3. Referring to Figure 4.13, which shows the temperature profiles of the unexposed face of Assembly 2, the moisture draw off temperature plateau in the test #3, occurs between 7 and 28 minutes from the start of fire exposure.

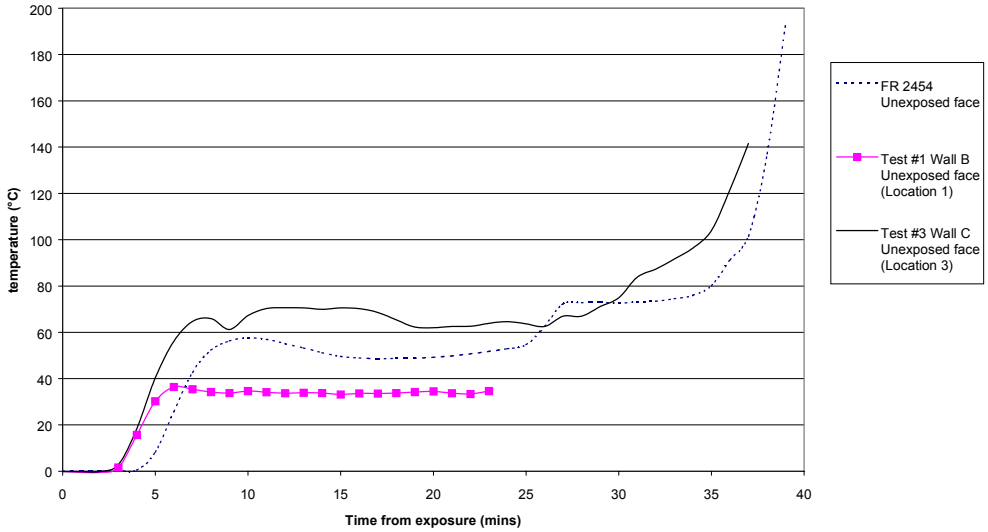

NB: Test #3 Wall C had 13mm Fyreline Plasterboard installed instead of specified 10mm

Figure 4.13 – Assembly 2 unexposed face temperature rise profiles at failure locations

Since the fire exposure and temperature at the unexposed panel in the cavity are relatively constant during this period of time (Figure 4.12 and 4.14 respectively), it can be assumed that the time for moisture draw off is proportional to the thickness of the lining.

Therefore, moisture draw off from 10mm of plasterboard lining will equate to $\frac{10mm}{13mm} \times (28-7)$, giving an equivalent temperature plateau of 16 minutes. Therefore the temperature plateau would end at 23 minutes from exposure (had 10mm lining been used). From the end of the moisture draw off plateau, the conduction calculation as described in Section 3.5.1, and obtained by Equations 3-1 to 3-3, where the average exposure temperature on the unexposed lining in the cavity is assumed constant at 500°C (Figure 4.14).

Failure due to an average temperature rise of 140°C occurs 1 minutes 50 seconds after the plateau ends (Figure 4.15), giving a rounded down failure time of 24 minutes for Assembly 2 in Test #3.

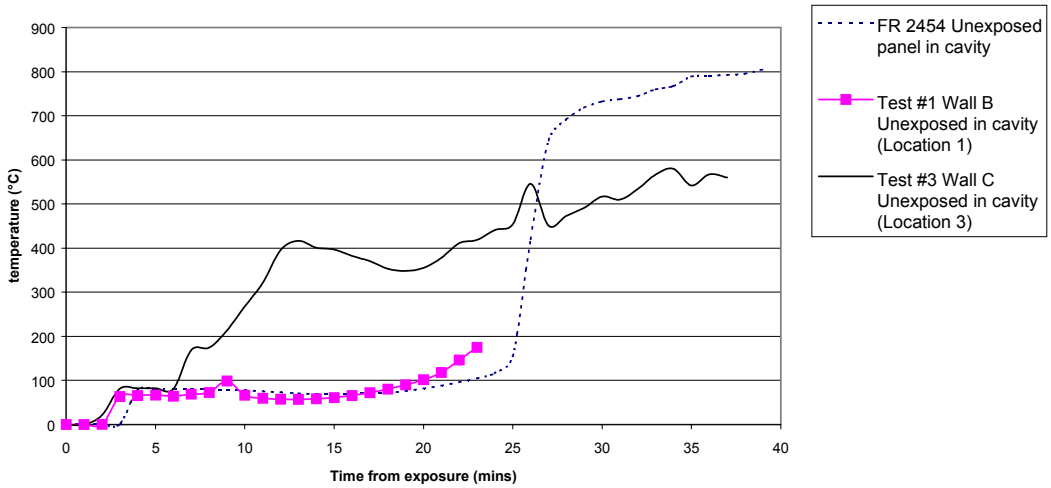

Figure 4.14 – Assembly 2 unexposed panel in cavity temperature rise profiles at failure locations

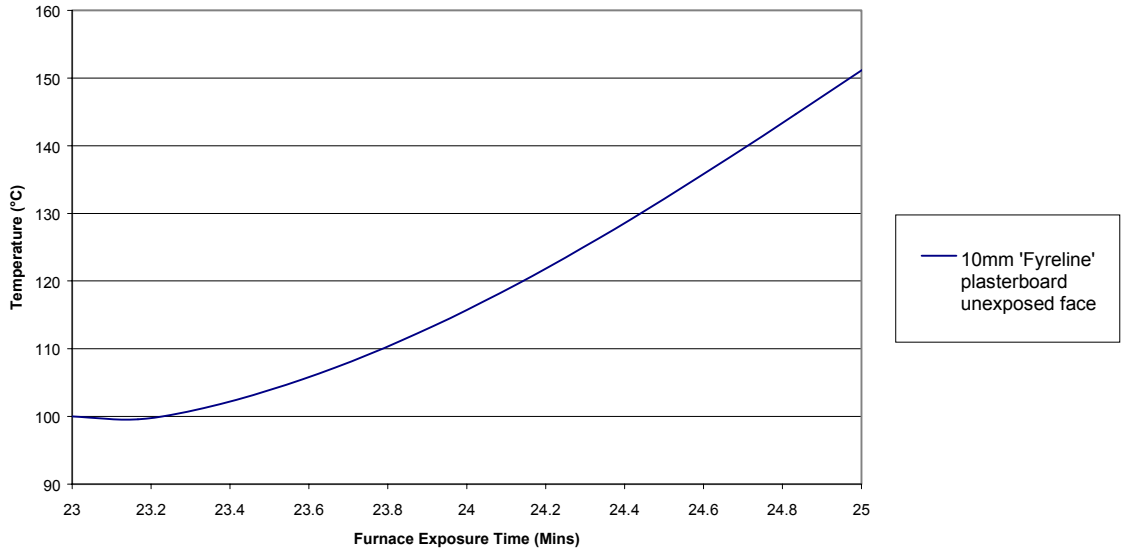

Figure 4.15 –Temperature rise of 10mm 'Fyreline' plasterboard to failure time - Assembly 2, test #3

4.9.6 Time to Failure of Assembly 4 in Tests #1 and #3 'by Assessment'

As it was not possible to test the ceiling/floor assembly for structural failure, as would be done in the standard furnace test, using an applied load, estimation of the failure times for Assembly 4 has been carried out using a comparison of the data obtained from the compartment tests and the standard fire test data (BRANZ FR1572). The following assessment of compartment test failure times is carried out with reference to Figures 4.16-18.

From Figure 4.16, which shows the assembly temperatures of the exposed panel in the cavity, the test results for test #1 and #3 show that the temperature at which the underside of the joists will begin charring (300°C) is reached within 18 minutes from exposure, for each test. In the standard test, this charring temperature is not reached until 24 minutes from the standard fire exposure. Therefore an additional 6 minutes of charring occurring at the underside of the timber joists is evident from the compartment test data.

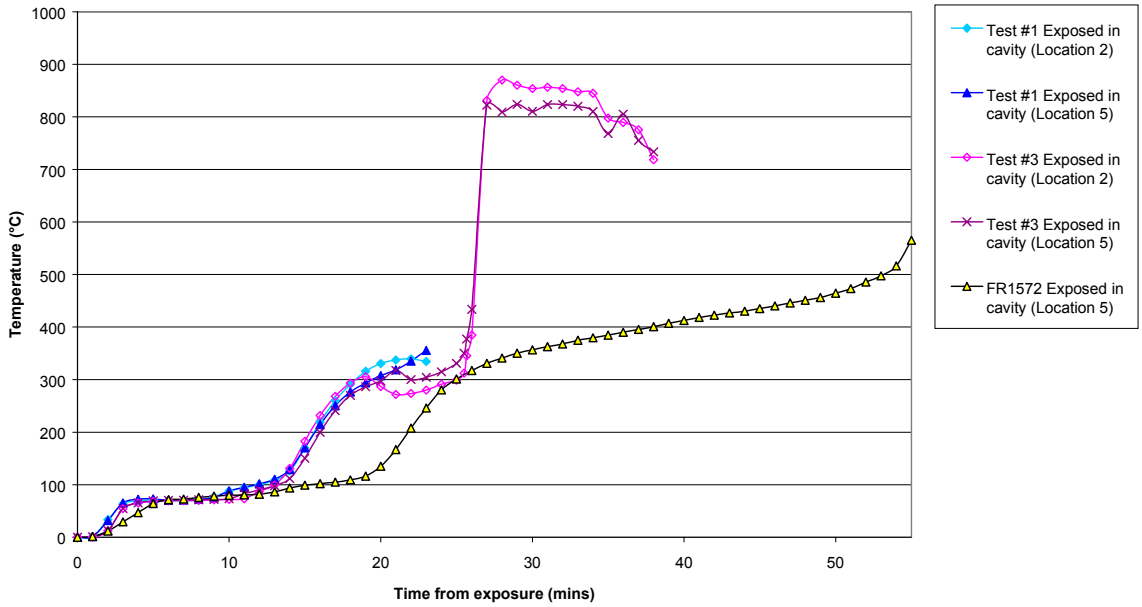

Figure 4.16 – Assembly 4 exposed panel in cavity temperature rise profiles at failure locations

The mid cavity profile, shown in Figure 4.17, indicates charring of the joist webs occurring once the ceiling lining has fallen. The time at which the plasterboard ceiling lining fell off in compartment test #3 at 23 minutes 35 seconds from exposure, exposing the joists to the fire exposure, is clearly evident by the rapid rise in temperature at this time. Mid web temperatures in the standard fire test do not reach charring levels until 50 minutes after exposure to the standard fire. 5 minutes after this, at 55 minutes, the assembly failed in the standard test. Since the charring of the web is considered to be the primary mechanism of early failure of the assembly, this time lag between commencement of web charring and failure to the standard test has been applied to the test #3, giving a failure time, by assessment of 28 minutes from exposure. There would be a higher mass loading applied during a standard fire test at 50-55minutes into the standard test, compared with that at a point 24-29 minutes into a test, which would make the 'assessment' appear to be too conservative. However, the increased charring

rates occurring to the web (refer to Section 4.10 of this report), as a result of the more severe fire exposure, are considered to be a reasonable trade off, such that the assessment is not deemed too conservative.

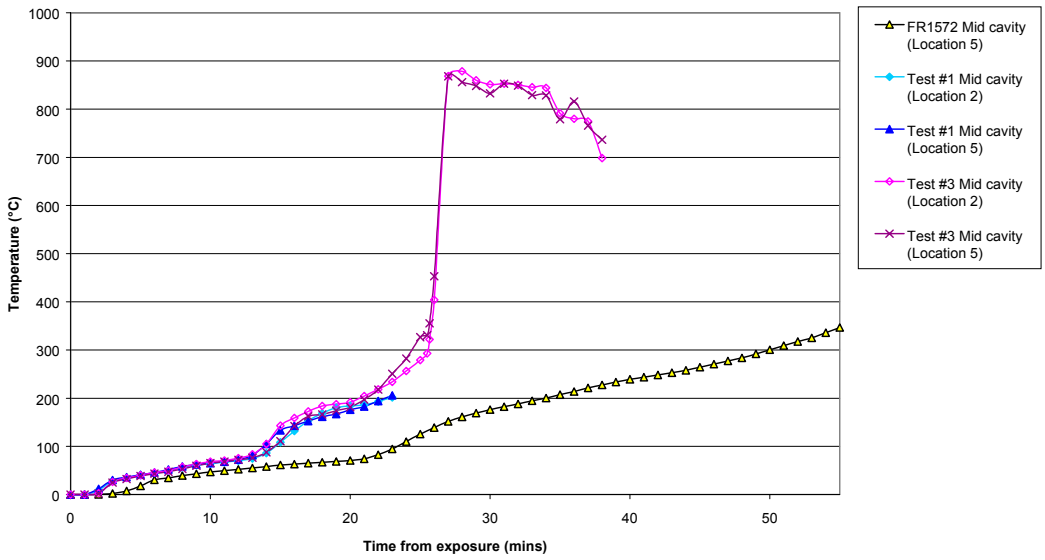

Figure 4.17 – Assembly 4 mid cavity temperature rise profiles at failure locations

A similar failure criterion can be applied to the test #1 ceiling/floor assembly, in which the ceiling lining had not fallen off by the time the test was terminated 25 minutes from ignition. At the time of test termination, the test #1 ceiling mid cavity temperatures as shown in Figure 4.17 Show that the cavity temperature has a lag of 2 minutes, compared with the corresponding test #3 mid cavity temperature. Extrapolating the temperatures based on the lag of 2 minutes provides a failure time of 30 minutes from exposure, by assessment. Although the test was terminated at 25 minutes after ignition, the continuing fire severity beyond this time, as predicted (Figure 4.18), would not have been expected to rapidly diminish below 900°C after the time of failure. This exposure is still considerably more severe than the standard fire test severity at that time, and leads to the conclusion that this 'assessment' of the fire severity and subsequent failure time of 30 minutes for assembly 4 in compartment test #1, is a reasonable assessment. Examination of the structural mechanisms of failure would lead to a more accurate assessment. However, such examination is beyond the scope of this project.

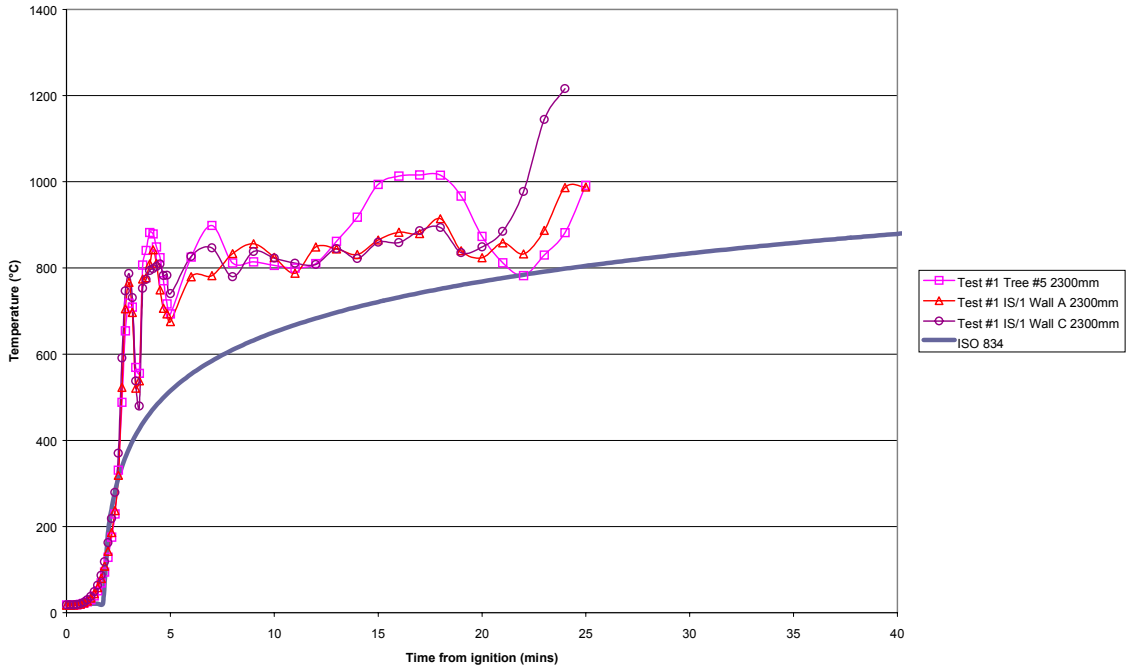

Figure 4.18 – Assembly 4 Test #1 fire exposure

4.9.7 Time to Failure of Assembly 8 'by Assessment'

As previously described for Assembly 4, it was not possible to test ceiling/floor assembly #8 for structural failure, as would be done in the standard furnace test, using an applied load. Therefore estimation of the failure times for Assembly 8 has been carried out using a comparison of the data obtained from the compartment tests and the standard fire test data (BRANZ FR1370). The following assessment of compartment test failure times is carried out with reference to Figure 4.19, which shows the temperature profiles through the test assembly.

Figure 4.19, which shows the assembly temperatures of the exposed panel in the cavity. The test results for test #2 show that the temperature at which the underside of the joists will begin charring (300°C) is reached within 31minutes from exposure. In the standard test, this charring temperature is not reached until 41 minutes from the standard fire exposure. Therefore an additional 10 minutes of charring occurring at the underside of the timber joists is evident from the compartment test data.

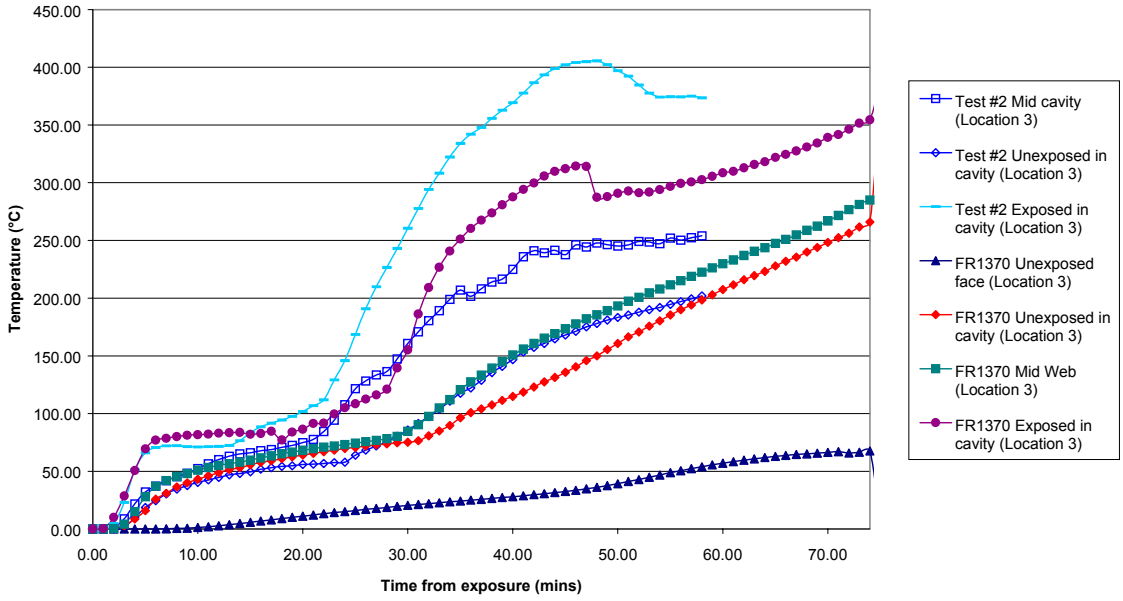

NB: Temperature results from thermocouples on unexposed lining in cavity ignored

Figure 4.19 – Assembly 8 temperature rise profiles at failure locations

It should be noted that the ceiling plasterboard lining did not fall from the joists during the test. The mid cavity profile, shown in Figure 4.19, indicates charring of the joist webs did not occur at any point in the duration of the test, suggesting no weakening of the strength of the beam within the web. Mid web temperatures in the standard fire test also did not reach charring levels during the 75 minutes of exposure to the standard ISO 834 test. By extrapolation, it can be seen that the compartment temperatures at all locations through the profile of the assembly are dropping off and falling to levels where, at 75 minutes they would be at, or below the temperatures recorded during the standard furnace test. This is a result of the exposure from the fire falling to temperatures below the standard ISO 834 exposure from 39 minutes into the compartment test (Figure 4.20).

The temperatures recorded in test #2 of the exposed lining in the cavity, suggest that the charring was occurring for a longer duration and at a marginally higher rate than the standard test. This factor, in conjunction with a similar increasing load, as would be applied to the assembly to test for structural resistance, suggest that Assembly 2 would fail structurally before the 75 minute standard furnace test failure time (BRANZ FR1370). The exact failure time, however, cannot be assessed from the temperature data alone. Structural analysis of this assembly's failure is beyond the scope of this project.

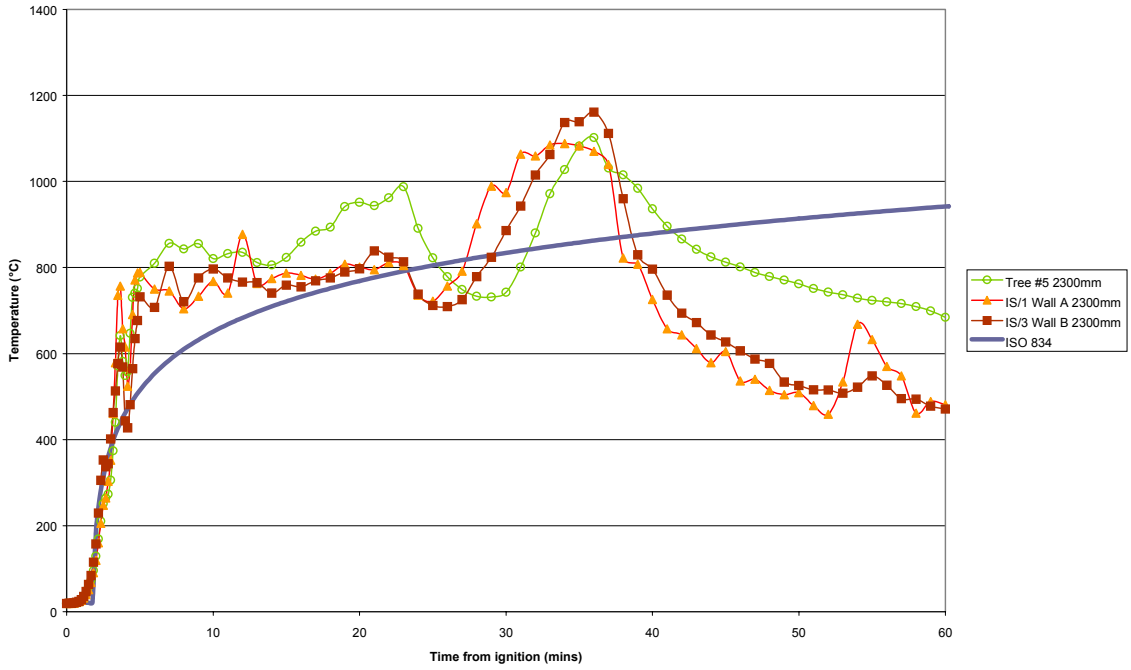

Figure 4.20 – Assembly 8 fire exposure

4.10 Charring Rates

Figures 4.21, 4.22 and 4.23 show the temperature profiles through the dummy column, and their associated fire exposures, for tests #1, #2, and #3 respectively. A brief description of the results will be provided in this section. Detailed analysis of the results is beyond the scope of this report.

In test #1, the sheath thermocouple, located 40mm from the fire exposure, malfunctioned during the test. However, as the duration of the test was relatively short and charring temperatures were not reached at the thermocouple 30mm from the fire exposure, this malfunction does not affect the results obtained.

Only the thermocouples 5mm and 10mm reached charring temperatures (300°C) in test #1 (Figure 4.21). Charring temperatures were reached at 13 minutes and 21 minutes from exposure, respectively.

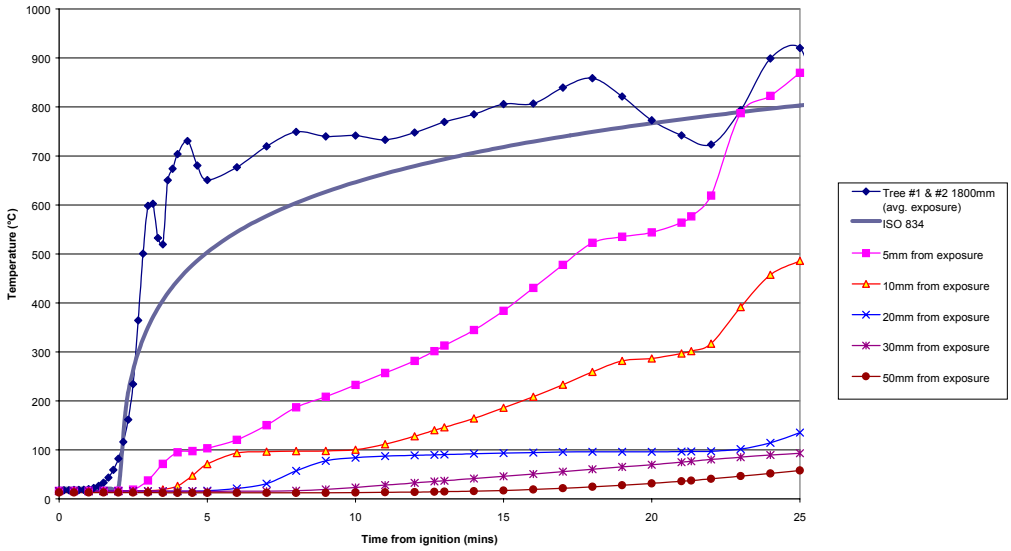

Figure 4.21 – Test #1 Dummy column exposure and temperature profile chart

All thermocouples in tests #2 reached charring temperatures at 16, 19, 30, 42, 44 and 46 minutes, for thermocouples 5 - 50mm from the fire exposure, respectively. It is apparent, from the relatively short duration of time between the three thermocouples furthest away from the fire exposure, that the dummy column had become thermally thin, and that the remaining core was exposed to the fire exposure from three sides. Therefore the calculated charring rates to these thermocouples, as shown in Table 4.2, are unrealistically fast. It is suggested that the charring rates to thermocouples 40mm and 50mm from the exposure be ignored for this reason.

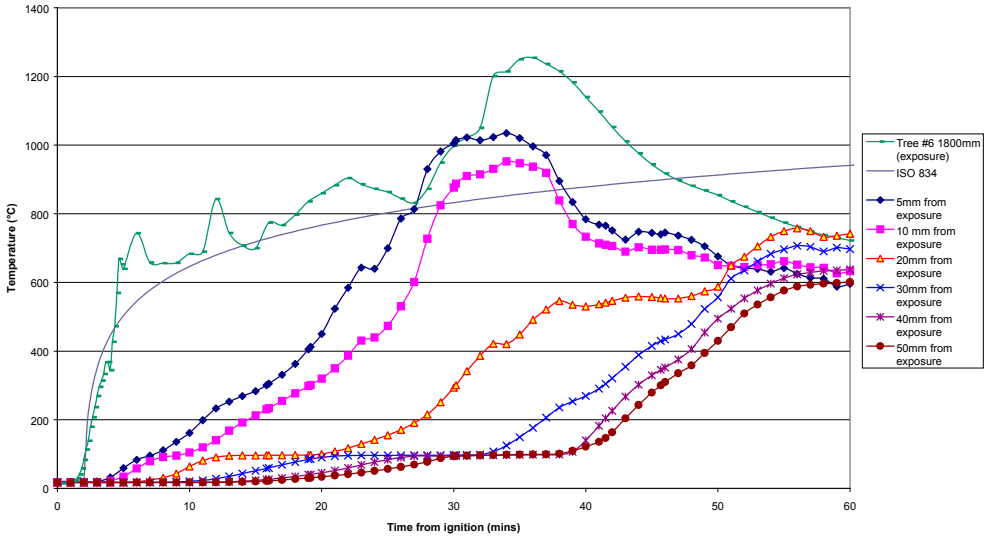

Figure 4.22 – Test #2 Dummy column exposure and temperature profile chart

In test #3, the thermocouples 5 – 30mm from the fire exposure reached charring temperatures at 9, 13, 21 and 36 minutes, respectively.

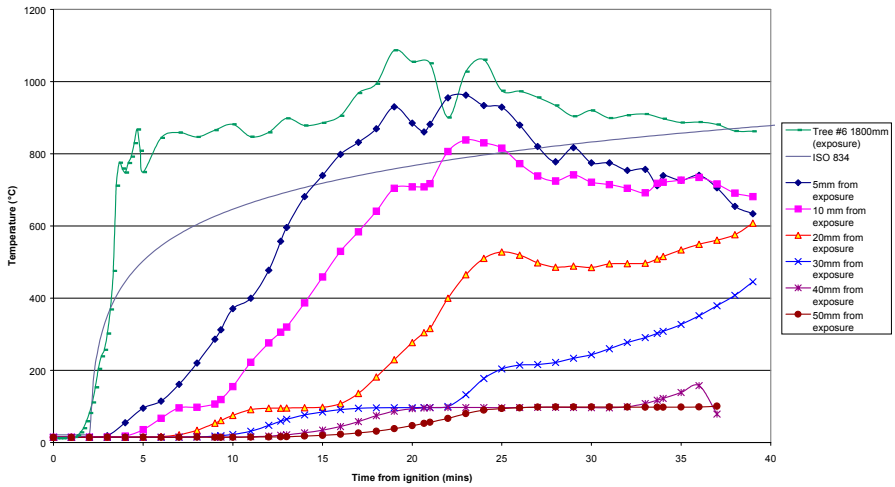

Figure 4.23 – Test #3 Dummy column exposure and temperature profile chart

Charring rates have been calculated for distances from the fire exposure to the thermocouple achieving charring temperatures, and additionally for distances between adjacent thermocouples achieving charring temperatures. The results are summarised in Table 4.2.

It is evident that for fires more severe than the standard furnace test fire exposure, charring rates can be significantly higher than the design charring rates applied (refer to Section 3.8 for description). The results from tests #2 and #3, in particular, reaching as much as 1.07mm/min, show that the standard rate of charring (0.65mm/min) used in design would appear to be insufficient for fires of severity greater than the standard fire test severity. Further analysis is beyond the scope of this project. The detailed examination of charring rates in realistic fires would be a recommended topic for further research.

CHAR RATES (mm/min)			
	Test #1	Test #2	Test #3
0 - 5mm	0.47	0.36	0.68
0 - 10mm	0.52	0.58	0.94
0 - 20mm	-	0.71	1.07
0 - 30mm	-	0.76	0.95
0 - 40mm	-	0.95 (ignore)	-
0 - 50mm	-	1.15 (ignore)	-
0 - 5mm	0.47	0.36	0.68
5 - 10mm	0.58	1.50	1.50
10 - 20mm	-	0.91	1.25
20 - 30mm	-	0.88	0.77
30 - 40mm	-	4.00 (ignore)	-
40 - 50mm	-	6.00 (ignore)	-

Table 4.2 – Dummy column char rates summary

4.11 Room Test Pressures

Figure 4.24 and 4.25 show the compartment pressures during tests #2 and #3 respectively. Pressures in test #2 are generally higher than test #3, as would be expected, since the test #2 compartment had a smaller ventilation opening than the compartment in test #3.

Figure 4.24 shows the rise in room pressure peaking at 20Pa after 5 minutes. The pressure in the room then remains generally constant until 37 minutes into the test, when room pressure begins to decline. This corresponds with when a section of Wall C (Assembly 7) fell from the compartment, creating an opening, and additionally coincides with the start of the fire decay phase.

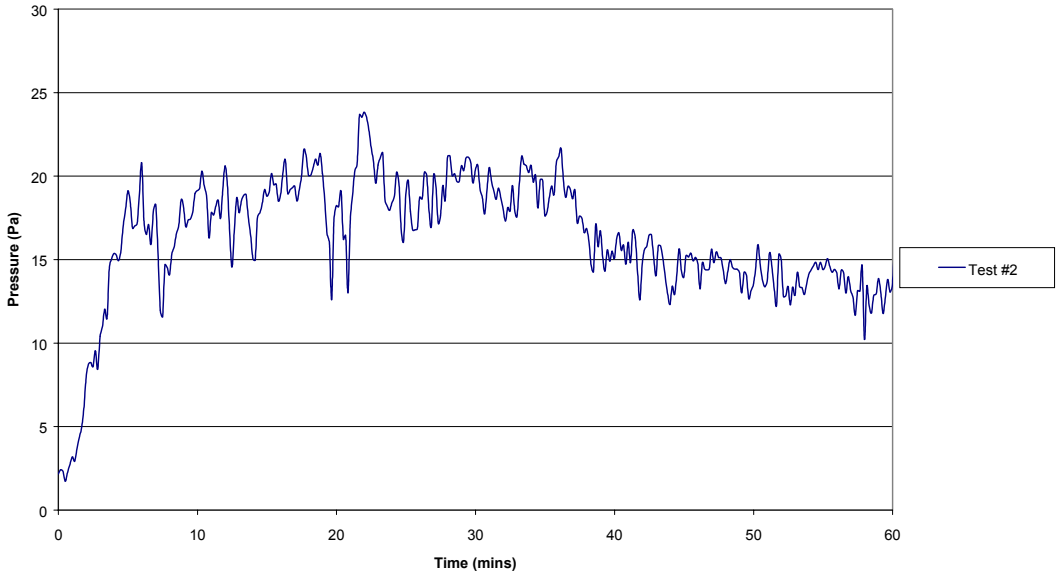

Figure 4.24 – Test #2 fire compartment pressure

Figure 4.25 shows the rise in room pressure peaking at 15Pa after 4 minutes. The pressure in the room then slowly rises to a peak of 19Pa until about 18 minutes into the test, when room pressure begins to decline. This corresponds with when a section of Wall B (Assembly 3) fell from the compartment, creating an opening. The steep decline in pressure after 23 minutes is due to pressure probe malfunction at this point in the test.

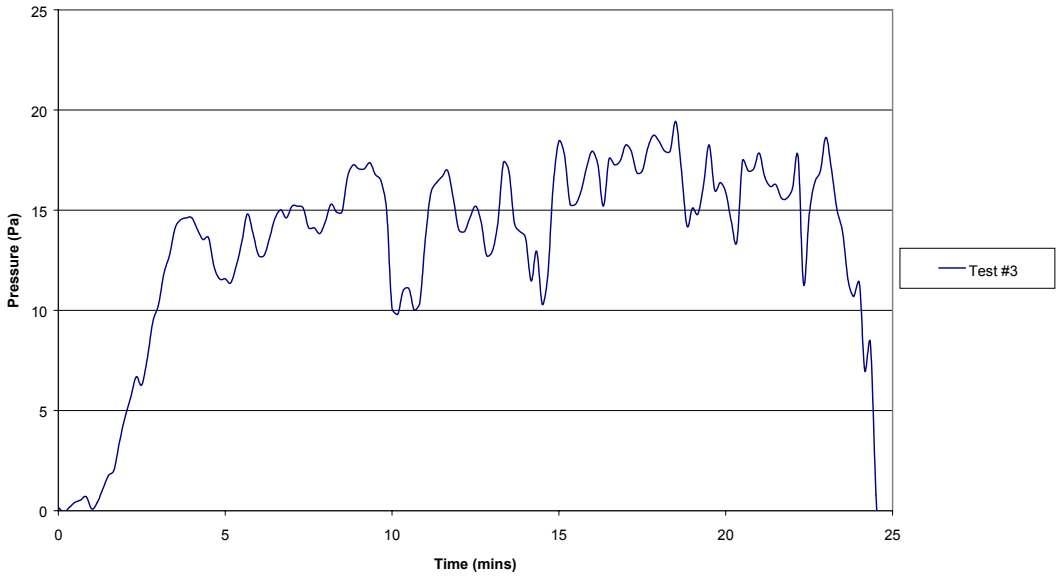

Figure 4.25 – Test #3 fire compartment pressure

5 Compartment Test Analyses

5.1 General

This section of the report provides analyses of the results and details a method to correlate the real fire exposure and the varying time to failures, with the standard test fire exposure and failure times, for those assemblies tested.

5.2 Correlation of Fire Severity with Assembly Fire Resistance

5.2.1 Radiant Exposure Area Correlation Description

To establish the time to failure of non-loadbearing assemblies in a real fire, a method of quantifying a real fire severity with the standard test fire severity is proposed. This method expands further, the equal area concept of fire severity as previously discussed in Section 2.4.5. The equal area concept of fire severity based on the compartment temperature has been recognised as being theoretically inappropriate in assessing a fires severity. The main reason given for this was that the predominant mode of heat transfer to an assembly, post-flashover, is that of radiant heat transfer (Babrauskas 1976). Radiant heat transfer is a function of the temperature, T (K), raised to the fourth power. Therefore taking a direct area under a time-temperature exposure curve cannot truly reflect the severity of a fire. It is therefore proposed to use an approach where the severity of a fire is established from the total energy impinging upon the surface of an assembly, expressed as the area under a plot of the emissive power ($\dot{Q}'' = \varepsilon\sigma T^4$) of the compartment gases versus time. To simplify calculations, the emissivity of the gases is conservatively taken as 1. The area under the curve is expressed mathematically as:

$$area = \int_0^t \dot{Q}''dt = \varepsilon\sigma \int_0^t (T^4)dt \quad \text{(units: kJ/m}^2\text{)} \qquad \textbf{Equation 5-1}$$

The method assumes that the compartment test fires and standard furnace test fires are identical in energy characteristics, and that convective components of the fire's heat transfer to the assembly are of equal proportion to the whole energy transfer in both test fires. Therefore, the radiation fire severity in each test type can be correlated.

This approach can be applied to any fire exposure time-temperature profile. Applying the radiant exposure area concept to the standard ISO 834 time-temperature relationship will provide a measure of fire severity at any time on that curve. This measure of fire severity can then simply be equated to a real fire exposure having the same radiant exposure area, giving an equivalent fire severity. Therefore, if the failure time of an assembly, when exposed to the ISO 834 exposure, is known, and a real fire exposure is known or predicted, the failure time of that assembly in the real fire exposure can be determined. This is shown graphically in Figure 5.1.

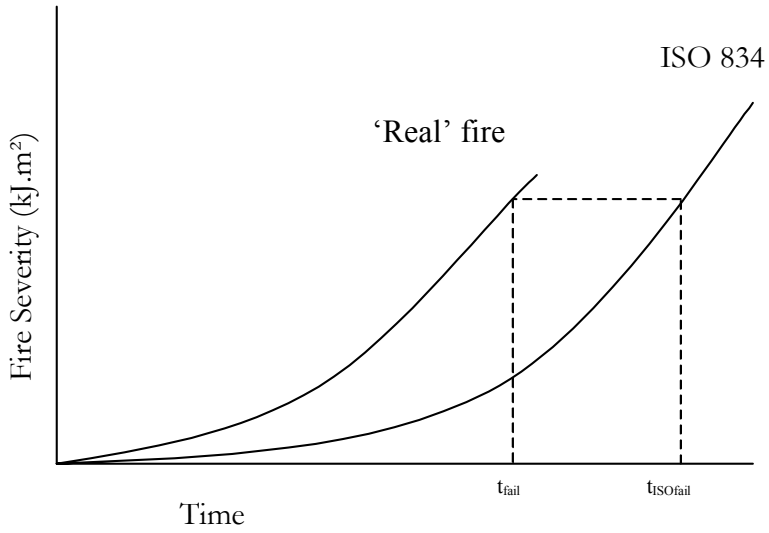

Figure 5.1 – Radiant Exposure Area Concept of Equivalent Fire Severity

5.3 Radiant Exposure Area Correlation Applied to Compartment Test Assemblies

5.3.1 Assembly 1 Radiant Exposure Area Correlation

Figure 5.2 shows the fire exposure temperatures measured at the respective tree, or trees, adjacent to assembly 1 in tests #1 and #3.

Applying the radiant exposure area correlation, Assembly #1 failed in the standard furnace test at 42 minutes, at which time it had been exposed to 2061kJ/m². The times at which Assembly 1 is exposed to this same level of fire exposure in tests #1 and #3, are 24 and 16 minutes, respectively, as shown in Figure 5.3. The actual time of assembly failure in tests #1 and #3, were 21 and 18 minutes respectively. The method provides conservative estimates of the insulation failure times of the assembly.

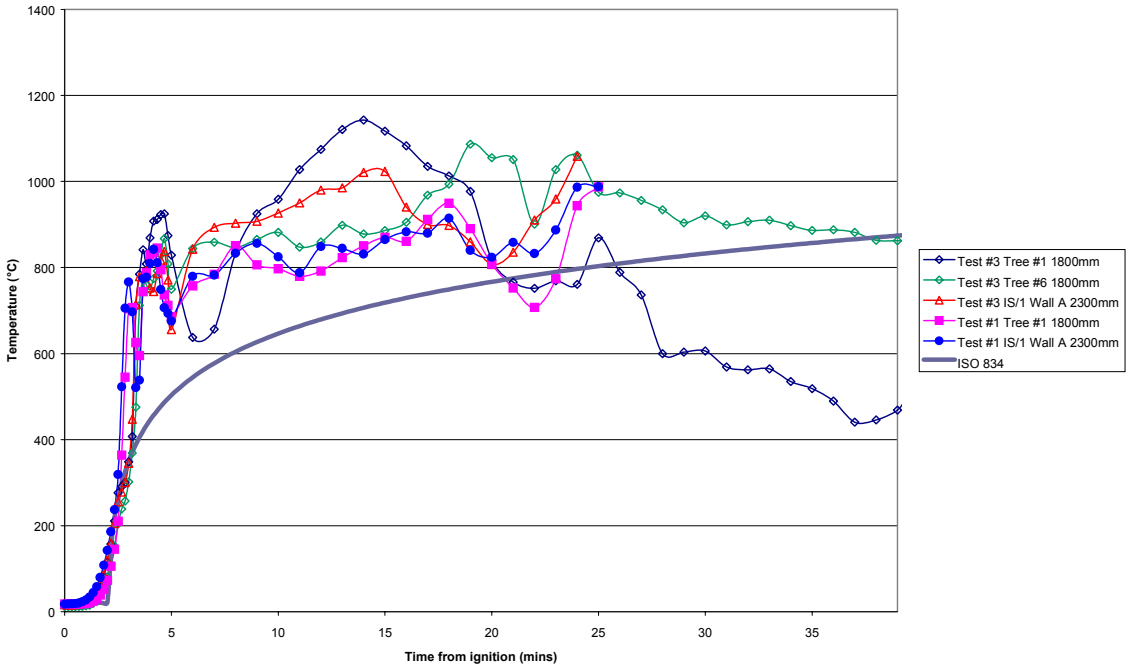

Figure 5.2 – Assembly 1 fire exposure

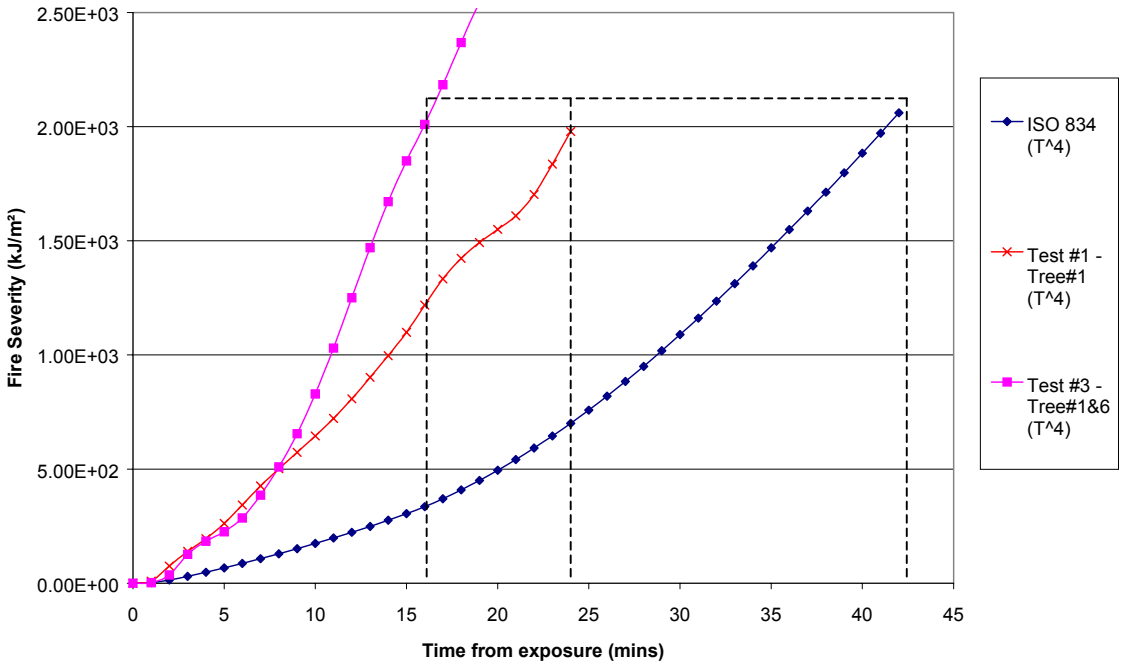

Figure 5.3 – Assembly 1 radiant exposure area correlation failure graph

5.3.2 Assembly 2 Radiant Exposure Area Correlation

Figure 4.12 (Section 4.9.5) shows the fire exposure temperatures measured at the respective tree, or trees, adjacent to Assembly 2 in tests #1 and #3. Applying the radiant exposure area correlation, Assembly 2 failed in the standard furnace test at 39 minutes, at which time it had been exposed to 1798kJ/m². The times at which Assembly 2 is exposed to this same level of fire exposure in tests #1 and #3, are 30 and 18 minutes, respectively, as shown in Figure 5.4. The actual time of assembly failure in tests #1 and #3, were 36 and 24 minutes respectively. The method provides conservative estimates of the insulation failure times of the assembly.

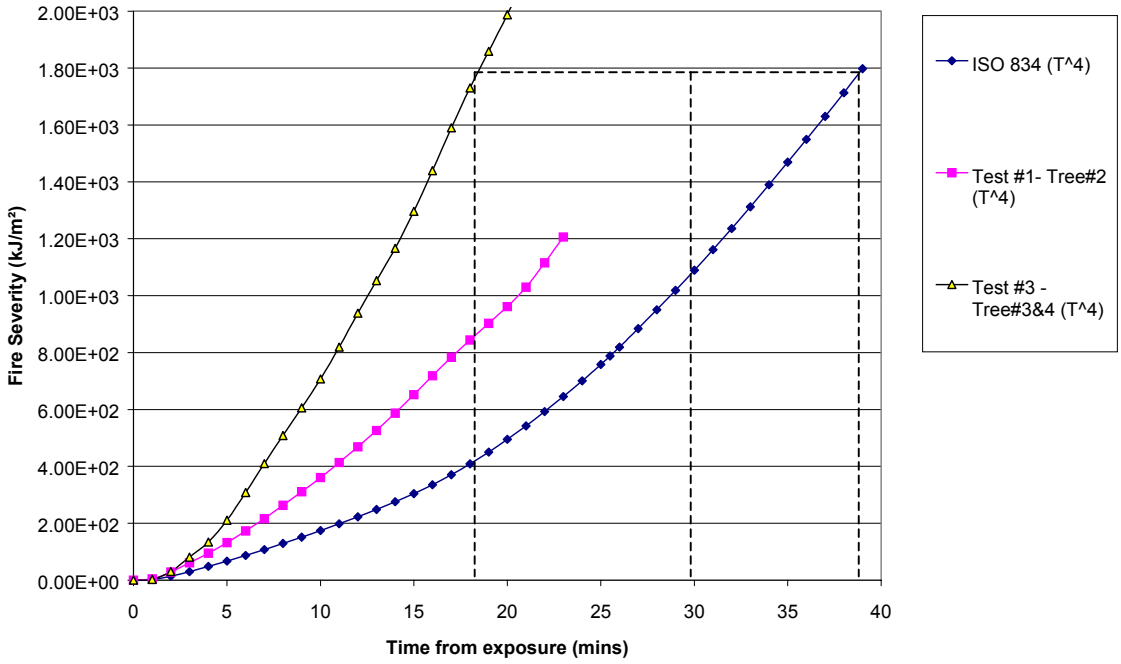

Figure 5.4 – Assembly 2 radiant exposure area correlation failure graph

5.3.3 Assembly 3 Radiant Exposure Area Correlation

Figure 5.5 shows the fire exposure temperatures measured at the respective tree, or trees, adjacent to assembly 3 in tests #1 and #3.

Applying the radiant exposure area correlation, Assembly #3 failed in the standard furnace test at 34 minutes, at which time it had been exposed to 1390kJ/m². The times at which Assembly 3 is exposed to this same level of fire exposure in tests #1 and #3, are 14 and 13 minutes, respectively, as shown in Figure 5.6. The actual time of assembly failure in tests #1 and #3,

were 19 and 17 minutes respectively. The method provides conservative estimates of the failure times of the assembly.

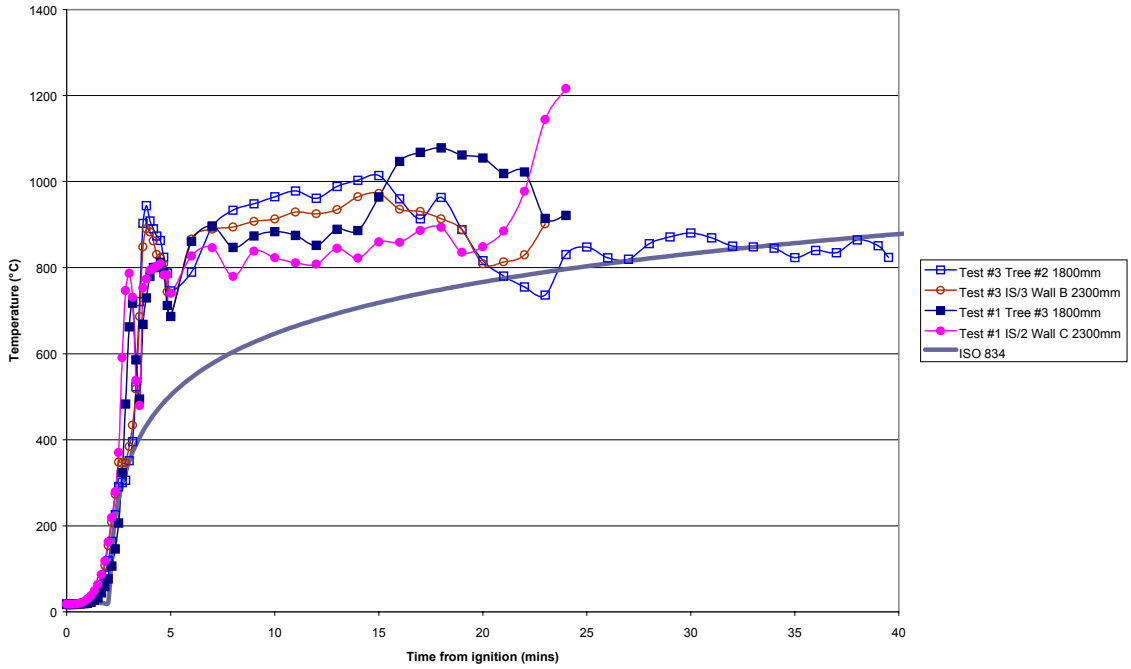

Figure 5.5 – Assembly 3 fire exposure

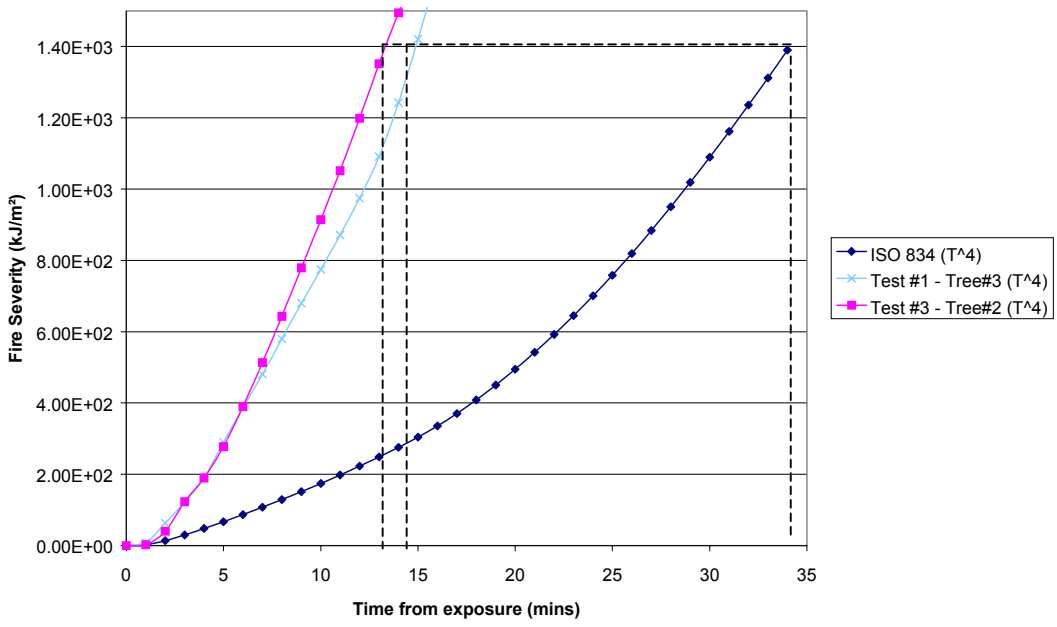

Figure 5.6 – Assembly 3 radiant exposure area correlation failure graph

5.3.4 Assembly 4 Radiant Exposure Area Correlation

Figure 5.7 shows the fire exposure temperatures measured at the respective tree, or trees, adjacent to assembly 4 in tests #1 and #3.

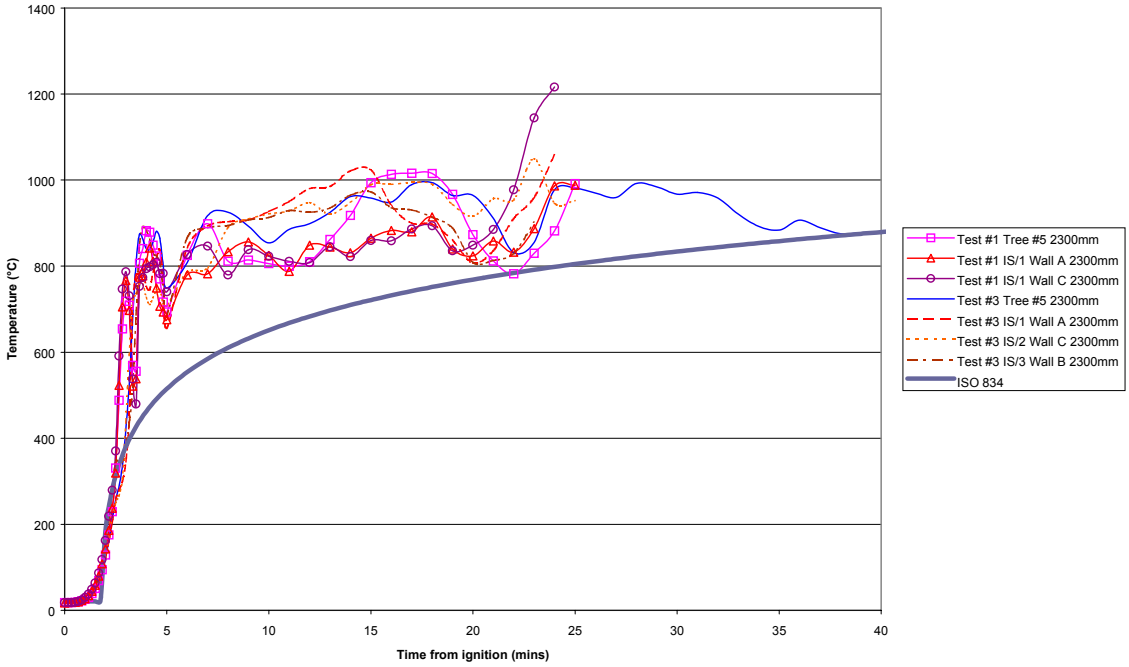

Figure 5.7 – Assembly 4 fire exposure

Applying the radiant exposure area correlation, Assembly 4 failed in the standard furnace test at 55 minutes (structural failure), at which time it had been exposed to 4247kJ/m². The times at which Assembly 4 is exposed to this same level of fire exposure in tests #1 and #3, are 43 and 38 minutes (by extrapolation), respectively, as shown in Figure 5.8. The actual time of assembly failure in tests #1 and #3, were 30 and 28 minutes respectively. The method provides non-conservative results for this floor/ceiling assembly.

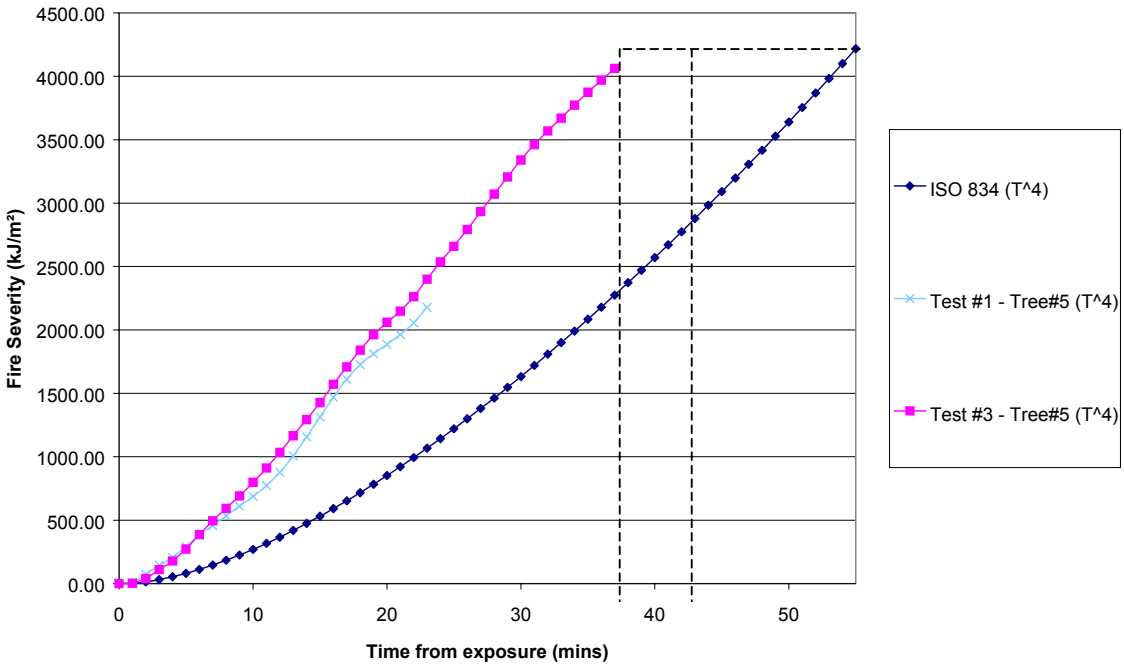

Figure 5.8 – Assembly 4 radiant exposure area correlation failure graph

5.3.5 Assembly 5 Radiant Exposure Area Correlation

Figure 5.9 shows the fire exposure temperatures measured at the respective tree, or trees, adjacent to assembly 5 in test #2.

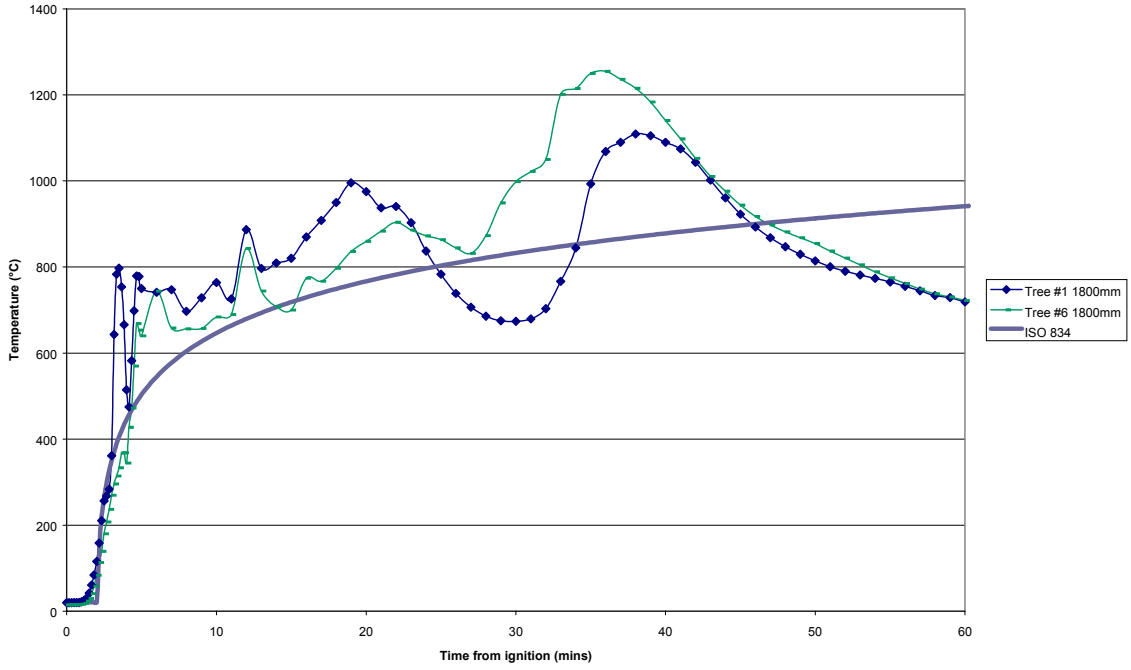

Figure 5.9 – Assembly 5 fire exposure

Applying the radiant exposure area correlation, Assembly 5 failed in the standard furnace test at 68 minutes, at which time it had been exposed to 5903kJ/m². The times at which Assembly 5 is exposed to this same level of fire exposure in test #2, is 44 minutes, as shown in Figure 5.10. The actual time of assembly failure in test #2 was 51 minutes. The method provides a conservative estimate of the insulation failure time of the assembly.

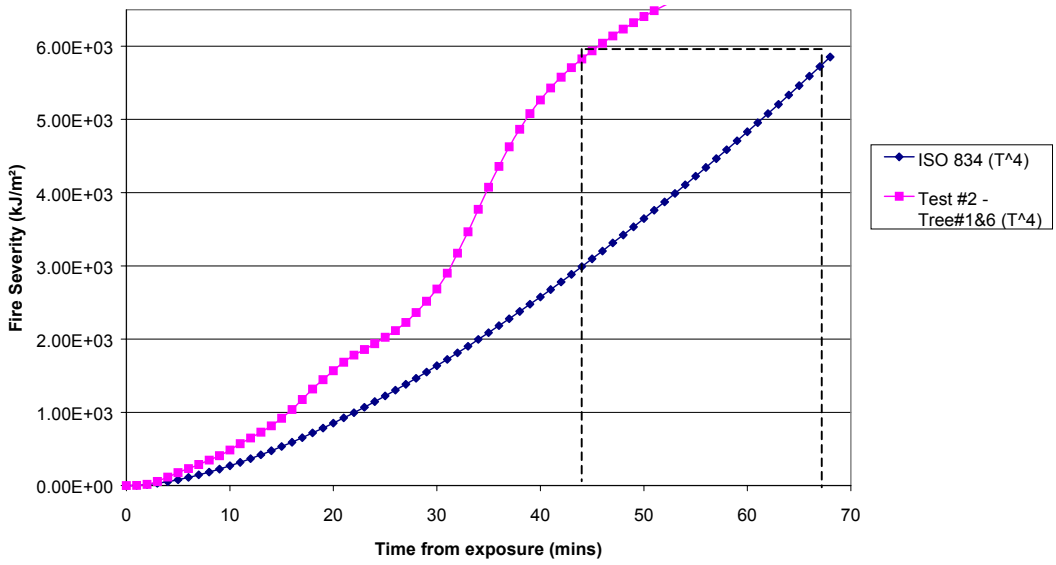

Figure 5.10 – Assembly 5 radiant exposure area correlation failure graph

5.3.6 Assembly 6 Radiant Exposure Area Correlation

Figure 5.11 shows the fire exposure temperatures measured at the respective tree, or trees, adjacent to assembly 6 in test #2.

Applying the radiant exposure area correlation, Assembly 6 failed in the standard furnace test at 58 minutes, at which time it had been exposed to 4631kJ/m². The times at which Assembly 6 is exposed to this same level of fire exposure in test #2, is 42 minutes, as shown in Figure 5.12. The actual time of assembly failure in test #2 was 55 minutes. The method provides a conservative estimate of the insulation failure time of the assembly.

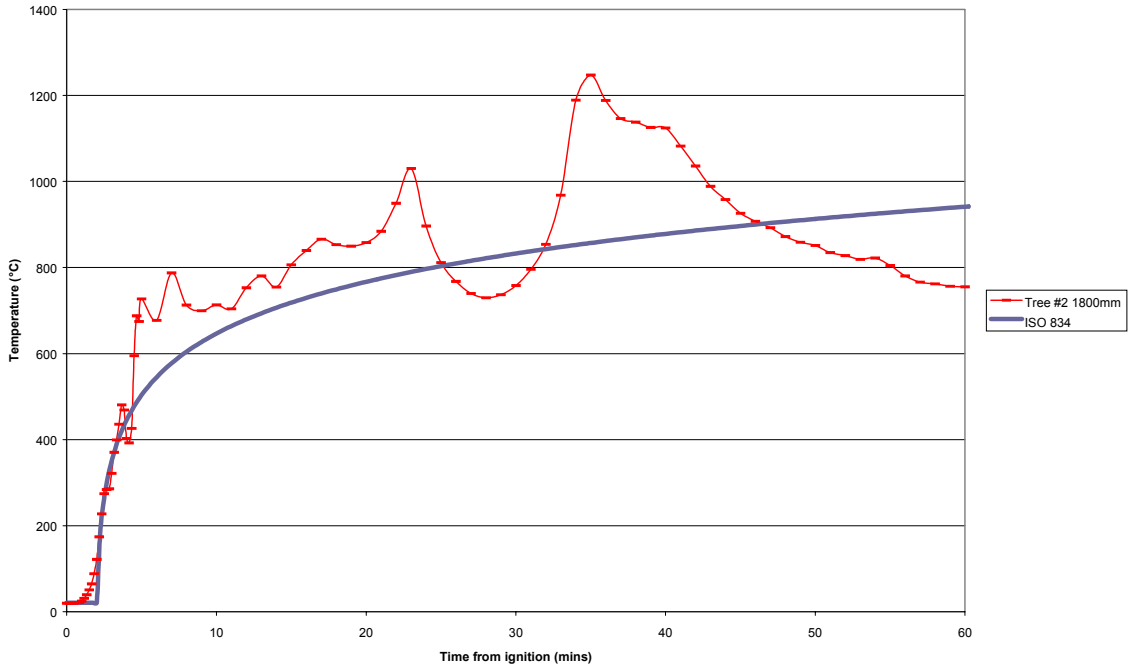

Figure 5.11 – Assembly 6 fire exposure

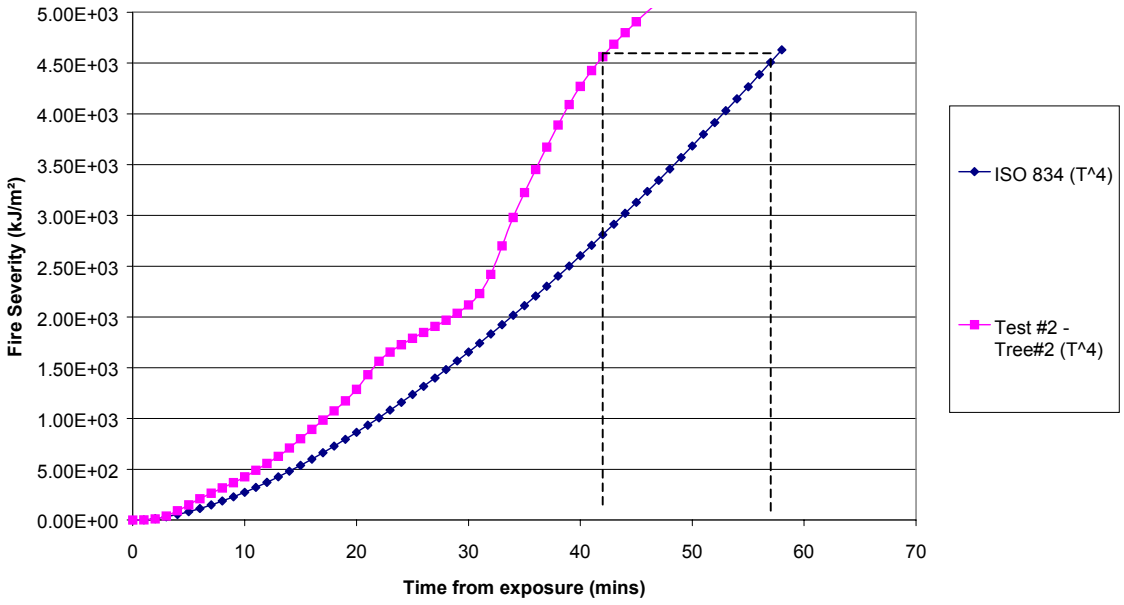

Figure 5.12 – Assembly 6 radiant exposure area correlation failure graph

5.3.7 Assembly 7 Radiant Exposure Area Correlation

Figure 5.13 shows the fire exposure temperatures measured at the respective tree, or trees, adjacent to assembly 7 in test #2, and additionally the pilot furnace test temperatures (BRANZ FP2881).

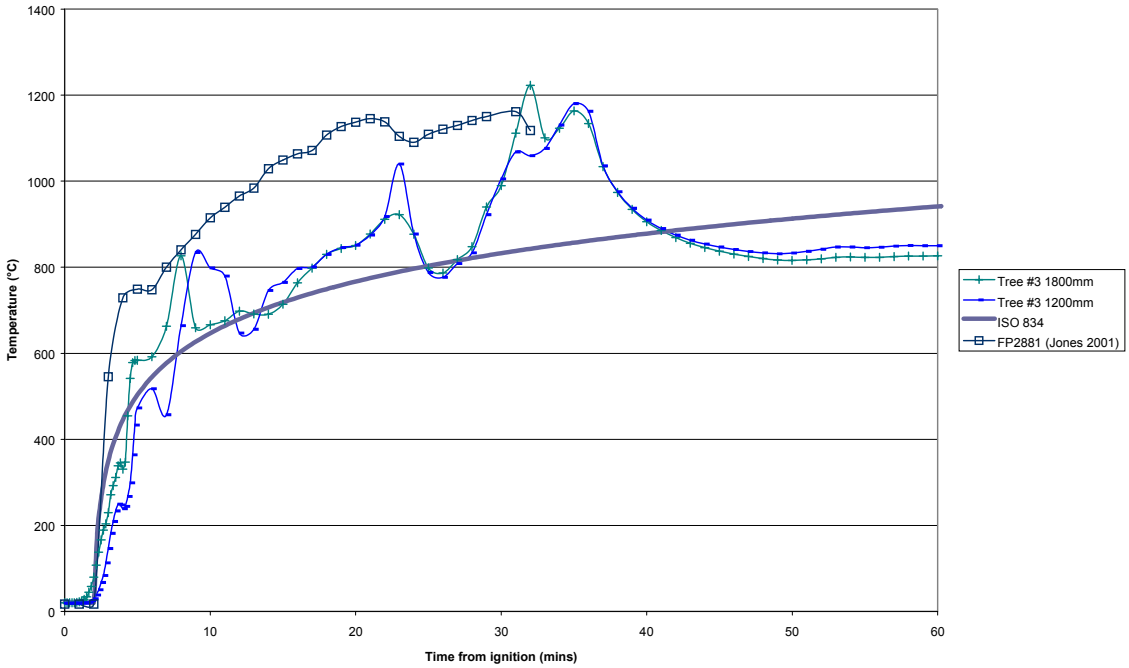

Figure 5.13 – Assembly 7 fire exposure

Applying the radiant exposure area correlation, Assembly 7 failed in the standard furnace test at 63 minutes (insulation), at which time it had been exposed to 5261kJ/m². The times at which Assembly 7 is exposed to this same level of fire exposure in tests #2 and in FP2881, are 45 and 31 minutes (by extrapolation), respectively, as shown in Figure 5.14. The actual time of assembly failure in tests #2 and FP2881 were 35 minutes and 28 minutes (integrity failures), respectively. The method provides a non-conservative estimate of the integrity failure time of this assembly, for both tests. However, the results are less non-conservative for the pilot scale test exposure, suggesting the assembly was closer to failing on insulation than in the compartment test. The apparent earlier integrity failure of the compartment test, compared with the pilot furnace test is probably due to the differing sizes of the test assembly in each case, resulting in differing deflection mechanisms. Examination of this phenomenon is beyond the scope of this project, but may be a topic for future research.

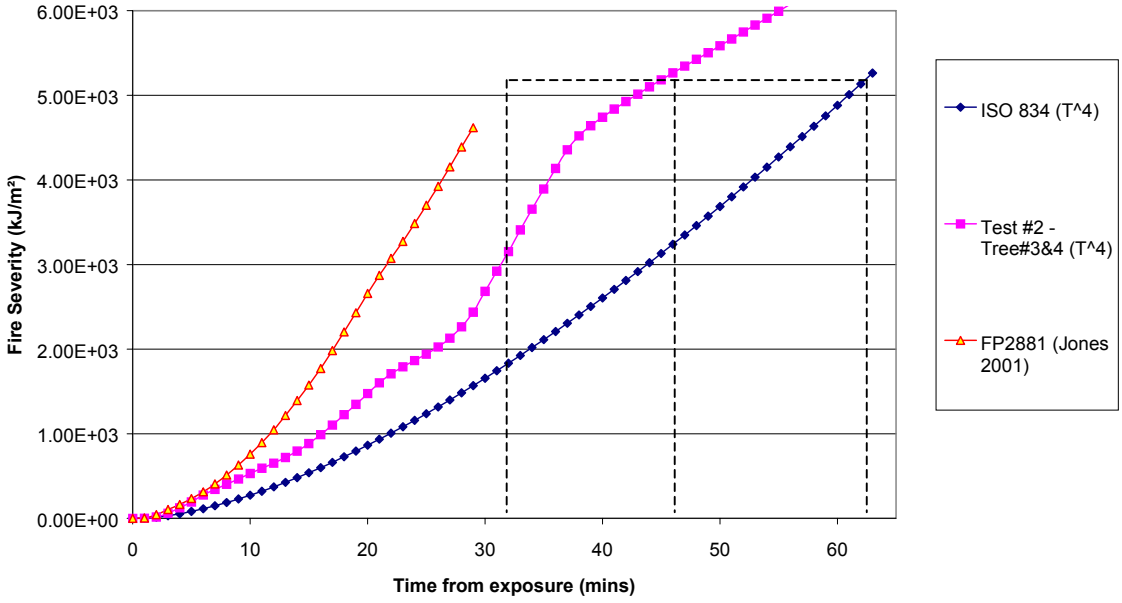

Figure 5.14 – Assembly 7 radiant exposure area correlation failure graph

5.3.8 Assembly 8 Radiant Exposure Area Correlation

Figure 4.20 (Section 4.9.7) shows the fire exposure temperatures measured at the respective tree, or trees, adjacent to assembly 8 in test #2.

Applying the radiant exposure area correlation, Assembly 8 failed in the standard furnace test at 74 minutes, at which time it had been exposed to 6708kJ/m². The times at which Assembly 8 is exposed to this same level of fire exposure in test #2, is 89 minutes (extrapolated), as shown in Figure 5.15. The actual time of assembly failure in test #2 was could not be assessed accurately, but was expected to be within the limits of 58-75 minutes (refer to section 4.9.7). The method result suggests that prediction of structural failure of the assembly is non-conservative.

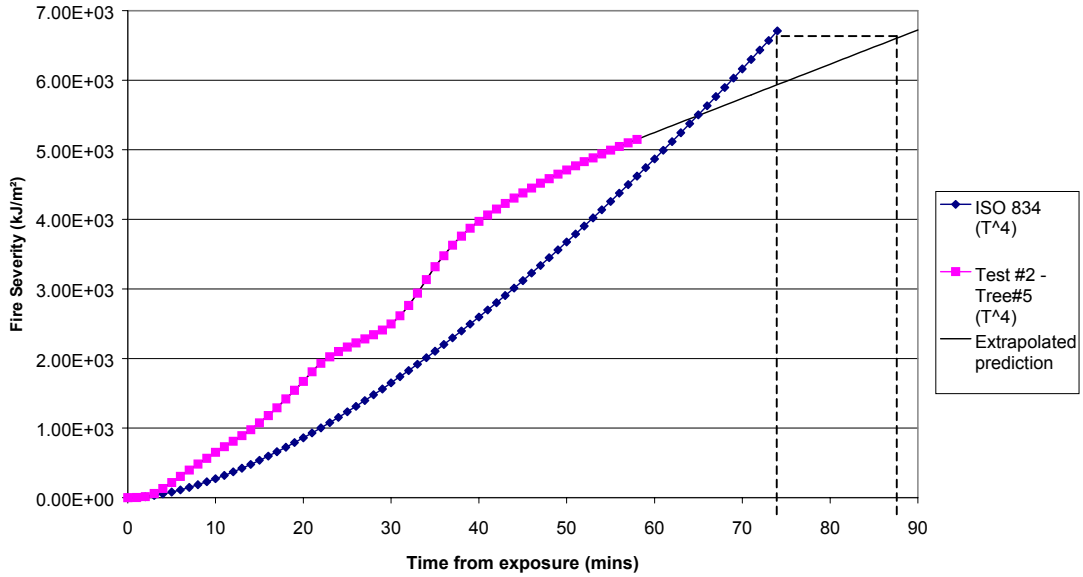

Figure 5.15 – Assembly 8 radiant exposure area correlation failure graph

5.3.9 Assembly 9 Radiant Exposure Area Correlation

Figure 5.16 shows the fire exposure temperatures measured at the respective tree, or trees, adjacent to assembly 9 in test #1.

Applying the radiant exposure area correlation, Assembly 9 failed in the standard furnace test at 74 minutes, at which time it had been exposed to 1820kJ/m². The times at which Assembly 9 is exposed to this same level of fire exposure in test #1, is 24 minutes (extrapolated), as shown in Figure 5.17. The actual time of assembly failure in test #2 was 20. The method generally provides reasonable agreement, slightly on the non-conservative side.

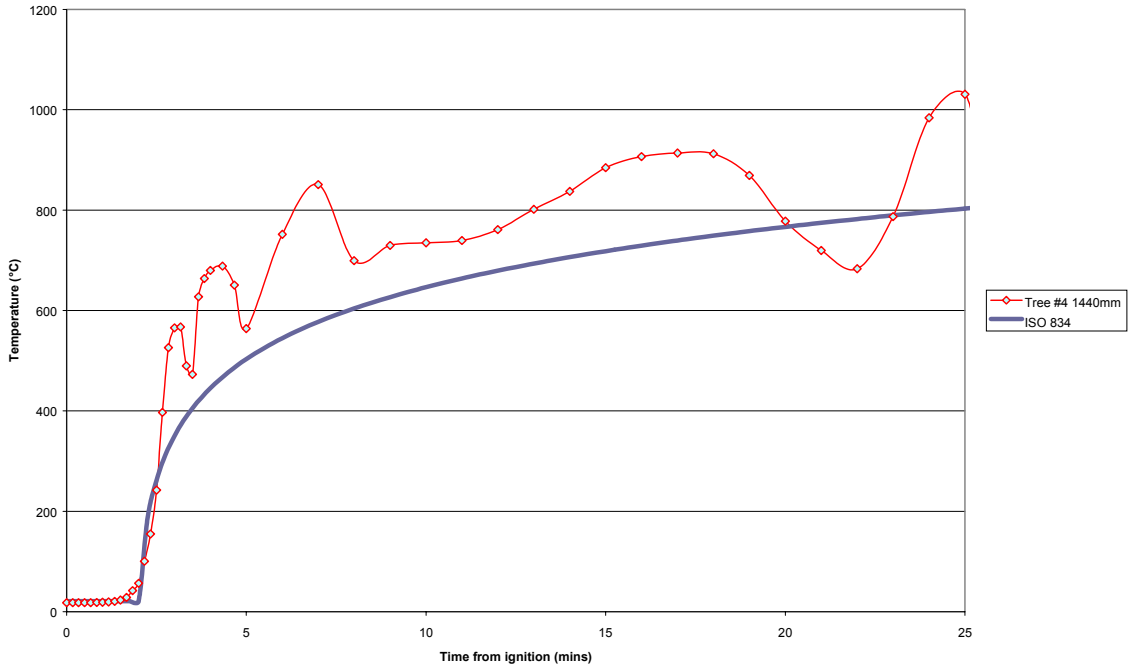

Figure 5.16 – Assembly 9 fire exposure

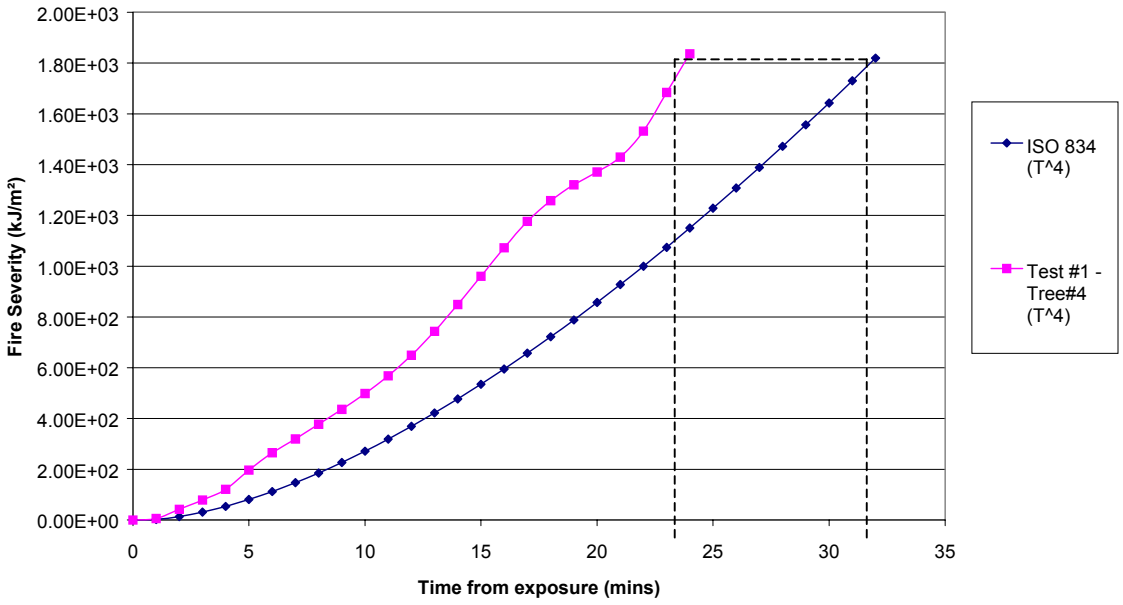

Figure 5.17 – Assembly 9 radiant exposure area correlation failure graph

5.4 Analysis of Radiant Exposure Area Method

A summary of test and the radiant exposure area correlation failure times for each assembly are shown in Table 5.1. Additionally included, for information and comparison, are results of ISO compartment assembly failure time prediction based on Thomas' method (Thomas, G et al 2002), which was described previously, in Section 2.4.9.

Assembly Reference	Test #	Test Assemblies Times to Failure, t_{fail} (mins)			
		ISO 834	Compartment tests	Prediction Methods	
				T^4 Area Method	Thomas' correlation
1	#1	42	21	24	18
1	#3	42	18	16	15
2	#1	39	36	30	17
2	#3	39	24	18	14
3	#1	34	19	14	15
3	#3	34	17	13	13
4	#1	55	30	43	24
4	#3	55	28	38	20
5	#2	68	51	44	38
6	#2	58	55	42	25
7	#2	63	35	45	27
7 (Jones 2001)	BRANZ FP2881	63	28	31	-
8	#2	74	$58<t_{fail}<75$	89	32
9	#1	32	20	24	14

Table 5.1 – Summary of assemblies' test and prediction methods failure times

The scatter chart in Figure 5.18 shows the radiant exposure area correlation predictions of times to failure against the actual test failure times. This shows graphically that all insulation failures were predicted with a reasonable level of conservativeness (above the line). The one exception to this was assembly 1 in test #1, which actually failed in 21 minutes, with the prediction estimating 24 minutes. Additionally, the 30 minute rated LSF assembly, which failed on integrity in both tests, shows conservative prediction.

The remainder, which are non-conservative (below the line) are the ceiling /floor assemblies, which would have failed on the structural criterion, the fire door and 60 minute rated LSF assembly which failed on integrity in test #2 and the pilot furnace test (Jones 2001).

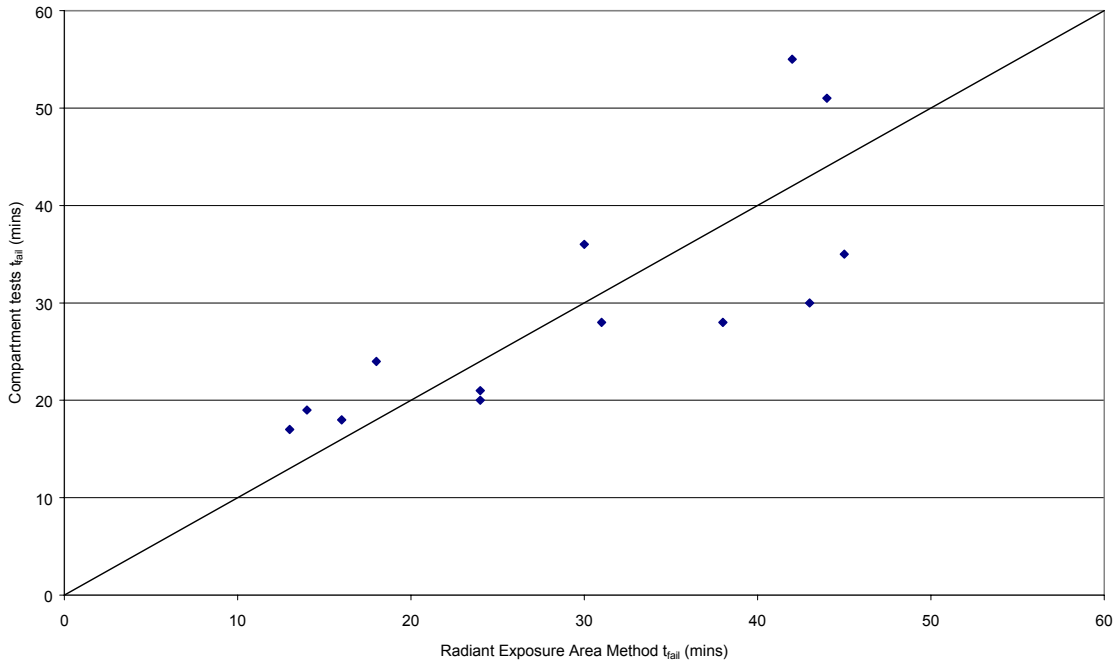

Figure 5.18 – Radiant Exposure Area Correlation t_{fail} Vs Compartment Tests t_{fail}

For wall assembly insulation failure prediction, the proposed radiant exposure area correlation provides very good conservative agreement, for real fire exposure. Exceptions to this were found to be for steel framed assemblies, particularly Assembly 7, which was found to fail on integrity, at exposures more severe than the standard fire test exposure, due to noticeable deflections causing linings to fall from the framing. A safety factor of 0.75, when multiplied by the correlation predicted time to failure, provides a conservative failure time (34 minutes). However, application of such an approach as this should made with caution, by a designer/engineer, as no thorough validation of such a factor of safety has been carried out. Such validation would be a topic for further research. Thomas' method for prediction of assembly failure (insulation) provides results, which are generally more conservative than the radiant exposure area correlation.

When the correlation is used for prediction of integrity failure of the fire door assembly (9), the result gives relatively good agreement, however, it is slightly (4 minutes) on the non-conservative side. Thomas' method provides reasonable agreement, 6 minutes, on the conservative side. Fire door assemblies of this type of construction (refer to Section for description), tend to fail the

standard furnace test on integrity. This suggests that there are more failure mechanisms involved in this type of assembly's failure, than purely a thermal mechanism. A multiplication safety factor of 0.75, which when multiplied by the radiant exposure area correlation predicted result gives a conservative result (18 minutes). However, application of such an approach as this should made with caution, by a designer/engineer, as no thorough validation has been carried out. The one, standard test, integrity failed assembly tested, is not considered by the writer to be a sufficiently large enough sample of tests, to completely validate the correlation for integrity failure. On the basis of the results, and until both methods are fully validated for integrity failure, it would be recommended to use the more conservative of the two, Thomas's method.

Predictions, using the radiant exposure area correlation, of the structural failure of the ceiling/floor assemblies tested (4 and 8) are non-conservative. As with the integrity failed assembly, this is a result of there being more failure mechanisms involved in this type of assembly's failure, than purely a thermal mechanism. Thomas's method provides varying levels of conservativeness for the floor/ceiling systems. This is possibly due to the use of the time equivalent equation (Equation 2-5, Section 2.4.8), which is used for structural fire design purposes. In lieu of there being no alternative conservative approach, it is suggested that Thomas's method be employed to predict structural failure of loadbearing light framed assemblies, until further validation is done. Further research on load bearing assemblies is recommended.

5.4.1 Example of Practical Application of Radiant Exposure Correlation Method of Assembly Failure Prediction

The radiant exposure area correlation has been shown to provide good conservative agreement of insulation failure prediction of non-loadbearing assemblies. Therefore, the engineer, to predict assembly insulation failure of an assembly, could apply the method to any design fire exposure.

As an example, application of the method has been made using the Eurocode modified parametric method, as described in Section 3.7.5, to derive design fires of varying severities. The severities of the several design fires calculated for this example, were for a fire compartment of identical geometry to the ISO room and FLEDs of 800MJ/m² and 400MJ/m². The ventilation

openings were modified, for each FLED design fire, such that the opening factor, F_v, as derived by Equation 2-2, ranged from 0.1 (large opening) to 0.01 (small opening).

Notional assemblies of 30FRR and 60FRR were employed to establish predicted failure times. Applying the radiant exposure area correlation to the standard ISO 834 exposure, the 30FRR and 60 FRR assemblies fail when exposed to a fire severity of 1665kJ/m² and 4903kJ/m² respectively.

The times when the assemblies are predicted to fail, when exposed to the Eurocode modified parametric fire exposures, for differing ventilation conditions at each FLED, are shown graphically in Figures 5.19 and 5.20. The curves shown in Figures 5.19 and 5.20 do not show rounded curves, due to rounding down of the times to failure to the nearest minute. If the predicted time to the equivalent fire severity is greater than the FRR, the system will not fail. If the opening factor, F_v, is off the top of the curve, this represents a short sharp fire, which has burnt itself out before failure of the barrier occurs.

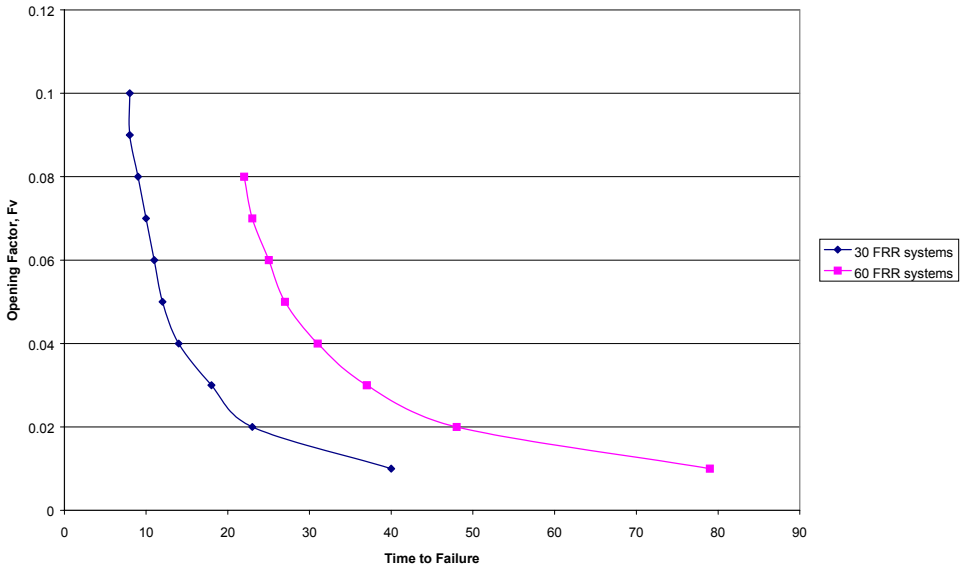

Figure 5.19 – Assembly failure prediction charts for Eurocode modified parametric exposure with 800MJ/m² FLED

From Figure 5.19, it can be seen that the ISO 834 is equivalent to a Eurocode modified parametric fire of 800MJ/m² FLED and F_v of 0.015. No failures of 60 FRR systems were predicted for a Eurocode modified parametric curve at 400MJ/m² FLED.

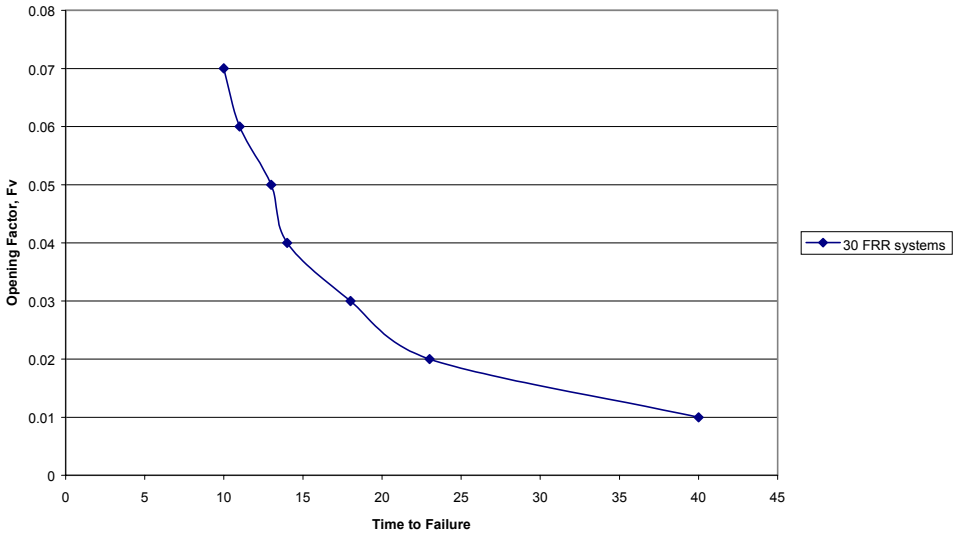

Figure 5.20– Assembly failure prediction charts for Eurocode modified parametric exposure with 400MJ/m² FLED

It can be seen from the charts shown in Figures 5.19 and 5.20, that based on the particular design fire methodology used (i.e. Eurocode modified parametric, or similar), a designer, or engineer, can determine a failure time for a non-loadbearing assembly, if they know the FLED and ventilation conditions.

The above representation could also be applied by manufacturers of such assemblies. Manufacturers' literature could produce such charts, which would advise designers and engineers on selection of their products. The failure prediction curves could be applied at various time increments of FRR and FLEDS. To assist designers further with the application of the radiant exposure area correlation, it would be recommended for manufacturers to detail more accurate assembly standard test failure times (i.e. rounded down to the nearest 5-10 minutes, as oppose to the nearest half hour). This would avoid being over conservative in failure time prediction. Table 5.2 shows the radiant fire severity of the standard furnace test fire exposure at increments of10 minutes. Designers could apply such tabulated data to establish when their 'design' fire would cause assembly failure.

ISO 834 Exposure Time (mins)	Radiant Fire Severity (kJ/m²)
30	1665
40	2718
50	3703
60	4903
70	6206
80	7602
90	9083

Table 5.2 – Standard ISO 834 radiant fire severity

5.4.2 Limitations of Radiant Exposure Area Correlation

The method is based on a comparison of measured temperatures, both in standard furnace tests and in the compartment tests. Errors associated with temperature measurement are considered to be the same for both methods, as instrumentation used in the compartment tests was the same as that used in the furnace tests.

The radiant exposure area correlation should not be applied to make assessment of structural failure of loadbearing assembly. The method provides good conservative agreement of the thermal mechanism of an insulation failure, but does not account for other mechanisms involved with structural failure. The method requires further validation, or factor of safety applied, if necessary, for prediction of integrity failure of a system.

6 Calorimeter Tests

6.1 General

Cone and ISO room calorimeter tests were undertaken on the foam and fabric selection to establish the energy release rates and heat of combustion of the synthetic fuels used in the compartment tests. Only the rate of heat release, total energy release and effective heat of combustion shall be detailed in this section of the report. For information regarding detailed gas analysis of the products of combustion of burning synthetic fuels and upholstered furniture, refer to references quoted in Section 3 of this report.

This section overviews the equipment and methodology used at BRANZ and details the results and findings.

6.2 Cone Calorimeter Test

6.2.1 Introduction

The cone calorimeter in use at BRANZ is able to measure a range of material fire properties, including:

- Rate of heat release
- Total energy release
- Effective heat of combustion
- Mass loss
- Time to ignition
- Smoke obscuration

Cone testing of the synthetic materials used in the compartment tests has been carried out in accordance with ISO 5660-1 (1993b) and the protocol set out in Appendix 6 of the CBUF final report (Sundström 1995).

6.2.2 Equipment and Instrumentation

Figure 6.1 shows a schematic representation of the cone calorimeter test equipment used for the sample testing.

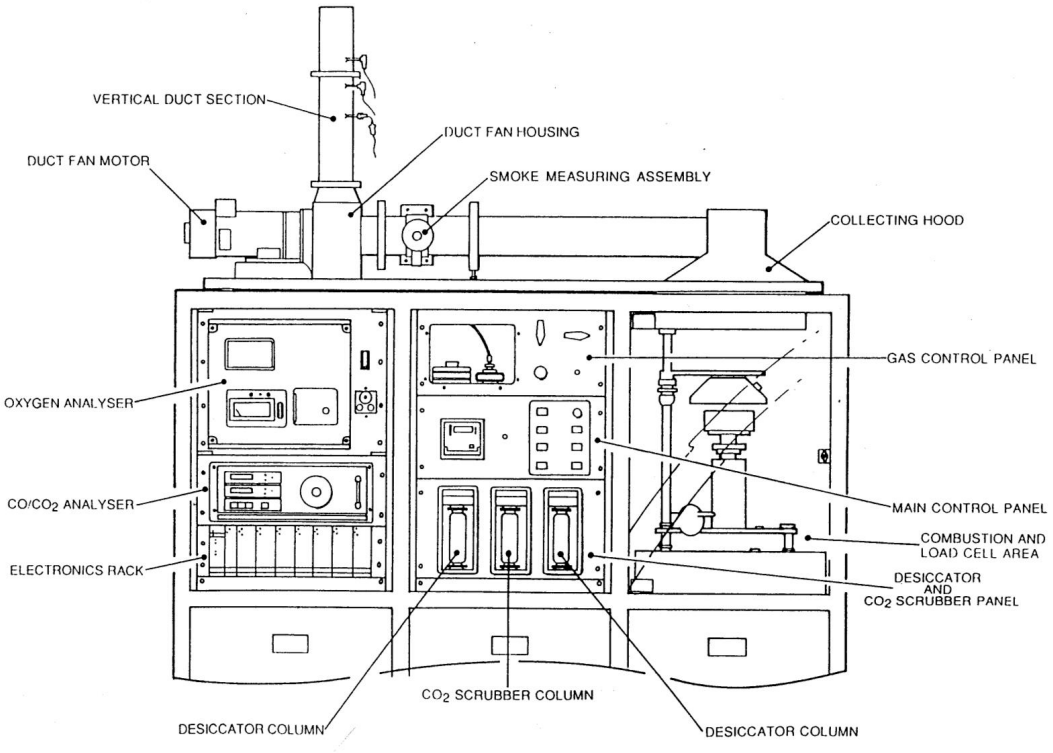

Figure 6.1 – Cone Calorimeter Test Apparatus Schematic

The complete apparatus consists of four distinct sections of equipment:

- Cone heater and load cell
- Gas train and control panel bay
- Analyser bay
- Ducting section

The cone heater and load cell section of the apparatus is shown in greater detail in Figure 6.2. The cone element is mounted internally on a double-skinned insulated truncated cone. Its maximum load is 5kW at 240VAC, enabling irradiance levels between 0-110kW/m² to be achieved. The distance between the top of the sample and the base of the cone should be 25mm. The cone has three 3mm (OD) type K stainless steel sheathed thermocouples symmetrically around and in contact with the element.

The spark igniter should be located 13mm above the centre of the sample. The igniter will not operate if the safety doors around the sample testing reaction area are left open whilst trying to operate the equipment.

The load cell is mounted on a platform with a level indicator and has a 500g dynamic range.

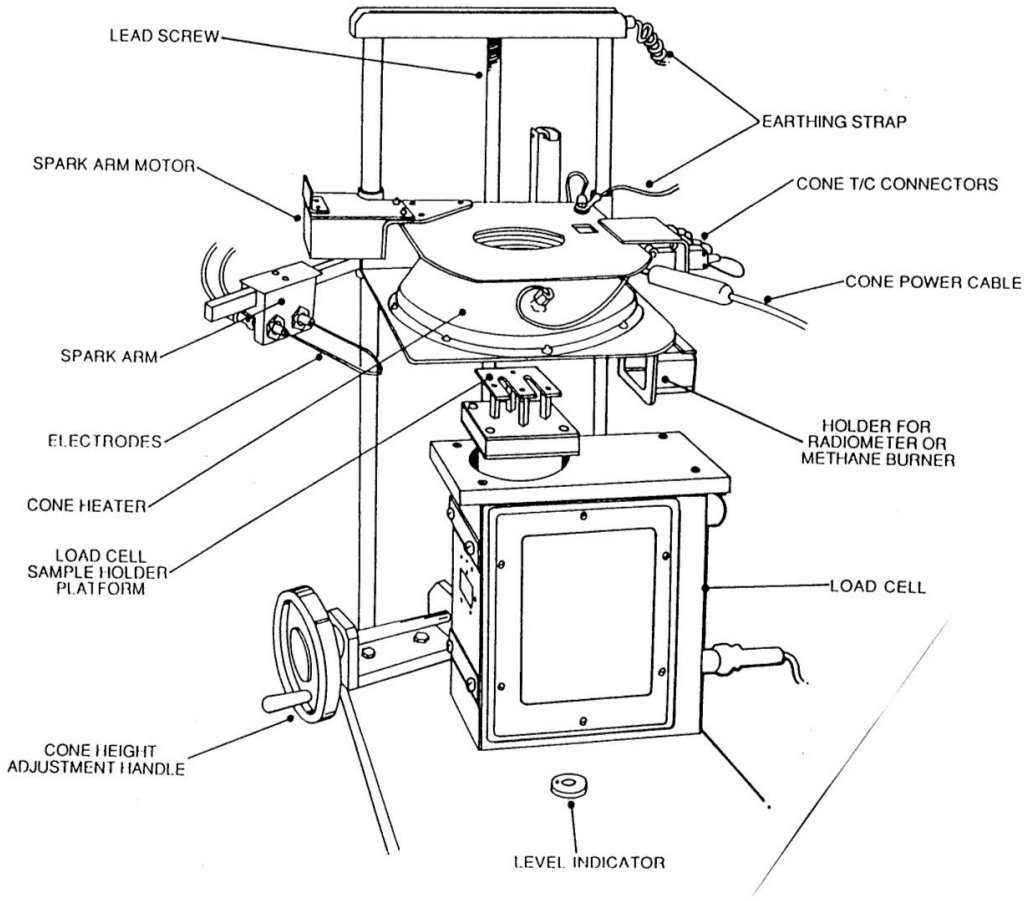

Figure 6.2 – Cone Heater and Load Cell Schematic

For calibration of the cone heater, there is a methane burner and radiometer (heat flux meter).

The main gas train of the apparatus consists of several filtering and scrubbing components used prior to gas analysis. These items include:

- Filters (and soot mass train) for soot removal
- Pump to draw out sampling gas
- Cold trap to condense out moisture
- Drying columns for further moisture removal

- CO_2 drying column to prevent CO_2 passing into the oxygen analyser

The gas analysing section of the test apparatus include a Servomex 540A oxygen analyser, and a Siemens Ultramat 22P analyser for CO and CO_2 monitoring of samples. Additionally in this section of the apparatus are all the electronic interfaces for the recording of data.

The ducting section (114mm ID) begins with a rectangular hood situated immediately above the cone and between this point and the gas exhaust to atmosphere includes the following instrumentation:

- Soot mass probe
- Ring sampler
- Smoke thermocouple
- Laser optical system
- Fan and orifice plate in vertical section of ductwork

6.2.3 Experimental Procedure

6.2.3.1 Calibration of Equipment

Gas analysers were calibrated using gases of known concentrations. The apparatus is first calibrated using atmospheric oxygen levels to provide a voltage at the analyser corresponding to 21% atmospheric O_2 levels. Nitrogen is then used to 'zero' the O_2 analyser. CO_2 and CO analysers were not operating at the time of the tests.

The heat release rate (HRR) from the apparatus is calibrated using a 5kW Methane burn. With the knowledge that 12.54MJ/kg heat of combustion is produced when O_2 is present, the required gas flow rate can be set to provide a 5kW flame. The results from the calibration data verify a constant HRR curve at 5kW. During this process the oxygen analyser is re-checked to ensure it is reading 20.95% volts.

The heat flux of the cone heater is calibrated with the use of a calibration table containing the heater temperatures corresponding to various common irradiance heat fluxes and additionally

the corresponding millivolt outputs for the flux gauge used for final adjustment of the controller set point.

6.2.3.2 Test Fuel Sample Preparation

Three foam and fabric samples were used for the cone calorimeter testing. The foam and fabric is as previously described in Section 3 of this report.

Each foam sample was cut into 102.5mm x 102.5mm x 50mm thick and their weight was recorded. Fabric samples were cut 200mm x 200mm square and their weight recorded. The fabric was then cut using the 'fabric cutting template' shown in Appendix A6 of the CBUF final report, and re-weighed.

The fabric shells were constructed with a non-acrylic based adhesive. The foam sample is then placed into the fabric shell, which had been allowed to cure for 24 hours, to produce the composite fuel sample. Aluminium foil trays were constructed to enable collection of residue and by-products created during the testing procedure. The completed fuel samples and foil trays (Figure 6.3) were cured in a conditioning chamber at 23°C (±3°C) and 50% RH (±5%) for 24 hours prior to testing. The weights recorded are shown in Table 6.1.

6.2.3.3 Testing Procedure

Cone calorimeter apparatus is housed internally in a draught free environment at ambient temperature and humidity conditions. The tests were carried out with at a cone heater radiant heat flux of 35kW/m². Samples were located in a tests sample holder and placed on the load cell sample holder platform such that the top of the sample is 25mm from the base of the heating element. Once in place, the sample is exposed to the radiant heat flux and the apparatus shield door is closed. The spark igniter is activated on closing of the doors. Upon sustained ignition, an 'ignition' button is pressed, which records time and withdraws the spark igniter arm automatically. The end of each test was declared when flaming had stopped. Data collection on each test was continued for 2 minutes after the test end to allow conditions to return to ambient.

The results of the three sample tests were recorded and individual HRR's were calculated. An average HRR for all three was then obtained.

Figure 6.3 – Foam and fabric sample in holder (typical)

6.2.4 Results and Calculations

6.2.4.1 Heat Release Rates

Calculation of the HRR is based upon oxygen consumption calorimetry detailed by Janssens (1995). The HRR for most organic compounds can be determined by measurement of the amount of oxygen consumed during combustion. Huggett (1980) showed that organic compounds produce an average heat of combustion of 13.1MJ/kg of O_2. This value varies by ±4% for a range of organic liquids, polymers and fuels (ie Methane has a heat of combustion of 12.54MJ/kg of O_2 as mentioned earlier in this section). As a result, the value of 13.1MJ/kg can be used to an accuracy of ±5%.

Only the O_2 analyser was in operation for the tests, so the HRR, $\dot{q}$, of the samples was calculated using:

$$\dot{q} = E \frac{\phi}{1+\phi(\alpha-1)} \dot{m}_e \frac{M_{O_2}}{M_a} \left(1 - X^a_{H_2O} - X^a_{CO_2}\right) X^{A^a}_{O_2} \qquad \textbf{Equation 6-1}$$

with

$$\phi = \frac{X^{A^a}_{O_2} - X^{A^e}_{O_2}}{\left(1 - X^{A^e}_{O_2}\right) X^{A^a}_{O_2}} \qquad \textbf{Equation 6-2}$$

and where the actual mole fraction of water vapour, $X^{a}_{H_2O}$, in the ambient air, is determined by:

$$X^{a}_{H_2O} = \frac{RH}{100} \frac{\exp\left(23.2 - \frac{3816}{T_{ref} - 46}\right)}{101325}$$ **Equation 6-3**

The results obtained for the foam fabric samples from the calorimetry tests and calculations are summarised in Table 6.1.

Sample	Mass (g)		Density (kg/m³)		Peak HRR, $\dot{q}''_{peak}$ (kW/m²)	Total Heat Released, q''_{total} (MJ/m²)
	Foam	Fabric	Foam	Composite		
1	15.4	9.6	29.6	48.1	341.6	68.24
2	15.4	9.4	29.6	47.7	369.6	67.66
3	15.5	9.5	29.8	48.1	363.0	67.45
Average	**15.4**	**9.5**	**29.7**	**48.0**	**354.4**	**67.78**

Table 6.1 – Cone calorimeter test HRR of foam and fabric samples

Figure 6.4 shows the resulting averaged HRR chart obtained from the cone calorimeter test on the foam and fabric samples.

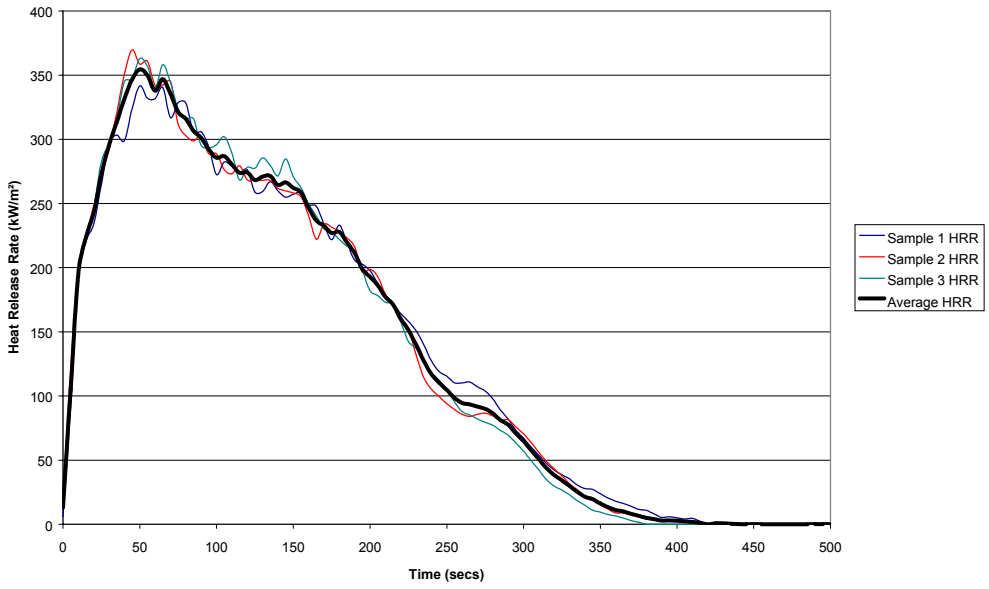

Figure 6.4 – Cone calorimeter foam and fabric HRR

6.2.4.2 Heat of Combustion

The energy release from the foam samples during each test is shown in Figure 6.5.

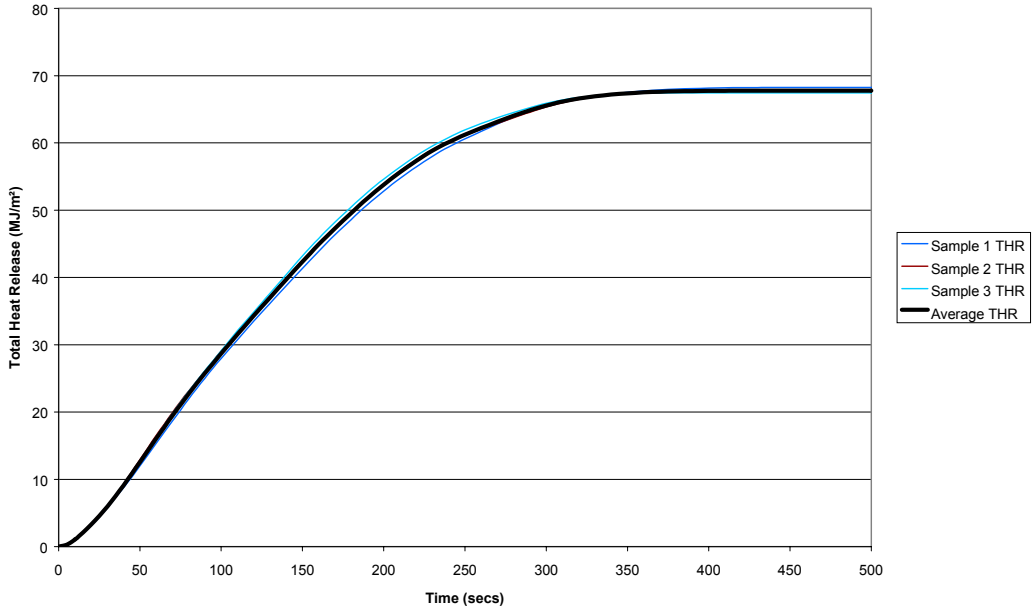

Figure 6.5 – Cone calorimeter foam and fabric THR

The effective heat of combustion, $\Delta h_{c.eff}$, is calculated over the duration of the test period, by the following equation:

$$\Delta h_{c.eff} = \frac{\sum \dot{q}(t)\Delta t}{m_i - m_f}$$ **Equation 6-4**

Where the total energy released was 677.81kW, and the average values for m_i and m_f were 24.93g and 0.50g respectively, the average heat of combustion for the foam and fabric samples was therefore 27.7MJ/kg.

6.3 ISO Room Calorimeter Test

6.3.1 Introduction

A full-scale fire test room built to internationally recognised standards (ISO 1993) has been constructed at BRANZ. As a first use of the new test facilities, a calorimeter ISO room burn was undertaken to allow us to provide more specific details of the foam and fabric cushions selected for the room compartment test. The two seater chair foam and fabric arrangement used in compartment test #1 burn was tested in the calorimeter room. It was not possible to test the three seater chair arrangement, as used in compartment tests #2 and #3, as the ISO room set up cannot cater for such a large fuel source. Heat release rates and additional heat of combustion results have been obtained.

6.3.2 ISO Room Construction and Setup

The ISO room, with geometry as shown in Figure 6.6 (ISO 1993), is constructed of lightweight concrete with internal dimensions of 3.6m(L) x 2.4m(W) x 2.4m(H), with a vent opening dimension of 2m(H) x 0.8m(W). In order to replicate the test compartment environment and thermal properties, the ISO room was internally lined with 13mm 'standard' gypsum plasterboard (Figure 6.7). With the plasterboard linings, the clear internal dimensions were 3.57m(L) x 2.38m (W) 2.3m(H).

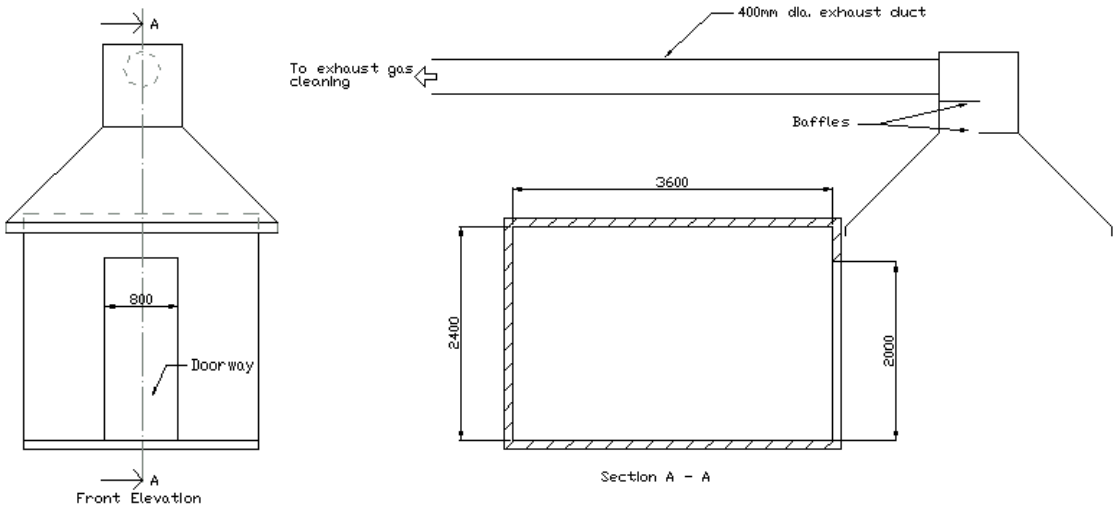

Figure 6.6 – ISO room calorimeter schematic

Figure 6.7 – ISO room set up and room linings

The fuel tested was the two-seater foam and fabric arrangement used in compartment Test #1. The chair was located in an identical position to that in test #1 (Figure 3.20 and 6.7).

The products of combustion from foam and fabric cushions burning within the ISO room are collected outside the opening through a hood and extracted via a sheet metal ductwork distribution system. The products of combustion are then analysed by gas sampling equipment.

6.3.3 Equipment and Instrumentation

A single thermocouple tree was located in the same position as that used for Tree #5 in compartment test #1 (Figure 3.31). The crimped quick-tip thermocouples on the tree were placed at heights of 2300mm, 2100mm, 1800mm, 1200mm and 300mm above the floor. Additionally, a crimped quick-tip thermocouple was located at the point of ignition (Figure 3.18).

The instrumentation consists of a gas analysis console and a ducting insert. The console houses instrumentation to measure oxygen depletion, CO/CO_2 production and soot mass sampling. The ducting insert is fitted with a sampling probe, CO/CO_2 gas train, bi-directional probe for volume flow monitoring, flow thermocouple and smoke thermocouple. Figures 6.8 and 6.9 show the gas analysis console and ducting insert respectively.

Figure 6.8 – ISO room gas analysis rack

Figure 6.9 – Ducting insert instrumentation

The main gas train of the apparatus consists of several filtering and scrubbing components used prior to gas analysis. These items include:

- Sampling probe
- Filters for soot removal
- Cooling column
- Gas path pump
- Drying columns for further moisture removal
- CO_2 drying column to prevent CO_2 passing into the oxygen analyser
- O_2, CO_2 and CO analysers

The gas analysing section of the test apparatus for O_2, CO and CO_2 monitoring of samples is a modified Servomex 4000 model. The range settings for the equipment are 0-25% for O_2, 0-10% for CO_2, and 0-1% for CO. Additionally in this section of the apparatus are all the electronic interfaces for the recording of data.

The flow and smoke thermocouples in the ducting insert are 1.5mm type K sheathed thermocouples.

6.3.4 Experimental Procedure

6.3.4.1 Calibration of Equipment

The O_2 analyser is calibrated using the same method described for calibration of the cone calorimeter tests O_2 analyser. Nitrogen is then used to 'zero' the O_2 analyser. The CO/CO_2 analyser is calibrated by the introduction of known concentrations of the gases, and is zeroed with the introduction of Nitrogen.

The heat release rate (HRR) measurements are calibrated using a Propane burner. A pre-determined gas flow rate can be set to provide a designated flame output (kW).

6.3.4.2 Test Fuel Sample - Two-seater chair

The two-seater chair arrangement as used in compartment test #1 was employed for the ISO room test. Figures 3.15 and 3.17 show the geometry of the foam cushions and the steel seat framing used, respectively. The fabric was fixed over the foam and standard staples were used for joining seams and edges. Overlapping edges of fabric were cut off. The weights recorded are shown in Table 6.3.

6.3.4.3 Testing Procedure

The chair was positioned in the compartment in the same location as in compartment test #1. The ignition source was a cotton wool swab soaked lightly with methylated spirits. The ignition source was located centrally along the chair at the corner join of the seat cushion and the seat back cushion. Data acquisition was commenced prior to ignition and continued for a period of 10 minutes after the fuel source had burnt out.

The results of the test were recorded and the HRR was calculated.

6.3.5 Results and Calculations

6.3.5.1 Test Observations

The sequence of photos shown in Figure 6.10 show the general observations that can be made from the experiment.

1 min

1min 30 secs

1 min 50 secs

2min 20 secs

2mins 35 secs

3 mins 05 secs

3 mins 20 secs

3 mins 55 secs

4 mins 40 secs

Figure 6.10 ISO room calorimeter photo sequence

Following the ignition, the fire grew steadily, spreading up and along the seat back cushions, with the smoke layer getting thicker and darker. At 1 minute 30 seconds, the black smoke exiting the opening became visible. By 2 minutes, melted and burning foam could be observed falling from the chair to form a pool at the floor. With the fire growing noticeably more intense with the increased pooling, flashover occurred at 2 minutes and 50 seconds from ignition. Post flashover, ventilation controlled burning continued for approximately 1 minute before a rapid decay became evident. Small quantities of flaming were still evident where melted plastics had collected in certain places on the steel chair framing and on the floor. No flaming was evident after 10 minutes from ignition.

6.3.5.2 Temperatures

Figure 6.11 shows the temperatures at the thermocouple locations, and the corresponding temperatures of the equivalent thermocouples used in compartment test #1.

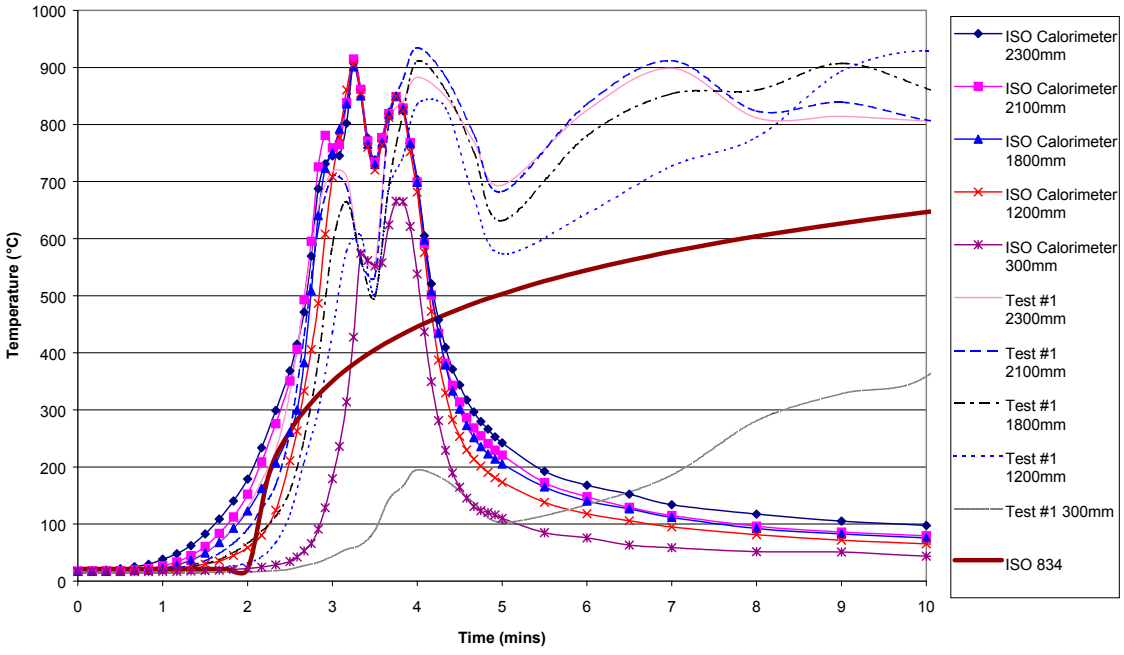

Figure 6.11 ISO room calorimeter test temperatures

The temperatures recorded at the thermocouples in the ISO room calorimeter test show a slightly faster rate of temperature rise within the compartment compared with the compartment test #1 results. The different observed times to flashover confirm this difference in temperature rise. Flashover in the calorimeter test was achieved at a time of 2 minutes 55 seconds after ignition, whereas in compartment test #1 flashover was reached at a time of 3 minutes 30

seconds. For both tests, peak temperatures at flashover rose to just above 900°C. In Test #1, the slight lag, compared with the calorimeter test, in reaching peak temperatures is die to the cribs in test #1 acting as a heat sink to some extent. It is also clear that the upper layer temperatures at which flashover in the room occurred are different. Flashover occurred at a temperature of approximately 750°C and 550°C in the room calorimeter test and compartment test #1 respectively. An analysis of the reason for this phenomenon is beyond the scope of this report and would be a suggested research area in the future. The decay of the chairs in the two tests can be seen to start at differing times of 3minutes 45 seconds and 4 minutes for the calorimeter test and compartment test #1 respectively, with the crib burning of test #1 becoming evident at 5 minutes, when the chair PU foam burning diminishes.

There are several variables, which result in the compartment test #1 temperatures rising at a slightly slower rate than observed in the ISO room calorimeter test. These variables include:

- Wind factors in the outdoor test compared with the ISO calorimeter test. The ISO calorimeter room can generally be considered to be free from wind effects.

- The wood cribs in the compartment tests invariably act as a heat sink and absorbed some heat release to some extent. As no cribs were in the ISO calorimeter test, such heat absorption by the cribs could not occur.

Considering the differing variables, the temperature readings obtained in both tests provide similar indications of the rate of rapid rise to above 900°C, which can be generated within a compartment of that geometry, by the two-seater chair arrangement, within the first five minutes of a 'real' fire.

6.3.5.3 Heat Release Rate

As with the cone calorimeter test, calculation of the HRR is based upon oxygen consumption calorimetry detailed by Janssens (1995). However, unlike the cone testing, additional CO and CO_2 analysers were used for the ISO room test.

Therefore a modified equation for the HRR, $\dot{q}$, is applied, where:

$$\dot{q} = \left[E\phi - (E_{CO} - E)\frac{1-\phi}{2}\frac{X_{CO}^{A^e}}{X_{O_2}^{A^e}} \right] . \frac{\dot{m}_e}{1+\phi(\alpha-1)} \frac{M_{O_2}}{M_a} \left(1 - X_{H_2O}^{A^a}\right) X_{O_2}^{A^a} \quad \textbf{Equation 6-5}$$

with

$$\phi = \frac{X_{O_2}^{A^a}\left(1 - X_{CO_2}^{A^e} - X_{CO}^{A^e}\right) - X_{O_2}^{A^e}\left(1 - X_{CO_2}^{A^a}\right)}{\left(1 - X_{O_2}^{A^e} - X_{CO_2}^{A^e} - X_{CO}^{A^e}\right) X_{O_2}^{A^a}} \quad \textbf{Equation 6-6}$$

The actual mole fraction of water vapour, $X_{H_2O}^{a}$, in the ambient air, is determined in the same way as for the cone calorimetry (Equation6-3). The results are summarised in Table 6.2.

ISO room calorimeter test - Two-seater chair arrangement					
Mass (kg)		Density (kg/m³)		Peak HRR, $\dot{Q}_{peak}$ (kW)	Total Heat Released, Q_{total} (MJ)
Foam	Fabric	Foam	Composite		
5.98	1.80	28.48	37.05	3,060	271.5

Table 6.2 – ISO room calorimeter test peak HRR and total heat release

Figure 6.12 shows the HRR chart obtained from the ISO room calorimeter test on the two–seater chair arrangement.

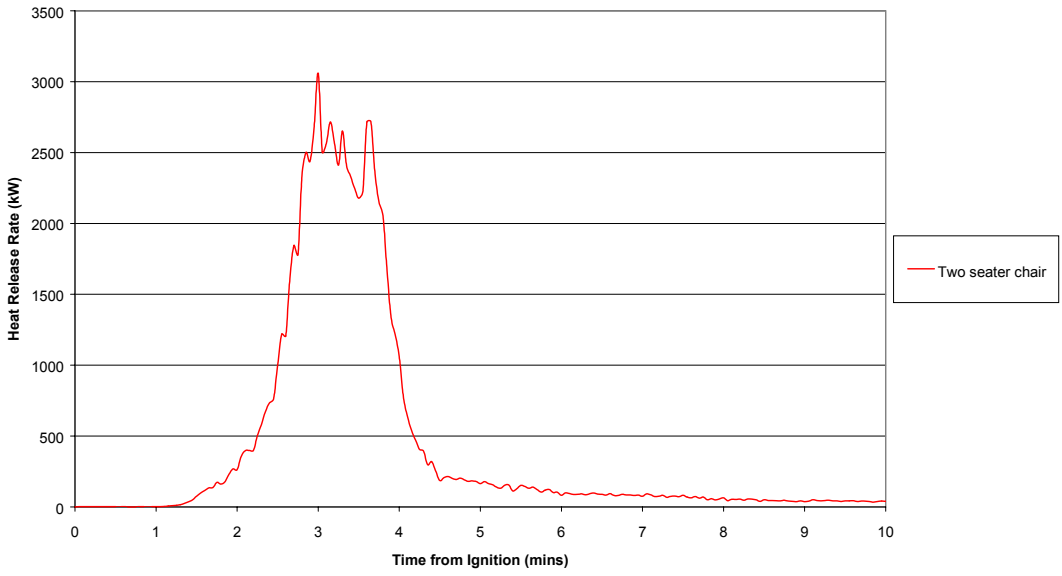

Figure 6.12 Two-seater chair HRR chart

The results show a rapid rise to a peak heat release of 3MW. However, an apparent steady state heat release of 2.5MW is evident for a duration of over a minutes burning time. The rapid decay associated with such fuels is much in evidence.

It should be noted that the results for heat release rate include some quantity heat release as a result of the burning paper lining from gypsum plasterboard. The level of contribution of paper heat release at any specific time cannot accurately be assessed to modify the chart accordingly. However, the level of heat release attributed by the paper at any given time is relatively small when compared with the chair heat release at that same time. Therefore, the HRR as shown in Figure 5.12 can generally be considered to be solely that of the two-seater chair cushions.

6.3.5.4 Heat of Combustion

The effective heat of combustion, $\Delta h_{c.eff}$, was calculated over the duration of the test period, and as given by Equation 6-4. The total heat release of the ISO room burn is shown graphically in Figure 6.13.

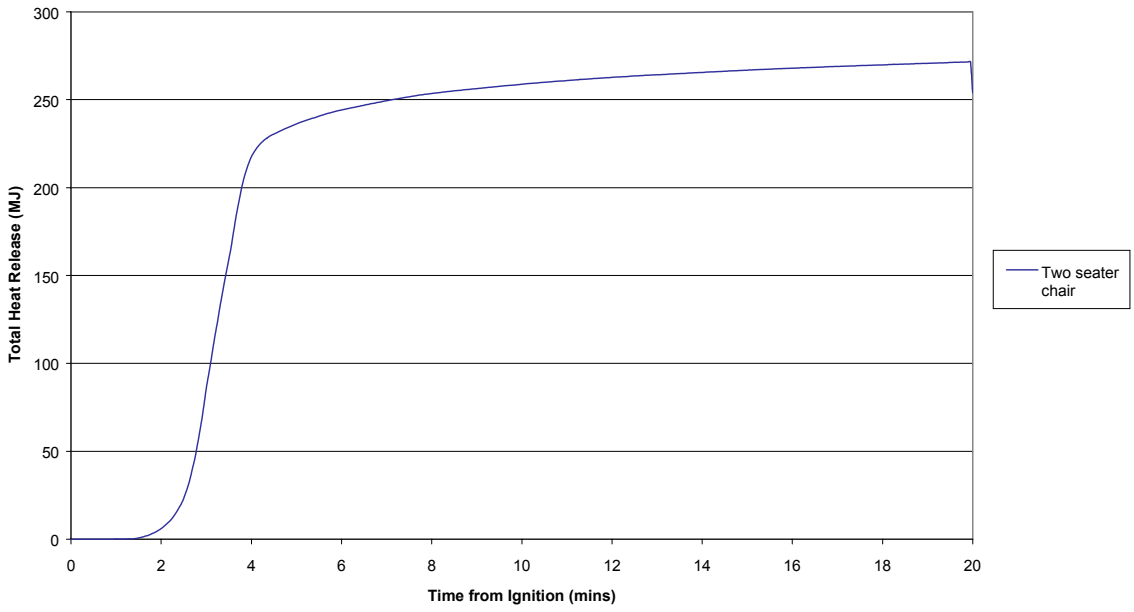

Figure 6.13 ISO room calorimeter test total heat release

Where the final mass for this combination of burnt foam and fabric is 2% of the initial mass (Coles 2001 – Sample K26), the effective heat of combustion, $\Delta h_{c.eff}$, was calculated at 35.6MJ/kg of foam and fabric cushions, assuming that only the chair fuel burning contributed to

the test results. This effective heat of combustion is significantly higher than the figure of 23.6MJ/kg, which Cole (2001) achieved in cone calorimeter samples of the same materials. The reason for this is easily explained. As mentioned previously, the total heat release includes a quantity from the paper lining of the plasterboard burning, and at any given time of the test the contribution of the paper heat release has been considered to be negligible when compared with the chair heat release at that same given time. However, the overall contribution of paper heat release over the duration of the test data collection (ie 20minutes) is clearly of significance to the correct calculation of the chair $\Delta h_{c.eff}$. Since the total heat release from the test produces such a significantly higher $\Delta h_{c.eff}$ than expected, an estimate of the contribution of paper heat release is required.

The total surface area of exposed paper lining was 42.8m². From post-test observations of the level of burnt internal surfaces, it has been assumed that all internal wall and ceiling surfaces and three-quarters of the floor surface area contributed to the total heat release. Where the paper thickness is 0.3mm and an assumed density of 550kg/m³ (Buchanan 2001b - similar to wood), the total mass of paper contributing to the heat release during the test is estimated as 6.7kg. The $\Delta h_{c.eff}$ of paper is assumed to be the same as wood, at 12MJ/kg (Babrauskas 1995). Therefore, the energy release, throughout the duration of the test, attributed to the paper lining of the plasterboard is estimated to be 80.5MJ. Deducting the paper heat release content from the total test heat release gives 191MJ, which can be assumed to be the total heat release due solely to the foam and fabric cushions burning. Where the final mass of the fuels after the test is assumed to be 2% of the initial mass, this provides a $\Delta h_{c.eff}$, for the foam and fabric, of 25.1MJ/m². When checked against the cone calorimeter test result of 27.7MJ/kg, this was a reasonable estimate.

7 Summary and Conclusions

7.1 Summary

This study was carried out to develop a correlation between the standard furnace test fire exposure and realistic fire exposures, and determine the failure time of a non-loadbearing assembly when exposed to such fires.

An overview of fire resistance, fire severity, New Zealand Building Code fire resistance requirements and assembly fire resistance testing methods has been undertaken in the form of a literature review.

Three full-scale compartment tests were carried out to obtain time-temperature histories within the compartment and failure times for assemblies of various constructions when exposed to the compartment fire exposures. Each compartment was constructed to enable testing of several assemblies in a single test. Extensive temperature data was obtained. Results of the compartment tests were compared with standard furnace test data for each assembly.

A method of predicting assembly failure times when exposed to real fire exposures has been proposed. The method is based on a correlation of the cumulative radiant heat energy that would impact on an assembly up to the time of failure during a standard test, and the equivalent time at which a real fire exposure would have produced the same level of energy impact to cause failure. This method is called the 'radiant exposure area method'.

7.2 Conclusions

The following conclusions have been found further to the results and analyses of the compartment fire tests:

- The failure times of the test assemblies in the compartment tests confirm that the typical light timber/steel framed assemblies exposed to realistic fires, will fail at times significantly less than the FRR derived from standard tests, for fires which are more severe than the standard tests fire exposure. Appropriate modifications to the FRR requirements in the Approved Documents should be made to reflect this.

- The 'radiant exposure area correlation' provides good agreement and reasonably conservative prediction of non-loadbearing wall assembly insulation failure. For specific design fires with varying ventilation conditions, assembly failure curves can be produced.

- When exposed to more severe fire exposures than the standard fire test, light steel framed plasterboard wall assemblies fail on the integrity criteria. As a result, the radiant exposure area correlation cannot reliably predict failure of LSF assemblies, since mechanisms other than thermal heat transfer are involved, such as rate and extent of deflection of steel framing. Further development of the method with the use of factors of safety is required, to incorporate such mechanisms of LSF assembly integrity failure.

- The radiant exposure area correlation is inappropriate for prediction of structural failure of loadbearing assemblies. Factors of safety need to be incorporated into the method, or alternative approaches need to be developed.

7.3 Recommendations

The following recommendations are advised:

- The radiant exposure area correlation of assembly insulation failure prediction for non- loadbearing wall assemblies be employed, by building designers, engineers, and the territorial authorities, to ensure the Approved Documents F ratings are met in a realistic fire exposure. This would require an increase in FRRs, where appropriate, for real fire exposures more severe than the standard furnace test exposure.

- The Approved Documents F ratings terminology should be modified to represent a 'real time' value.

- To assist designers further with the application of the radiant exposure area correlation, it would be recommended for manufacturers to detail more accurate assembly standard test failure times (i.e. rounded down to the nearest 5-10 minutes, as oppose to the nearest half hour). This would avoid over conservativism of failure time prediction.

- Further research, is recommended, to make a full assessment as to whether the radiant exposure area method is suitable for use on assemblies that fail the standard furnace test on integrity, and/or validate Thomas' method for use. Specific assemblies include fire doors and proprietary fittings used, where wall penetrations are a concern (ie fire dampers, pipe collars etc) should be researched further to establish whether the radiant exposure area method is appropriate, or whether a suitable modification to the method can be applied for integrity failure (i.e. factors of safety).

- The mechanisms of integrity failure of light steel framed wall systems, when exposed to more severe fires than the standard test fire exposure, require further research to develop factors of safety into the radiant exposure area method, or to reduce the likelihood of integrity failure. Particular attention is required to evaluate the level steel framing deflection and the effect of assembly size on

assembly failure times, when exposed to fires more severe than the standard test fire exposure.

- In lieu of there being no alternative conservative approach to the structural failure prediction of light weight loadbearing assemblies, it is suggested that Thomas's method be employed to predict structural failure of loadbearing light framed assemblies. Further research on structural failure of load bearing assemblies, exposed to realistic fires, is recommended.

- A quantitative survey of the site installed construction quality and level of workmanship, of LTF and LSF assemblies used as fire barriers, should be undertaken. The results of the survey should be incorporated into the building code fire endurance requirements using a probabilistic risk assessment approach.

- The detailed examination of charring rates in realistic fires would be a recommended topic for further research.

8 References

(ASTM 1995), ASTM E119, *Standard Test Methods for Fire Tests of Building Construction and Materials*, 1995, American Society for Testing and Materials, Philadelphia, United States of America.

(Babrauskas 1976), V Babrauskas, *Fire Endurance in Buildings*, 1976, Fire Research Group, Report No. UCB FRG 76-16, University of California-Berkeley, United States of America.

(Babrauskas et al 1978a), V Babrauskas, R B Williamson, *Postflashover Compartment Fires – Basis of a Theoretical Model*, 1978, Fire and Materials, Vol. 2, No. 2., pp39-53.

(Babrauskas et al 1978b), V Babrauskas, R B Williamson, *The Historical Basis of Fire Resistance Testing – Part I and Part II*, 1974, Fire Technology, 14/3&4.

(Babrauskas 1979), V Babrauskas, *COMPF2, A Program for Calculating Post-Flashover Fire Temperatures*, 1979, US Department of Commerce/National Bureau of Standards, NBS Technical Note 991, Gaithersburg, USA.

(Babrauskas et al 1979a), V Babrauskas, U G Wickström, *Thermoplastic Pool Compartment Fires*, 1979, Combustion and Flame, Vol. 34, pp195-202.

(Babrauskas 1995), V Babrauskas, *Burning Rates*, Section 3/Chapter 1, SFPE Handbook of Fire Protection Engineering, 2nd Edition, 1995, Society of Fire Protection Engineers, USA.

(Barnett 2002), C R Barnett, *BFD Curve – A New Empirical Model for Fire Compartment Temperatures*, Macdonald Barnett Partners Ltd, Consulting Engineers, Auckland, New Zealand.

(BIA 2001), *Approved Documents C/AS1,* 2001, Building Industry Authority (BIA), New Zealand.

(Blackmore et al 1999), J Blackmore, C Brescianini, G Collins, M A Delichatsios, G Everingham, J Hooke, R Ralph, I Thomas, P Beever, *Fire Code Reform Centre, Project 3: Fire Resistance and Non Combustibility, Part 3: Room and Furnace Tests of Fire Rated Construction*, July 1999, Fire Code Reform Centre Ltd/CSIRO Division of Building, Construction and Engineering, NSW, Australia.

(BRANZ FP2881), *FP 2881: Pilot Furnace Test of a Non-loadbearing Steel Framed Wall Lined with 12.5mm GIB® Fyreline Gibralter Board*, 2001, Building Research Association of New Zealand, Wellington, New Zealand. (Confidential -referenced with permission of manufacturer).

(BRANZ FR1370), *FR 1370: Report on the Fire Resistance Properties of a Loadbearing Floor/Ceiling System*, September 1988, BRANZ Test Report, Building Research Association of New Zealand, Wellington, New Zealand. (Confidential -referenced with permission of manufacturer).

(BRANZ FR1391), *FR 1391: Report on the Fire Resistance Properties of a Non-loadbearing Steel Framed Wall Lined with One Layer of 10mm GIB® Foam Gibralter Board*, BRANZ Test Report, Building Research Association of New Zealand, Wellington, New Zealand. (Confidential -referenced with permission of manufacturer).

(BRANZ FR1405), *FR 1405: Report on the Fire Resistance Properties of the Side-hung Single-leaf Fireguard 30 Fire Doorset*, September 1988, BRANZ Test Report, Building Research Association of New Zealand, Wellington, New Zealand. (Confidential -referenced with permission of manufacturer).

(BRANZ FR1571), *FR 1571: Report on the Fire Resistance Properties of a Loadbearing Timber Framed Wall Lined with 12.5mm GIB® Fyreline Gibralter Board*, October 1990, BRANZ Test Report, Building Research Association of New Zealand, Wellington, New Zealand. (Confidential -referenced with permission of manufacturer).

(BRANZ FR1572), *FR 1572: Report on the Fire Resistance Properties of a Loadbearing Floor/Ceiling System*, November 1990, BRANZ Test Report, Building Research Association of New Zealand, Wellington, New Zealand. (Confidential -referenced with permission of manufacturer).

(BRANZ FR1579), *FR 1579: Report on the Fire Resistance Properties of a Non-loadbearing Steel Framed Wall Lined with 12.5mm GIB® Fyreline Gibralter Board*, 1990, BRANZ Test Report, Building Research Association of New Zealand, Wellington, New Zealand. (Confidential -referenced with permission of manufacturer).

(BRANZ FR1712), *FR 1712: Report on the Fire Resistance Properties of a Loadbearing Timber Framed Wall Lined Each Side with One Layer of 9.5mm GIB® Fyreline Gibralter Board*, July 1992, BRANZ Test

Report, Building Research Association of New Zealand, Wellington, New Zealand. (Confidential -referenced with permission of manufacturer).

(BRANZ FR2454), *FR 2454: Report on the Fire Resistance Properties of a Load Bearing Timber Framed Wall*, BRANZ Test Report, Building Research Association of New Zealand, Wellington, New Zealand. (Confidential -referenced with permission of manufacturer).

(BRANZ FR2493), *FR 2493: Report on the Fire Resistance Properties of a Load Bearing Timber Framed Wall*, BRANZ Test Report, Building Research Association of New Zealand, Wellington, New Zealand. (Confidential -referenced with permission of manufacturer).

(BRANZ 2000), C Wade, *BRANZFIRE Technical Reference Guide*, BRANZ Study Report No.92, 2000, Building Research Association of New Zealand, Wellington, New Zealand.

(BSI 1987), British Standard, BS 476: Parts 20-24, *Fire Tests on Building Materials and Structures*, 1987, British Standards Institution, United Kingdom.

(Buchanan 1994), A H Buchanan, *Fire Engineering for a Performance Based Code*, 1994, Fire Safety Journal, Vol. 23, pp1-16.

(Buchanan 2001a), A H Buchanan, *Structural Design for Fire Safety,* 2001, John Wiley & Sons, UK.

(Buchanan 2001b), A H Buchanan, *Fire Engineering Design Guide,* 2001, Centre for Advanced Engineering, Christchurch, New Zealand.

(Buchanan et al 2001), A H Buchanan, J T Gerlich, *Evacuation Times and Fire Resistance Ratings – How realistic are they?*, Build, May/June 2001, pp21-23.

(Caro et al 1995), T C Caro, J A Milke, *A Survey of Fuel loads in Office Buildings*, November 1995 (issued September 1996), NIST Report NIS-GCR-96-697, Building and Fire Research Laboratory, National Institute of Standards and Technology, Gaithersburg, MD 20899, USA.

(CIB 1986), CIB-W14, *Design Guide – Structural Fire Safety*, Fire Safety Journal, Vol. 10, No. 2, pp75-138, 1986.

(Coles 2001), A R Coles, *Flammability of Upholstered Furniture Using Cone Calorimeter*, Fire Engineering Research Report 01/1, 2001, University of Canterbury, New Zealand.

(Collier 2000), P C R Collier, *Fire Resistance of Lightweight Framed Construction*, Fire Engineering Research Report 00/2, 2000, University of Canterbury, New Zealand.

(Cooper 1995), L Y Cooper, *Compartment Fire Generated Environment and Smoke Modelling*, Section 3/Chapter 10, SFPE Handbook of Fire Protection Engineering, 2nd Edition, 1995, Society of Fire Protection Engineers, USA.

(Cooper et al 1996), L Y Cooper, K D Steckler, *Methodology for Developing and Implementing Alternative Temperature-Time Curves for Testing the Fire Resistance of Barriers for Nuclear Power Plant Applications*, 1996, NIST Report NISTIR 5842. Building and Fire Research Laboratory, National Institute of Standards and Technology, Gaithersburg, MD 20899, USA.

(Cooper 1997), L Y Cooper, *The Thermal Response of Gypsum-Panel/Steel Stud Wall Systems Exposed to Fire Environments – A Simulation for the use in Zone-Type Fire Models*, 1997, NIST Report NISTIR 6027. Building and Fire Research Laboratory, National Institute of Standards and Technology, Gaithersburg, MD 20899, USA.

(Cooper et al 2000), L Y Cooper, P A Reneke, *A Prototype Model for Simulating Barrier fire Performance: CFAST.GYPST – for Evaluating the Response of Gypsum Panel/Steel-Stud Wall Systems*, February 2000, NIST Report NISTIR 6482. Building and Fire Research Laboratory, National Institute of Standards and Technology, Gaithersburg, MD 20899, USA.

(Culver 1976), C G Culver, *Survey Results for Fire Loads and Live Loads in Office Buildings*, NMS Building Science Series 85, Gaithersburg, MD: NBS, 1976, USA..

(Denize 2000), H Denize, *The Combustion Behaviour of Upholstered Furniture Materials in New Zealand*, Fire Engineering Research Report, 2000, University of Canterbury, New Zealand.

(Duncan 2001), C Duncan, *History of the Standard Time-Temperature Fire Curve*, BRANZ Report FSR495, Building Research Association of New Zealand, Wellington, New Zealand. (Confidential -referenced with permission of Winstone Wallboards Ltd.).

(EC1 1996), *Eurocode 1: Basis of Design and Design Actions on Structures*, *Part 2-2: Actions on Structures Exposed to Fire*, ENV 1991-2-2:1996, European Committee for Standardisation, Brussels.

(EC5 1994), *Eurocode 5: Design of Timber Structures*, ENV 1995-1-2:General Rules - Structural Fire Design, European Committee for Standardisation, Brussels.

(England et al 2000), J P England, S A Young, M C Hui, N Kurban, *Guide for the Design of Fire Resistant Barriers and Structures*, 2000, Warrington Fire and Research (Aust) Pty Ltd, Victoria, Australia.

(Enright 2000), P A Enright, *Heat Release and Combustion Behaviour of Upholstered Furniture*, 2000, Thesis in Doctor of Philosophy, University of Canterbury, Christchurch, New Zealand.

(Firestone 1999), J Firestone, *An Analysis of Furniture Heat Release Rates by the Nordtest*, Fire Engineering Research Report, 1999, University of Canterbury, New Zealand.

(Gerlich 1995), *Design of Loadbearing Light Steel Frame Walls for Fire Resistance*, Fire Engineering Research Report 95/3, 1995, University of Canterbury, Christchurch, New Zealand.

(Girgis 2000), N Girgis, *Full-Scale Compartment Fire Experiments*, Fire Engineering Research Report, 2000, University of Canterbury, New Zealand.

(Harmathy 1987), P Z Harmathy, *On the Equivalent Fire Exposure*, 1987, Fire and Materials, Vol. 11, pp95-104.

(Huggett 1980), C Huggett, *Estimation of Rate of Heat Release by Means of Oxygen Consumption Measurements*, 1980, Fire and Materials, Vol. 4, No. 2.

(Incropera and DeWitt 1996), F P Incropera, D P DeWitt, *Fundamentals of Heat and Mass Transfer*, Fourth Edition, 1996, John Wiley and Sons Publications, USA.

(ISO 1975), ISO 834, 1975, *Fire Resistance Tests – Elements of Building Construction*, 1975, International Organization for Standardisation, Switzerland.

(ISO 1993a), ISO 9705 , 1993 *Fire Tests – Full Scale Room Test for Surface Products*, 1993, International Organisation for Standardisation, Switzerland.

(ISO 1993b), ISO 5660 Part 1, 1993 *Fire Tests – Reaction to Fire Part 1: Heat Release Rate from Building Products*, 1993, International Organisation for Standardisation, Switzerland.

(Janssens 1995), M Janssens, *Calorimetry*, Section 3/Chapter 2, SFPE Handbook of Fire Protection Engineering, 2nd Edition, 1995, Society of Fire Protection Engineers, USA.

(Jones et al 1990), W W Jones, G P Forney, *A Programmer's Reference for CFAST, The Unified Model of Fire Growth and Smoke Transport*, Technical Note 1283, National Institute of Standards and Technology, Gaithersburg MD, 1990.

(Jones 2001), Bevan H Jones, *Performance of Gypsum Plasterboard Assemblies Exposed to Real Building Fires*, Fire Engineering Research Report, 2001, University of Canterbury, New Zealand.

(Karsson et al 2000), B Karlsson, J G Quintiere, *Enclosure Fire Dynamics*, 2000, CRC Press LLC.

(Kawagoe 1958), K Kawagoe, *Fire Behaviour in Rooms*, 1958, Report No.27, 2000, Building Research Institute, Tokyo.

(Kirby et al 1994), B R Kirby, D E Wainman, L N Tomlinson, T R Kay, B N Peacock, *Natural Fires in Large Scale Compartments- A British Steel Technical*, Fire Research Station Collaborative Project, British Steel Technical, Swinden Laboratories, UK.

(Law 1997), M Law, *A Review of Formulae for T-Equivalent*, 1997, 5th IAFSS Symposium, Melbourne Australia.

(Lie 1974), T T Lie, *Characteristic Temperature Curves for Various Fire Severities*, 1974, Fire Technology, Vol. 10, No. 4, pp315-326.

(NZBC, 1992), *New Zealand Building Code,* Building Regulations, 1992, New Zealand.

(NZS 1993), *Code of Practise for Timber Design. NZS 3603: 1993,* Standards New Zealand.

(SAA 1990), *AS 1530: Part 4: Fire Resistance Tests of Elements of Building Construction, 1997*, Standards Association of Australia, NSW, Australia.

(SAA 1998), *AS/NZS 3837: 1998 Method for Test for Heat and Smoke Release Rates for Materials and Products Using an Oxygen Consumption Calorimeter, 1998*, New Zealand Standards & Standards Association of Australia.

(Sultan et al 2000), M A Sultan, V K R Kodur, *Light-weight Frame Wall Assemblies: Parameters for Consideration in Fire Resistance Performance-Based Design*, 2000, Fire Technology, Vol. 36, No. 2, pp75-88.

(Sundström 1995), B Sundström, *CBUF Fire Safety of Upholstered Furniture – the final report on the CBUF research programme*, 1995, European Commission Measurements and Testing Report EUR 16477 EN.

(Thomas, G 1997), G C Thomas, *Fire Resistance of Light Timber Framed Walls and Floors*, 1997, Fire Engineering Research Report 97/7, University of Canterbury, Christchurch, New Zealand.

(Thomas, G et al 2002), G C Thomas, D Lloyd, *Fire Resistance of Structural Components Protecting Escape Routes,* Proceedings of the Second International Workshop: 'Structures in Fire', 18th & 19th March 2002, Christchurch, New Zealand.

(Walton et al 1995), W D Walton, P H Thomas, *Estimating Temperatures in Compartment Fires*, Section 3/Chapter 6, SFPE Handbook of Fire Protection Engineering, 2nd Edition, 1995, Society of Fire Protection Engineers, USA.

(Winstone Wallboards 2001), *GIB® Fire Rated Systems*, August 2001, Winstone Wallboards Ltd, Auckland, New Zealand.

(Yii 2000), H W Yii, *Effect of Surface Area and Thickness on Fire Loads*, Fire Engineering Research Report, 2000, University of Canterbury, New Zealand.

A. Appendix A – Construction Drawings and Photos

NOTE: - Timber framing was nominal 90mm x 45mm kiln dried Radiata pine. Not 90mm x 35mm laser framing as indicated.

TEST #1 – Half hour rated systems:

Walls Plan Layout:

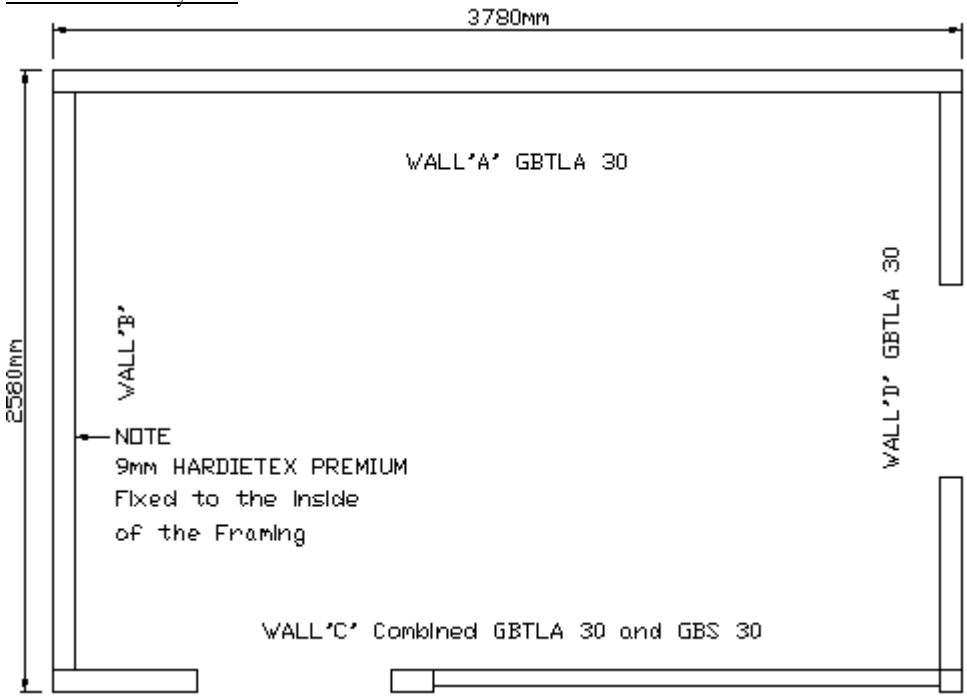

Wall A Elevation:

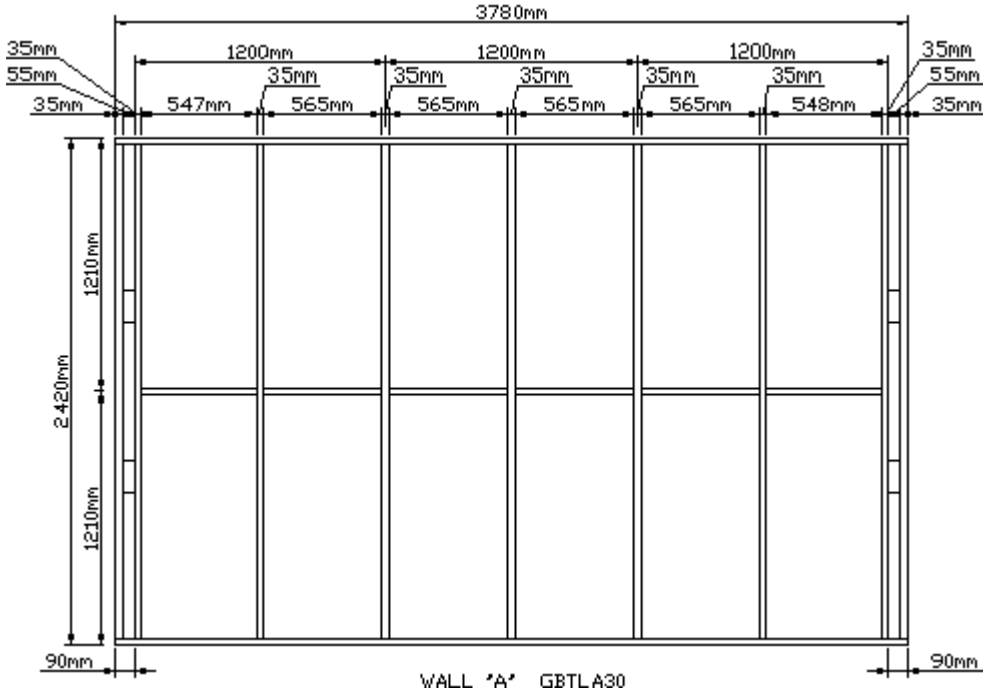

Appendix A – Construction Drawings and Photos

Wall A Section and Construction Photo:

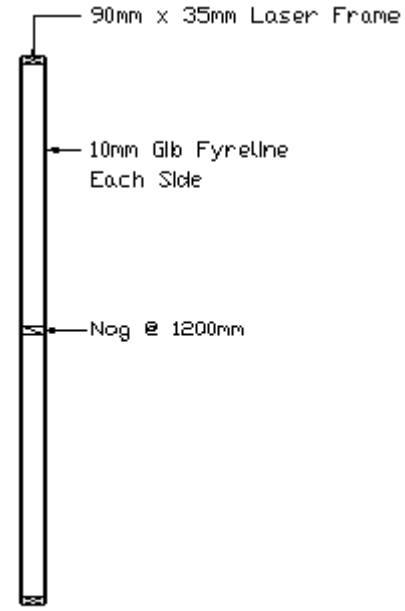

WALL 'A'
GBTLA 30

Wall B Elevation and Construction Photo:

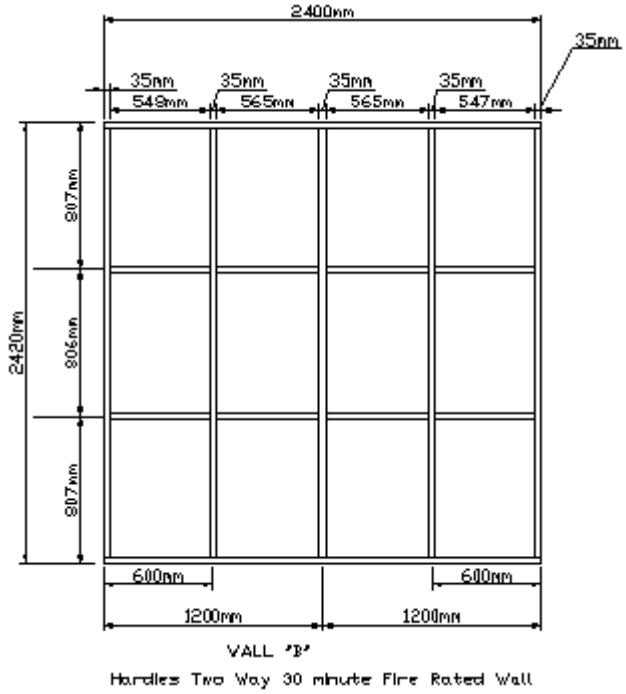

WALL 'B'
Handles Two Way 30 minute Fire Rated Wall

Wall B Section:

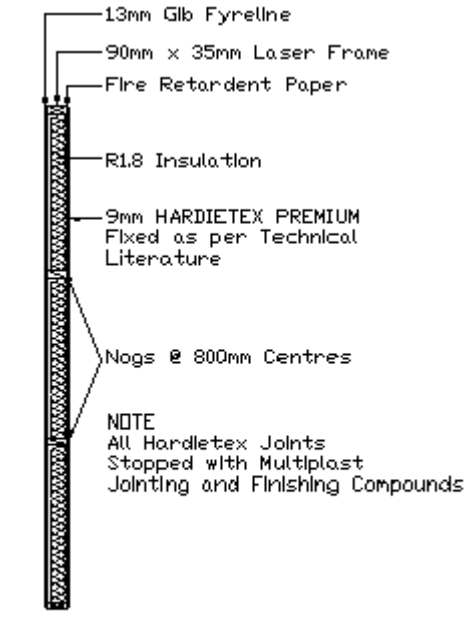

Wall C and Fire Door Framing Elevation:

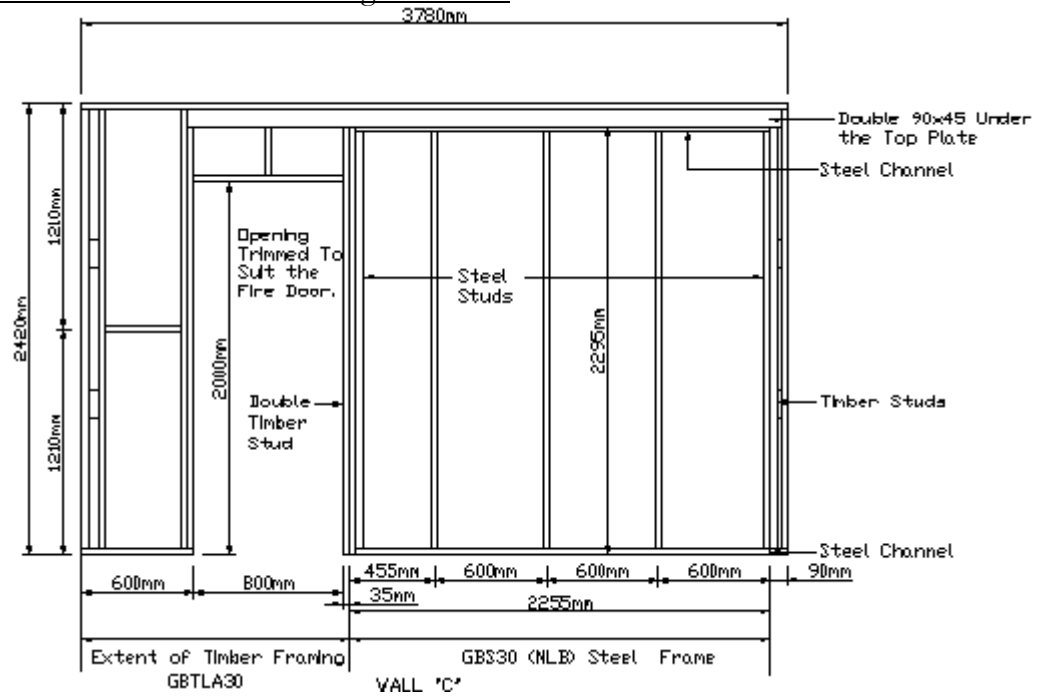

Appendix A – Construction Drawings and Photos

Wall C and Fire Door Section:

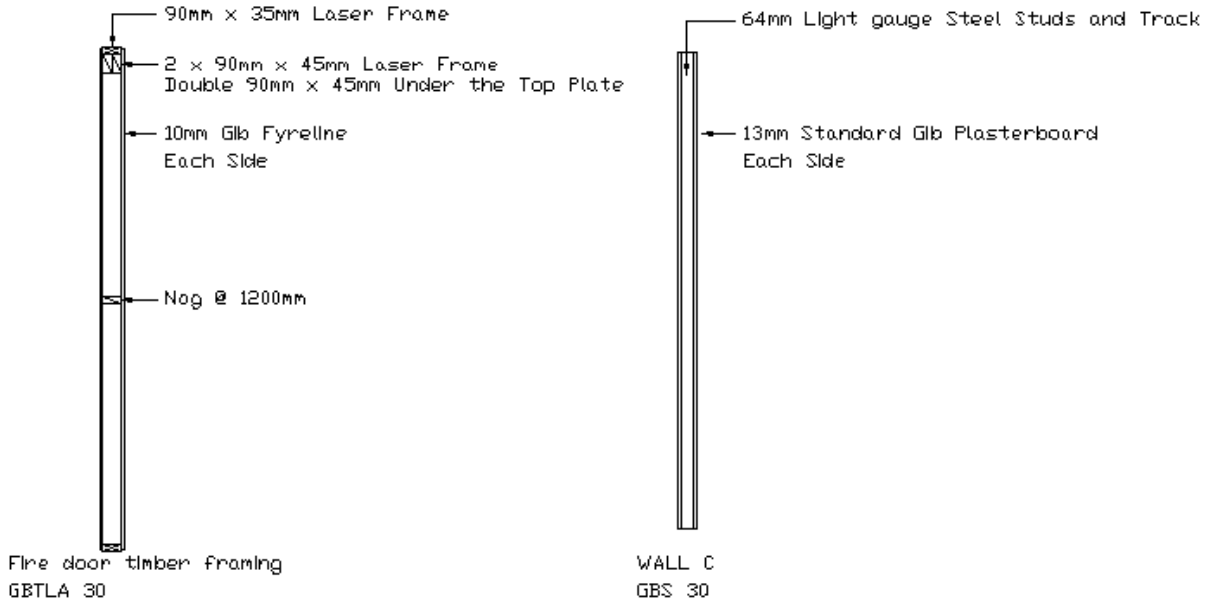

Wall C Construction Photo:

Appendix A – Construction Drawings and Photos

Wall Opening Elevation and Section:

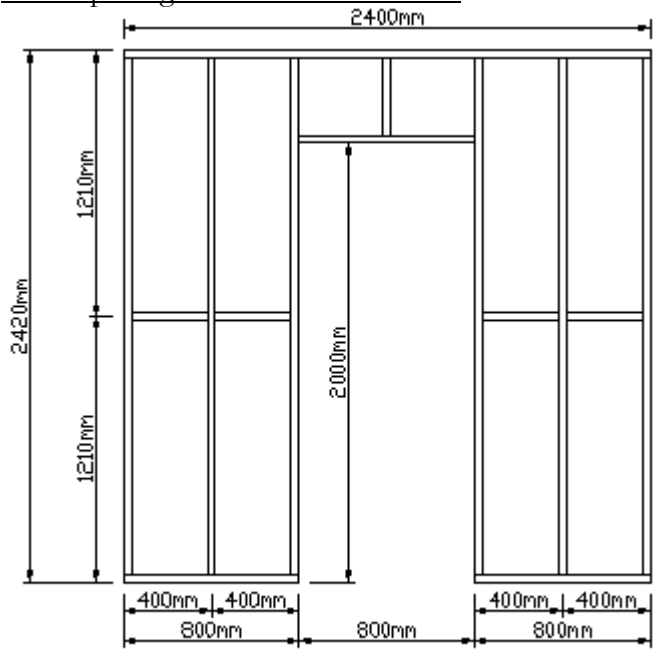

WALL Opening GBTLA30

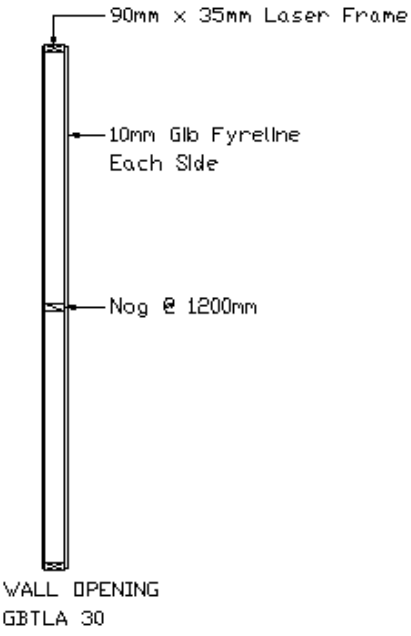

WALL OPENING
GBTLA 30

Ceiling set out and Construction Photo:

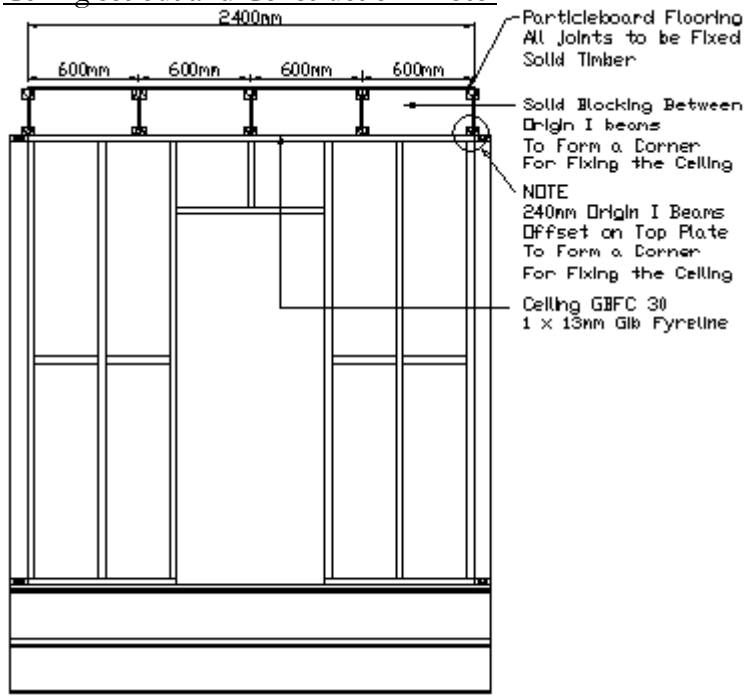

Appendix A – Construction Drawings and Photos

Floor Plan:

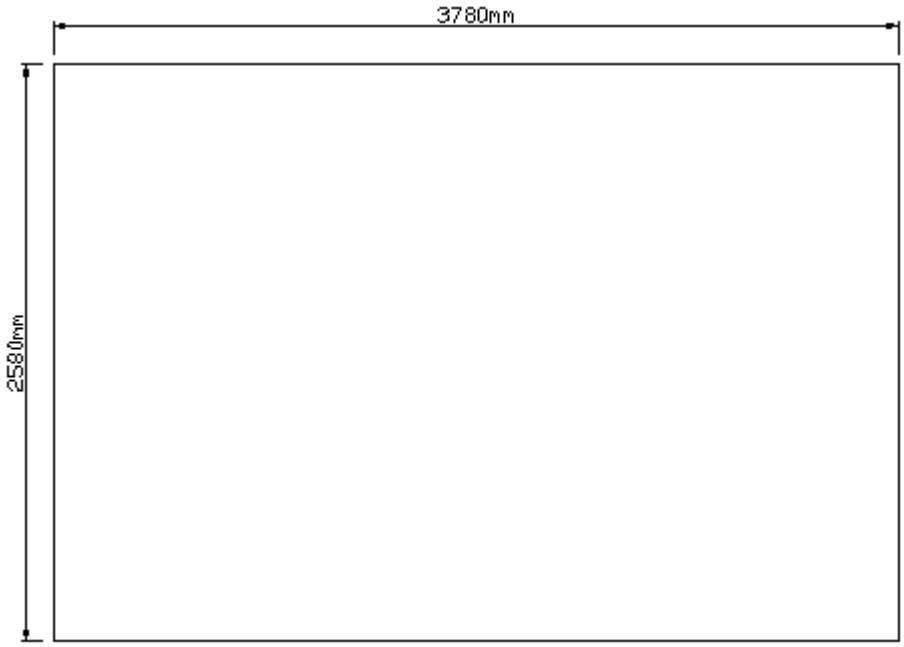

Floor Plan

Floor Section:

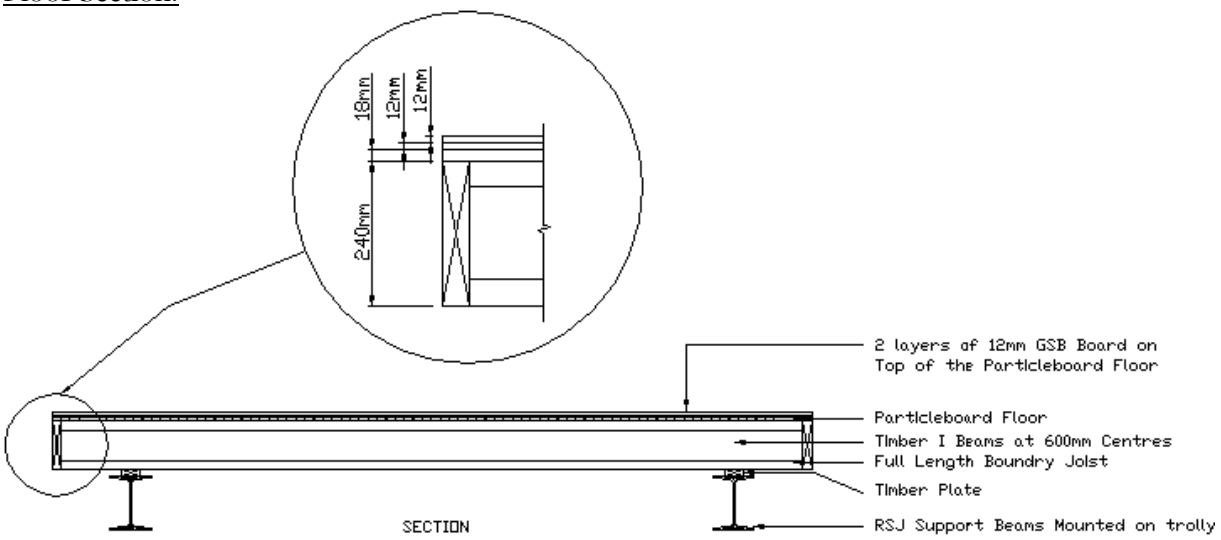

Floor I Beam set out:

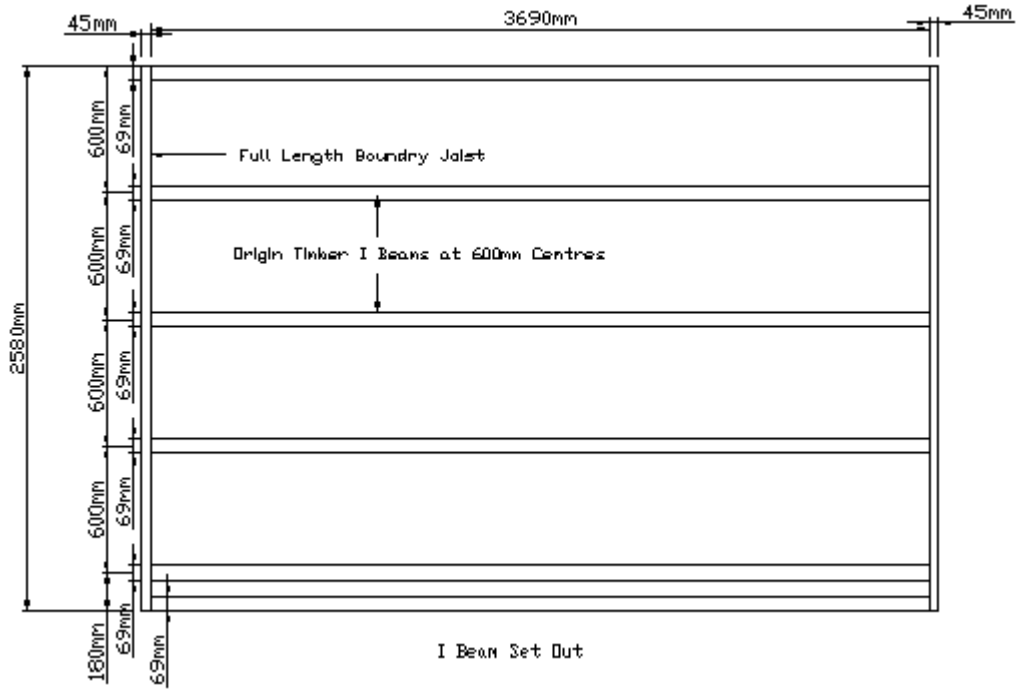

TEST #2 – One hour rated systems:

Walls Plan Layout:

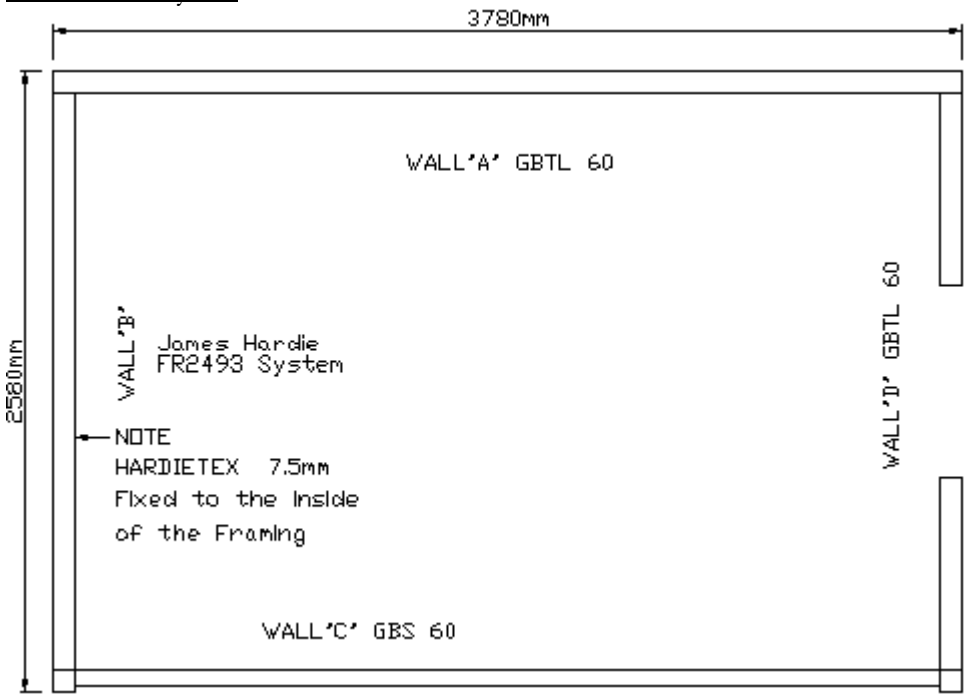

Wall A Elevation:
Refer to Test#1 framing construction details.

Wall A Section:
Construction details as given for Test#1 drawing. 13mm 'Fyreline' plasterboard lining on both side of the framing.

Wall B Elevation:
Refer to Test#1 framing construction details.

Wall B Section:

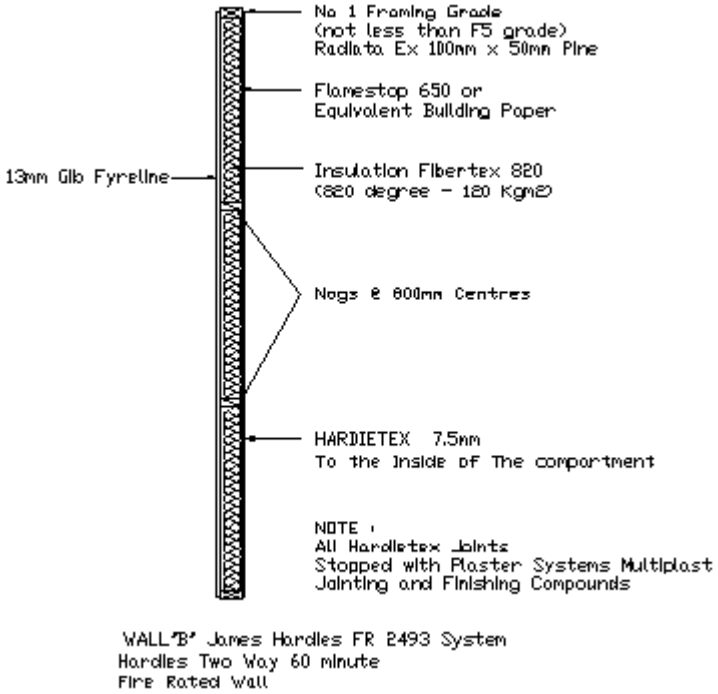

WALL'B' James Hardies FR 2493 System
Hardies Two Way 60 minute
Fire Rated Wall

Wall C Elevation:

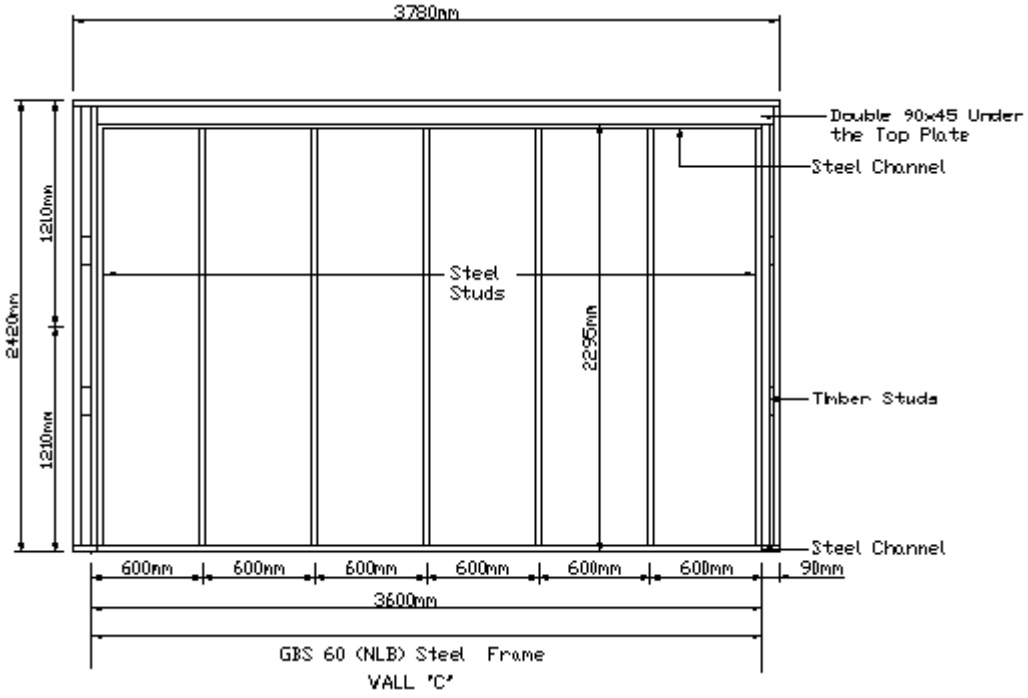

Wall C Section:
Construction details as given for Test#1 drawing. 13mm 'Fyreline' plasterboard lining on both side of the framing.

Wall C Construction Photo:

Wall Opening Elevation:
Refer to Test#1 framing construction details.

Wall Opening Section:
Construction details as given for Test#1 drawing. 13mm 'Fyreline' plasterboard lining on both side of the framing.

Ceiling set out:
Construction details as given for Test#1 drawing. 16mm 'Fyreline' plasterboard lining on underside of ceiling construction.

Floor Plan:
Refer to Test #1 Floor Plan.

Floor Section:
Refer to Test #1 Floor Section.

Floor I Beam set out:
Refer to Test #1 Floor I Beam set out.

TEST #3 – Half hour rated systems:

Walls Plan Layout:

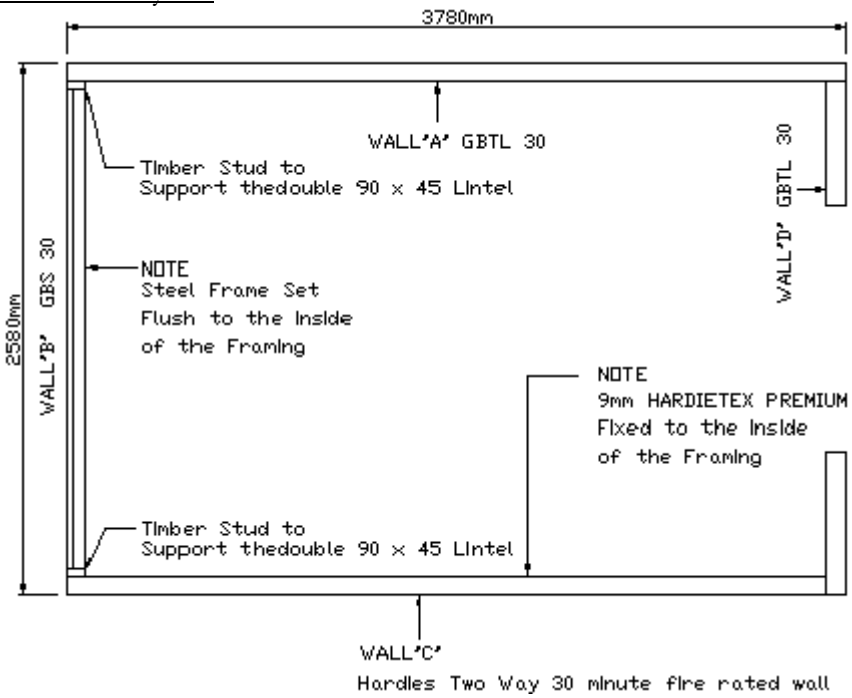

Wall A Elevation:
Refer to Test #1 Wall A elevation details

Wall A Section:
Refer to Test #1 Wall A section details

Wall B Elevation:

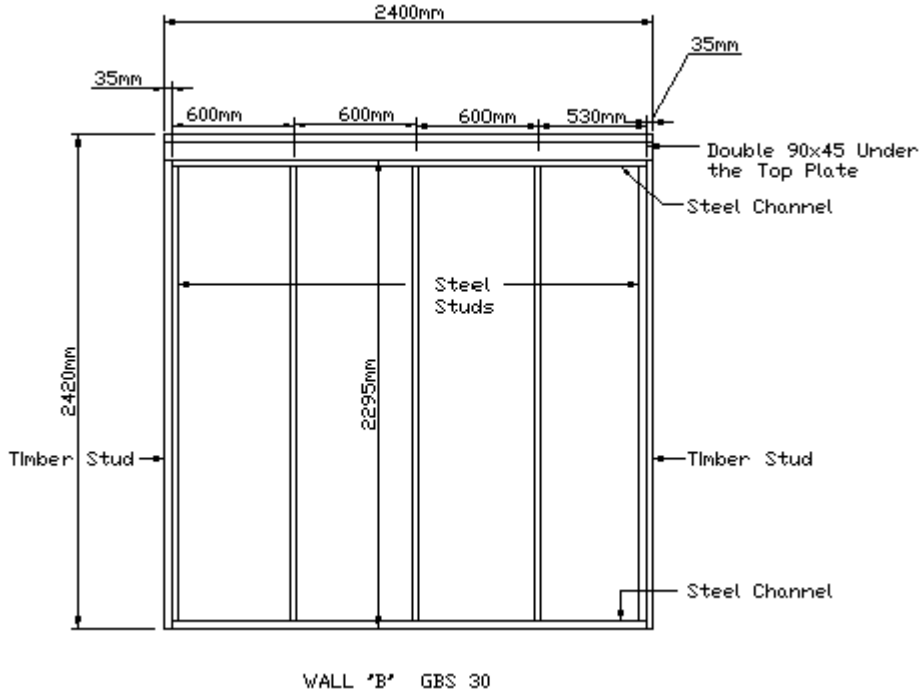

Wall B Section:
Refer to Test #1 Wall C section details

Wall C Framing Elevation:

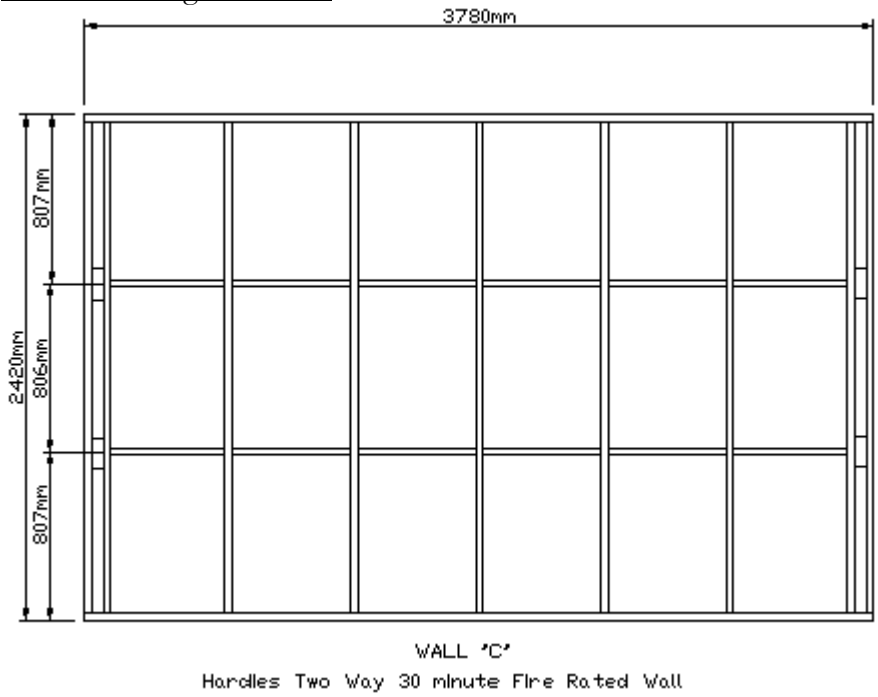

Wall C Framing Construction Photo:

Wall C Section:
Refer to Test #1 Wall B section details

Wall Opening Elevation:

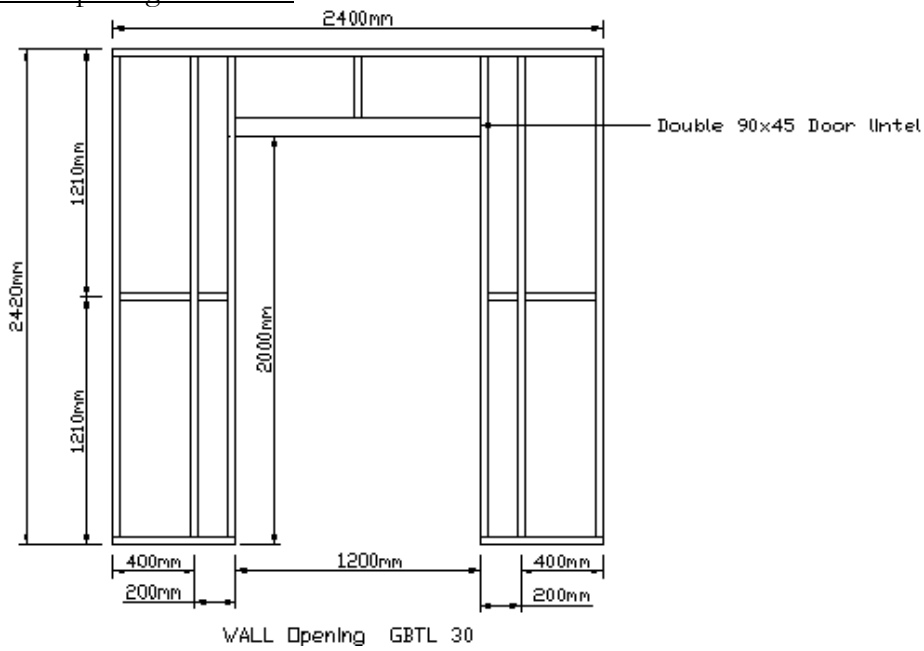

Wall Opening Section:
Refer to Test #1 wall opening section

Ceiling set out:

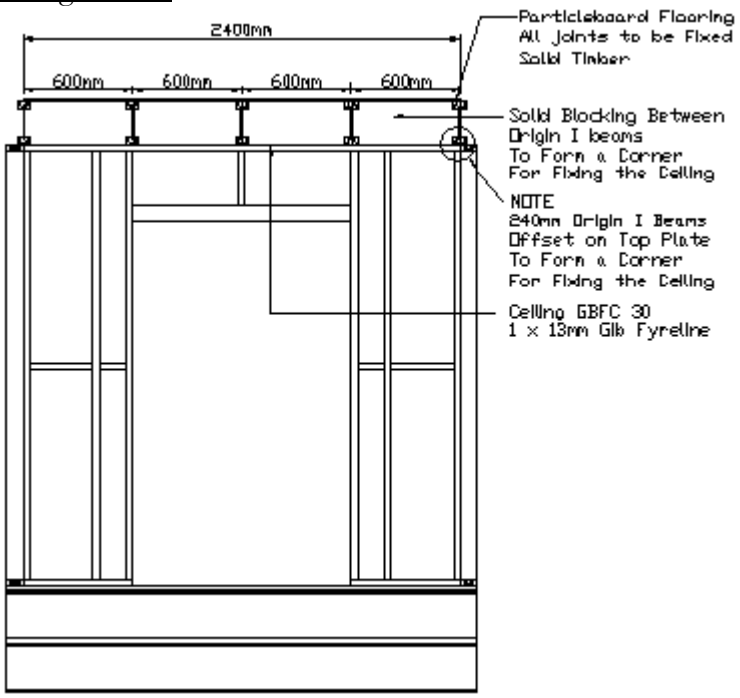

Floor Plan:
Refer to Test #1 Floor Plan.

Floor Section:
Refer to Test #1 Floor Section.

Floor I Beam set out:
Refer to Test #1 Floor I Beam set out.

B. Appendix B – Thermocouple References and Data Logger Channel

Test #1:

Channel	t/c ref	Description
1	WA/1-1	Wall A Location 1 - Unexposed face (disc t/c)
2	WA/2-1	Wall A Location 2 - Unexposed face (disc t/c)
3	WA/3-1	Wall A Location 3 - Unexposed face (disc t/c)
4	WA/4-1	Wall A Location 4 - Unexposed face (disc t/c)
5	WA/5-1	Wall A Location 5 - Unexposed face (disc t/c)
6	WA/1-2	Wall A Location 1 - Unexposed panel in cavity (disc t/c)
7	WA/2-2	Wall A Location 2 - Unexposed panel in cavity (disc t/c)
8	WA/3-2	Wall A Location 3 - Unexposed panel in cavity (disc t/c)
9	WA/4-2	Wall A Location 4 - Unexposed panel in cavity (disc t/c)
10	WA/5-2	Wall A Location 5 - Unexposed panel in cavity (disc t/c)
11	WA/1-3	Wall A Location 1 - Exposed panel in cavity (disc t/c)
12	WA/2-3	Wall A Location 2 - Exposed panel in cavity (disc t/c)
13	WA/3-3	Wall A Location 3 - Exposed panel in cavity (disc t/c)
14	WA/4-3	Wall A Location 4 - Exposed panel in cavity (disc t/c)
15	WA/5-3	Wall A Location 5 - Exposed panel in cavity (disc t/c)
16	WB/1-1	Wall B Location 1 - Unexposed face (disc t/c)
17	WB/2-1	Wall B Location 2 - Unexposed face (disc t/c)
18	WB/3-1	Wall B Location 3 - Unexposed face (disc t/c)
19	WB/4-1	Wall B Location 4 - Unexposed face (disc t/c)
20	WB/5-1	Wall B Location 5 - Unexposed face (disc t/c)
21	WB/1-2	Wall B Location 1 - Unexposed panel in cavity (disc t/c)
22	WB/2-2	Wall B Location 2 - Unexposed panel in cavity (disc t/c)
23	WB/3-2	Wall B Location 3 - Unexposed panel in cavity (disc t/c)
24	WB/4-2	Wall B Location 4 - Unexposed panel in cavity (disc t/c)
25	WB/5-2	Wall B Location 5 - Unexposed panel in cavity (disc t/c)
26	WB/1-3	Wall B Location 1 - Exposed panel in cavity (disc t/c)
27	WB/2-3	Wall B Location 2 - Exposed panel in cavity (disc t/c) **(rogue – no readings)**
28	WB/3-3	Wall B Location 3 - Exposed panel in cavity (disc t/c)
29	WB/4-3	Wall B Location 4 - Exposed panel in cavity (disc t/c)
30	WB/5-3	Wall B Location 5 - Exposed panel in cavity (disc t/c)
31	WC/1-1	Wall C Location 1 - Unexposed face (disc t/c)
32	WC/2-1	Wall C Location 2 - Unexposed face (disc t/c)
33	WC/3-1	Wall C Location 3 - Unexposed face (disc t/c)
34	WC/4-1	Wall C Location 4 - Unexposed face (disc t/c)
35	WC/5-1	Wall C Location 5 - Unexposed face (disc t/c)
36	WC/1-2	Wall C Location 1 - Unexposed panel in cavity (disc t/c) **(rogue – no readings)**
37	WC/2-2	Wall C Location 2 - Unexposed panel in cavity (disc t/c)
38	WC/3-2	Wall C Location 3 - Unexposed panel in cavity (disc t/c)

39	WC/4-2	Wall C Location 4 - Unexposed panel in cavity (disc t/c)
40	WC/5-2	Wall C Location 5 - Unexposed panel in cavity (disc t/c)
41	WC/1-3	Wall C Location 1 - Exposed panel in cavity (disc t/c)
42	WC/2-3	Wall C Location 2 - Exposed panel in cavity (disc t/c)
43	WC/3-3	Wall C Location 3 - Exposed panel in cavity (disc t/c)
44	WC/4-3	Wall C Location 4 - Exposed panel in cavity (disc t/c)
45	WC/5-3	Wall C Location 5 - Exposed panel in cavity (disc t/c)
46	WC/7-1	Wall C Location 7 – Steel stud Unexposed panel in cavity (disc t/c – card backed)
47	WC/6-1	Wall C Location 6 – Steel stud Unexposed panel in cavity (rivetted t/c)
48	WC/7-2	Wall C Location 7 - Steel stud mid web in cavity (disc t/c – card backed)
49	WC/6-2	Wall C Location 6 - Steel stud mid web in cavity (rivetted t/c)
50	WC/7-3	Wall C Location 7 – Steel stud Exposed panel in cavity (disc t/c – card backed)
51	WC/6-3	Wall C Location 6 – Steel stud Exposed panel in cavity (rivetted t/c)
52	CLG/1-1	Ceiling Location 1 - Unexposed face (disc t/c)
53	CLG/2-1	Ceiling Location 2 - Unexposed face (disc t/c)
54	CLG/3-1	Ceiling Location 3 - Unexposed face (disc t/c)
55	CLG/4-1	Ceiling Location 4 - Unexposed face (disc t/c)
56	CLG/5-1	Ceiling Location 5 - Unexposed face (disc t/c)
57	CLG/1-2	Ceiling Location 1 - Unexposed panel in cavity (disc t/c)
58	CLG/2-2	Ceiling Location 2 - Unexposed panel in cavity (disc t/c)
59	CLG/3-2	Ceiling Location 3 - Unexposed panel in cavity (disc t/c)
60	CLG/4-2	Ceiling Location 4 - Unexposed panel in cavity (disc t/c)
61	CLG/5-2	Ceiling Location 5 - Unexposed panel in cavity (disc t/c)
62	CLG/1-3	Ceiling Location 1 – Cavity mid web (disc t/c)
63	CLG/2-3	Ceiling Location 2 – Cavity mid web (disc t/c)
64	CLG/3-3	Ceiling Location 3 – Cavity mid web (disc t/c)
65	CLG/4-3	Ceiling Location 4 – Cavity mid web (disc t/c)
66	CLG/5-3	Ceiling Location 5 - Cavity mid web (disc t/c)
67	CLG/1-4	Ceiling Location 1 - Exposed panel in cavity (disc t/c)
68	CLG/2-4	Ceiling Location 2 - Exposed panel in cavity (disc t/c)
69	CLG/3-4	Ceiling Location 3 - Exposed panel in cavity (disc t/c)
70	CLG/4-4	Ceiling Location 4 - Exposed panel in cavity (disc t/c)
71	CLG/5-4	Ceiling Location 5 - Exposed panel in cavity (disc t/c)
72	FD/1	Fire door Location 1 - Unexposed face (disc t/c)
73	FD/2	Fire door Location 2 - Unexposed face (disc t/c)
74	FD/3	Fire door Location 3 - Unexposed face (disc t/c)
75	FD/4	Fire door Location 4 - Unexposed face (disc t/c)
76	FD/5	Fire door Location 5 - Unexposed face (disc t/c)
77	FD/6	Fire door Location 6 - Unexposed face (disc t/c)
78	FD/7	Fire door Location 7 - Unexposed face (disc t/c)
79	FD/8	Fire door Location 8 - Unexposed face (disc t/c)
80	FLR/1	Floor Location 1 – Mid 'Fiberock' layers(disc t/c)
81	FLR/2	Floor Location 2 – Mid 'Fiberock' layers(disc t/c)
82	FLR/3	Floor Location 3 – Mid 'Fiberock' layers(disc t/c)

83	FLR/4	Floor Location 4 – Mid 'Fiberock' layers(disc t/c)
84	FLR/5	Floor Location 5 – Mid 'Fiberock' layers(disc t/c)
85	T1/1	Tree #1 – Wall A 1800mm height (quick tip t/c)
86	T1/2	Tree #1 – Wall A 1100mm height (quick tip t/c)
87	T1/3	Tree #1 – Wall A 600mm height (quick tip t/c)
88	T2/1	Tree #2 – Wall B 1800mm height (quick tip t/c)
89	T2/2	Tree #2 – Wall B 1200mm height (quick tip t/c)
90	T2/3	Tree #2 – Wall B 600mm height (quick tip t/c)
91	T3/1	Tree #3 – Wall C 1800mm height (quick tip t/c)
92	T3/2	Tree #3 – Wall C 1200mm height (quick tip t/c)
93	T3/3	Tree #3 – Wall C 600mm height (quick tip t/c)
94	T4/1	Tree #4 – Fire Door 1440mm height (quick tip t/c)
95	T4/2	Tree #4 – Fire Door 960mm height (quick tip t/c)
96	T4/3	Tree #4 – Fire Door 480mm height (quick tip t/c)
97	T5/1	Tree #5 – Central ceiling/floor 2400mm (quick tip t/c)
98	T5/2	Tree #5 – Central ceiling/floor 2300mm (quick tip t/c)
99	T5/3	Tree #5 – Central ceiling/floor 2100mm (quick tip t/c)
100	T5/4	Tree #5 – Central ceiling/floor 1800mm (quick tip t/c)
101	T5/5	Tree #5 – Central ceiling/floor 1200mm (quick tip t/c)
102	T5/6	Tree #5 – Central ceiling/floor 300mm (quick tip t/c)
103	T5/7	Tree #5 – Central ceiling/floor 100mm (quick tip t/c)
104	IG/1	Ignition location fire exposed at couch –Mid width at location of corner of cushion back and seat join (disc t/c)
105	IS/1	Iso-sheath t/c - Wall A 2300mm
106	IS/2	Iso-sheath t/c - Wall C 2300mm
107	DC/1	Dummy Column Location 1 - Sheathed t/c 5mm from fire exposure
108	DC/2	Dummy Column Location 2 - Sheathed t/c 10mm from fire exposure
109	DC/3	Dummy Column Location 3 - Sheathed t/c 20mm from fire exposure
110	DC/4	Dummy Column Location 4 - Sheathed t/c 30mm from fire exposure
111	DC/5	Dummy Column Location 5 - Sheathed t/c 40mm from fire exposure
112	DC/6	Dummy Column Location 6 - Sheathed t/c 50mm from fire exposure
	LC/1	Load cell #1
	LC/2	Load cell #2
	LC/3	Load cell #3
	LC/4	Load cell #4

Test #2:

Channel	t/c ref	Description
1	WA/1-1	Wall A Location 1 - Unexposed face (disc t/c)
2	WA/2-1	Wall A Location 2 - Unexposed face (disc t/c)
3	WA/3-1	Wall A Location 3 - Unexposed face (disc t/c)
4	WA/4-1	Wall A Location 4 - Unexposed face (disc t/c)
5	WA/5-1	Wall A Location 5 - Unexposed face (disc t/c)
6	WA/1-2	Wall A Location 1 - Unexposed panel in cavity (disc t/c)
7	WA/2-2	Wall A Location 2 - Unexposed panel in cavity (disc t/c)
8	WA/3-2	Wall A Location 3 - Unexposed panel in cavity (disc t/c)
9	WA/4-2	Wall A Location 4 - Unexposed panel in cavity (disc t/c)
10	WA/5-2	Wall A Location 5 - Unexposed panel in cavity (disc t/c)
11	WA/1-3	Wall A Location 1 - Exposed panel in cavity (disc t/c)
12	WA/2-3	Wall A Location 2 - Exposed panel in cavity (disc t/c)
13	WA/3-3	Wall A Location 3 - Exposed panel in cavity (disc t/c)
14	WA/4-3	Wall A Location 4 - Exposed panel in cavity (disc t/c)
15	WA/5-3	Wall A Location 5 - Exposed panel in cavity (disc t/c)
16	WB/1-1	Wall B Location 1 - Unexposed face (disc t/c)
17	WB/2-1	Wall B Location 2 - Unexposed face (disc t/c)
18	WB/3-1	Wall B Location 3 - Unexposed face (disc t/c)
19	WB/4-1	Wall B Location 4 - Unexposed face (disc t/c)
20	WB/5-1	Wall B Location 5 - Unexposed face (disc t/c)
21	WB/1-2	Wall B Location 1 - Unexposed panel in cavity (disc t/c)
22	WB/2-2	Wall B Location 2 - Unexposed panel in cavity (disc t/c)
23	WB/3-2	Wall B Location 3 - Unexposed panel in cavity (disc t/c)
24	WB/4-2	Wall B Location 4 - Unexposed panel in cavity (disc t/c)
25	WB/5-2	Wall B Location 5 - Unexposed panel in cavity (disc t/c)
26	WB/1-3	Wall B Location 1 - Exposed panel in cavity (disc t/c)
27	WB/2-3	Wall B Location 2 - Exposed panel in cavity (disc t/c)
28	WB/3-3	Wall B Location 3 - Exposed panel in cavity (disc t/c)
29	WB/4-3	Wall B Location 4 - Exposed panel in cavity (disc t/c)
30	WB/5-3	Wall B Location 5 - Exposed panel in cavity (disc t/c)
31	WC/1-1	Wall C Location 1 - Unexposed face (disc t/c)
32	WC/2-1	Wall C Location 2 - Unexposed face (disc t/c)
33	WC/3-1	Wall C Location 3 - Unexposed face (disc t/c)
34	WC/4-1	Wall C Location 4 - Unexposed face (disc t/c)
35	WC/5-1	Wall C Location 5 - Unexposed face (disc t/c)
36	WC/1-2	Wall C Location 1 - Unexposed panel in cavity (disc t/c)
37	WC/2-2	Wall C Location 2 - Unexposed panel in cavity (disc t/c)
38	WC/3-2	Wall C Location 3 - Unexposed panel in cavity (disc t/c)
39	WC/4-2	Wall C Location 4 - Unexposed panel in cavity (disc t/c)
40	WC/5-2	Wall C Location 5 - Unexposed panel in cavity (disc t/c)
41	WC/1-3	Wall C Location 1 - Exposed panel in cavity (disc t/c)
42	WC/2-3	Wall C Location 2 - Exposed panel in cavity (disc t/c)
43	WC/3-3	Wall C Location 3 - Exposed panel in cavity (disc t/c)
44	WC/4-3	Wall C Location 4 - Exposed panel in cavity (disc t/c)
45	WC/5-3	Wall C Location 5 - Exposed panel in cavity (disc t/c)

46	**WC/7-1**	**Wall C Location 7 – Steel stud 1 Unexposed panel in cavity (rivetted t/c)**
47	**WC/6-1**	**Wall C Location 6 – Steel stud 2 Unexposed panel in cavity (rivetted t/c)**
48	**WC/7-2**	**Wall C Location 7 - Steel stud 1 mid web in cavity (rivetted t/c)**
49	**WC/6-2**	**Wall C Location 6 - Steel stud 2 mid web in cavity (rivetted t/c)**
50	**WC/7-3**	**Wall C Location 7 – Steel stud 1 Exposed panel in cavity (rivetted t/c)**
51	**WC/6-3**	**Wall C Location 6 – Steel stud 2 Exposed panel in cavity (rivetted t/c)**
52	CLG/1-1	Ceiling Location 1 - Unexposed face (disc t/c)
53	CLG/2-1	Ceiling Location 2 - Unexposed face (disc t/c)
54	CLG/3-1	Ceiling Location 3 - Unexposed face (disc t/c)
55	CLG/4-1	Ceiling Location 4 - Unexposed face (disc t/c)
56	CLG/5-1	Ceiling Location 5 - Unexposed face (disc t/c)
57	CLG/1-2	Ceiling Location 1 - Unexposed panel in cavity (disc t/c)
58	CLG/2-2	Ceiling Location 2 - Unexposed panel in cavity (disc t/c)
59	CLG/3-2	Ceiling Location 3 - Unexposed panel in cavity (disc t/c)
60	CLG/4-2	Ceiling Location 4 - Unexposed panel in cavity (disc t/c)
61	CLG/5-2	Ceiling Location 5 - Unexposed panel in cavity (disc t/c)
62	CLG/1-3	Ceiling Location 1 – Cavity mid web (disc t/c)
63	CLG/2-3	Ceiling Location 2 – Cavity mid web (disc t/c)
64	CLG/3-3	Ceiling Location 3 – Cavity mid web (disc t/c)
65	CLG/4-3	Ceiling Location 4 – Cavity mid web (disc t/c)
66	CLG/5-3	Ceiling Location 5 - Cavity mid web (disc t/c)
67	CLG/1-4	Ceiling Location 1 - Exposed panel in cavity (disc t/c)
68	CLG/2-4	Ceiling Location 2 - Exposed panel in cavity (disc t/c)
69	CLG/3-4	Ceiling Location 3 - Exposed panel in cavity (disc t/c)
70	CLG/4-4	Ceiling Location 4 - Exposed panel in cavity (disc t/c)
71	CLG/5-4	Ceiling Location 5 - Exposed panel in cavity (disc t/c)
72	**Spare**	**Spare**
73	**Spare**	**Spare**
74	**Spare**	**Spare**
75	**T6/1**	**Tree #6 – Wall A 1800mm height (quick tip t/c)**
76	**T6/2**	**Tree #6 – Wall A 1100mm height (quick tip t/c)**
77	**T6/3**	**Tree #6 – Wall A 600mm height (quick tip t/c)**
78	**IS/3**	**Iso-sheath t/c - Wall B 2300mm**
79	**FLR/6**	**Floor Location 6 – Mid 'Fiberock' layers(disc t/c)**
80	FLR/1	Floor Location 1 – Mid 'Fiberock' layers(disc t/c)
81	FLR/2	Floor Location 2 – Mid 'Fiberock' layers(disc t/c)
82	FLR/3	Floor Location 3 – Mid 'Fiberock' layers(disc t/c)
83	FLR/4	Floor Location 4 – Mid 'Fiberock' layers(disc t/c)
84	FLR/5	Floor Location 5 – Mid 'Fiberock' layers(disc t/c)
85	T1/1	Tree #1 – Wall A 1800mm height (quick tip t/c)
86	T1/2	Tree #1 – Wall A 1100mm height (quick tip t/c)
87	T1/3	Tree #1 – Wall A 600mm height (quick tip t/c)

88	T2/1	Tree #2 – Wall B 1800mm height (quick tip t/c)
89	T2/2	Tree #2 – Wall B 1200mm height (quick tip t/c)
90	T2/3	Tree #2 – Wall B 600mm height (quick tip t/c)
91	T3/1	Tree #3 – Wall C 1800mm height (quick tip t/c)
92	T3/2	Tree #3 – Wall C 1200mm height (quick tip t/c)
93	T3/3	Tree #3 – Wall C 600mm height (quick tip t/c)
94	**T4/1**	**Tree #4 – Wall C 1800mm height (quick tip t/c)**
95	**T4/2**	**Tree #4 – Wall C 1200mm height (quick tip t/c)**
96	**T4/3**	**Tree #4 – Wall C 600mm height (quick tip t/c)**
97	T5/1	Tree #5 – Central ceiling/floor 2400mm (quick tip t/c)
98	T5/2	Tree #5 – Central ceiling/floor 2300mm (quick tip t/c)
99	T5/3	Tree #5 – Central ceiling/floor 2100mm (quick tip t/c)
100	T5/4	Tree #5 – Central ceiling/floor 1800mm (quick tip t/c)
101	T5/5	Tree #5 – Central ceiling/floor 1200mm (quick tip t/c)
102	T5/6	Tree #5 – Central ceiling/floor 300mm (quick tip t/c)
103	T5/7	Tree #5 – Central ceiling/floor 100mm (quick tip t/c)
104	IG/1	Ignition location fire exposed at couch –Mid width at location of corner of cushion back and seat join (disc t/c)
105	IS/1	Iso-sheath t/c - Wall A 2300mm
106	IS/2	Iso-sheath t/c - Wall C 2300mm
107	DC/1	Dummy Column Location 1 - Sheathed t/c 5mm from fire exposure
108	DC/2	Dummy Column Location 2 - Sheathed t/c 10mm from fire exposure
109	DC/3	Dummy Column Location 3 - Sheathed t/c 20mm from fire exposure
110	DC/4	Dummy Column Location 4 - Sheathed t/c 30mm from fire exposure
111	DC/5	Dummy Column Location 5 - Sheathed t/c 40mm from fire exposure
112	DC/6	Dummy Column Location 6 - Sheathed t/c 50mm from fire exposure
	LC/1	Load cell #1
	LC/2	Load cell #2
	LC/3	Load cell #3
	LC/4	Load cell #4

Note: Bold references denote changes from Test #1

Test #3:

Channel	t/c ref	Description
1	WA/1-1	Wall A Location 1 - Unexposed face (disc t/c)
2	WA/2-1	Wall A Location 2 - Unexposed face (disc t/c)
3	WA/3-1	Wall A Location 3 - Unexposed face (disc t/c)
4	WA/4-1	Wall A Location 4 - Unexposed face (disc t/c)
5	WA/5-1	Wall A Location 5 - Unexposed face (disc t/c)
6	WA/1-2	Wall A Location 1 - Unexposed panel in cavity (disc t/c)
7	WA/2-2	Wall A Location 2 - Unexposed panel in cavity (disc t/c)
8	WA/3-2	Wall A Location 3 - Unexposed panel in cavity (disc t/c)
9	WA/4-2	Wall A Location 4 - Unexposed panel in cavity (disc t/c)
10	WA/5-2	Wall A Location 5 - Unexposed panel in cavity (disc t/c)
11	WA/1-3	Wall A Location 1 - Exposed panel in cavity (disc t/c)
12	WA/2-3	Wall A Location 2 - Exposed panel in cavity (disc t/c)
13	WA/3-3	Wall A Location 3 - Exposed panel in cavity (disc t/c)
14	WA/4-3	Wall A Location 4 - Exposed panel in cavity (disc t/c)
15	WA/5-3	Wall A Location 5 - Exposed panel in cavity (disc t/c)
16	WB/1-1	Wall B Location 1 - Unexposed face (disc t/c)
17	WB/2-1	Wall B Location 2 - Unexposed face (disc t/c)
18	WB/3-1	Wall B Location 3 - Unexposed face (disc t/c)
19	WB/4-1	Wall B Location 4 - Unexposed face (disc t/c)
20	WB/5-1	Wall B Location 5 - Unexposed face (disc t/c)
21	WB/1-2	Wall B Location 1 - Unexposed panel in cavity (disc t/c)
22	WB/2-2	Wall B Location 2 - Unexposed panel in cavity (disc t/c)
23	WB/3-2	Wall B Location 3 - Unexposed panel in cavity (disc t/c)
24	WB/4-2	Wall B Location 4 - Unexposed panel in cavity (disc t/c)
25	WB/5-2	Wall B Location 5 - Unexposed panel in cavity (disc t/c)
26	WB/1-3	Wall B Location 1 - Exposed panel in cavity (disc t/c)
27	WB/2-3	Wall B Location 2 - Exposed panel in cavity (disc t/c)
28	WB/3-3	Wall B Location 3 - Exposed panel in cavity (disc t/c)
29	WB/4-3	Wall B Location 4 - Exposed panel in cavity (disc t/c)
30	WB/5-3	Wall B Location 5 - Exposed panel in cavity (disc t/c)
31	WC/1-1	Wall C Location 1 - Unexposed face (disc t/c)
32	WC/2-1	Wall C Location 2 - Unexposed face (disc t/c)
33	WC/3-1	Wall C Location 3 - Unexposed face (disc t/c)
34	WC/4-1	Wall C Location 4 - Unexposed face (disc t/c)
35	WC/5-1	Wall C Location 5 - Unexposed face (disc t/c)
36	WC/1-2	Wall C Location 1 - Unexposed panel in cavity (disc t/c)
37	WC/2-2	Wall C Location 2 - Unexposed panel in cavity (disc t/c)
38	WC/3-2	Wall C Location 3 - Unexposed panel in cavity (disc t/c)
39	WC/4-2	Wall C Location 4 - Unexposed panel in cavity (disc t/c)
40	WC/5-2	Wall C Location 5 - Unexposed panel in cavity (disc t/c)
41	WC/1-3	Wall C Location 1 - Exposed panel in cavity (disc t/c)
42	WC/2-3	Wall C Location 2 - Exposed panel in cavity (disc t/c)
43	WC/3-3	Wall C Location 3 - Exposed panel in cavity (disc t/c)
44	WC/4-3	Wall C Location 4 - Exposed panel in cavity (disc t/c)
45	WC/5-3	Wall C Location 5 - Exposed panel in cavity (disc t/c)

46	**WB/7-1**	**Wall C Location 7 – Steel stud 1 Unexposed panel in cavity (rivetted t/c)**
47	**WB/6-1**	**Wall C Location 6 – Steel stud 2 Unexposed panel in cavity (rivetted t/c)**
48	**WB/7-2**	**Wall C Location 7 - Steel stud 1 mid web in cavity (rivetted t/c)**
49	**WB/6-2**	**Wall C Location 6 - Steel stud 2 mid web in cavity (rivetted t/c)**
50	**WB/7-3**	**Wall C Location 7 – Steel stud 1 Exposed panel in cavity (rivetted t/c)**
51	**WB/6-3**	**Wall C Location 6 – Steel stud 2 Exposed panel in cavity (rivetted t/c)**
52	CLG/1-1	Ceiling Location 1 - Unexposed face (disc t/c)
53	CLG/2-1	Ceiling Location 2 - Unexposed face (disc t/c)
54	CLG/3-1	Ceiling Location 3 - Unexposed face (disc t/c)
55	CLG/4-1	Ceiling Location 4 - Unexposed face (disc t/c)
56	CLG/5-1	Ceiling Location 5 - Unexposed face (disc t/c)
57	CLG/1-2	Ceiling Location 1 - Unexposed panel in cavity (disc t/c)
58	CLG/2-2	Ceiling Location 2 - Unexposed panel in cavity (disc t/c)
59	CLG/3-2	Ceiling Location 3 - Unexposed panel in cavity (disc t/c)
60	CLG/4-2	Ceiling Location 4 - Unexposed panel in cavity (disc t/c)
61	CLG/5-2	Ceiling Location 5 - Unexposed panel in cavity (disc t/c)
62	CLG/1-3	Ceiling Location 1 – Cavity mid web (disc t/c)
63	CLG/2-3	Ceiling Location 2 – Cavity mid web (disc t/c)
64	CLG/3-3	Ceiling Location 3 – Cavity mid web (disc t/c)
65	CLG/4-3	Ceiling Location 4 – Cavity mid web (disc t/c)
66	CLG/5-3	Ceiling Location 5 - Cavity mid web (disc t/c)
67	CLG/1-4	Ceiling Location 1 - Exposed panel in cavity (disc t/c)
68	CLG/2-4	Ceiling Location 2 - Exposed panel in cavity (disc t/c)
69	CLG/3-4	Ceiling Location 3 - Exposed panel in cavity (disc t/c)
70	CLG/4-4	Ceiling Location 4 - Exposed panel in cavity (disc t/c)
71	CLG/5-4	Ceiling Location 5 - Exposed panel in cavity (disc t/c)
72	**Spare**	**Spare**
73	**Spare**	**Spare**
74	**Spare**	**Spare**
75	**T6/1**	**Tree #6 – Wall A 1800mm height (quick tip t/c)**
76	**T6/2**	**Tree #6 – Wall A 1100mm height (quick tip t/c)**
77	**T6/3**	**Tree #6 – Wall A 600mm height (quick tip t/c)**
78	**IS/3**	**Iso-sheath t/c - Wall B 2300mm**
79	**FLR/6**	**Floor Location 6 – Mid 'Fiberock' layers(disc t/c)**
80	FLR/1	Floor Location 1 – Mid 'Fiberock' layers(disc t/c)
81	FLR/2	Floor Location 2 – Mid 'Fiberock' layers(disc t/c)
82	FLR/3	Floor Location 3 – Mid 'Fiberock' layers(disc t/c)
83	FLR/4	Floor Location 4 – Mid 'Fiberock' layers(disc t/c)
84	FLR/5	Floor Location 5 – Mid 'Fiberock' layers(disc t/c)
85	T1/1	Tree #1 – Wall A 1800mm height (quick tip t/c)
86	T1/2	Tree #1 – Wall A 1100mm height (quick tip t/c)
87	T1/3	Tree #1 – Wall A 600mm height (quick tip t/c)

88	T2/1	Tree #2 – Wall B 1800mm height (quick tip t/c)
89	T2/2	Tree #2 – Wall B 1200mm height (quick tip t/c)
90	T2/3	Tree #2 – Wall B 600mm height (quick tip t/c)
91	T3/1	Tree #3 – Wall C 1800mm height (quick tip t/c)
92	T3/2	Tree #3 – Wall C 1200mm height (quick tip t/c)
93	T3/3	Tree #3 – Wall C 600mm height (quick tip t/c)
94	**T4/1**	**Tree #4 – Wall C 1800mm height (quick tip t/c)**
95	**T4/2**	**Tree #4 – Wall C 1200mm height (quick tip t/c)**
96	**T4/3**	**Tree #4 – Wall C 600mm height (quick tip t/c)**
97	T5/1	Tree #5 – Central ceiling/floor 2400mm (quick tip t/c)
98	T5/2	Tree #5 – Central ceiling/floor 2300mm (quick tip t/c)
99	T5/3	Tree #5 – Central ceiling/floor 2100mm (quick tip t/c)
100	T5/4	Tree #5 – Central ceiling/floor 1800mm (quick tip t/c)
101	T5/5	Tree #5 – Central ceiling/floor 1200mm (quick tip t/c)
102	T5/6	Tree #5 – Central ceiling/floor 300mm (quick tip t/c)
103	T5/7	Tree #5 – Central ceiling/floor 100mm (quick tip t/c)
104	IG/1	Ignition location fire exposed at couch –Mid width at location of corner of cushion back and seat join (disc t/c)
105	IS/1	Iso-sheath t/c - Wall A 2300mm
106	IS/2	Iso-sheath t/c - Wall C 2300mm
107	DC/1	Dummy Column Location 1 - Sheathed t/c 5mm from fire exposure
108	DC/2	Dummy Column Location 2 - Sheathed t/c 10mm from fire exposure
109	DC/3	Dummy Column Location 3 - Sheathed t/c 20mm from fire exposure
110	DC/4	Dummy Column Location 4 - Sheathed t/c 30mm from fire exposure
111	DC/5	Dummy Column Location 5 - Sheathed t/c 40mm from fire exposure
112	DC/6	Dummy Column Location 6 - Sheathed t/c 50mm from fire exposure
	LC/1	Load cell #1 **(Rogue – no readings)**
	LC/2	Load cell #2
	LC/3	Load cell #3
	LC/4	Load cell #4

Note: Bold references denote changes from Test #1

C. Appendix C – Test Observations and Photos

Test #1 - 800MJ/m² FLED, 30min rated constructions

Time	Observations
1:30	Smoke begins to exit compartment through the vent opening.
2:00	Chair seats and backs fully involved in flame.
2:30	PU foam seats dripping melted burning fuel to form pool at floor level.
3:30	Flashover under PU foam burning regime. Cribs begin to ignite at high level.
4:15	PU foam burning diminishes as PU fuel source is burnt out. Crib fuel controlled burning becomes predominant burning regime.
5:00	Crib burning becomes ventilation controlled.
6:30	Smoke visible around construction joints of wall C and additionally the framing of fire door.
13:00	Flames escape through gap at bottom of fire door – not greater than 10 second duration exceeded, therefore, no failure.
17:00	Pieces of charred crib fall to floor. Wall B plasterboard joints show signs of darkening and smoke visible.
18:15	Middle cribs in the compartment collapse into heap on the floor.
19:00	Front cribs in the compartment by the opening collapse into heap on the floor.
20:00	Sound of internal plasterboard lining falling off within the compartment.
21:55	Wall C has large integrity failure and a big section of the wall collapses outwards. Flames now burning outside of this newly formed opening.
22:30	Fire door has an integrity failure. Flames burning through top of door and frame.
23:00	Wall A integrity failure. Flames burning through plasterboard joints.
25:00	Test terminated due to fire exposure to adjacent building. Extinguishment of fire commences.

Test #1 – 45 sec

Test #1 – 1 min 30 sec

3 min 35 sec

Appendix C – Test Observations and Photos

3 min 45 sec

4 min 20 sec

5 min 10 sec

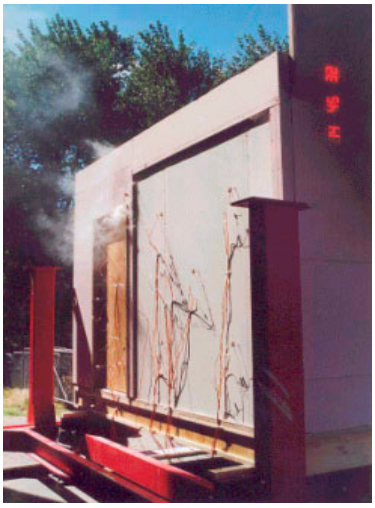

5 min 15 sec

5 min 45 sec

9 min 35 sec

10 min 55 sec

12 min 55 sec (Wall C & fire door)

16 min 25 sec

Appendix C – Test Observations and Photos

18 min 35 sec

19 min 40 sec

22 min (Assembly #3 integrity failure)

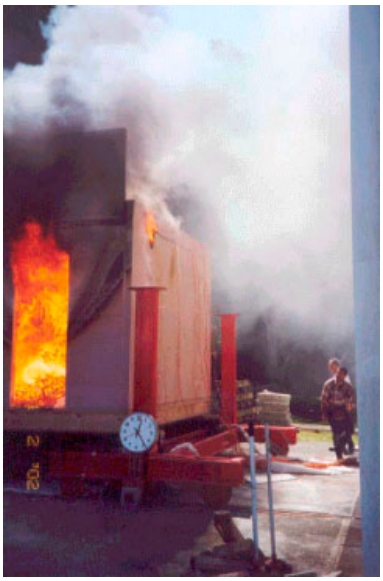

23 min 40 sec (Assembly #1 integrity failure)

22 min 30 sec (Fire door integrity failure)

Test #2 - 1200MJ/m² FLED, 60min rated constructions

Time	Observations
00:45	Flame height to top of seat back cushion
1:30	Flame spread across whole middle seat back cushion
1:25	Smoke begins to exit compartment through the vent opening.
2:00	PU foam seats dripping melted burning fuel to form pool at floor level.
2:30	Chair seats and backs fully involved in flame.
4:30	Flashover under PU foam burning regime. Cribs begin to ignite at high level.
5:30	Front cribs ignite at high level
6:00	Flames begin burning outside compartment.
6:30	PU foam burning diminishes as PU fuel source is burnt out. Crib ventilation controlled burning becomes predominant burning regime.
10:00	Paper from shield above opening burning off.
11:20	Extremely high/rich concentration of smoke bellowing out of compartment. Diluting to within it's flammability limits and igniting away from the opening.
13:00	All cribs full involved
17:20	Pieces of charred crib begin to fall to floor.
21:50	Middle cribs in the compartment collapse inwards. Air path into compartment still visible.
22:40	Front cribs in the compartment by the opening collapse into heap on the floor, noticeably blocking opening and air path into compartment.
22:55	Pieces of charred crib sticks falling out of compartment
23:00	Thermal deformations and deflections noticeable in steel stud framed wall (Wall C).
26:50	Noticeably cooler fire evident – still ventilation controlled burning.
33:00	Inside cement-fibre sheet of Wall B cracking and sections falling away.
33:30	Burning of Wall A timber framing evident.
34:00	Fuel controlled burning regime become prominent.
35:00	Inside plasterboard lining falls inwards from steel stud framed Wall C.
37:30	Wall C has large integrity failure and a big section of the wall collapses outwards. Still fuel controlled burning.
40:00	Timber frame above Wall C flaming.
51:00	Wall B has first signs of scorching discolouration across a significant section
51:30	Large cracking sound from inside compartment. Possibly a ceiling beam.
52:40	Inside plasterboard lining of Wall A falls away from framing.
53:00	Wall A insulation failure - scorching significantly in the vicinity of Location 3 thermocouple.
57:00	Wall B insulation failure – scorching discolouration across significant sections of wall.
60:00	Test terminated. Extinguishment of fire commences.

Appendix C – Test Observations and Photos

10 sec

45 sec

1 min

1 min 15 sec

2 min 05 sec

2 min 30 sec

4 min 30 sec

5 min

6 min 25 sec

Appendix C – Test Observations and Photos

7 min 35 sec

9 min

13 min 20 sec

16 min

21 min 20 sec

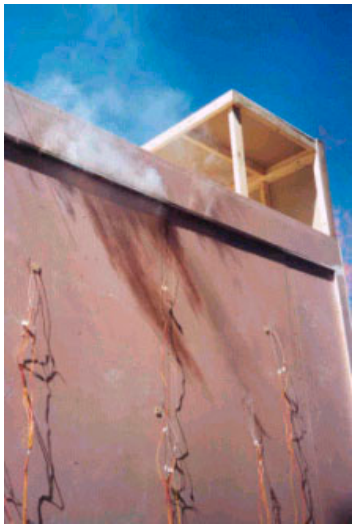

24 min 30 sec

25 min 55 sec

28 mins 40 secs

31 min 30 sec

34 mins 40 secs

36 min 35 sec

37 min 10 sec

37 min 30 sec (Assembly #7)

39 min 30 sec

54 min (Assembly #5)

55 min

57 min (Assembly #6)

Test #3 - 800MJ/m² FLED, 30min rated constructions:

Time	Observations
1:00	Flame above seat back height. Flame approximately half seat back cushion width (350mm)
1:30	Smoke begins to exit compartment through the vent opening.
2:00	Flame spread across whole middle seat back cushion.
2:15	PU foam seats dripping melted and burning fuel to form pool at floor level.
2:30	Chair seats and backs fully involved in flame.
3:00	Seat back cushions completely melted from seat frame and pooling at floor level.
3:15	Flashover under PU foam burning regime. Ventilation controlled burning of PU foam begins. Cribs begin to ignite at high level.
4:30	Large noise heard from within compartment - cement fibre board lining cracking and exposing insulation at several locations.
4:45	PU foam burning diminishes as PU fuel source is burnt out. Crib fuel controlled burning becomes predominant burning regime.
5:30	Crib burning becomes ventilation controlled.
6:15	Top of front cribs ignite.
7:00	A piece small piece of cement fibre lining falls onto steel chair frames. Flame from top of front cribs spreading slowly to bottom of cribs.
10:00	All of cribs fully involved in flame.
14:00	Slight darkening on unexposed plasterboard lining occurring due to heat at a location on the perimeter of steel stud wall (Wall B).
15:30	Deflection in steel stud framed wall (Wall B) becoming evident.
16:40	Noise from within compartment of a plasterboard lining falling from it's framing.
17:30	Scorching occurring at high level along the central joints of the steel stud system (Wall B).
19:00	Heavy scorching along joint of steel stud wall. Insulation failure of Wall B.
19:15	Light discolouration along joint of cement fibre lined wall (Wall C).
19:30	Rear cribs collapse inwards.
20:00	Middle cribs in the compartment collapse inwards on the floor.
20:30	Heavy scorching and burning paper on unexposed section of plasterboard lined, light timber framed wall. Insulation failure of Wall A.
21:30	Front cribs (Wall A side) collapse inwards on the floor.
22:30	Front cribs (Wall C side) collapse inwards on the floor.
23:15	Wall B has large integrity failure and approximately half of the wall collapses outwards. Increased ventilation evident.
23:20	Fire fuel controlled burning (and decay) begins due to increased ventilation and cooling effect of air.
25:20	Ceiling assembly exposed plasterboard lining at rear of compartment falls from ceiling frame. Remainder of steel stud (Wall B) collapses outwards from compartment.
26:00	Ceiling structure fully involved in flames.
28:00	Ceiling assembly exposed plasterboard lining at front of compartment falls from ceiling frame.
34:00	Ceiling joists show visible signs of being burnt out. Failure of the ceiling prior to this time is likely to have occurred.
39:30	Test terminated. Extinguishment of fire commences.

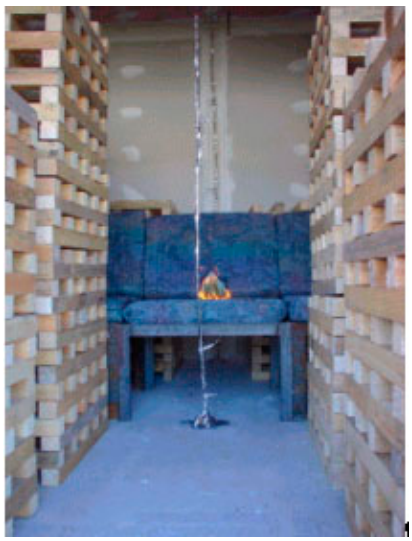

00 mins 10secs

1min 00 secs

2mins 00 secs

2 mins 30 secs

3 mins 00 secs

4 mins 25 secs

6 mins 00 secs

8 mins 00 secs

12 mins 40 secs

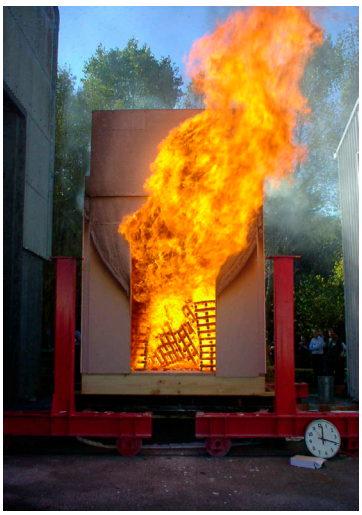

18 mins 55 secs

19 mins 30 secs

20 mins 00 secs

21 mins 00 secs

23 mins 00 secs

25 mins 00 secs

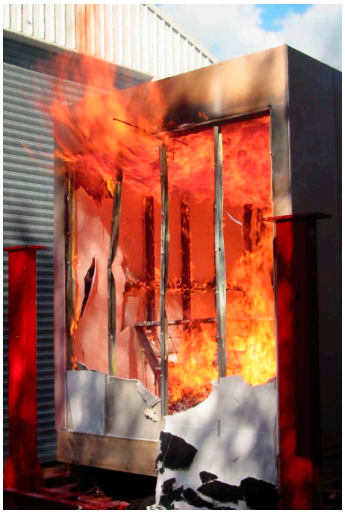

27 mins 00 secs

33 mins 00 secs

38 mins 00 secs

D. Appendix D – Crib Moisture Content Monitoring

Moisture Content Monitoring Sheet - Test #1

TIMBER SAMPLES weighing during drying:

Timber samples associated with 800MJ/m² compartment test.

INITIAL MONITORING DATE: 21st February 2002

Sample 1		Sample 2	
Dimensions (mm): Width	50	Dimensions (mm): Width	50
Length	650	Length	650
Thickness	50	Thickness	50
Volume (m³)	0.0016	Volume (m³)	0.0016
Undried Weight (kg):	0.790	Undried Weight (kg):	0.799

INITIAL 'MOISTURE METER' MOISTURE CONTENT:

Moisture Content (with moisture meter)	
Sample 1	**Sample 2**
13%	13%

Weight during drying @ 85°C :

Date	Weight (kg)	
	Sample 1	**Sample 2**
22/02/02	0.693	0.701
25/02/02	0.689	0.698
26/02/02	0.689	0.698

Weight per m³ at time of test:

$$= \frac{Undried\ weight\ (kg)}{Volume\ (m^3)}$$

Moisture content % at time of test:

$$= \frac{Undried\ weight - Final\ dry\ weight}{Final\ dry\ weight} \times 100\%$$

Sample 1	Sample 2
0.790 / 0.0016	0.799 / 0.0016
494 kg/m³	499 kg/m³
Average	496.5 kg/m³

Sample 1	Sample 2
0.101 / 0.689	0.101 / 0.698
14.7 %	14.5 %
Average	14.6 %

Moisture Content Monitoring Sheet - Test #2

TIMBER SAMPLES weighing during drying:

Timber samples associated with 1200MJ/m² compartment test.

INITIAL MONITORING DATE: 7th March 2002

Sample 1		Sample 2	
Dimensions (mm): Width	50	Dimensions (mm): Width	50
Length	650	Length	650
Thickness	50	Thickness	50
Volume (m³)	0.0016	Volume (m³)	0.0016
Undried Weight (kg):	0.720	Undried Weight (kg):	0.720

INITIAL 'MOISTURE METER' MOISTURE CONTENT:

Moisture Content (with moisture meter)	
Sample 1	**Sample 2**
13.25%	13%

Weight during drying @ 85°C :

Date	Weight (kg)	
	Sample 1	**Sample 2**
08/03/02	0.636	0.641
11/03/02	0.632	0.638
12/03/02	0.631	0.638
13/03/02	0.631	0.638

Weight per m³ at time of test $= \frac{Undried\ weight\ (kg)}{Volume\ (m^3)}$

Moisture content % at time of test $= \frac{Undried\ weight - Final\ dry\ weight}{Final\ dry\ weight} \times 100\%$

Sample 1	Sample 2
$\frac{0.720}{0.0016}$	$\frac{0.725}{0.0016}$
450 kg/m³	453.1 kg/m³
Average	451.6 kg/m³

Sample 1	Sample 2
$\frac{0.089}{0.631}$	$\frac{0.087}{0.638}$
14.1 %	13.6 %
Average	13.9 %

Moisture Content Monitoring Sheet - Test #3

TIMBER SAMPLES weighing during drying:

Timber samples associated with 800MJ/m² compartment test.

INITIAL MONITORING DATE: 11th April 2002

Sample 1		Sample 2	
Dimensions (mm): Width	53	Dimensions (mm): Width	55
Length	652	Length	652
Thickness	44	Thickness	45
Volume (m³)	0.0015	Volume (m³)	0.0016
Undried Weight (kg):	0.778	Undried Weight (kg):	0.731

INITIAL 'MOISTURE METER' MOISTURE CONTENT:

Moisture Content (with moisture meter)	
Sample 1	**Sample 2**
14%	15%

Weight during drying @ 85°C :

Date	Weight (kg)	
	Sample 1	**Sample 2**
17/04/02	0.668	0.631
18/04/02	0.668	0.631

Weight per m³ at time of test

$$= \frac{Undried\ weight\ (kg)}{Volume\ (m^3)}$$

Moisture content % at time of test

$$= \frac{Undried\ weight - Final\ dry\ weight}{Final\ dry\ weight} \times 100\%$$

Sample 1	Sample 2
0.778 / 0.0015	0.731 / 0.0016
518.7 kg/m³	456.9 kg/m³
Average	487.8 kg/m³

Sample 1	Sample 2
0.11 / 0.668	0.1 / 0.631
16.5 %	15.8 %
Average	16.2 %

E. Appendix E – BRANZFIRE Addendum Notes and Fire Input Data

(**BRANZfire 2000) – Addendum Notes:**

BRANZFIRE 2002.2 has had basic postflashover model added. The user can elect to use the model by selecting the option available in the <Tools> <Options> <Postflashover> screen. Input required is the average effective heat of combustion for the total fuel load in the room (kJ/g), the fire load energy per unit floor area (MJ/m^2), the average fuel density (kg/m^3) and a characteristic stick thickness (m) based on the assumption that the majority of the fuel in the room is representative of wood cribs.

The pyrolysis model included is based on COMPF2, where the ventilation controlled mass loss rate is given by

$$0.12\ A_v\ H_v^{0.5}\ (kg/s)$$

and the fuel surface area controlled mass loss rate (for wood cribs) is given by :

$$4 / \text{Fuel Thickness} * \text{initial mass} * vp * (\text{mass remaining} / \text{initial mass})^{0.5}$$

where

$$vp = 0.0000022 \times \text{Fuel Thickness}^{-0.6}\ \text{(wood crib fire regression rate)}$$

Following flashover, the lesser of the fuel surface area and the ventilation-limited burning rate is used to determine the theoretical rate of heat release from the fire, and this overides any fire object heat release rate input specified by the user in the 'postflashover' stage. The switch to the postflashover model occurs when the incident radiant heat flux on the floor exceeds 20 kW/m^2. Additionally, in the postflashover stage, the mass entrained by the plume is taken as:

$$\text{Mass\_Plume} = 0.011 * q * (z / (q \wedge (2 / 5))) \wedge 0.566$$

where z is the layer height above the floor and q is the heat release rate (based on the MacCaffrey entrainment correlation for the flaming region). Thus the postflashover model can be used provided an initial fire object is selected that is sufficient to cause 'flashover' in the room i.e. cause an incident radiant heat flux on the floor that exceeds 20 kW/m^2.

(**BRANZfire 2000) – Input Data Test #1:**

```
Input Filename : \\erika\branzcw$\vb\branzfire_source\data2\JN1n.mod
BRANZFIRE Multi-Compartment Fire Model (Ver 2002.2)
Copyright Notice - This software is provided for evaluation only and may
not be used for commercial purposes.
Compartment Test 1,  800 MJ/m²  (with 80% fuel consumed)
Description of Rooms:
Room  1  :
         Room Length (m) =                                  3.60
         Room Width (m) =                                   2.40
         Maximum Room Height (m) =                          2.40
         Minimum Room Height (m) =                          2.40
         Floor Elevation (m) =                              0.000
         Room  1  has a flat ceiling.

         Wall Surface is plasterboard
         Wall Density (kg/m3) =                             810.0
         Wall Conductivity (W/m.K) =                        0.160
         Wall Emissivity =                                  0.88
         Wall Thickness (mm) =                              13.0

         Ceiling Surface is plasterboard
         Ceiling Density (kg/m3) =                          810.0
         Ceiling Conductivity (W/m.K) =                     0.160
         Ceiling Emissivity =                               0.88
         Ceiling Thickness (mm) =                           13.0

         Floor Surface is plasterboard
         Floor Density (kg/m3) =                            810.0
         Floor Conductivity (W/m.K) =                       0.160
         Floor Emissivity =                                 0.88
         Floor Thickness = (mm)                             25.0
============


Description of Wall Vents:
From room  1  to outside, Vent No 1
                  Vent Width (m) =                          0.800
                  Vent Height (m) =                         2.000
                  Vent Sill Height (m) =                    0.000
                  Vent Soffit Height (m) =                  2.000
                  Opening Time (sec) =                      0
                  Closing Time (sec) =                      0
============
Description of Ceiling/Floor Vents
============
Ambient Conditions:
Interior Temp (C) =                                         20.0
Exterior Temp (C) =                                         20.0
Relative Humidity (%) =                                     65
============
Tenability Parameters:
Monitoring Height for Visibility and FED (m) =              1.50
Occupant Activity Level =                                   Light
Visibility calculations assume:                             reflective signs
FED Start Time (sec)                                        0
FED End Time (sec)                                          1200
============
Sprinkler / Detector Parameters:
No thermal detector or sprinkler installed.
============
Mechanical Ventilation (to/from outside):
Mechanical Ventilation not installed in Room 1
============
Description of the Fire:
Radiant Loss Fraction =                                     0.35
Underventilated Soot Yield Factor =                         1.00
Smoke Emission Coefficent (1/m) =                           0.80
Characteristic Mass Loss per Unit Area (kg/s.m2) =          0.011
```

Air Entrainment in Plume uses McCaffrey (recommended)

Burning Object No 1:

Located in Room	1
Energy Yield (kJ/g) =	25.0
CO2 Yield (kg/kg fuel) =	1.500
Soot Yield (kg/kg fuel) =	0.194
H2O Yield (kg/kg fuel) =	0.442
Fire Height (m) =	0.300
Fire Location (m) =	Centre

Time (sec)	Heat Release (kW)
0	0
100	674
200	2500
300	1900
400	660
500	312
600	200
700	100
800	50
900	0
1000	0

Summary of End-Point Conditions in Room of Fire Origin
Upper Layer Temperature Exceeds 600 deg C at 162.0 Seconds.
Initial Time-Step = 1.00 seconds.
Computer Run-Time = 553.3 seconds.

(BRANZfire 2000) – Input Data Test #2:

```
Input Filename : S:\Job Files\FQ Research\FQ0590 - compartment
fires\JN2n.mod
BRANZFIRE Multi-Compartment Fire Model (Ver 2002.2)
Copyright Notice - This software is provided for evaluation only and may
not be used for commercial purposes.
Compartment Test 2,  1200 MJ/m² (with 80% fuel consumed)
Description of Rooms:
Room  1  :
         Room Length (m) =                                  3.60
         Room Width (m) =                                   2.40
         Maximum Room Height (m) =                          2.40
         Minimum Room Height (m) =                          2.40
         Floor Elevation (m) =                              0.000
         Room  1  has a flat ceiling.

         Wall Surface is plasterboard
         Wall Density (kg/m3) =                             810.0
         Wall Conductivity (W/m.K) =                        0.160
         Wall Emissivity =                                  0.88
         Wall Thickness (mm) =                              13.0

         Ceiling Surface is plasterboard
         Ceiling Density (kg/m3) =                          810.0
         Ceiling Conductivity (W/m.K) =                     0.160
         Ceiling Emissivity =                               0.88
         Ceiling Thickness (mm) =                           13.0

         Floor Surface is plasterboard
         Floor Density (kg/m3) =                            810.0
         Floor Conductivity (W/m.K) =                       0.160
         Floor Emissivity =                                 0.88
         Floor Thickness = (mm)                             25.0
============


Description of Wall Vents:
From room  1  to outside, Vent No 1
                  Vent Width (m) =                          0.800
                  Vent Height (m) =                         2.000
                  Vent Sill Height (m) =                    0.000
                  Vent Soffit Height (m) =                  2.000
                  Opening Time (sec) =                      0
                  Closing Time (sec) =                      0
============
Description of Ceiling/Floor Vents
============
Ambient Conditions:
Interior Temp (C) =                                         20.0
Exterior Temp (C) =                                         20.0
Relative Humidity (%) =                                     65
============
Tenability Parameters:
Monitoring Height for Visibility and FED (m) =              1.50
Occupant Activity Level =                                   Light
Visibility calculations assume:                             reflective signs
FED Start Time (sec)                                        0
FED End Time (sec)                                          1200
============
Sprinkler / Detector Parameters:
No thermal detector or sprinkler installed.
============
Mechanical Ventilation (to/from outside):
Mechanical Ventilation not installed in Room 1
============
Description of the Fire:
Radiant Loss Fraction =                                     0.35
Underventilated Soot Yield Factor =                         1.00
Smoke Emission Coefficent (1/m) =                           0.80
Characteristic Mass Loss per Unit Area (kg/s.m2) =          0.011
```

```
Air Entrainment in Plume uses McCaffrey (recommended)

Burning Object No 1:
              Located in Room                              1
              Energy Yield (kJ/g) =                        25.0
              CO2 Yield (kg/kg fuel) =                     1.500
              Soot Yield (kg/kg fuel) =                    0.194
              H2O Yield (kg/kg fuel) =                     0.442
              Fire Height (m) =                            0.300
              Fire Location (m) =                          Centre

              Time (sec)              Heat Release (kW)
               0                      0
               100                    674
               200                    2500
               300                    1900
               400                    660
               500                    312
               600                    200
               700                    100
               800                    50
               900                    0
               1000                   0
============
Summary of End-Point Conditions in Room of Fire Origin
Upper Layer Temperature Exceeds 600 deg C at 162.0 Seconds.
Initial Time-Step = 1.00 seconds.
Computer Run-Time = 762.8 seconds.
```

(BRANZfire 2000) – Input Data Test #3:

```
Input Filename : P:\vb\branzfire_source\data2\JN3n.mod
BRANZFIRE Multi-Compartment Fire Model (Ver 2002.2)
Copyright Notice - This software is provided for evaluation only and may
not be used for commercial purposes.
Compartment Test 3,  800 MJ/m²
============
Description of Rooms:
Room  1  :
         Room Length (m) =                              3.60
         Room Width (m) =                               2.40
         Maximum Room Height (m) =                      2.40
         Minimum Room Height (m) =                      2.40
         Floor Elevation (m) =                          0.000
         Room  1  has a flat ceiling.

         Wall Surface is plasterboard
         Wall Density (kg/m3) =                         810.0
         Wall Conductivity (W/m.K) =                    0.160
         Wall Emissivity =                              0.88
         Wall Thickness (mm) =                          13.0

         Ceiling Surface is plasterboard
         Ceiling Density (kg/m3) =                      810.0
         Ceiling Conductivity (W/m.K) =                 0.160
         Ceiling Emissivity =                           0.88
         Ceiling Thickness (mm) =                       13.0

         Floor Surface is plasterboard
         Floor Density (kg/m3) =                        810.0
         Floor Conductivity (W/m.K) =                   0.160
         Floor Emissivity =                             0.88
         Floor Thickness = (mm)                         25.0
============

Description of Wall Vents:
From room  1  to outside, Vent No 1
                  Vent Width (m) =                      1.200
                  Vent Height (m) =                     2.000
                  Vent Sill Height (m) =                0.000
                  Vent Soffit Height (m) =              2.000
                  Opening Time (sec) =                  0
                  Closing Time (sec) =                  0
============
Description of Ceiling/Floor Vents
============
Ambient Conditions:
Interior Temp (C) =                                     20.0
Exterior Temp (C) =                                     15.0
Relative Humidity (%) =                                 65
============
Tenability Parameters:
Monitoring Height for Visibility and FED (m) =          1.50
Occupant Activity Level =                               Light
Visibility calculations assume:                         reflective signs
FED Start Time (sec)                                    0
FED End Time (sec)                                      1200
============
Sprinkler / Detector Parameters:
No thermal detector or sprinkler installed.
============
Mechanical Ventilation (to/from outside):
Mechanical Ventilation not installed in Room 1
============
Description of the Fire:
Radiant Loss Fraction =                                 0.35
Underventilated Soot Yield Factor =                     1.00
Smoke Emission Coefficent (1/m) =                       0.80
Characteristic Mass Loss per Unit Area (kg/s.m2) =      0.011
Air Entrainment in Plume uses McCaffrey (recommended)
```

```
Burning Object No 1:
               Located in Room                              1
               Energy Yield (kJ/g) =                        25.0
               CO2 Yield (kg/kg fuel) =                     1.500
               Soot Yield (kg/kg fuel) =                    0.194
               H2O Yield (kg/kg fuel) =                     0.442
               Fire Height (m) =                            0.300
               Fire Location (m) =                          Centre

               Time (sec)              Heat Release (kW)
                0                      0
                100                    674
                200                    2500
                300                    1900
                400                    660
                500                    312
                600                    200
                700                    100
                800                    50
                900                    0
                1000                   0
                1100                   0
                1200                   0
                1300                   0
                1400                   0
                1500                   0
============
Event Log:
The Sprinkler/Detector Did Not Actuate.
Summary of End-Point Conditions in Room of Fire Origin:
Upper Layer Temperature Exceeds 600 deg C at 187.0 Seconds.
Initial Time-Step = 1.00 seconds.
Computer Run-Time = 334.7 seconds.
```

F. Appendix F –Conduction Calculation Spreadsheets

Spreadsheet calculation for Evaluation of FRR 'by Opinion' for Nominal Half Hour Steel Stud Framed Wall Assembly #3 (achieving an average rise of 140°C):

Ambient temperature =	293	°C	
Specific heat capacity, Cp =	2000	J/kg K	Buchanan 2001a
Density, ρ =	670	kg/m³	
Thermal conductivity, k =	0.1	W/mK	
Heat Transfer Coefficient, h =	6	W/m² K	(assumed free convection - source Incropera & Dewitt Table 1.1)
Stephan boltzmann constant, σ =	5.67E-08	W/m² K⁴	
Emmissivity, ε =	0.88		(assumed - source Incropera & Dewitt Table A.12)
Δt =	10	seconds	
Δx =	0.0033	m	

	Time			Node 0	Node 1	Node 2	Node 3	Node 4			
	(secs)	(min)	(hrs)	(°K)	(°K)	(°K)	(°K)	(°K)	(°K)	Temp rise	
33	0	0.00	0.00	1124.4	855.9	638.3	491.9	408.7	373	100	
33.167	10	0.17	0.00	1125.2	860	644	497	413	379	106	
33.333	20	0.33	0.01	1126.0	864	650	503	417	385	111.75	
33.5	30	0.50	0.01	1126.7	868	656	508	422	390	117.22	
33.667	40	0.67	0.01	1127.5	872	661	513	426	396	122.53	
33.833	50	0.83	0.01	1128.3	876	667	518	431	401	127.73	
34	60	1.00	0.02	1129.0	880	672	523	436	406	132.86	
34.167	70	1.17	0.02	1129.8	883	677	529	441	411	137.93	
34.333	80	1.33	0.02	1130.5	887	682	534	446	416	142.98	failure
34.5	90	1.50	0.03	1131.3	890	687	539	451	421	148.01	
34.667	100	1.67	0.03	1132.0	893	691	544	456	426	153.02	

Spreadsheet calculation for Evaluation of Failure Time 'by Opinion' Assembly #2 in Test #3 (achieving an average rise of 140°C):

Ambient temperature =	293	°C	
Specific heat capacity, Cp =	2000	J/kg K	Buchanan 2001a
Density, ρ =	670	kg/m³	
Thermal conductivity, k =	0.1	W/mK	
Heat Transfer Coefficient, h =	6	W/m² K	(assumed free convection - source Incropera & Dewitt Table 1.1)
Stephan boltzmann constant, σ =	5.67E-08	W/m² K⁴	
Emmissivity, ε =	0.88		(assumed - source Incropera & Dewitt Table A.12)
Δt =	10	seconds	
Δx =	0.0020	m	

	Time			Node 0	Node 1	Node 2	Node 3	Node 4			
	(secs)	(min)	(hrs)	(°K)	(°K)	(°K)	(°K)	(°K)	(°K)	Temp rise	
23	0	0.00	0.00	773.0	538.1	440.6	390.1	372.0	373	100	
23.167	10	0.17	0.00	773.0	569	451	397	376	373	100	
23.333	20	0.33	0.01	773.0	588	465	405	380	374	101	
23.5	30	0.50	0.01	773.0	602	479	413	384	377	104	
23.667	40	0.67	0.01	773.0	613	492	421	389	380	107	
23.833	50	0.83	0.01	773.0	622	503	430	394	384	111	
24	60	1.00	0.02	773.0	629	513	438	400	389	116	
24.167	70	1.17	0.02	773.0	635	522	447	406	394	121	
24.333	80	1.33	0.02	773.0	641	531	454	412	399	126	
24.5	90	1.50	0.03	773.0	646	538	462	419	405	132	
24.667	100	1.67	0.03	773.0	650	545	469	425	411	138	
24.833	110	1.83	0.03	773.0	654	552	477	432	418	145	failure
25	120	2.00	0.03	773.0	658	558	483	439	424	151	
25.167	130	2.17	0.04	773.0	661	564	490	446	431	158	

G. Appendix G – Compartment Test Assemblies Temperature Profiles

Assembly #1 Temperature Profiles:

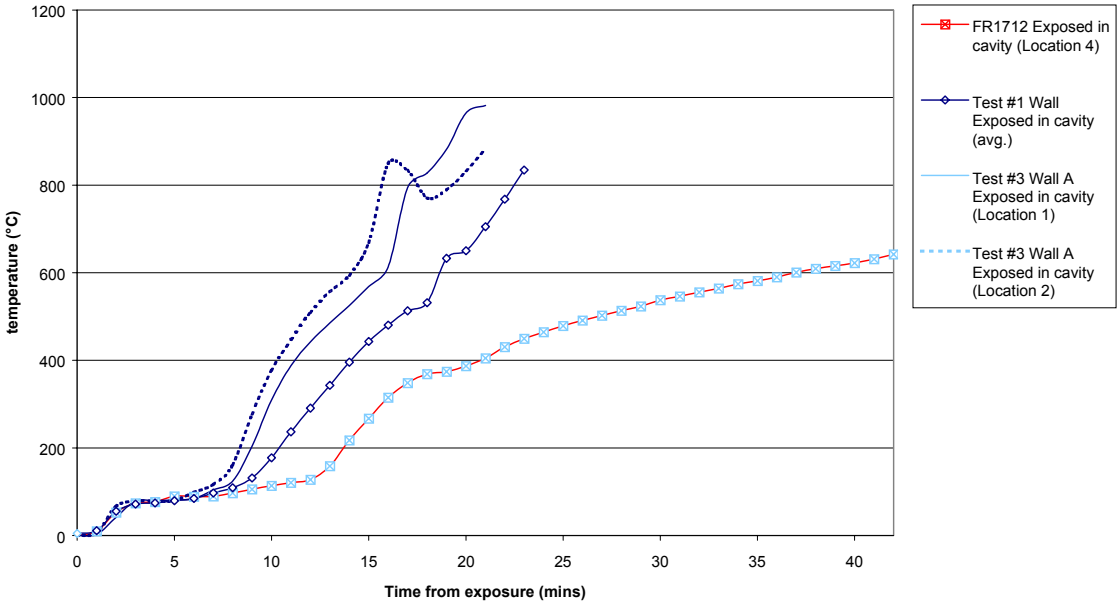

Assembly #1 exposed panel in cavity temperature rise profiles at failure locations

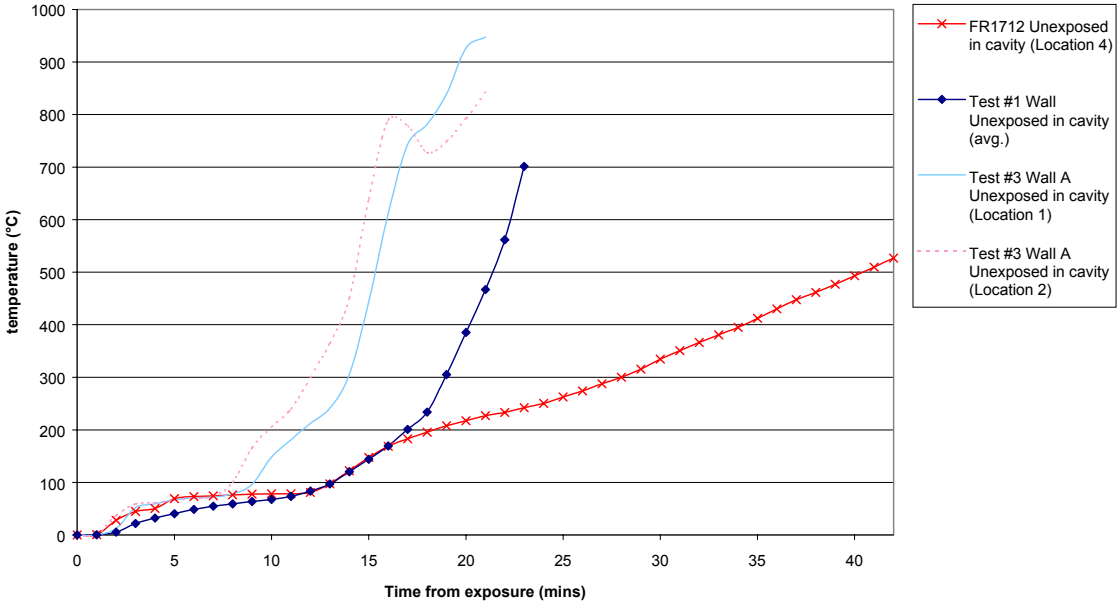

Assembly #1 unexposed panel in cavity temperature rise profiles at failure locations

Assembly #2 Temperature Profiles:

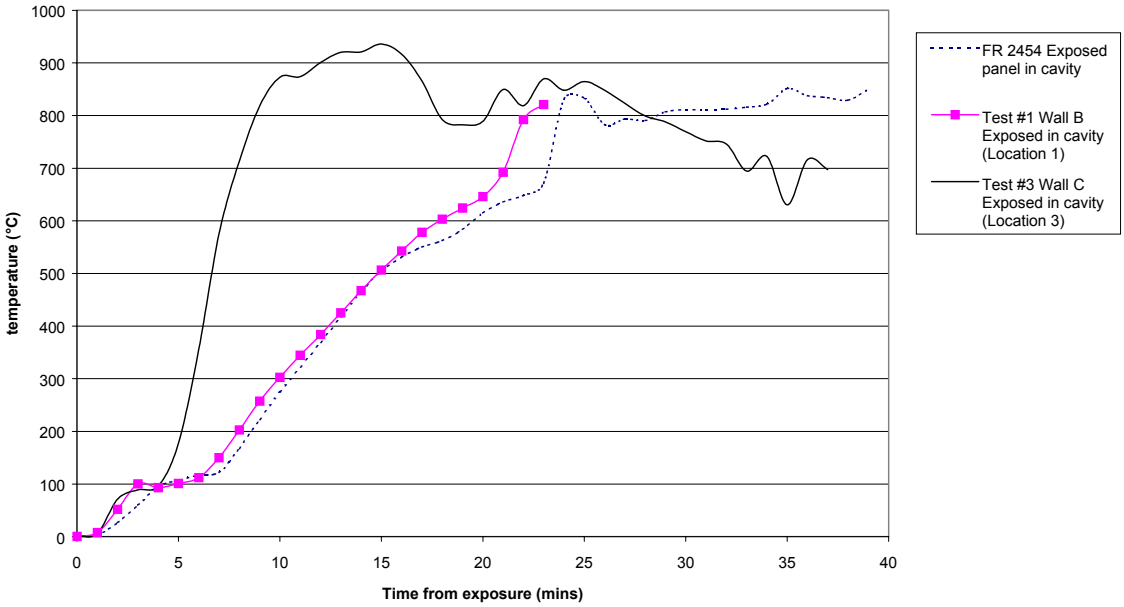

Assembly #2 exposed panel in cavity temperature rise profiles at failure locations

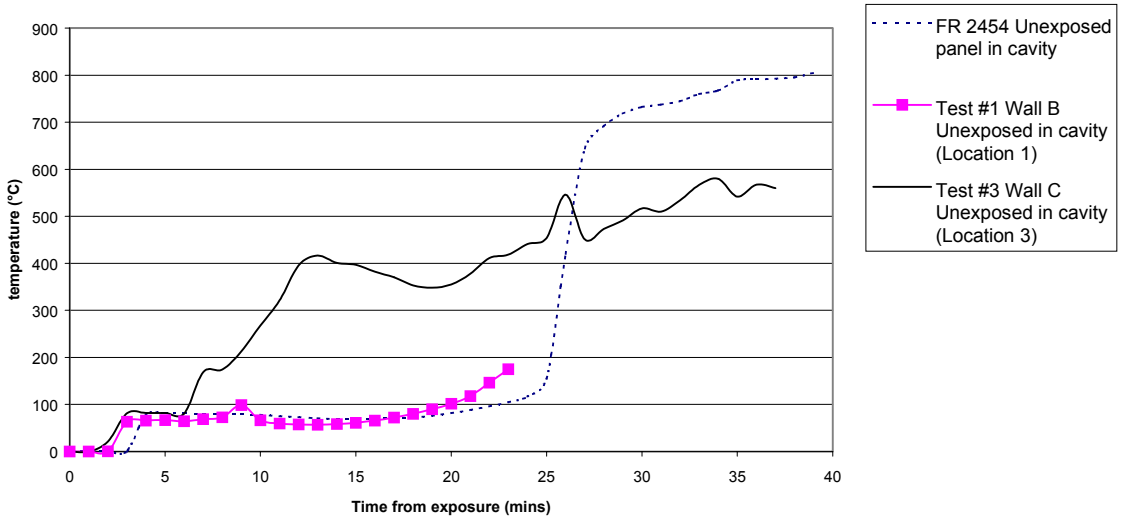

Assembly #2 unexposed panel in cavity temperature rise profiles at failure locations

Assembly #3 Temperature Profiles:

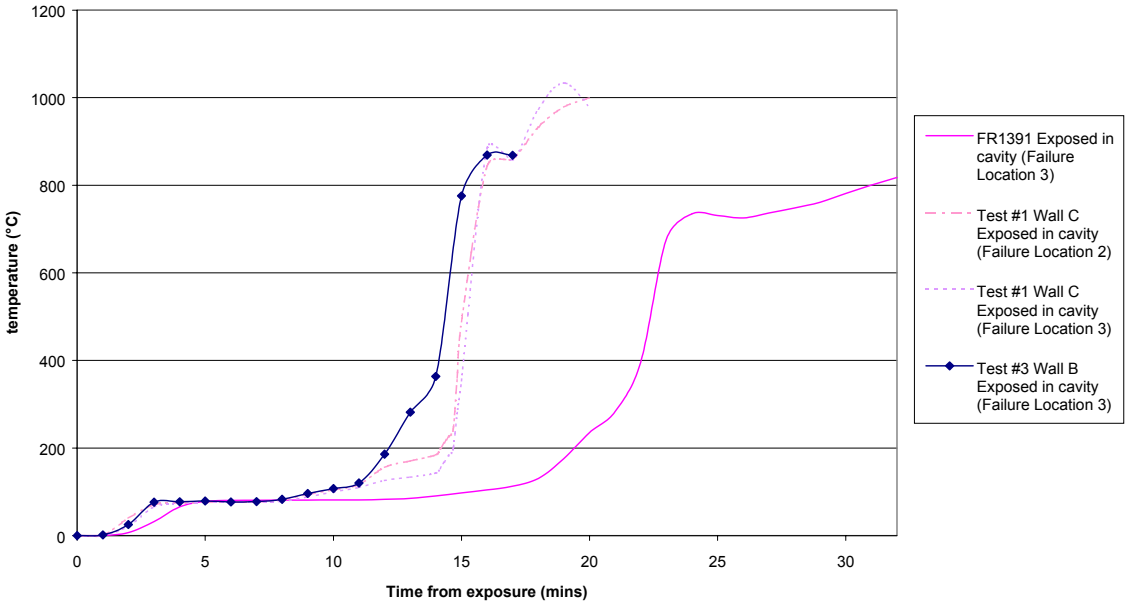

Assembly #3 exposed panel in cavity temperature rise profiles at failure locations

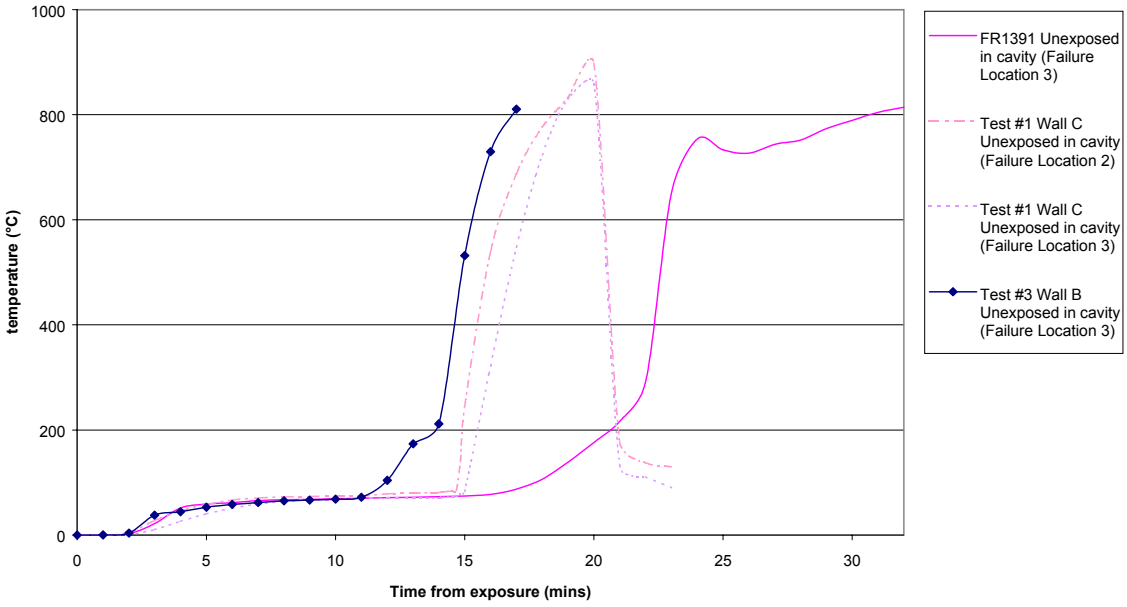

Assembly #3 unexposed panel in cavity temperature rise profiles at failure locations

Assembly #4 Temperature Profiles:

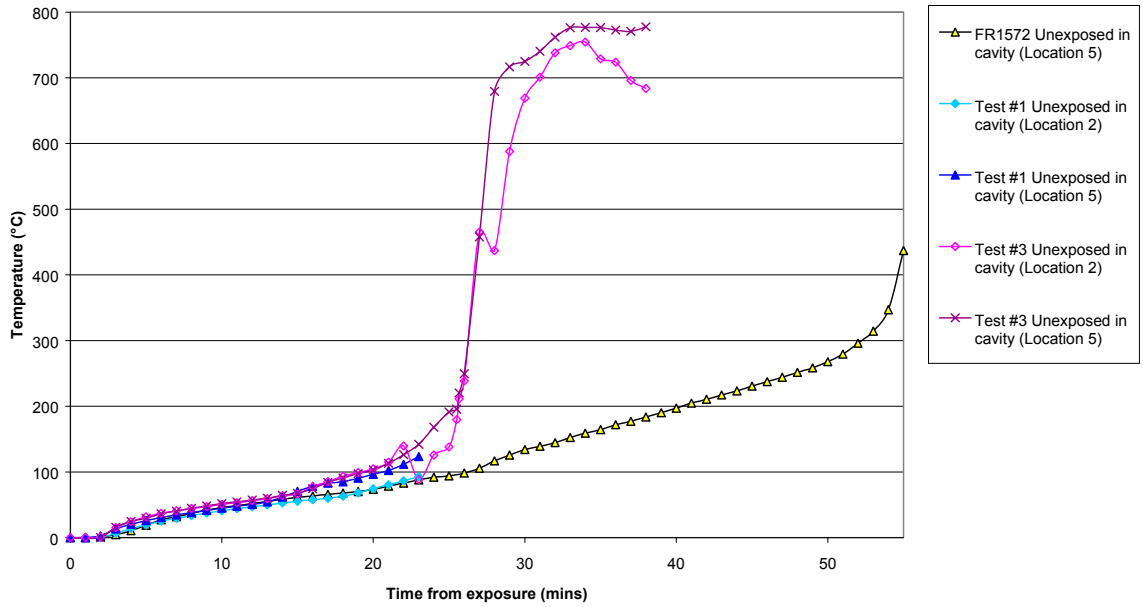

Assembly #4 unexposed panel in cavity temperature rise profiles at failure locations

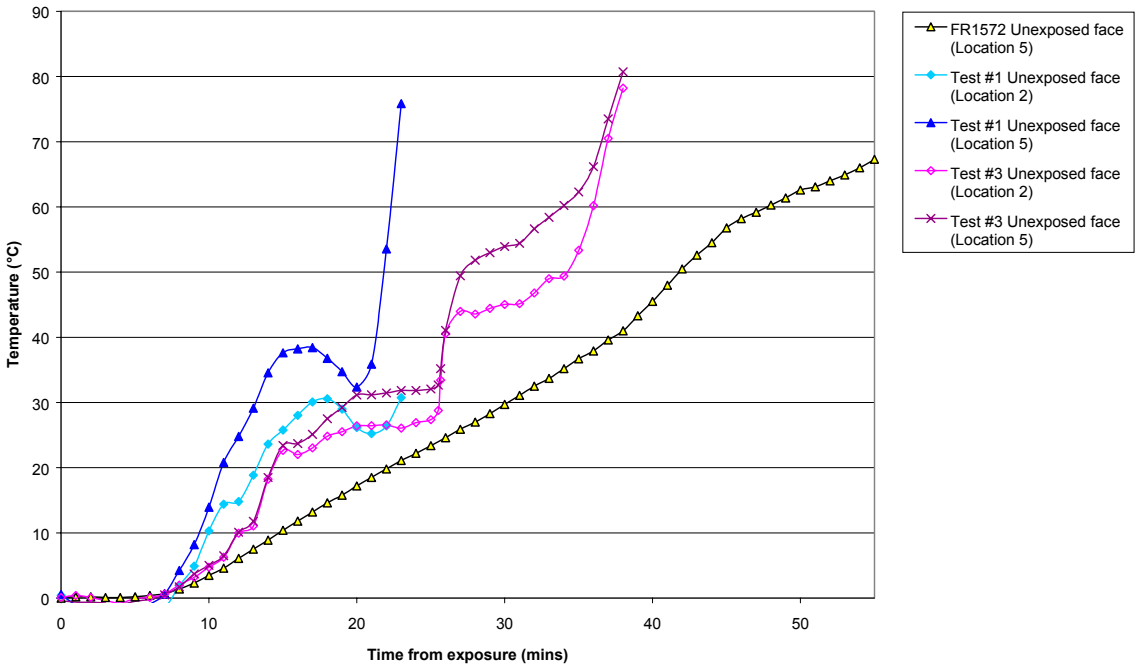

Assembly #4 unexposed face temperature rise profiles at failure locations

Assembly #9 Temperature Profiles:

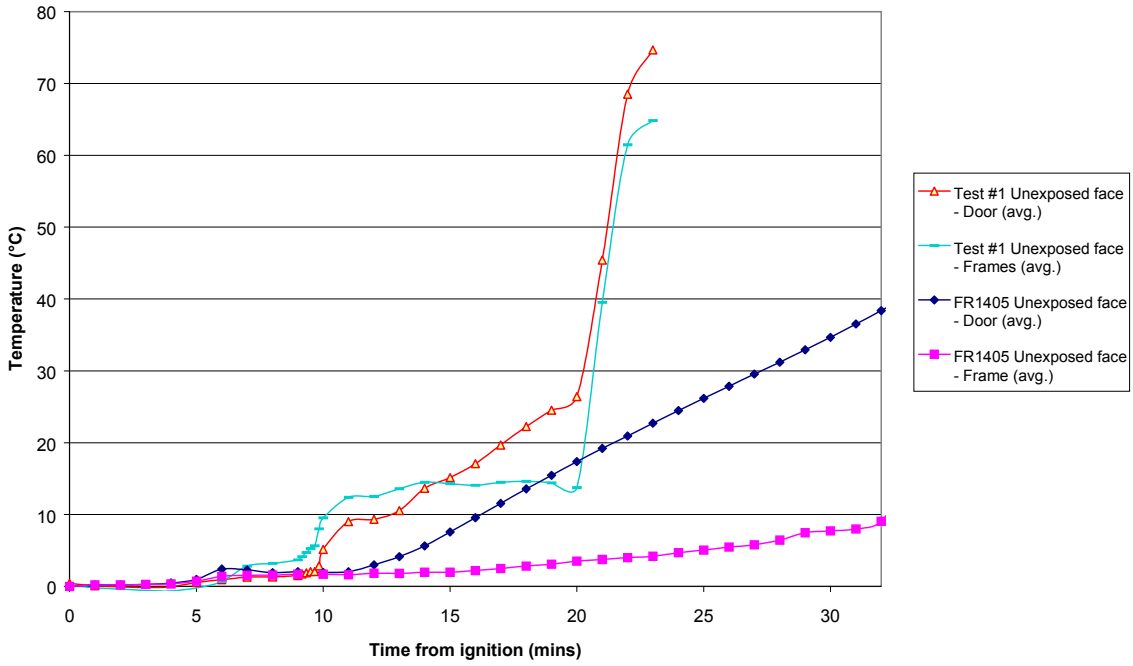

Assembly #9 unexposed face temperature rise profiles at failure locations

H. Appendix H – Compartment Tests Floor Temperatures

Compartment Floor Temperature Profiles:

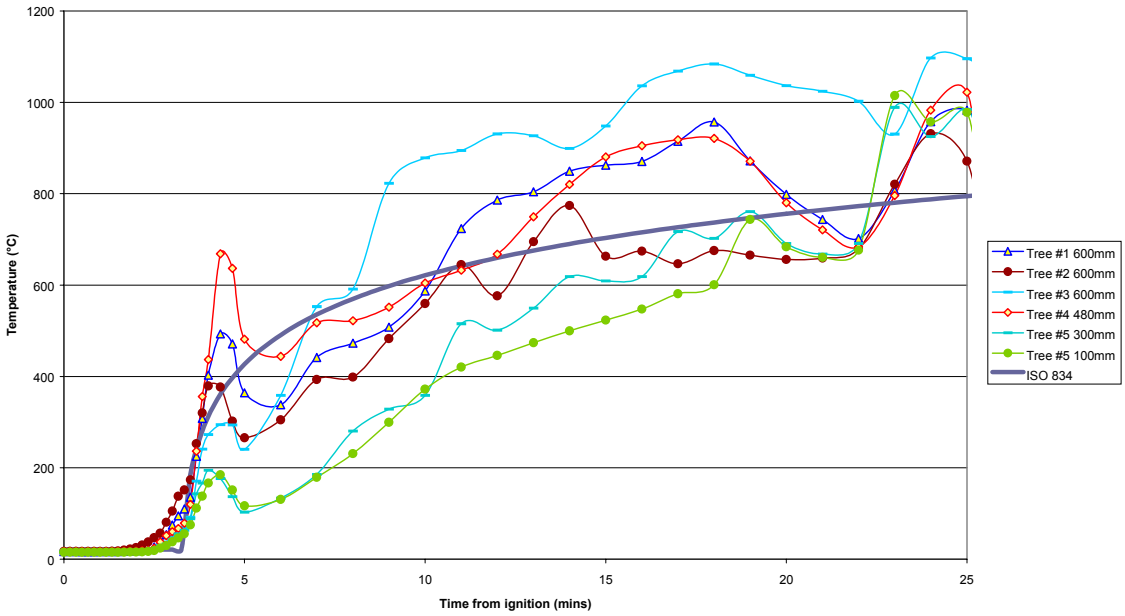

NB: Exposure 3.25mins after ignition

Test #1 Floor Exposure

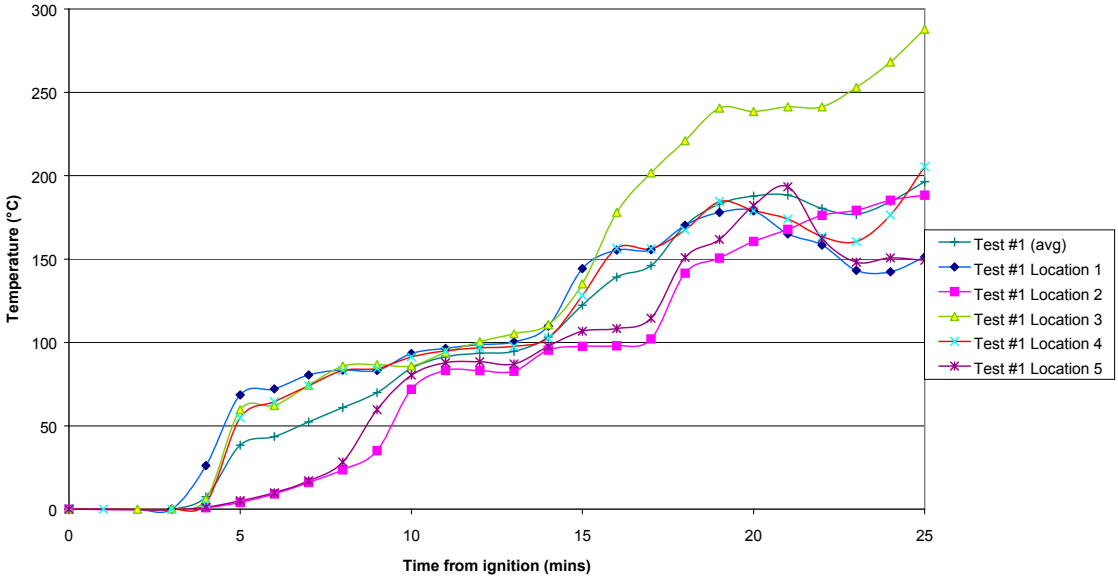

Test # 1 inter floor lining temperature rise profiles

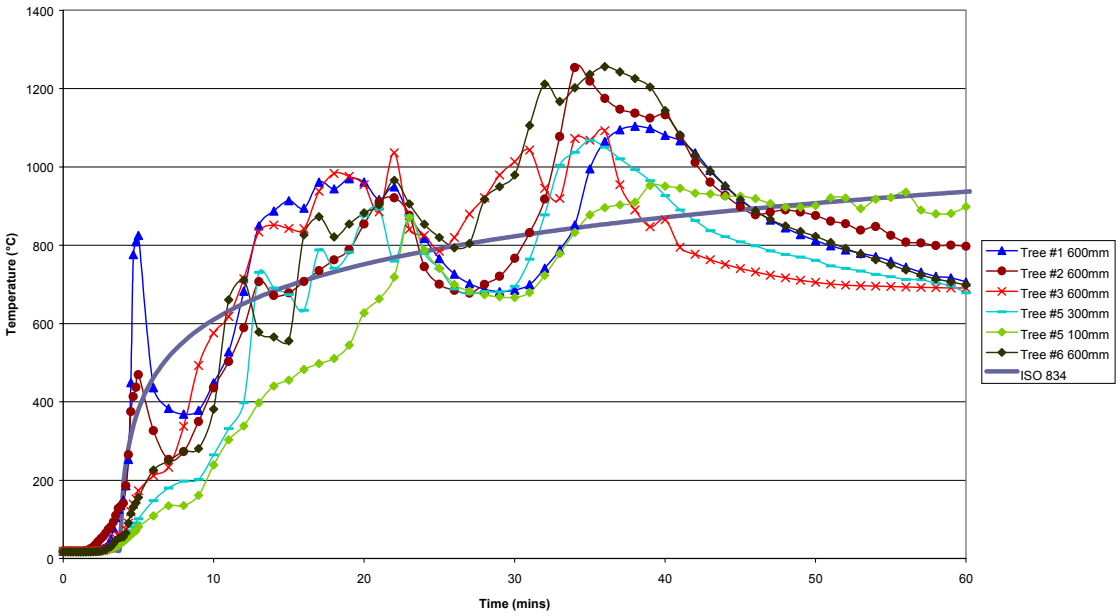

NB: Exposure 3.75mins after ignition

Test #2 Floor Exposure

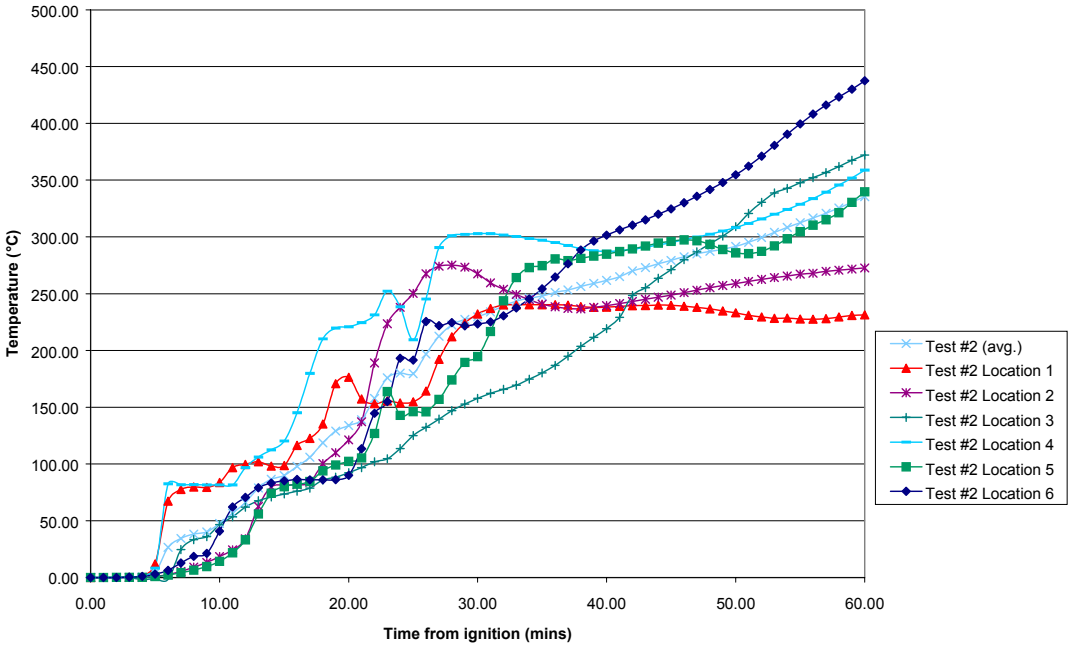

Test #2 inter floor lining temperature rise profiles

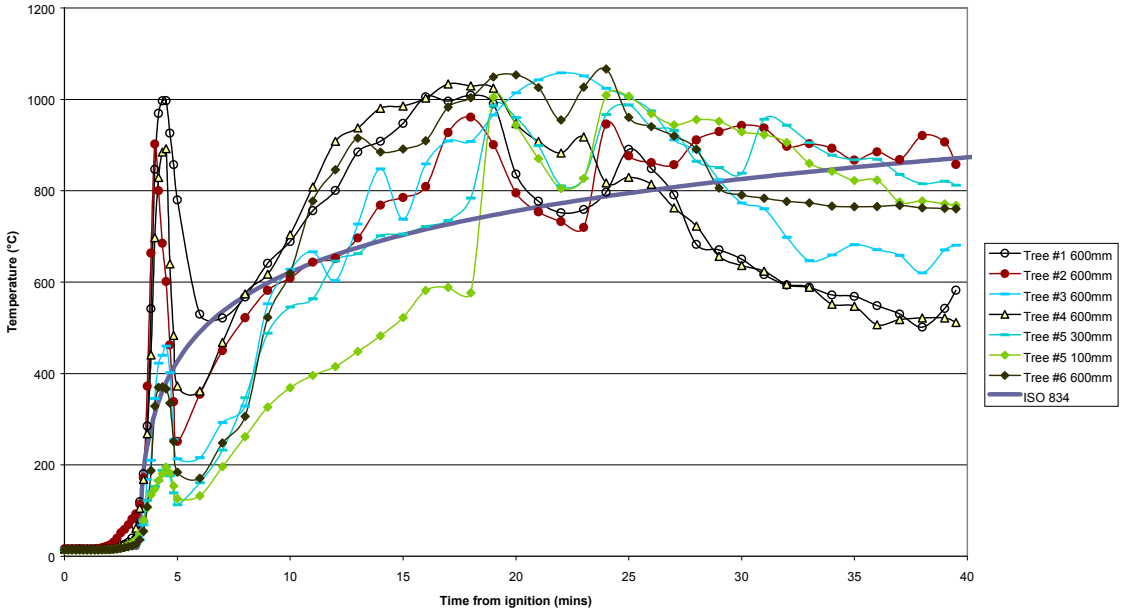

NB: Exposure 3.25mins from ignition

Test #3 Floor Exposure

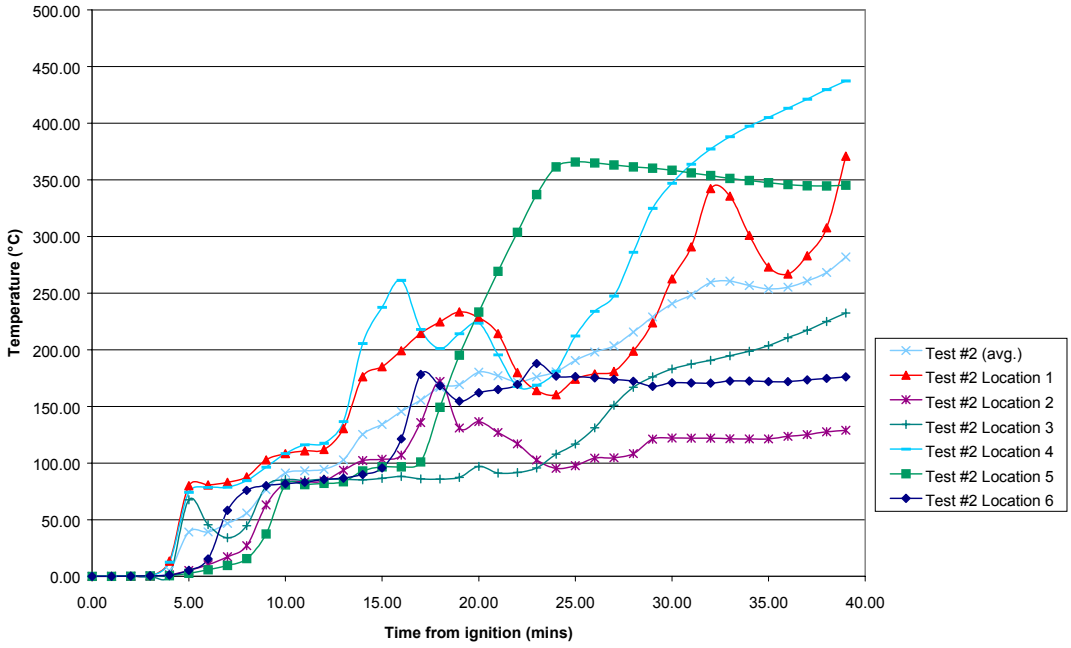

Test #3 inter floor lining temperature rise profiles